Comparative morphometric and molecular genetic analyses of Triatominae (Hemiptera: Reduviidae)

James S. Patterson

2007

Thesis submitted to the University of London in fulfilment to the requirements for the degree of Doctor of Philosophy (Ph.D.)

Supervisor: Prof. Michael A. Miles

Pathogen Molecular Biology Unit, Department of Infectious and Tropical Diseases,
London School of Hygiene & Tropical Medicine.
University of London

Abstract

Triatomine bugs (Hemiptera: Reduviidae: Triatominae) are the vectors of Chagas disease in South and Central America. Chagas disease predominantly affects poor rural communities with simply constructed housing susceptible to infestation by triatomines. Chagas disease is restricted to the Americas largely due to the limited distribution of triatomine bugs. The global diversity of triatomines is ~130 species, of which only ~10% are known to occur outside the Americas, one species (*Triatoma rubrofasciata*) is tropicopolitan, and the others are concentrated on the Indian subcontinent (*Linshcosteus spp.*) and adjacent south east Asian island groups (*Triatoma spp.*).

The main objectives of this PhD programme were to: a) assess the facility of morphometric approaches (measurement and robust statistical analysis of morphological variation) in the study of population structure of vector species with proximal domestic and silvatic distributions to detect population structure and give information on the risk of reinvasion, b) study interspecific and higher taxonomic level relationships of New World and Old World triatomine bugs. To these ends geometric morphometric analyses were conducted in concert with molecular genetic analyses of mitochondrial and nuclear DNA sequences. The principal question being: Does the relatively low cost method of morphometrics reveal patterns consistent with population structure, as otherwise determined by more expensive molecular genotyping methods? Or are such patterns disrupted by environmental effects and intraspecific convergent/divergent morphological evolution?

Combined morphometrics and molecular genetics were used to study vector populations in three of the countries that continue to be most affected by Chagas disease. In Venezuela and Ecuador *Rhodnius* species (*R. prolixus* and *R. ecuadoriensis* respectively) were studied, in areas where they occur in both domestic and silvatic environments, and in Paraguay *T. infestans* from a domestic and a putative silvatic focus. Head and wing morphometrics were compared to mitochondrial DNA sequence data to assess the population structure and disparity among domestic and silvatic samples in each case. The results presented suggest that head shape variation is subject to morphological plasticity and/or selective pressure and functional constraint and does not correlate well with the

phylogeny. However, in all examples, wing shape was found to be congruent with the phylogenetic patterns inferred from sequence analysis. Consequently, it is recommended that wing shape and not head shape be used in morphometric assessments of population dynamics. It is also asserted here that if population structure is suggested by morphometrics, it should be followed by robust population genetic analysis. As such, morphometrics could be used as a tool for broad surveillance to identify areas of concern. A further objective was to elucidate the broader phylogeny of Triatominae and their relationships with other reduviid subfamilies. To investigate the debated polyphyletic origin of the Triatominae molecular approaches were used.

Combined head and wing morphometric and molecular genetic analyses of New World and Old World Triatominae have revealed patterns of convergent morphological evolution (among New World and Old World *Triatoma*) and striking examples of strongly divergent morphological evolution (between Old World *Triatoma* and *Linshcosteus*).

Applying a molecular clock based on the rate of sequence divergence for a fragment of ribosomal DNA (D2-28S), calibrated to the fossil record and vicariant events (the divergence of ancestral lineages due to separation by topographical or ecological barriers) it has been possible to reconstruct a likely evolutionary history for the Triatominae and the Reduviidae as a whole.

The weight of evidence presented supports a polyphylectic origin for blood-feeding for the Triatominae. The apparent independent development of blood feeding among the main lineages of the Triatominae represented by the genera *Triatoma* and *Rhodnius* highlights a fundamental biological difference among important vector species. This difference is likely to become evident in the eventual post genomic era in studies of vector/parasite interactions and it highlights the importance of sequencing genomes from different vector genera.

Acknowledgements

My deepest gratitude goes to my supervisor Prof. Michael Miles, and my other mentors, Dr Chris Schofield, and Dr Jean-Pierre Dujardin.

For advice and companionship in the field, lab, and office I thank Dr Matthew Yeo, Dr Isabel Mauricio and Dr Michael Gaunt. In particular it was my pleasure to work closely on projects with Dr Sinead Fitzpatrick, Dr Fernando Abad-Franch, and Dr Fernando Monteiro.

I owe a large debt of gratitude to friends and collaborators for their generous hospitality and companionship: Dr Jose Jurberg, Dr Cleber Galvao, Dr Dayse de Silva Rocha and all at the International Laboratory for Reference and Taxonomy of Triatominae, Instituto Oswaldo Cruz , Rio de Janeiro, Brasil. Dr Dora Feliciangeli and all at BIOMED, University of Carabobo, Maracay, Venezuela. Dr Antonieta Rojas de Arias, Nidia Acosta and all at the Instituto de Investigaciones en Ciencias de la Salud, Universidad Nacional de Asunción, Paraguay. Dr D. Ambrose & Dr. K. Rajen of the Entomology Research unit, St Xavier's College, Palayankottai, India.

Many thanks to Mick Webb of the Natural History Museum London, Dr R. T. Schuh of the American Museum of Natural History New York, Dr T. J. Henry of the National Museum of Natural History, Smithsonian Institute, Washington DC, for access to collections.

Apologies to those who have been omitted due to lapse of memory or for the sake of brevity.

This work was funded by the Sir Halley Stewart Trust, the European commission funded ALFA programme and the ECLAT network.

Lastly and most importantly I thank my friends (many mentioned above) and family for their encouragement, support and patience. I couldn't have done it without you!

For Olga and Toby.

Contents

1 General introduction

1.1 Chagas disease

1.1.1 Epidemiology

Chagas disease, named after the Brazilian physician Carlos Chagas, who first described it in 1909, is a chronic and largely incurable parasitic infection that causes much morbidity and mortality. Chagas disease (also known as American trypanosomiasis) is a threat to almost a quarter of the population of Central and South America, associated with poverty in rural areas of 21 countries. Little more than a decade ago approximately 16-18 million people were thought to be infected with 100 million at risk (WHO, 1991). In 1996 it was estimated that of those infected, 6 million would develop clinical symptoms and 45000 would die per year (Rozendaal, 1997). As a result of efforts to control disease transmission, by 2003 an estimated 13 million people were infected with ~3 million symptomatic cases and a reduced annual incidence of 200,000 cases in 15 countries (WHO, 2003). Current estimates are as low as 9.8 million Remme *et al.,* (2006). The disease is most commonly associated with the rural poor and for this reason has historically struggled against the political climate to receive due recognition. Chagas disease is thought to be one of the principal reasons for the impoverishment of many areas of South America, and is believed to be responsible for the loss of 649,000 disability adjusted life years (DALYs) (WHO, 2002). The zoonotic aetiology of Chagas disease is complex and continues to require further research. In the United States, the disease exists almost exclusively as a zoonosis; only five autochthonous cases have been reported in humans (Herwaldt, 2000). However, recent studies (Beard, 2003) highlight the veterinary importance of the disease in the USA. Chagas disease continues to be

ranked as the most serious parasitic disease of the Americas. Its economic impact is more significant than the combined effects of other parasitic diseases, such as malaria, leishmaniasis, and schistosomiasis (Dias & Schofield 1999). In terms of DALYs, Chagas disease has been ranked as the third most serious parasitic disease in the world after malaria and schistosomiasis (World Bank, 1993).

The causative agent of Chagas disease is the flagellate protozoan *Trypanosoma* (*Schizotrypanum*) *cruzi*. Transmission usually occurs via the faeces of infected triatomine bugs (Triatominae: Reduviidae: Hemiptera). However a small percentage of cases are attributable to unscreened blood transfusions and congenital transmission. Most species of Triatominae occupy silvatic ecotopes in association with their respective vertebrate hosts. Examples include bird-nests, opossum lodges, rock-piles, hollow trees, rodent nests, and bat caves. These associations highlight the zoonotic origins of Chagas disease.

1.1.2 Life cycle

Triatomine bugs become infected with trypomastigote forms of *T. cruzi* during feeding on an infected vertebrate host. The parasites multiply and differentiate in the insect gut, yielding infective metacyclic trypomastigotes. During a subsequent blood meal on a second vertebrate host, the trypomastigotes are excreted in the insect faeces, often near the site of the bite wound. The host becomes infected through mucous membranes, conjunctivae, or breaks in the skin. On entering the host, the trypomastigotes invade the host cells where they differentiate into intracellular amastigotes. The amastigotes multiply and differentiate into trypomastigotes, which are released into the circulation as bloodstream trypomastigotes. Unlike human African trypanosomes, *T. brucei spp.* the bloodstream trypomastigotes of *T. cruzi* do

not replicate. Replication resumes when the parasites enter another cell, usually cardiac muscle, smooth muscle or skeletal muscle but also many other cell types. Alternatively a trypomastigote can be ingested by another vector and begin the cycle again. See fig. 1 for a summary of the life cycle.

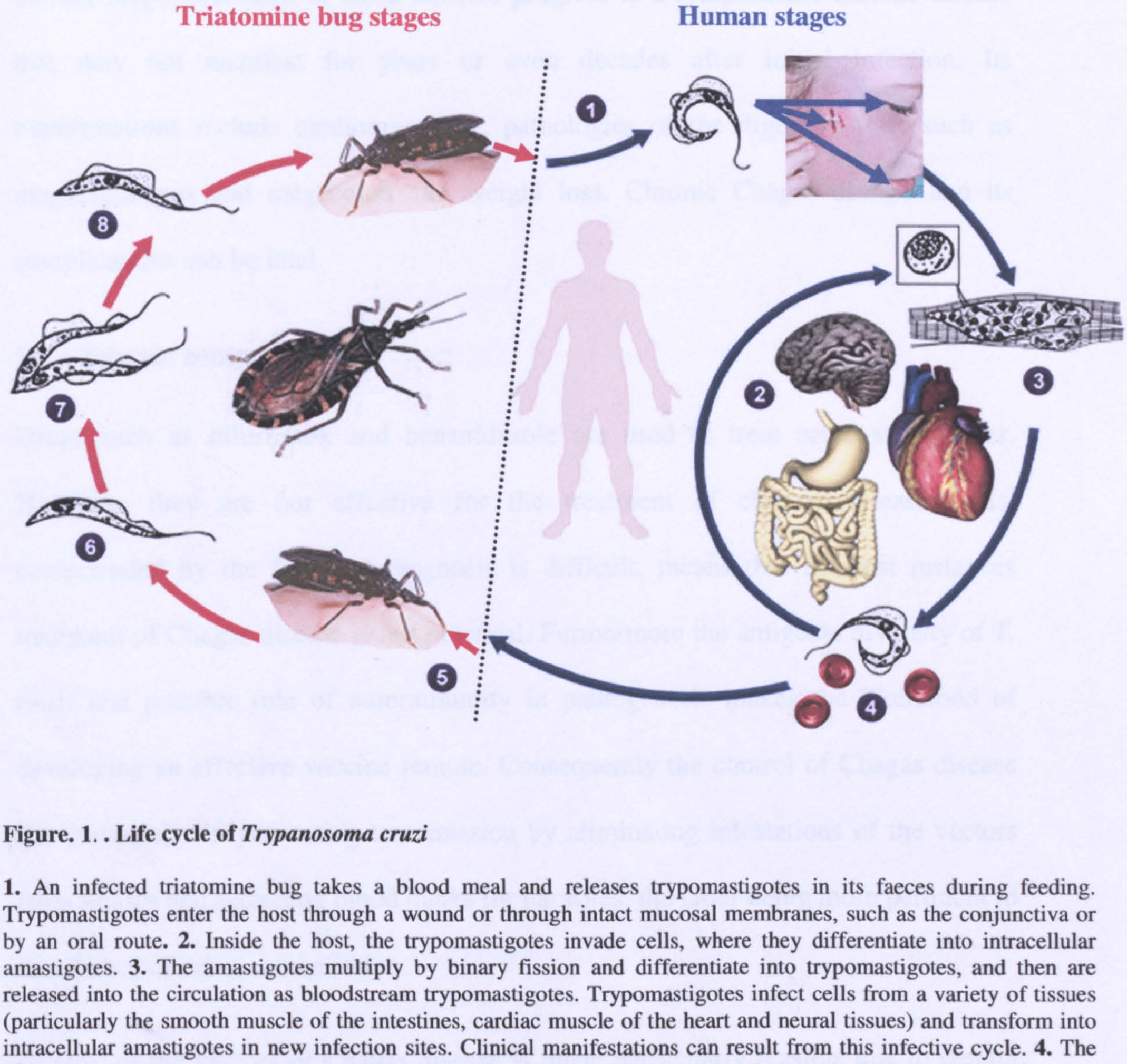

Figure. 1. . Life cycle of *Trypanosoma cruzi*

1. An infected triatomine bug takes a blood meal and releases trypomastigotes in its faeces during feeding. Trypomastigotes enter the host through a wound or through intact mucosal membranes, such as the conjunctiva or by an oral route**. 2.** Inside the host, the trypomastigotes invade cells, where they differentiate into intracellular amastigotes. **3.** The amastigotes multiply by binary fission and differentiate into trypomastigotes, and then are released into the circulation as bloodstream trypomastigotes. Trypomastigotes infect cells from a variety of tissues (particularly the smooth muscle of the intestines, cardiac muscle of the heart and neural tissues) and transform into intracellular amastigotes in new infection sites. Clinical manifestations can result from this infective cycle. **4.** The bloodstream trypomastigotes do not replicate. Replication resumes only when the parasites enter another cell or are ingested by another vector. **5.** A triatomine bug becomes infected by feeding on human or animal blood that contains circulating parasites. **6**. The ingested trypomastigotes transform into epimastigotes in the vector's midgut. **7.** The parasites multiply and differentiate in the midgut. **8**. Finally they differentiate into infective metacyclic trypomastigotes in the hindgut .

1.1.3 Clinical features

A local oedema (chagoma or Romaña's sign) can appear at the site of inoculation. The acute phase is usually asymptomatic, but can present with manifestations that include fever, anorexia, lymphadenopathy, mild hepatosplenomegaly, and myocarditis. Most acute cases resolve over a period of 2 to 3 months and lapse into an asymptomatic chronic stage. One third of those infected progress to a symptomatic chronic disease that may not manifest for years or even decades after initial infection. Its manifestations include cardiomyopathy, pathologies of the digestive tract such as megaesophagus and megacolon and weight loss. Chronic Chagas disease and its complications can be fatal.

1.2 Disease control

Drugs such as nifurtimox and benznidazole are used to treat acute stage cases. However, they are not effective for the treatment of chronic disease. This, compounded by the fact that diagnosis is difficult, means that in most instances treatment of Chagas disease is not practical. Furthermore the antigenic diversity of *T. cruzi* and possible role of autoimmunity in pathogenesis makes the likelihood of developing an effective vaccine remote. Consequently the control of Chagas disease lies principally in preventing transmission by eliminating infestations of the vectors from houses and screening blood banks for parasites, the latter being more pertinent to the control of urban transmission.

Control of the vectors of Chagas disease is made particularly feasible due to certain biological characteristics of domestic triatomine populations. Unlike many medically important vectors triatomine bugs have three basic characteristics, highlighted by Schofield (1994), which render them vulnerable to control interventions. Firstly, they

are slowly reproducing *K*-strategists, with a low rate of genetic rearrangement, and low capacity for active dispersal. Secondly, they have limited genetic diversity within populations and consequently low likelihood of developing insecticide resistance. Their third weak point is that all developmental stages are present in the house and therefore vulnerable to control interventions.

1.2.1 Methods of vector control

In the control of triatomine bugs, efforts fall mainly into three spheres; application of residual insecticides to houses, public health education, and house improvement. Much research has been dedicated to finding new, more effective and specific methods of eliminating domestic triatomines, summarised by Schofield (1985). Insect pathogens have been considered (Ryckman & Blankenship, 1984) most notably steinermatid nematodes and *Metarrhizium* fungi. Despite being safe to mammals, they are limited by low humidity and high temperatures, expensive to produce, and so far ineffective in field trials. Microhymenopterous Scelinoid egg-parasitoids have been another contender, highly specific and safe, however they are also expensive and have failed in field trials. Genetic control using sterilised or sub-sterile males is technically difficult due to the holocentric nature of bug chromosomes. The holocentric chromosomes of Hemiptera respond differently to radiation compared to Diptera where there are localized centromeres. Consequently, the established protocols of sterilising flies by radiation are ineffective for bugs and cannot simply be transferred. It may also be considered unethical since males (sterile or not) are also potential vectors of *T. cruzi*.

Chemosterilants have also been considered, but they would be a danger to occupants and relatively expensive. Traps baited with pheromones have been found to be

ineffective in both the laboratory and field trials. Insect growth regulators, specifically juvenile hormone mimics or precocenes act to disrupt natural moulting activity in nymphs giving rise to precocious sterile adultoids (Patterson & Schwarz, 1977). Precocenes also have some ovicidal activity. Although juvenile hormone analogues are often species specific and benign to mammals, their specificity limits their potential on the commercial market. Slow release formulations have been tested in the field but found to be practically ineffective for the control of triatomines (Schofield *et al.*, 1987).

Finally, the most recent development in the exploration of biological control methodology is to exploit the populations of symbiotic bacteria that bugs have in their intestinal tract. It is possible to genetically modify these bacteria to produce antitrypanosomal gene products, and place them back into their insect host, generating paratransgenic bugs, thereby resulting in insects that are incapable of transmitting Chagas disease. The method has been developed by Beard *et al.*, (2002) and they propose that it might be used as a tool for integrated vector control in the future.

1.2.2 Control strategy

Coordinated control activities, (Dias, 1987) have led to the development of a systematic approach to the control of triatomine bugs. This strategy was principally developed in Brazil, financed by SUCAM (Superintendancia de Campanhas de Saude Publica), an agency of the Brazilian Ministry of Health. This strategy comprises three phases; preparatory, attack, and vigilance, with the general goal of eliminating domestic populations of bugs and preventing reinfestation.

In the preparatory phase all houses in an endemic area are mapped and a sample examined manually through searches with flashlights and forceps, this may be

supplemented with spraying with irritant pyrethroids in an attempt to dislodge insects hiding in crevices. These preliminary surveys allow costs to be calculated, and detailed planning of intervention logistics.

In the attack phase the intervention method is employed comprehensively. For example, in a house spraying intervention all houses and outbuildings are sprayed irrespective of whether they are known to be infested with bugs. Spraying is then only repeated fully if >5% of houses are infested.

In the vigilance phase, houses are sampled periodically through a surveillance system set up with the local community and supported by health education. The conventional method of surveillance is collecting by hand, as in the preparatory phase. A passive method of surveillance is to use sensor boxes, e.g. 'Maria Sensor' developed in Argentina (WHO, 1991) or the Gómez-Núñez box utilised in Brazil (Pinchin *et al.*, 1981, Marsden & Penna 1982). These are artificial refuges made simply from cardboard, with holes in the sides to allow bug entry, and pleated paper inside provides resting sites. These boxes are placed on internal walls of houses, often close to beds. The boxes are checked periodically for live adults or nymphs, or other indirect evidence of bug activity, such as faecal smears on the paper, exuviae, or eggs. Vigilance can involve householder participation. In Brazil (Marsden & Penna, 1982) it was found to be feasible to supplement Gómez-Núñez boxes with educational posters and plastic bags, into which people could deposit bugs they found in their houses.

1.2.3 Control programmes

1.2.3.1 The southern cone initiative

In Brasilia, in June 1991, Ministers of Health of Argentina, Bolivia, Brazil, Chile,

Paraguay and Uruguay, met with the PAHO (Pan American Health Organisation) and launched an initiative for the elimination of Chagas disease in these countries by the end of the last century. The emphasis of the campaign was to use established triatomine control methods in a cooperative, international effort to eliminate domestic *Triatoma infestans* populations from these six southern most countries of South America. *T. infestans* is responsible for 80% of *T. cruzi* transmission in the southern cone countries (Schofield & Dias, 1999), with other species such as *T. brasiliensis* in northern Brazil and *Panstrongylus megistus* in Atlantic coastal regions being responsible for 10%. The remaining 10% is attributable to unscreened blood transfusion and congenital routes. To facilitate the elimination of *T. infestans*, an Intergovernmental Commission (composed of technical representatives of each Ministry) was formed to implement and evaluate the control programmes in each member country, and to administer funding arrangements. They meet annually to monitor progress in operations. This collaboration was instigated as, by 1990, it was clear that the control of Chagas was not failing due to a lack of biological, technical or operational knowledge, but because of political and economic limitations (Dias, 1991). Chagas was not given priority, partly because it was endemic and rural and not urban and epidemic (Schofield & Dias, 1999). This was exemplified in Brazil in1986, as resources were diverted from triatomine control to combat the incursion of *Aedes aegypti* and dengue epidemics in the Atlantic, coastal cities. Although uncomplicated dengue is rarely fatal, the resounding political outcry forced the diversion of funds. Prior to the southern cone initiative, existing programmes in the individual countries were generally underfunded and given insufficient priority. In a sense, the southern cone initiative can be seen as a scientific response to political uncertainty (*cf.* Schofield & Dias, 1999).

Most important achievements of the programme

(source: WHO web site)

- Reduction by 72% of the incidence of human infection in children and young adults in the countries of the initiative of the southern cone.

- 1997: Uruguay is certified free of vectorial and transfusional transmission of Chagas disease.

- 1999: Chile is certified free of vectorial and transfusional transmission of Chagas disease.

- 2000: Ten out of the twelve endemic states of Brazil are certified free of vectorial and transfusional transmission of Chagas disease.

1.2.3.2 Control in northern South America and Central America

Control activities in northern and western South America and Central America are divided into two initiatives; The Andean initiative (Colombia, Ecuador, Peru and Venezuela) and the Central American initiative (Belize, Costa Rica, El Salvador, Guatemala, Honduras, Mexico, Nicaragua and Panama). These two programmes have more complications than the southern cone initiative because there are more vector species involved, some of which, unlike *T. infestans,* have widespread silvatic foci which pose the threat of reinvasion of houses post-intervention. There is also less political cohesion in coordinating efforts between countries.

In 1993 the first phase of the Central American and Andean initiatives began with the emphasis on screening blood banks for parasites. The vector control phase was launched in 1997, triggering a surge in research on the biology and systematics of triatomine species in these regions, with the aim to provide governments with recommendations on how to best proceed with control.

1.3 Biosystematics of the Triatominae

1.3.1 Systematics

The triatomine bugs (Hemiptera: Heteroptera: Cimicomorpha: Reduviidae: Triatominae) are an assemblage of reduviids defined by their obligate haematophagous behaviour (Jeannel, 1919; Usinger, 1939). There are ~130 recognised species of Triatominae, classified into 16 genera and 5 tribes (see Fig. 2)

The Reduviidae is one the largest and most morphologically diverse families of the true bugs, composed of approximately 23 subfamilies with some 6000 species. With the exception of a few aberrant plant feeding members (Bérenger & Pluot-Sigwalt 1997) and the Triatominae, all reduviids are predators of other invertebrates.

It is reasonably proposed that the Triatominae are derived from vertebrate nest dwelling predatory ancestors that adapted and evolved to exploit the niche of blood feeding on birds and mammals. However, there is some debate as to whether there was a single divergent event (monophyletic origin) or, as is hypothesised by some, a polyphyletic or diphyletic origin. Polyphyly for the Triatominae has been assumed by Dujardin *et al.,* (1999a), Stothard *et al.,* (1998), Lyman *et al.,* (1999) Carcavallo *et al.,* (1999), Marcilla *et al.,* (2001), and most notably by Schofield (1994, 1988, 1999, & 2000). Some of the evidence adduced is based on molecular and morphological differences between the two main tribes; Rhodniini and Triatomiini. Monophyly has been incrorrectly supported by Hypsa *et al.,* (2002) and alluded to by Gaunt & Miles (2000) in which they comment on a molecular clock that dates divergence between the two main genera/tribes; *Triatoma* and *Rhodnius* at ~ 40Mya, before the arrival of bats and rodents to South America and suggest that the ancestor of the two lineages would most likely already have adapted to exploit the marsupials and edentates extant 65 Mya. However, Gaunt & Miles (2002) later estimated the same divergence at ~95

Mya and correlated it with the emergence of palm trees with which extant *Rhodnius* have a close association. Clearly ancient divergence does not preclude the possibility that the divergent ancestors were predatory reduviids, separated by ecological specialisation and later adapting to haematophagy in parallel. Moreover, the numerous molecular phylogenetic studies to date (Stothard *et al.,* 1998 García & Powell 1998, García 1999 Lyman *et al.,* 1999, Monteiro *et al.,* 1999a,b, 2000, 2001 Bargues *et al.,* 2000, Marcilla *et al.,* 2001, Gaunt & Miles 2000, Hypša *et al.,* 2002 and Paula *et al.,* 2005) have failed to represent all of the triatomine tribes in a single analysis, and few representatives of other reduviid subfamilies have been included. The clarification of this debate forms one of the objectives of this work.

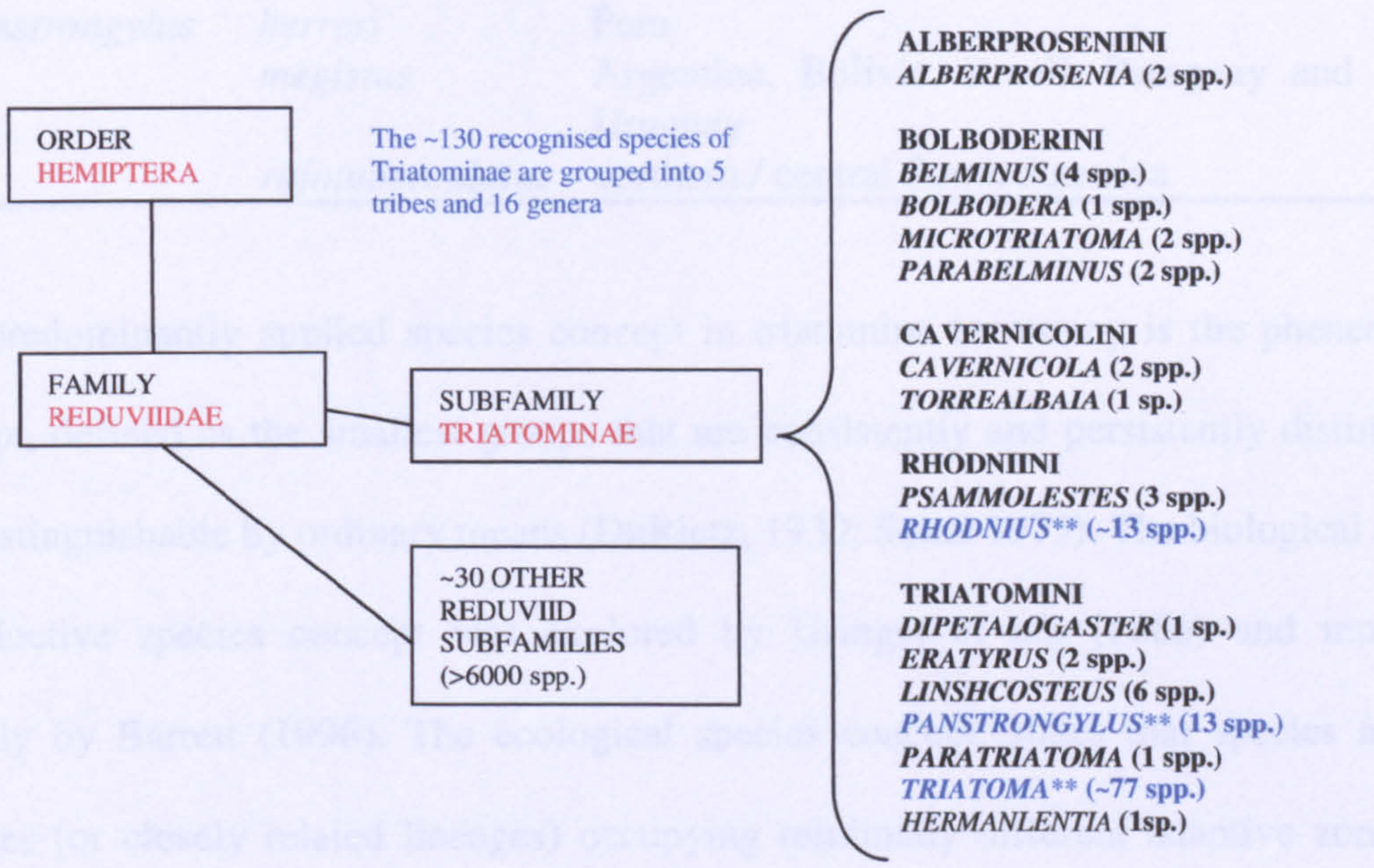

Figure. 2. Systematics of the Triatominae indicating the tribes, constituent genera and numbers of species within each. ** indicate the three genera containing the most important vector species

Of the ~130 described species of Triatominae most are unimportant as vectors as they generally remain restricted to silvatic ecotopes. Nevertheless, over 100 species have been reported as naturally or experimentally infected by *T. cruzi* (Schofield, 1994). Fortunately only twelve species, representing three genera have so far adapted to

regularly inhabit human environments and are of epidemiological importance in different geographical regions (Table.1). The five most significant vectors are generally considered to be *T. infestans, R. prolixus, P. megistus, T. dimidiata* and *T. brasiliensis* (Fig.3)

Table 1. The 12 most domesticated species of triatomine bug and their distributions.

Genus	*species*	Regions in which a vector
Triatoma	*barberi*	Mexico
	brasiliensis	northern Brazil
	dimidiata	Ecuador, Peru, Colombia and Central America
	infestans	southern South America
	maculata	Venezuela, Colombia,
	sordida	Argentina, Bolivia, Uruguay, Paraguay and Brazil
Rhodnius	*ecuadoriensis*	Ecuador and Peru
	pallescens	Panama and Colombia
	prolixus	Venezuela, Colombia and Central America
Panstrongylus	*herreri*	Peru
	megistus	Argentina, Bolivia, Brazil, Paraguay and Uruguay
	rufotuberculatus	northern / central South America

The predominantly applied species concept in triatomine taxonomy is the phenetic concept, defined as the smallest groups that are consistently and persistently distinct and distinguishable by ordinary means (DuRietz, 1930; Sokal 1973). The biological or reproductive species concept was explored by Usinger *et al.,* (1966) and more recently by Barrett (1996). The ecological species concept, states that species are lineages (or closely related lineages) occupying minimally different adaptive zones (Andersson 1990). This has been applied to triatomines in conjunction

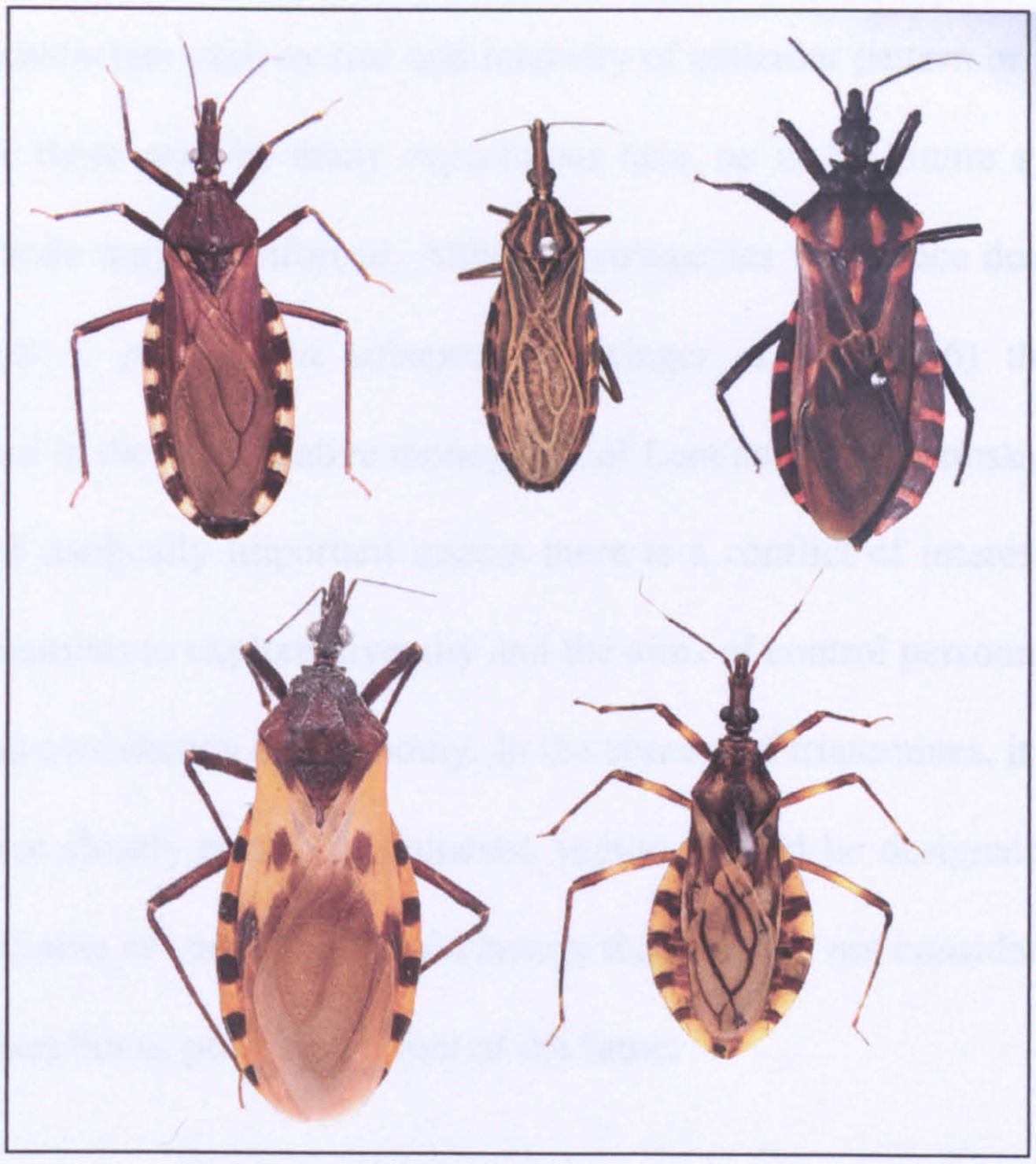

Figure. 3. Five most important vectors of Chagas disease. From left to right: above *T. infestans; Rhodnius prolixus; Panstrongylus megistus* (below) *Triatoma dimidiata; Triatoma brasiliensis* (see Table.1 for distributions)

with weak phenetic differences to distinguish between domestic and silvatic 'populations' e.g. *T. melanosoma,* a silvatic dark morph of the predominantly domestic *T. infestans.* Until recently it has not been possible to satisfactorily apply the phylogenetic species concept to triatomines. To date no cladistic analysis has been adequately concluded, probably due to a lack of well defined plesiomorphic and apomorphic morphological character states, however, molecular tools are increasingly applied to explore the phylogeny of the group (e.g. Hypsa *et al.,* 2002, Monteiro *et al.,* 2001, Lyman *et al.,* 1999, García & Powell1998, García *et al.,* 2001& Paula *et al.,*2005).

The morphospecies concept is historically the basis of triatomine taxonomy. Some species of *Rhodnius* and *Triatoma* have been described largely on the basis of inconsistent characters such as size and intensity of cuticular pattern or pigmentation. Some believe there may be many superfluous taxa, so in the future synonymies or subspecific ranks may be enforced. Although subspecies were once described e.g. *T. protracta* and *T. phyllosoma* subspecies (Usinger *et al.*, 1966) they were not accommodated in the authoritative monograph of Lent and Wygodzinsky (1979).

For groups of medically important insects there is a conflict of interest between the aims of taxonomists to explore diversity and the aims of control personnel to maintain simplicity and consistency of taxonomy. In the context of triatomines, it is crucial that silvatic species closely related to domestic vectors should be designated so as to be readily identifiable as such. This would ensure that they are not considered as abstract scientific names but as possible vectors of the future.

1.3.2 Taxonomy of the Triatominae

1.3.2.1 Morphological approaches

As stated, the main criteria used in the taxonomy of the Triatominae are morphological. Generally species can be distinguished by their external anatomical structures and/or by the pattern of their cuticular pigmentation. The works of Lent and Wygodzinsky (1979) and Carcavallo (1997) are detailed reviews and present effective keys for the identification of morphologically distinct species. The most discriminatory characters used at the species level are cuticular patterning and colouration of the head, pronotum, corium, connexivum and leg segments. Structure and shape of the pronotum and scutellum are also informative, as is cuticular texture. Relative metric characters (ratios) of the head, pronotum and mouthparts (rostral

segments) are also employed.

For the identification of most species of triatomine bugs these morphological parameters are sufficient. However there are some species with weak or inconsistent morphological distinctiveness and uncertain taxonomic status. To investigate such instances detailed studies of more differentiating characters have been undertaken:

The detailed internal and external structure of male genitalia has been scrutinized and used to define species (Lent & Wygodzinsky 1979), detect intraspecific variation (Lent & Jurberg 1985, Pires *et al.,* 1998) and infer phylogenetic relationships within the Triatominae. (Jurberg *et al.,* 1997, Lent & Wygodzinsky 1979). Another informative character is the number and arrangement of antennal sensilla, used for studying interspecific and intergeneric differences (Catalá & Schofield 1994, Catalá 1997, 2004, 2005 and Gracco & Catalá 2000)

Other detailed morphological investigations have focussed on the use of scanning electron microscopy to study eggshell structure (Barata 1996, 1998) and cuticular structures (Carcavallo *et al.*,1997).

1.3.2.2 Genetic approaches

1.3.2.2.1 Cytogenetic studies

Triatomine bugs have holocentric chromosomes. Studies of chromosome number, (summarised by Schofield 1988, and Panzera *et al.,* 1998) polymorphisms in C-banding of heterochromatin and meiotic behaviour (Panzera *et al.,* 1992, 1997, 1998,) have been used to study intraspecific variation and interspecific relationships.

1.3.2.2.2 Isoenzyme electrophoresis

This approach involves measuring a number of polymorphic allozyme loci and at each polymorphic locus quantifying the average heterozygosity. This method has been used

to address taxonomic issues and measure genetic diversity between populations (e.g. Dujardin *et al.*,1987 Costa *et al.*, 1997), and between species (e.g. López & Moreno 1995 García *et al.*, 1995, Dujardin *et al.*, 1999b, Solano 1996, Pereira *et al.*,1996). Particularly interesting works by Noireau *et al.*, (1998, 1999a) demonstrated cryptic speciation in *T. sordida* in Bolivia.

1.3.2.2.3 Microsatellites

Currently iosenzyme techniques are losing favour as tools for population genetics, as attention is increasingly diverted to microsatellite markers. Microsatellites are series of short, tandemly repeated, sequence motifs within the nuclear DNA. They are relatively neutral markers and much more polymorphic than allozymes, and therefore have the potential to give a higher resolution measurement of population structure and gene flow. They are potentially the most suitable tool for studying population genetics and addressing important questions of gene flow between domestic and silvatic bug populations. Preliminary characterisation of microsatellite markers for *R. pallescens* has been developed by Harry *et al.*, (1998). Markers for *T. infestans* have been developed by García *et al.*, (2004) and Marcet *et al.*, (2006), for *T. dimidiata* by Anderson *et al.*, (2002) and for *R. prolixus* by Fitzpatrick *et al.*, (submitted).

1.3.2.2.4 Random amplification of polymorphic DNA (RAPD)

This technique makes use of a battery of random primers to produce a profile of DNA fragments, subsequently visualised by electrophoresis as discrete banding patterns. This approach has been used to investigate interspecific relationships between closely related species of *Rhodnius* (García *et al.*, 1998) and to study intraspecific variability between populations of *T. infestans* and *T. sordida.* (Carlier *et al.*, 1996) and *T.*

brasiliensis (Borges *et al.*, 2000). RAPD analysis provides better resolution for detecting intraspecific variability than isoenzyme electrophoresis (Borges *et al.*, 2000). The drawbacks of RAPD analysis are that the technique is vulnerable to contamination. Also particular PCR conditions may give rise to different results, reducing reliability and reproducibility.

1.3.2.2.5 DNA sequencing

Sequencing of specific DNA fragments can serve as the ultimate indicators of genetic diversity, plus they also have the advantage of being good markers from which to infer phylogenetics.

Fragments of some protein coding genes of the mitochondrial DNA (mtDNA) are particularly useful for studies of intraspecific variation, as they have the potential to accumulate a high number of mutations in the form of nucleotide substitutions in the third codon positions. These "silent" substitutions render such genes as rapidly evolving markers (Simon *et al.*, 1994, Moor 1995).

A preliminary study of a 400bp fragment of the 16S ribosomal gene (Stothard *et al.*, 1998) demonstrated the facility of mtDNA sequencing to detect variation at intergeneric, interspecific and intraspecific levels. Fragments of three mitochondrial genes (12S and 16S ribosomal RNA and cytochrome oxidase I) were analysed to successfully infer phylogenetic relationships between members of the *T. infestans* complex (García & Powell 1998, García 1999)

Two further mitochondrial targets (cytochrome B and large subunit ribosomal RNA) have been analysed to construct phylogenies of *Rhodnius* and *Triatoma* (Lyman *et al.*, 1999, Monteiro *et al.*, 1999a,b, 2000, 2001, 2003, 2004). These studies have demonstrated the facility of mtDNA sequence analysis for studying the systematics and phylogenetics of triatomine bugs at both inter and intraspecific levels.

Genomic targets studied include the second internal transcribed spacer (ITS-2) of the nuclear ribosomal DNA (rDNA) (Bargues *et al.*, 2000, Marcilla *et al.*, 2001, 2002), 18S rDNA (Bargues *et al.*, 2000) and the D2 region of the 28S RNA gene (Monteiro *et al.*, 2000). ITS2 and 18S have generally been used to address higher taxonomic questions and for the development of molecular clocks (Bargues *et al.*, 2000). 28S RNA was used by Monteiro *et al.*, (2000) to support mtDNA in a phylogenetic analysis of the Rhodniini. See Abad-Franch & Monteiro (2005) for a comprehensive review of molecular genetic studies on triatomines.

1.3.2.3 Morphometrics

Morphometry is the measurement and analysis of form, and the main premise of morphometrics is that a statistical analysis of genetic variability expressed by morphological characters is a measure of population differentiation and ultimately speciation.

Current terminology describes morphometric techniques based on linear measurements, or ratios as "traditional morphometrics" and the newer approaches based or cartesian coordinates and superimposition procedures are referred to as "geometric morphometrics".

1.3.2.3.1 Traditional morphometrics

Morphometrics emerged as a discrete discipline only a few decades ago with its roots in the work of Sneath (1957). The rapid progression of computer technology has been the driving force behind the development of morphometrics, as the approach relies heavily on the application of rigorous multivariate statistics. Morphometrics has been applied to an array of biological sciences, including anatomy, anthropology, medicine

and palaeontology. A review by Daly (1985) examines the application of morphometrics to the study of insects. The first studies conducted on medically important insects were performed on mosquitoes by Rohlf (1963) and Coluzzi (1964). Later came studies on blackfies (Townson & Meredith 1979), sandflies (Ready *et al.*, 1982, Lane & Ready 1985) and ticks (Hutcheson *et al.*, 1995).

In the analysis of traditional morphometric data multivariate statistics are used to compare a selection of morphological measurements simultaneously. Prior to multivariate analysis data are log transformed to equalise variance among groups. Further transformation of the data to remove the element of size is also desirable, this allows partitioning of environmental (size related differences) from evolutionary or adaptive influences. Multivariate methods of canonical variate (multiple discriminant) analysis (CVA) and principal component analysis (PCA) are generally the techniques of choice. PCA and CVA essentially calculate linear combinations of the original variables to produce one or two components or functions, which represent the majority of the variability between the specimens.

1.3.2.3.2 Geometric morphometrics

With the traditional approach to morphometrics it is not possible to recover the shape of the original structure from the data matrices generated by multivariate analysis of distance measures, even as an abstract representation. The search for a more powerful approach designed for the analysis of shape data rather than the use of simple distance measures was the impetus behind the development of a new approach to morphometrics.

Geometric morphometrics has its conceptual roots in the remarkable work of D'Arcy Wentworth Thompson (1917), who depicted morphological shape changes or differences between taxa as transformational coordinate grids (Fig. 4.) However,

Thompson's examples were not constructed by any mathematical method, but were produced freehand. Through a progression of publications from the mid eighties (Bookstein, 1985) through to the early nineties (Rohlf & Bookstein, 1990, Bookstein, 1991, Rohlf & Marcus, 1993) a revolution occurred to bridge the gap between the inadequacies of traditional morphometrics and the visualization of shape change conceptualized by Thompson. Constructed on the basis of landmark coordinates, which reflect biological homology, geometric morphometrics involves the application of superimposition/procrustes methods, named after a character of Greek legend, who either stretched or mutilated people to fit into his bed. Essentially procrustes superimposition is based on the same premise; optimally overlaying images of two or more specimens so that their landmarks match as closely as possible. Differences in shape are given as residuals, shown graphically as displacement vectors. For the realisation of Thompson's work "thin–plate spline" analysis treats shape differences mathematically as deformations of a thin metal sheet. The functions used to fit compared landmark configurations are subsequently used as variables in multivariate analyses.

Geometric morphometric works on vectors include a phylogenetic study of mosquitoes at the generic level by Rohlf (2002) and an intraspecific study of sandflies by De la Riva *et al.*, (2001).

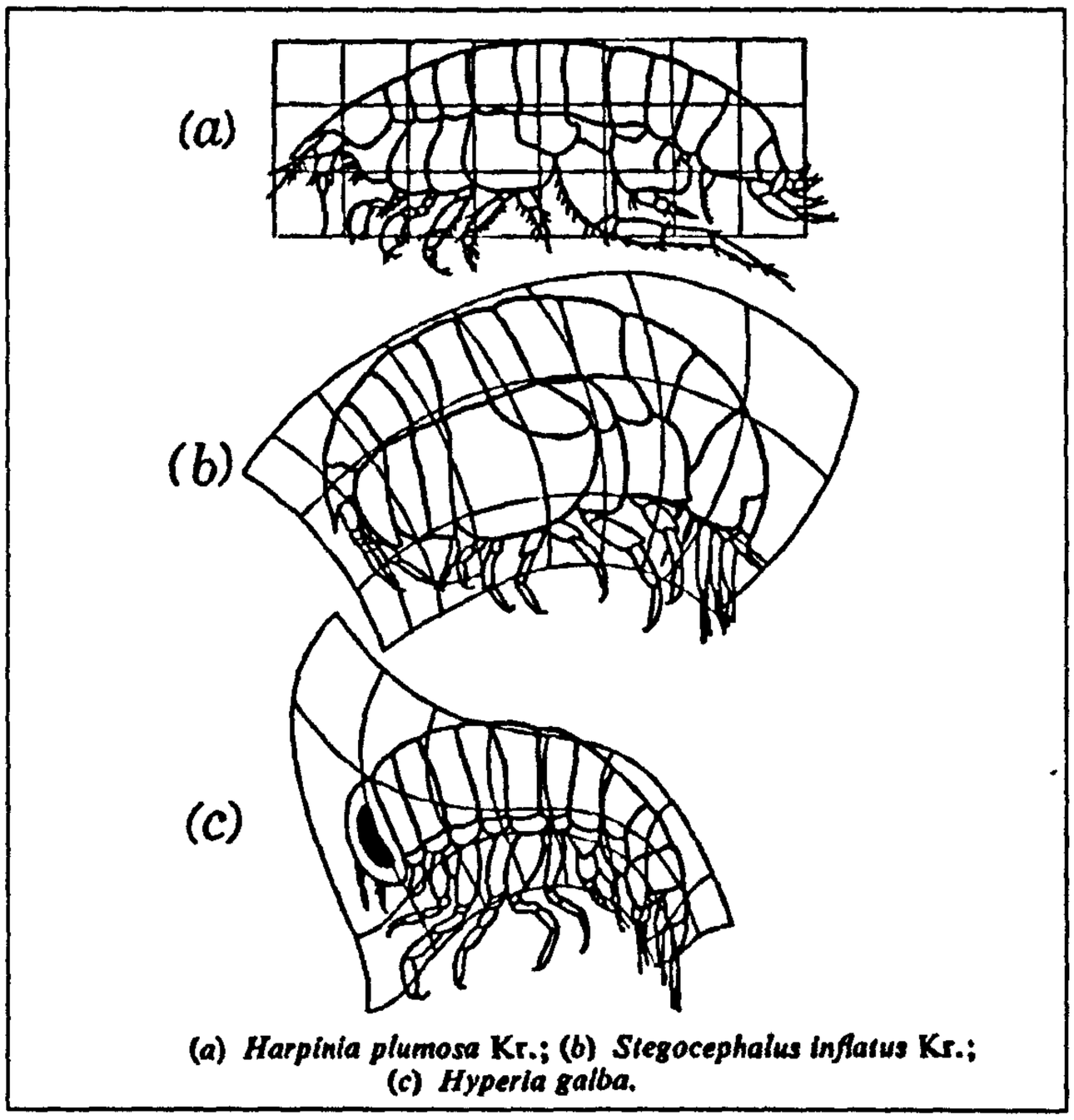

(a) *Harpinia plumosa* Kr.; (b) *Stegocephalus inflatus* Kr.; (c) *Hyperia galba.*

Figure. 4. Morphological differences between amphipod taxa explained by Transformational grids. (taken from; On Growth and Form, D'arcy Wentworth Thompson, 1917)

1.3.2.3.3 Morphometrics and triatomines

Over the last decade a trend has developed for the use of morphometrics in the investigation of the systematics and population biology of triatomine bugs, the principal proponents of which being Dujardin *et al.,* (1997a, 1997b, 1999c), Gorla *et al.*, (1993, 1997) and Harry (1994). Examples of these studies are summarised here on intraspecific variation between populations of *T. infestans* and *P. rufotuberculatus* in silvatic and domestic ecotopes (Dujardin *et al.,* 1998a, 1998b, & 1997b) and on interspecific variation between closely related species of *Rhodnius* (Harry, 1994). The main attraction of morphometrics is that it is far cheaper to implement than any of the molecular approaches outlined above.

A morphometric study by Harry (1994) addressed intraspecific variation of *R. prolixus* in Venezuela and examined its relatedness to *R. robustus* and other closely

related species, *R. nasutus* and *R. neglectus*. A further species, *R. pictipes* was included in the comparison as an out-group, known to be well differentiated from *R. prolixus* and related species. As mentioned, *R. prolixus* is the principal vector of *T. cruzi* in northern South America. *R. prolixus* was thought to be entirely domestic until 1961, when silvatic foci were discovered in the Llanos region of Venezuela (Gamboa, 1961, 1963). To confuse the issue *R. robustus* was then also discovered occurring sympatrically with *R. prolixus* in the Llanos and Andean regions. *R. robustus* is very similar in appearance, only distinguished from *R. prolixus* by ratio of head measurements and a few other minor morphological differences (Lent & Wygodzinsky, 1979). Harry (1994) attempted to elucidate the validity of the *R. robustus* species designation. However, morphometric analysis revealed that all the species were morphologically distinct, apart from *R. prolixus* and *R. robustus*. Therefore, at least for the single population of *R. robustus* sampled, its status as a species distinct from *R. prolixus* could not be upheld by morphometric analysis.

T. infestans, the principal vector of *T. cruzi* in the southernmost countries of South America is almost completely restricted to domestic and peridomestic ecotopes. Silvatic foci of *T. infestans* were, until recently (Noireau *et al.*, 2005a), thought only to exist in Cochabamba, Bolivia, occurring in rock piles in association with wild guinea pigs, *Galea musteloides*. This is believed to represent the original focus of the species (Schofield, 1994), probably becoming associated with man through the hunting and farming of guinea pigs. It is of interest to identify any measurable intraspecific differences between the two populations. Work had been done previously to establish the degree of isolation between populations in different ecotopes (Dujardin *et al.*, 1987). An isoenzyme electrophoresis study revealed no differences

between the silvatic and nearby domestic populations, found to be identical at 19 enzyme loci. Dujardin *et al.,* (1997a), used morphometric techniques to make the same comparison, including in the analysis specimens not differentiated by isoenzyme analysis ten years previously. They were able to demonstrate significant differences between domestic & silvatic populations. Another study (Dujardin *et al.*,1997b) aimed to establish whether or not post intervention (insecticide house spraying) recolonisation of domestic and peridomestic ecotopes was due to a recrudescence of survivors of the control effort or whether silvatic populations readily colonised the open niche. Specimens of domestic *T. infestans* were collected in a village close to Cochabamba in 1992 before insecticide spraying and 10 months later in 1993. Silvatic populations were collected from *G. musteloides* burrows in rock-piles in 1992 and again in 1995. The morphometric analysis supports the hypothesis that the re-infesting population post intervention was in fact a recrudescence of surviving members of the previous domestic population.

Utilising morphometrics, *P. rufotuberculatus* has also been investigated in relation to tendencies toward domesticity. (Dujardin *et al.*, 1998a) *P. rufotuberculatus* has been previously reported to be a widespread silvatic species with a distribution extending from Bolivia to Central America and Mexico (Lent & Wygodzinsky, 1979). The species is known to be attracted to light and is therefore an occasional visitor to houses (Schofield, 1994). However until recently there had been no reports of sustained domestic populations of *P. rufotuberculatus*. In the past few years there has been growing evidence for a trend of domiciliation of *P. rufotuberculatus* (Noireau *et al.*, 1994), with increasing reported occurrence in houses of the rural Nor Yungas province of La Paz. Since *T. infestans* is believed to have undergone adaptation to

domesticity two to three thousand years ago (C J Schofield & J P Dujardin pers.comm.), *P. rufotuberculatus* is interesting because it provides an opportunity to study the adaptive process of domestication in its earlier stages. Dujardin *et al.*, (1998a) collected bugs from houses in two neighbouring localities and compared them morphometrically with silvatic specimens. As with *Triatoma infestans* previously, the analysis differentiated between the populations. In this case a difference was also found between two geographically close domestic populations. However they were separated by a river, so the difference observed is possibly attributable to founder effects and genetic drift. Dimorphism was also observed between sexes in the domestic populations. This was interpreted by the authors to indicate recent adaptive tendencies toward domiciliation, as it can be related to accounts of laboratory colonies exhibiting a similar dimorphism between sexes (Jaramillo 2000).

In a review of morphometric techniques applied to the Triatominae (Dujardin *et al.*, 1999a) the polygenetic basis of morphology is highlighted and the utility for size-independent shape analysis to infer phylogenetics is discussed. Credence to this approach is presented in another study by Dujardin *et. al.* (1999b) in which isoenzyme evidence was correlated with morphometrics in a phylogenetic reconstruction of the Rhodniini. Another joint isoenzymic/morphometric study has also been applied to another group of haematophagous insects, the phlebotomine sandflies (Dujardin, 1997c).

Traditional morphometry, using distance measurements, does not allow recovery of variation that relates to the geometry of the original form (Rohlf and Marcus, 1993). In contrast, geometric morphometrics preserves the information on the shape of the organism and removes the effects of differences in growth (isometric size

differences), which generally have environmental causes. With growth effects removed significant differences between groups are attributable to shape alone, and shape variables mostly reflect adaptive (or genetic) effects rather than environmental.

All of the studies discussed above utilised traditional morphometric methodologies. Geometric morphometry has been applied to Triatominae for taxonomic purposes (Matias *et al.*, 2001, & Villegas *et al.*, 2002); to distinguish laboratory-reared and field specimens (Jaramillo *et al.*, 2002); and to assess variation among the chromatic morphs of *T. infestans* across an extensive geographical range (Gumiel *et al.*, 2003), and in the context of studying the eco-epidemiology of Chagas' disease in northern Argentina, Schachter-Broide *et al.*, (2004) used geometric morphometry in an attempted to study fine scale geographic spatial structuring of *T. infestans* populations.

Here I compare the morphometrics of three vector species implicated in disease transmission and apply some of the latest methods of comparative geometric morphometrics of different structures and to parallel analyses of mtDNA sequence data. The comparison of morphometric patterns to sequence data should help evaluate the facility of morphometric to serve as an effective tool for surveillance.

At the macroevolutionary level I will test the extent to which morphometry has congruence with molecular phylogenetics interspecifically and at higher taxonomic levels. Comparing variation of different morphological structures (head and wing) with phylogeny discontinuities or congruencies will reveal evolutionary histories and adaptive processes.

2 Aim and Objectives

2.1 Aim

The overall aim of this work is to determine whether the relatively low cost method of morphometrics demonstrates patterns consistent with population structure/phylogeny. Or are such patterns confounded intraspecifically by selection, morphological plasticity, and other environmental effects, and interspecifically by homoplasies due to convergent evolution.

2.2 Specific Objectives

- To compare novel geometric and traditional morphometric approaches with molecular genetics in the study of relationships between Old World and New World species of Triatominae; to test the phylogenetic facility of morphometrics against molecular, sequence based phylogenetics.
- To use molecular approaches to elucidate the broader phylogeny of Triatominae and their relationships with other reduviid subfamilies and to investigate the debated polyphyletic origin of the Triatominae.
- To use novel geometric morphometric approaches to study populations of *Rhodnius prolixus*, *Rhodnius ecuadoriensis* and *Triatoma infestans*, which are important as vectors in Venezuela, Ecuador and Paraguay respectively, in a comparison of domestic and silvatic populations, and in the context of strategies for the control of Chagas disease.

3 Materials & Methods

3.1 Morphometrics

3.1.1 Traditional morphometrics

3.1.1.1 Image collection and morphometry

Morphometry of the head capsule was used for this study because the head is the most rigid and easily preserved structure of the insect body. Furthermore, it is of proven taxonomic importance (Lent & Wygodzinsky 1979). A protocol of video photography and computerised image analysis was developed to collect morphometric data from the specimens observed. A Euromoex Eurocam microscope video camera was used, attached to the right eyepiece socket of a binocular dissecting microscope. Pinned museum specimens were mounted on a Bioquip entomology microscope stage to facilitate accurate orientation of the specimens. Illumination was provided by fibre optic light. The video camera was linked to a Zipshot image capture device configured to relay the captured still images to a computer via Arc Soft Photo Impression, version 2.5 software. Sigma Scan Pro, version 5.0.0 image analysis software was used to take measurements from stored images. Images were stored as high resolution JPG files. Three images were captured from each specimen: dorsal and lateral view of the head (x25 magnification) and dorsal view of wings (x8 magnification). Morphological measurements are described and displayed graphically by Fig. 5, which shows the measurement parameters overlaid on corresponding images.

Within Sigma Scan Pro the images were calibrated by a three-point calibration using an image of a 1cm grid graticule with 100μm graduations captured at the appropriate magnification. Measurements were made in Sigma Scan Pro by manual positioning of the

cursor at the relevant homologous points, defining the start and end of each anatomical measurement. All measurements were made by the same operator, and the values obtained were automatically recorded on spreadsheets.

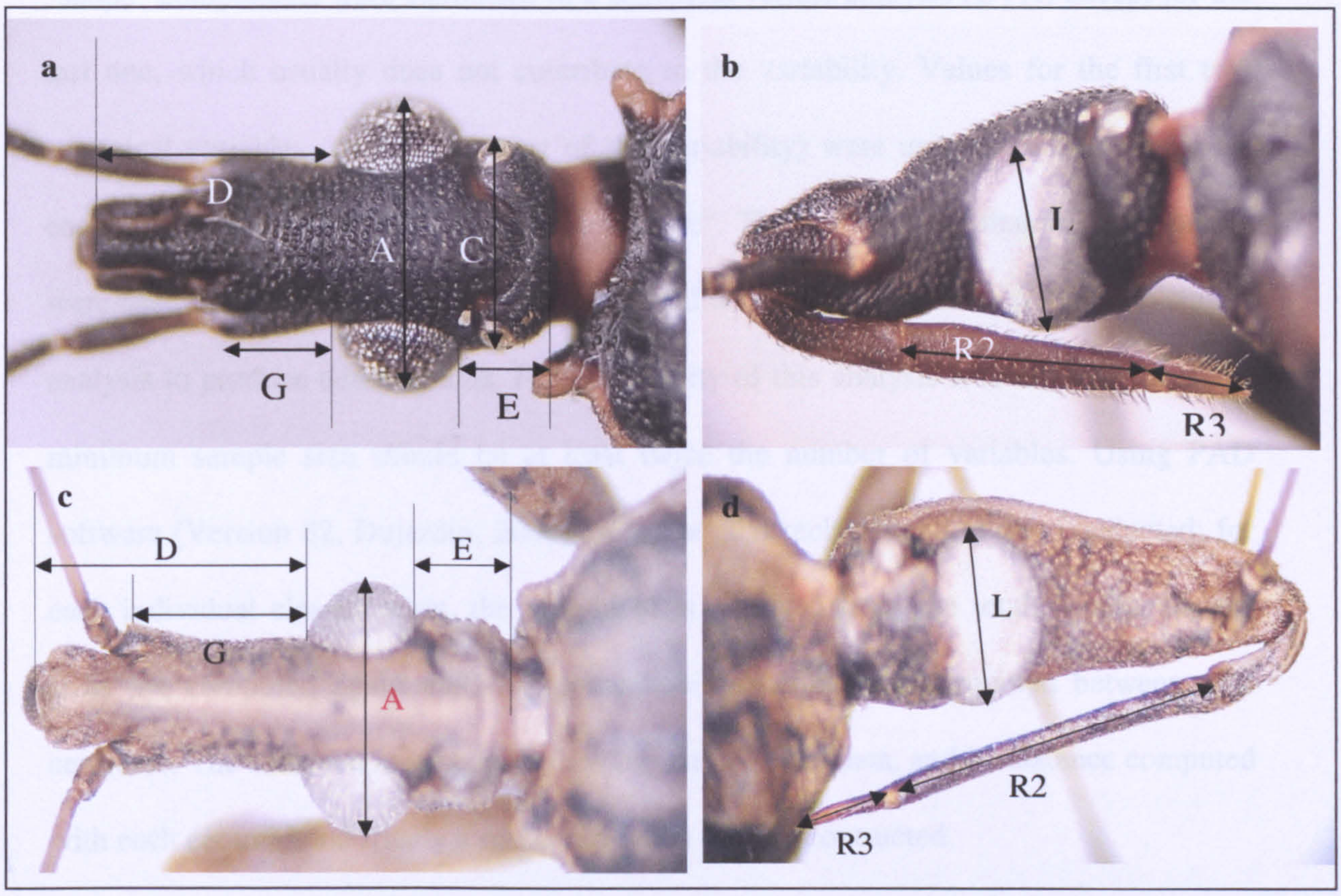

Figure 5. Views of the head indicating morphometric measurements taken. A = Outer distance between eyes, C = External distance between ocelli, D = Anteocular distance, E = Postocular distance; from the posterior edge of the eye to the beginning of the neck, G = Length of antenniferous tubercle; anterior edge of eye to furthest lateral extremity of antenniferous tubercle, L = Maximum diameter of the eye, R2 = Length of second rostral segment, and R3 = Length of third rostral segment. (a *Triatoma rubrofasciata* dorsal; b *T. rubrofasciata* lateral; c *Rhodnius ecuadoriensis* dorsal; d *R. ecuadoriensis* lateral).

3.1.1.2 Statistical analysis

Means and standard errors were calculated for the measurements of each species or population, and non parametric ANOVA (Kruskal-Wallis) tests were performed on log transformed data. Prior to multivariate analysis the data were adjusted to remove isometric size, in order to focus on evolutionary differences rather than those caused by

environmental factors (see: Claridge & Gillham 1992). This was achieved by log transforming the data and then subtracting the mean of each row (each row containing the measurements of one specimen). The resulting "log-shape ratios" (Durroch & Mosiman, 1985) were used as the input for a principal component analysis (PCA). The resulting "shape" components were submitted to a canonical variate analysis (CVA) except for the last one, which usually does not contribute to the variability. Values for the first two canonical variables (containing most of the variability) were used to plot positions for each specimen in the "shape discriminant space". The associated mahalanobis distances were used in an Unweighted Pair Group Method with Arithmetic mean (UPGMA) cluster analysis to produce dendrograms. For the validity of this analysis it is important that the minimum sample size should be at least twice the number of variables. Using PAD software (Version 82, Dujardin, 2006) cross checked reclassification was conducted; for each individual classification, the individual is removed from the total sample, sample sizes are computed again and the Mahalanobis distances are computed between new centroids. The removed individual is then used as external data, and its distance computed with each centroid and finally a re-classification table is contructed.

To elucidate relationships between similar groups it is necessary to account for allometric as well as isometric change. This was achieved by using a common (within-groups) principal component analysis (CPCA) (Klingenberg 1996): log transformed variables of similar groups were tested for their compatibility with a common allometric axis. The first CPC represents growth effects, so that discarding this allows the remaining CPC (allometry free variables) to be used as input for a further principal component analysis (multi group) and CVA (Dujardin & Le Pont 2000).

For both approaches, isometry-free and allometry-free, results were presented by plotting

the first two canonical variables (CV1 and CV2) with polygons enclosing each group. Multivariate significance of differences between groups was tested by the Wilk's lambda statistic (SAS Institute 2000). The statistics were performed using SPSS version 9.0., JMP 4.0.4, STATA 7.0 (SAS Institute 2000) and NTSSYS 2.10p (Rohlf, 2001).

3.1.2 Geometric morphometrics

3.1.2.1 Recording landmarks

Digital images of the head in dorsal view and/or lateral view and the wings, mounted between two microscope slides were captured using the protocol described in section 2.1.1. Subsequently each stored image was digitized for a series of 2 dimensional Cartesian coordinates (landmarks), which were automatically recorded using TPSDIG software (TPSdig version 1.2 Rolf 1997a). Figures 7 and 8 demonstrate the selection of landmarks used in the various experiments.

3.1.2.2 Superimposition

The raw x y landmark coordinates were subjected to procrustes superimposition (Bookstein 1991) and subsequently to a Thin Plate Spline analysis using TPSrelw version 1.2 (Rholf 1998a).

The procrustes superimposition is an iterative least square adjustment of all the figures after size normalization. This scaling is fundamental. A superimposition without size normalization will be biased. The procrustes superimpositon algorithms translate and rotate the landmark configurations to minimize the squared differences between landmarks. The procedure can be summarised by the following equation; $X_i = \rho_i(X_0 + D_i)H + 1\tau_i$. The terms relate to shape (X), scaling to centroid size (ρ), translation (τ), rotation (H), and D represents actual shape differences. After the

superimposition, a mean configuration (consensus) is computed. For each landmark, a procrustes residual is the difference between the position of specimen's landmark and position of the homologous landmark of the consensus. Technically after Generalised Procrustes Superimposition (GPS) each landmark configuration is represented by a point on a complexly curved multidimensional surface called Kendall's shape space. The dimensionality of this space is a function of the number of landmarks and can only be visualised satisfactorily as a sphere for triangles (3 landmarks) (Bookstein 1991). Because of the curved nature of shape space it has a non-Euclidean geometry. During thin plate spline (TPS) analysis points in shape space are projected on to a linear tangent plane with Euclidean geometry (Fig. 6). The underlying mathematics of TPS treats the landmark as

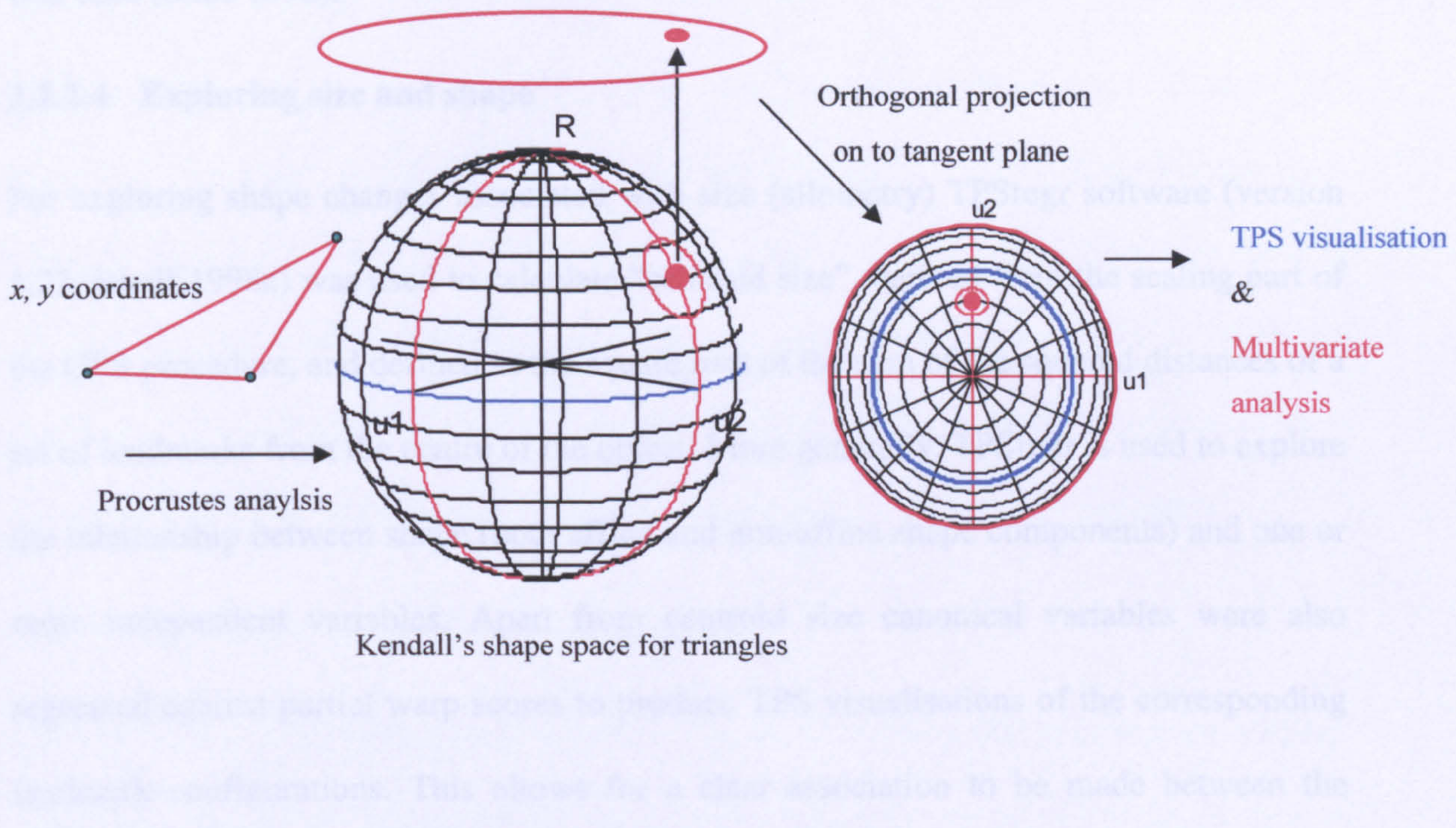

Figure 6. A diagrammatic representation of the mathematical procedures used to generate shape components from landmark data.

points on thin metal sheet, therefore differences between configurations are calculated as distortions in the TPS, termed "bending energy". The axes of the tangent space ("partial warps") are computed by eigenanalysis of the bending-energy matrix. TPS transformations/distortions are of two components, affine (global stretching, lines of grid remain parallel) and non-affine (non linear localised distortions "shape changes").

3.1.2.3 Multivariate analysis of geometric shape components

A principal component analysis of the partial warps including the affine and non-affine components delivers tangible shape components ("relative warps"), subsequently subjected to a discriminant analysis and cluster analysis as described previously.

For the pairwise comparison of mean landmark configurations Morpheus *et. al.* software was used (Slice 1998).

3.1.2.4 Exploring size and shape

For exploring shape changes associated with size (allometry) TPSregr software (version 1.22, Rholf 1998c) was used to calculate "centroid size", derived from the scaling part of the GPS procedure, and defined as the square root of the sum of the squared distances of a set of landmarks from the centre of the object. More generally, TPSregr is used to explore the relationship between shape (both affine and non-affine shape components) and one or more independent variables. Apart from centroid size canonical variables were also regressed against partial warp scores to produce TPS visualisations of the corresponding landmark configurations. This allows for a clear association to be made between the actual shape differences associated to the axis of discrimination. The tpsRegr program includes an overall multivariate test of how well variation in shape can be predicted using one or more independent variables. It uses multivariate multiple regression analysis,

which allows it to be used to fit a wide variety of multivariate general linear models. In addition to the usual Wilk's lambda test of significance, a generalization of Goodall's F-test and permutation tests are also performed.

3.1.2.5 Partial least squares analysis

To study the covariation between different sets of landmarks (i.e. head, dorsal and lateral views and wings) from the same individuals Two-block partial least-squares (2B-PLS) analysis was used. This relatively new statistical method (Sampson *et al.,* 1989) has only been demonstrated in the context of morphometrics in the past few years (Bookstein 1996, Rohlf & Corti 2000). This method differs from regression analysis in that the two sets of variables are treated symmetrically, rather than having independent variables and predicting variation in a set of dependent variables. To conduct 2B-PLS analysis in these studies TPSpls software (version 1.07 Rohlf 1997b) was used. 2B-PLS analysis constructs linear combinations of the partial warps, these new variables or "dimensions" account for as much as possible of the covariation between the two sets of shape data. Several dimensions are produced as with PCA and CVA, the first dimension usually accounts for the most covariance. Each dimension produced is tested for a significant correlation between the two shapes, a random permutation test with 999 replicates is used to test the probability of observed associations between the two sets of landmarks.

3.1.2.6 Identifying informative landmarks

In order to determine the relative importance of the landmarks and to determine whether there is redundancy in the landmarks necessary to define the shape of the dorsal view of the head or wings, landmarks and images were explored in conjunction using representative specimens of the groups (populations) compared. To accomplish this TPSsuper software (version 1.07 Rohlf 1998b) was used. The TPSsuper procedure

involves firstly conducting a GPA then "Unwarping" the images of each specimen so that the landmarks coincide with their positions in a consensus configuration. The TPS for the transformation from the configuration to each of the specimens is used for these computations. The final step is a process of averaging the unwarped images pixel by pixel. In the resulting average images those areas that appear fuzzy and "out of focus" correspond to those parts of the images that vary from specimen to specimen, in a way that is not well correlated with the variation in the positions of the landmarks. A stepwise reduction in the number of landmarks and repetition of the analysis highlights the minimum number of landmarks that are required to satisfactorily explain shape variation in a given set of species or populations.

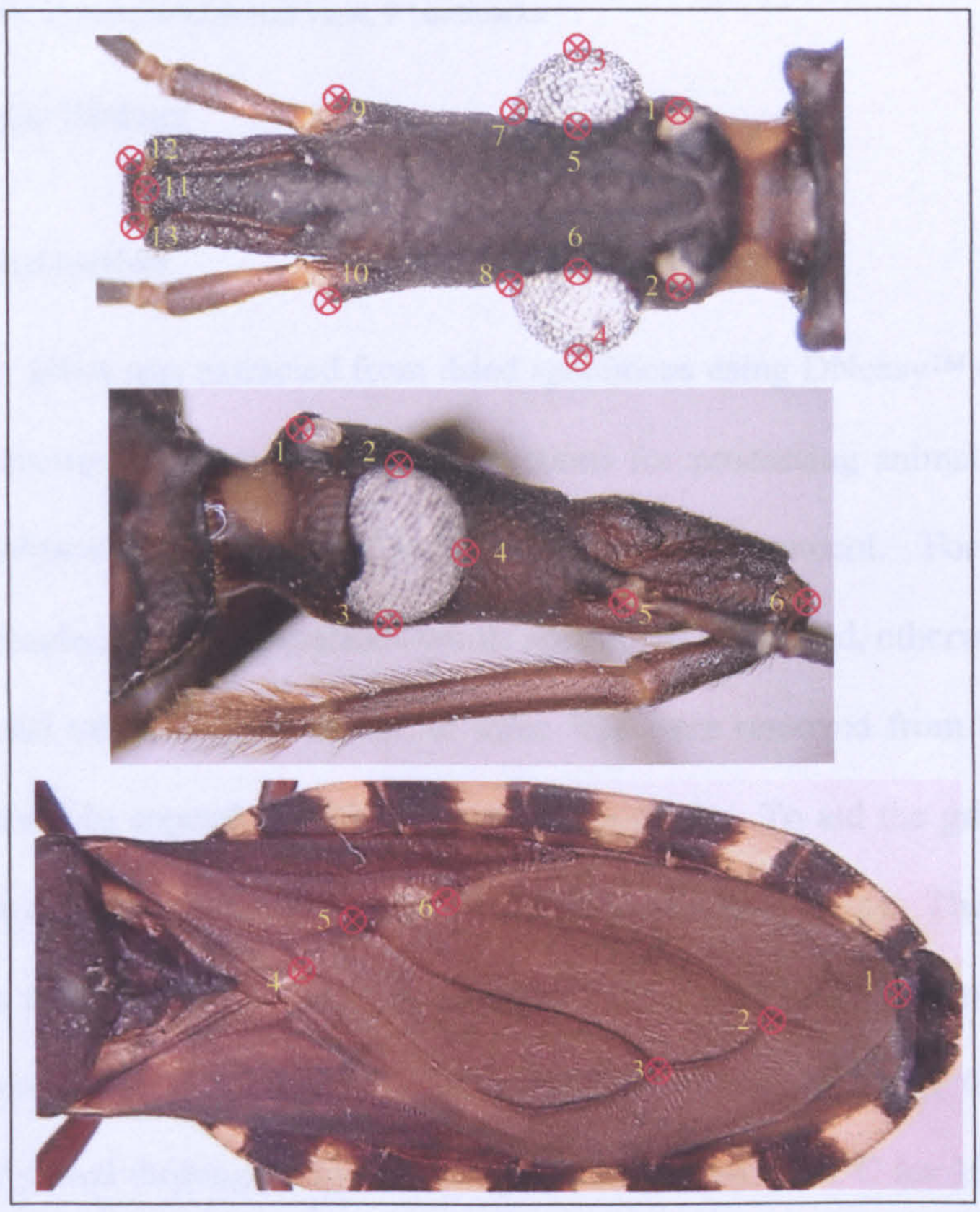

Figure. 7 Landmarks used for head and wing geometric morphometrics. This example features *T. infestans*. Upper; head dorsal view, 13 landmarks. Middle; head lateral view, 6 landmarks. Lower; wing, 6 landmarks

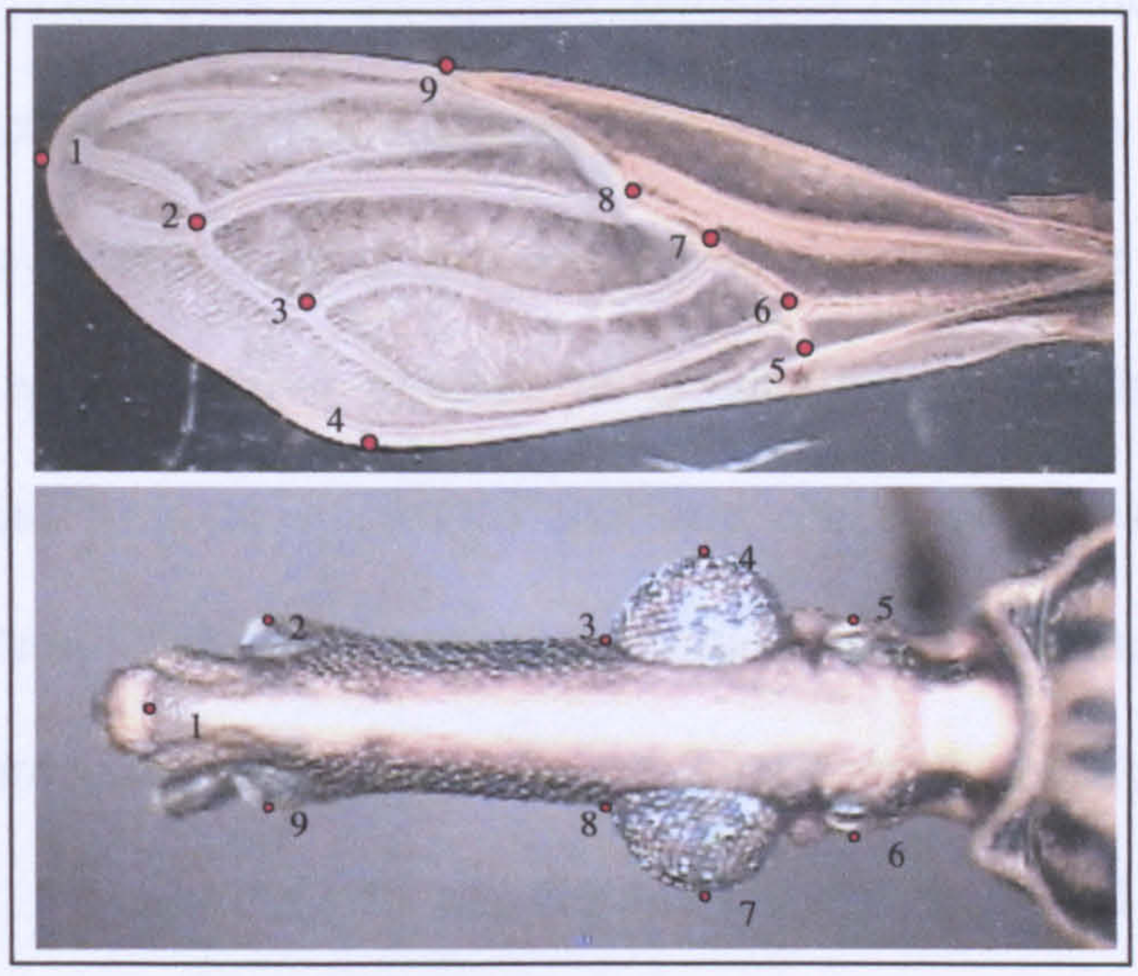

Figure. 8 Landmarks of head and wing used in the study of *R. prolixus* populations from Venezuela. Upper; wing, 9 landmarks. Lower; head dorsal view, 9 landmarks

3.2 Molecular Biology

3.2.1 DNA extraction

Total genomic DNA was extracted from dried specimens using DNeasy™ extraction kits (Qiagen), following the manufacturer's instructions for processing animal tissues. The following modifications were made to the recommended protocol. For extraction of DNA from nymphs, on some occasions whole specimens were used, otherwise from adult Triatominae and other Reduviidae one to three legs were removed from the specimens and homogenised in eppendorf tubes using a micro-pestle. To aid the grinding process the tubes were partially submerged in liquid nitrogen prior to crushing. The homogenised samples were mixed with 180 µl of lysis buffer (ATL) and 20 µl of proteinase k. and incubated overnight at 55°C. A further 200 µl of lysis buffer (AL) were then added and samples were mixed thoroughly by vortexing and incubated at 70°C for 10 minutes. 200 µl of ethanol were then added to each sample, mixed, and the liquid part of each

transferred to a DNeasy mini-column placed in a clean two millilitre collection tube. The columns were centrifuged at 8000 rpm for one minute discarding the flow through. 500 µl of washing buffer (AW1) was passed through the column by centrifugation at 8000 rpm for one minute and discarding the flow-through. The washing step was repeated using another washing buffer (AW2). After the second washing step the samples were centrifuged at 13,000 rpm for three minutes to ensure that the columns were dry. Columns were then transferred to sterile 1.5 millilitre centrifuge tubes and 200µl of elution buffer (AE) were applied directly to the membrane of the column. The columns were left to stand at room temperature for one to two hours and then centrifuged at 8000 rpm to elute the DNA. The elution step was repeated to give a second elution. DNA extracts were stored short-term at 4°C and at -20°C after completion of experimental work.

3.2.2 PCR amplification

3.2.2.1 Mitochondrial genes

Polymerase chain reaction (PCR) was used to amplify fragments of mitochondrial genes Cytochrome b (*cytb*) and Cytochrome Oxidase II (*coII).* A ~700bp fragment of *cytb* was amplified using primers *cytb* 7432F and *Cytb* 7433R (see Table. 2), these primers were demonstrated as effective for various triatomine species (Monteiro *et al.*, 2000). The primers were designed by comparisons of the conserved regions of the c*ytb* gene of *T. dimidiata* (Dotson & Beard, 2001) and other published insect c*ytb* sequences (Monteiro *et al.*, 2003). A further set of primers (c*ytb* 32F and c*ytb* 82R- degen) were used to amplify a smaller fragment of *cytb* (~600 bp). These primers were based on sequences provided by F. Monteiro with modification to introduce some degeneracy and facilitate amplification from diverse taxa. *coII* fragments were amplified using two pairs of primers (see Table 2)

corresponding to the first and second half of the gene with contiguity and together covering the whole gene (two fragments each ~350bp long). *coII*_2nd primers were modified from Simon *et al.* (1994) (C2-J-3400 & C2-N-3661) and *coII*_1st primers were designed using alignments of t-RNA-leu (region proceeding *coII* within the mitochondrial genome) and *coII* genes of *T. dimidiata* (Accession no. AF301594), an aphid; *Smynthurodes betae* (Aphidoidea: Homoptera) (Accession no. AF454630) and another Heteropteran; *Enchenopa binotata* (Membracidae) (Accession no. EBU77878).

Table 2. Primers used to amplify fragments of mitochondrial genes and the D2 region of 28S r-DNA

***COII*_1st_F**	**ATG ATT TTA AGC TTC ATT TAT AAA GAT**
***COII*_1st_R**	**GTC TGA ATA TCA TAT CTT CAA TAT CA**
*COII*_2nd_F	ATT GGC CAT CAA TGA TAT TGA
*COII*_2nd_R	CCA CAA ATT TCT GAG CAT TGT CCA
***Cytb*-32F**	**GGA CGW GGW ATT TAT TAT GGA TC**
***Cytb*-82R-DEGEN**	**ATT ACT CCT CCT AGY TTA TTA GGA ATT**
Cytb 7432F	GGA CGW GGW ATT TAT TAT GGA TC
Cytb 7433R	GCW CCA ATT CAR GTT ART AA
28S-D2-REV	**TTG GTC CGT GTT TCA AGA CGG G**
28S D2-FOR	**GCG AGT CGT GTT GCT TGA TAG TGC AG**

Standard degenerate code (N=ACGT, S=CG, W=AT, M=AC, K=GT, R=AG, Y=CT, V=ACG, H=ACT, D=AGT, B=GCT, replacing T with U for RNA), (ie W means a 50/50 ratio of A and T). Primers are listed in pairs (alternating bold and normal font)

PCR amplification was performed in a 50µl reaction mix containing 3.0µl of extracted DNA, 125pmol of each primer, 1 unit of Taq DNA polymerase (Bioline) 2mM of each dNTP, 1.5mM $MgCl_2$, 10mM TRIS-HCL pH 9.0, 50 mM KCL, 0.01% gelatin, 0.1% Triton X-100. Reaction conditions were as follows: an initial denaturation step at 95°C for

5 min followed by 35 cycles of denaturation at 95°C for 30 s, annealing at 50°C for 45 s, and extension at 72°C for 45 s, this was followed by a final extension step at 72°C for 5 min. Cycle amplification was performed on either a Primus 96 plus (MWG AG Biotech) or a PTC-100R (MJ research) thermal cycle sequencer.

Amplification was confirmed by running 3µl of PCR product alongside 5µl of HyperLadder IV (Bioline) on a 1% agarose gel (90V/30 mins) stained with ethidium bromide and visualized under ultraviolet light. Amplified products were subsequently purified using either a spin column format with QIAquick™ kit (Qiagen) or directly using DNAce Quick-clean™ (Bioline), using methods specified by the manufacturers. Purified products were rechecked by further agarose gel electrophoresis.

If weak bands were detected reaction conditions were modified as follows: in the reaction mix DNA volume was increased (up to 5-8µl) and 1 unit of Taq Extender™ (Stratagene) was used with Taq Extender buffer. Taq Extender™ is a PCR Taq additive that improves reliability and yield of standard Taq based amplifications. The PCR cycling conditions were also changed; the annealing temperature was lowered from 50°C to 45°C.

3.2.2.2 28S ribosomal DNA

D2 variable region of 28S r-DNA was amplified using primers previously used by Monteiro *et al.*, (2003). Standard PCR techniques were used to amplify ~650 bp fragment of the gene. The following cycling conditions were employed; 25 cycles of denaturation at 94°C for 1min, annealing at 50°C for 2 mins, and extension at 72°C for 2 mins. Cycle amplification was performed on either a Primus 96 plus (MWG AG Biotech) or a PTC-100R (MJ research) thermal cycle sequencer.

3.2.3 DNA sequencing

Purified PCR products were sequenced by fluorescent dye terminator chemistry using ABI Prism® BigdyeTM ready reaction kits V2.0 and V3.1 (Applied Biosystematics). Sequencing amplifications were performed in 10µl reactions. The reaction mix was as follows: 5-20ng of purified PCR product, 10pm forward or reverse primer, 1µl ready reaction premix, 1.5µl BigDye sequencing buffer. Purified PCR product concentration was approximated on band intensity from gel electrophoresis in comparison with the size standard Hyperladder IV. Sequencing reaction conditions were as follows: rapid thermal ramp to 96°C (ramp at 1°C/sec), 96°C for 30 s, rapid thermal ramp to 50°C (ramp at 1°C/sec), 50°C for 20s, rapid thermal ramp to 60°C (ramp at 1°C/sec), 60°C for 4 mins. The cycle was repeated 25 times.

Sequencing samples were purified to remove unincorporated dyes by isopropanol/ethanol precipitation in 1.5µl microcentrifuge tubes, following the ABI Prism® protocol for BigDyeTM V2.1. After clean up tubes were carefully labelled and kept at -20°C. Prior to electrophoresis 10µl HiDi formamide (ABI) was added to each sample and samples were then denatured at 95°C for 2-4mins.

3.2.4 Data analysis

Forward and reverse sequences were edited and aligned using the ClustalW algorithm (Thompson *et al.* 1994) in BioEdit software (version 7, Hall 1999) and ambiguities resolved, producing a reliable consensus sequence for each specimen analysed. Aligned consensus sequences were analysed as follows.

Phylogenetic and molecular evolutionary analyses were conducted using MEGA version 3.0 (Kumar, Tamura, Nei 2004). Statistical analysis of the data included the investigation of nucleotide and amino acid composition and substitution (transition/transversions and

synonymous/nonsynonymous substitutions). Nucleotide diversity was also estimated between collections sites and among all sequences analysed. The number of variable sites and their codon position together with the number of parsimonious informative sites and codon usage were also determined.

Phylogenetic analysis of aligned sequences was performed using both distance and character based methods. Neighbour-joining trees were constructed using various models of base substitution to produce matrices of pairwise genetic differences. Maximum parsimony analysis was also conducted to construct phlylogenetic trees using the branch and bound method of tree searching.

Maximum likelihood trees were generated using PAUP V 4.0 (Swofford, 2002). Parameters were estimated via maximum likelihood using a reiterative heuristic search strategy using TBR (tree-bisection-reconnection) and the Hasegawa-Kishino-Yano (HKY) model of base substitution.

For mitochondrial DNA targets haplotype networks were constructed using the programme TCS V1.20 (Clements *et al.* 2000). Networks were constructed according to the parsimony algorithm of Templeton *et al.* (1992). The programme calculates outgroup probabilities based on the frequencies of haplotypes by estimating haplotype age. Pairwise distances are used to calculate the maximum number of mutational connections between haplotypes and networks are created using the parsimony criterion.

3.2.5 Mantel tests.

To test for patterns of congruence between morphometric, genetic and geographical distance matrices Mantel tests (Mantel, 1967) were used to test for significant correlations

between pairs of distance matrices. Pairwise Mantel tests were conducted using GenAlEx (Peakall *et al.*, 2006). To assess significance, permutation tests were used, whereby the rows and columns of one of the matrices were subjected to 9999 random permutations, with the correlation being recalculated after each permutation. The significance of the observed correlation is the proportion of such permutations that lead to a higher correlation coefficient.

4 Morphometrics and phylogeny of the Old World and New World Triatominae: patterns of parallel and divergent morphological evolution

4.1 Part I: Population analysis of the tropicopolitan bug *Triatoma rubrofasciata* and relationships with endemic Old World and New World species of *Triatoma*

4.1.1 Introduction

Most of the ~130 species of triatomine bug occur only in the Americas, *T. rubrofasciata* however, is recorded from port areas throughout the tropics and subtropics, and a group of seven closely related species of *Triatoma* are known only from eastern Asia (Ryckman & Archbold, 1981).

The origin of *T. rubrofasciata* has long been a mystery. It is the type species of the genus (Lent & Wygodzinsky, 1979) and was the first species of *Triatoma* to be described, from a specimen collected in the then Dutch East Indies (now Indonesia) (De Geer, 1773). It has since been recorded from domestic habitats in port areas throughout the tropics and subtropics, and from more inland regions in some parts of northeast India (Assam), Vietnam (Kalshoven, 1970) and northeast Brazil (Ryckman & Archbold, 1981). It is frequently found in coastal cities of Brazil, especially the city of São Luis, Maranhão, where it causes public concern (Macario Rebelo *et al.*, 1999). Natural infection of *T. rubrofasciata* with *T. cruzi* has been reported in Brazil (Schofield, 1994) although the biting and defaecation habits of this bug make it a relatively inefficient vector (Braga & Lima, 1999). Also, in Brazil and parts of Southern Asia, *T. rubrofasciata* is commonly infected with the rat trypanosome, *Trypanosoma conorhini*, and is considered the main vector of this parasite which, like *T. cruzi*, is transmitted by host contamination with infected bug faeces (Hoare, 1972). *T. rubrofasciata* seems to have a close association with rats (*Rattus rattus*) and is assumed to have been transported on ships along early international trade routes during the 16^{th}-19^{th} centuries (Schofield, 1988, Gorla *et al.* 1997, Schofield *et al.*, 1999). Certainly the collective

distribution records of *T. rubrofasciata* (Ryckman & Archbold 1981) appear to correlate well with the major ports, European territories and trade routes of early post-Colombian history, but silvatic foci that might represent the original populations have not been reported.

T. rubrofasciata is known to be a morphologically variable species, ranging from orange marked specimens from South India (Gillett, 1934) to almost melanic forms in Hawaii (Lent & Wygodzinsky, 1979). However, several populations show superficial similarities to some North American species such as *T. sanguisuga* and *T. rubida*, which are also strongly associated with rodents (*Neotoma spp.*) (Usinger 1944). Presented here is a morphometric comparison of *T. rubrofasciata* with other species of *Triatoma*, including its seven Old World relatives (*T. amicitiae, T. bouvieri, T. cavernicola, T. leopoldi, T. migrans, T. pugasi, T. sinica*) designed to establish possible phylogenetic similarities that may indicate the most likely origin of *T. rubrofasciata*. These were subsequently tested by applying molecular phylogenetic analyses in parallel.

4.1.1.1 Traditional morphometrics

4.1.1.1.1 Material used in morphometrics

Most Old World species of *Triatoma* are rare, with some known only from the holotype specimens. Similarly, *T. rubrofasciata* is now difficult to collect from many of the Old World localities from where it has previously been recorded. Accordingly, this study made use of the museum collections held by the following six institutions: the Natural History Museum, London (NHM), The American Museum of Natural History, New York (AMNH), the National Museum of Natural History, Smithsonian Institute, Washington DC (SMITHS), the Instituto Oswaldo Cruz, Rio de Janeiro (FIOCRUZ), the Bishop Museum, Honolulu

(BISHOP), and the London School of Hygiene & Tropical Medicine (LSHTM). The pooled resources of these collections provided specimens of the following species.

4.1.1.1.1.1 Old World *Triatoma*

T. amicitiae (Lent, 1951). Known only from the female holotype (NHM collection) which was used in this study. Collected in southern Sri Lanka (Monteith, 1974).

T. bouvieri (Larrousse, 1924). Four specimens, two from the AMNH collection, collected in the Philippines, and two from the FIOCRUZ collection (collection locality unknown), previously held in the Copenhagen Museum. *T. bouvieri* has also been reported from Vietnam and the Nicobar Islands (Bay of Bengal) (Lent & Wygodzinsky, 1979).

T. cavernicola (Else & Cheong, 1977; in Else et al., 1977). Reported only from bat caves in Northern Malaysia; nine specimens were used: AMNH (2), BISHOP (1 paratype), FIOCRUZ (2 paratypes), NHM (4 paratypes). All these specimens appear to have been reared from a laboratory colony in Kuala Lumpur 1974-1975.

T. leopoldi (Schouteden, 1933) (= ***novaeguineae*** Miller, 1958). Six specimens were used: AMNH (1), FIOCRUZ (2), SMITHS (1) and BISHOP (2) collections. All had been collected in New Guinea. This species has also been reported from Australia (north Queensland) and some Indonesian islands (Monteith, 1974).

T. migrans (Breddin, 1903). (= ***pallidula*** Miller, 1941). This species has a broad distribution, recorded from localities in India, Indonesia, Malaysia, Philippines, Thailand and Australia (Ryckman & Archbold, 1981). A total of 27 specimens were used: AMNH (2), FIOCRUZ (4), BISHOP (4), NHM (17, including the holotype of *T. pallidula*).

T. pugasi (Lent, 1953). This little known species has only been recorded from Java, Indonesia (Lent & Wygodzinsky 1979). Three specimens were used, the holotype (NHM), and two paratypes (FIOCRUZ).

T. sinica (Hsaio, 1965). This species has only been recorded from China (Nanjing) (Lent & Wygodzinsky 1979). One female paratype (AMNH) specimen was used.

Triatoma rubrofasciata (De Geer, 1773). From the six collections, a total of 90 *T. rubrofasciata* was used. For the analysis, these were grouped by geographical region (Table 3).

Table 3. Specimens of *T. rubrofasciata* from each collection, showing sample sizes and geographical origin.

Geographical grouping		NHM	AMNH	SMITHS	FIOCRUZ	BISHOP	Total
Brazil: São Luis, Belém, Bahia, Rio de Janeiro, Salvador, Pernambuco	BR	-	3	-	12	-	15
Caribbean: Jamaica, Virgin Islands, Cuba, Haiti	CA	3	-	12	-	-	15
Hawaii	HA	-	2	2	-	11	15
Indo china: Burma, Thailand, Vietnam, Malaya	IC	7	-	5	-	3	15
South India: Pondicherry, Mangalore, Mysore, Coimbatore, Bombay,	SI	-	5	4	4	2	15
South Pacific: Philippines, Borneo, Java, Sumatra,	SP	-	5	6	4	-	15
Total per collection		10	15	29	20	16	90

Source of specimens: The Natural History Museum, London (NHM), The American Museum of Natural History, New York (AMNH), the National Museum of Natural History, Smithsonian Institute, Washington DC (SMITHS), the Instituto Oswaldo Cruz, Rio de Janeiro (FIOCRUZ), the Bishop Museum, Honolulu (BISHOP),

4.1.1.1.1.2 New World Triatoma

New World species of *Triatoma* were selected to represent the main species groups and complexes as suggested by Lent & Wygodzinsky (1979) and Schofield (1988) as follows (Table 4): (for details on the distribution of New World bugs see Patterson *et al.* (2001))

Table 4. Specimens of New World species from each collection, showing sample sizes for each species.

Species complex	Species	NHM	AMNH	LSHTM	FIOCRUZ	Total (n)
infestans	*T. rubrovaria*	-	7	-	15	22
	T. infestans	-	18	-	-	18
phyllosoma	*T. pallidipennis*	7	-	9	-	16
flavida	*T. flavida*	-	-	14	-	14
lecticularia	*T. sanguisuga*	-	15	-	21	36
-	*T. gerstaeckeri*	-	10	-	5	15
	T. rubida	-	21	-	13	34
protracta	*T. protracta*	5	-	14	-	19
	Total per collection	12	71	37	54	174

For photographs of representative specimens of species used in this chapter see Fig. 93 in the appendix
Source of specimens:The Natural History Museum, London (NHM), The American Museum of Natural History, New York (AMNH), the Instituto Oswaldo Cruz, Rio de Janeiro (FIOCRUZ), and the London School of Hygiene & Tropical Medicine (LSHTM).

4.1.2 Results

4.1.2.1 Morphometrics

4.1.2.1.1 Traditional Morphometrics of head shape

4.1.2.1.1.1 Univariate analysis

Comparing all species, Kruskal Wallis tests (Materials and methods) were significant for all variables (P=<0.0001). An intraspecific test on the allopatric populations of *T. rubrofasciata* also revealed significant differences (P=<0.001) for all variables apart from R2 with a lower level of significance (P<0.01) and R3 for which there was no significant difference between groups (P=0.38). Means and standard deviations are summarised in Patterson *et al.* (2001).

4.1.2.1.1.2 Isometry-free analysis

For the isometry-free analysis of all groups the CVA was significant (Table 5), reflected by a high level of correct reclassification. The dendrogram constructed by UPGMA cluster analysis using Mahalanobis distances (excluding pooled Old World group, Fig. 9) represents the taxonomic relationship between species further exemplified by the relative positions of groups in the discriminant space defined by CV1 and CV2 (Fig. 10), cumulatively representing 77.1% of the variance.

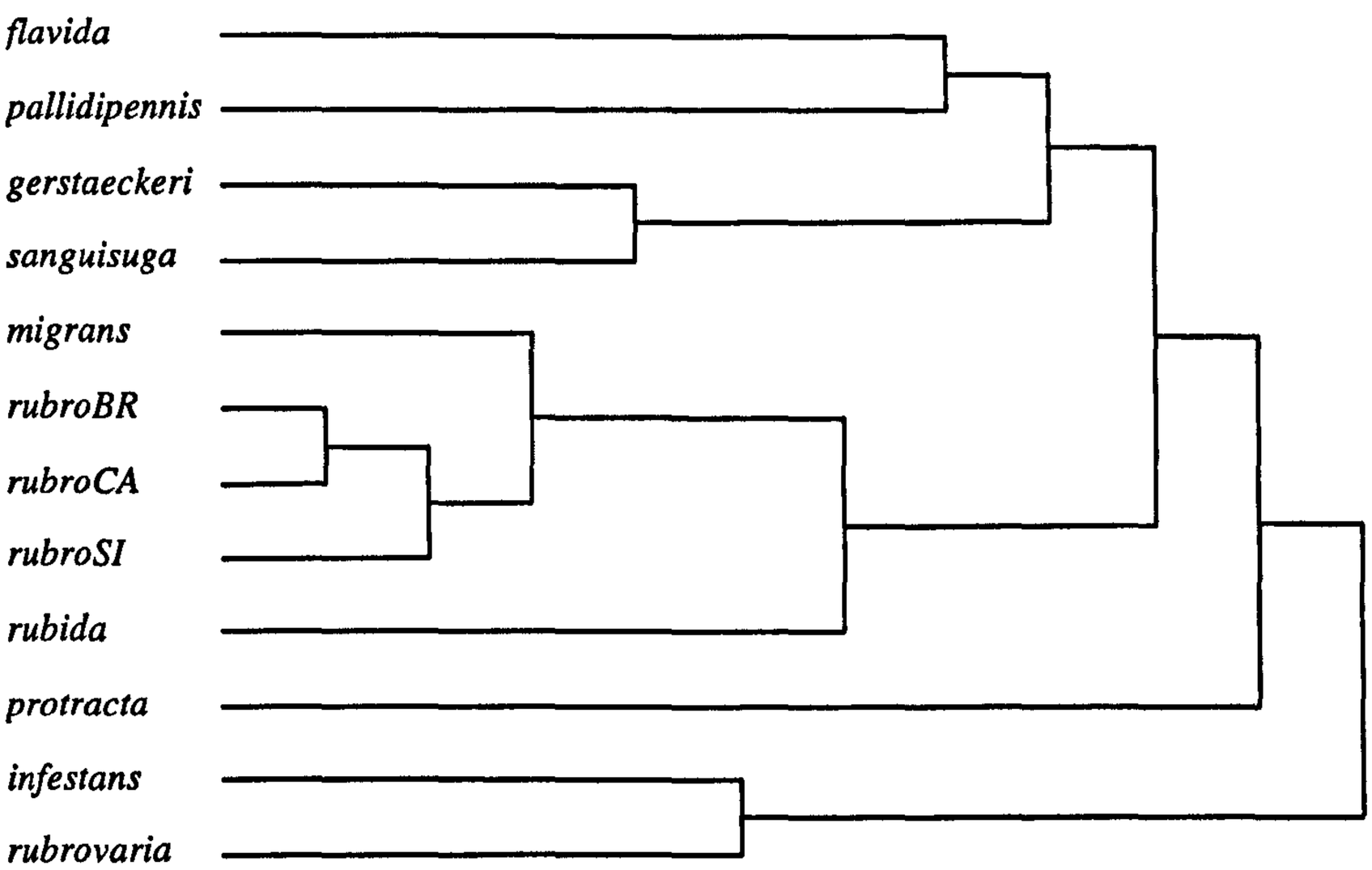

Figure 9. Traditional head morphometrics of Old and New World *Triatoma* species: UPGMA dendrogram derived from Mahalanobis distances after isometry-free analysis. rubroBR, rubroCA, rubroSI represent populations of *T. rubrofasciata* (see Tble. 3).

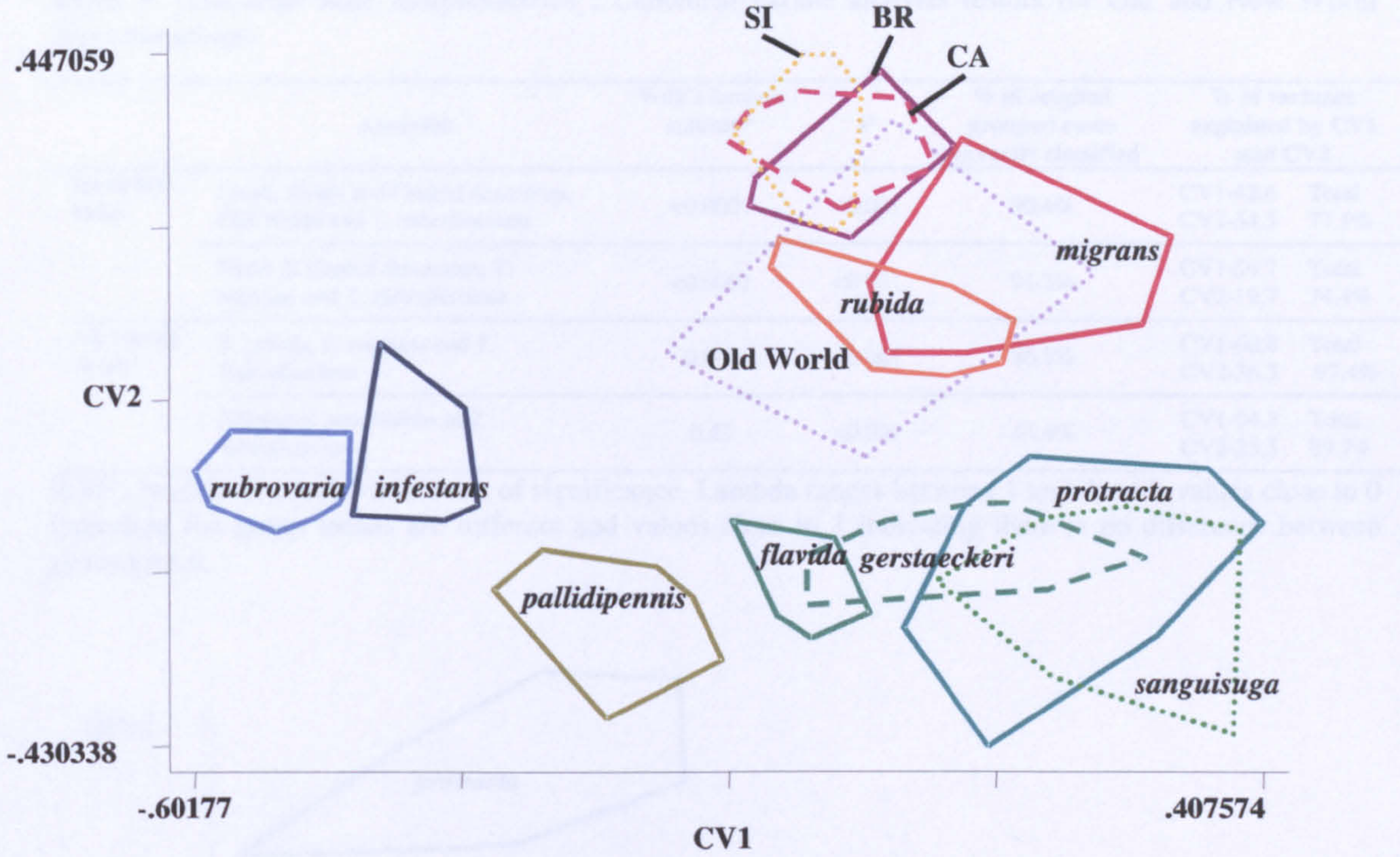

Figure 10. Traditional head morphometrics: Canonical variate analysis of Old and New World *Triatoma* species: isometry–free analysis. Old World represents a pooled group of *T. amicitae, T. bouvieri, T. cavernicola, T. leopoldi, T. pugasi* and *T. sinica.* SI, BR and CA represent populations of *T. rubrofasciata* (see Table 5.). Polygons enclose specimens of each group.

A further isometry-free analysis excluded South American and the pooled group of Old World species. This analysis was also highly significant (Table 5) with 91.3% correct reclassification. Removing the apparent outgroups (*T. infestans* and *T. rubrovaria)* clarified the relationships between North and Central American species, *T. rubrofasciata* and the Old World *T. migrans* (Fig. 11). CV1, explaining 54.7 % of the variance, and clearly groups *T. rubida* with *T. migrans* and *T. rubrofasciata.*

Table 5 Traditional head morphometrics : Canonical variate analysis results for Old and New World *Triatoma* groups.

	Analyses	Wilk's lambda statistic*	P	% of original grouped cases correctly classified	% of variance explained by CV1 and CV2
Isometry-Free	South, North and Central American, Old World and *T. rubrofasciata*	<0.0001	<0.001	90.4%	CV1-42.6 Total CV2-34.5 77.1%
	North & Central American, *T. migrans* and *T. rubrofasciata*	<0.0001	<0.001	91.3%	CV1-54.7 Total CV2-19.7 74.4%
Allometry -Free	*T. rubida, T. migrans* and *T. Rubrofasciata*	0.049	<0.001	86.7%	CV1-60.8 Total CV2-36.5 97.4%
	Allopatric populations of *T. rubrofasciata*	0.47	<0.001	44.4%	CV1-64.2 Total CV2-25.5 89.7%

Wilk's lambda is a multivariate test of significance. Lambda ranges between 1 and 0, with values close to 0 indicating the group means are different and values close to 1 indicating there is no difference between group means.

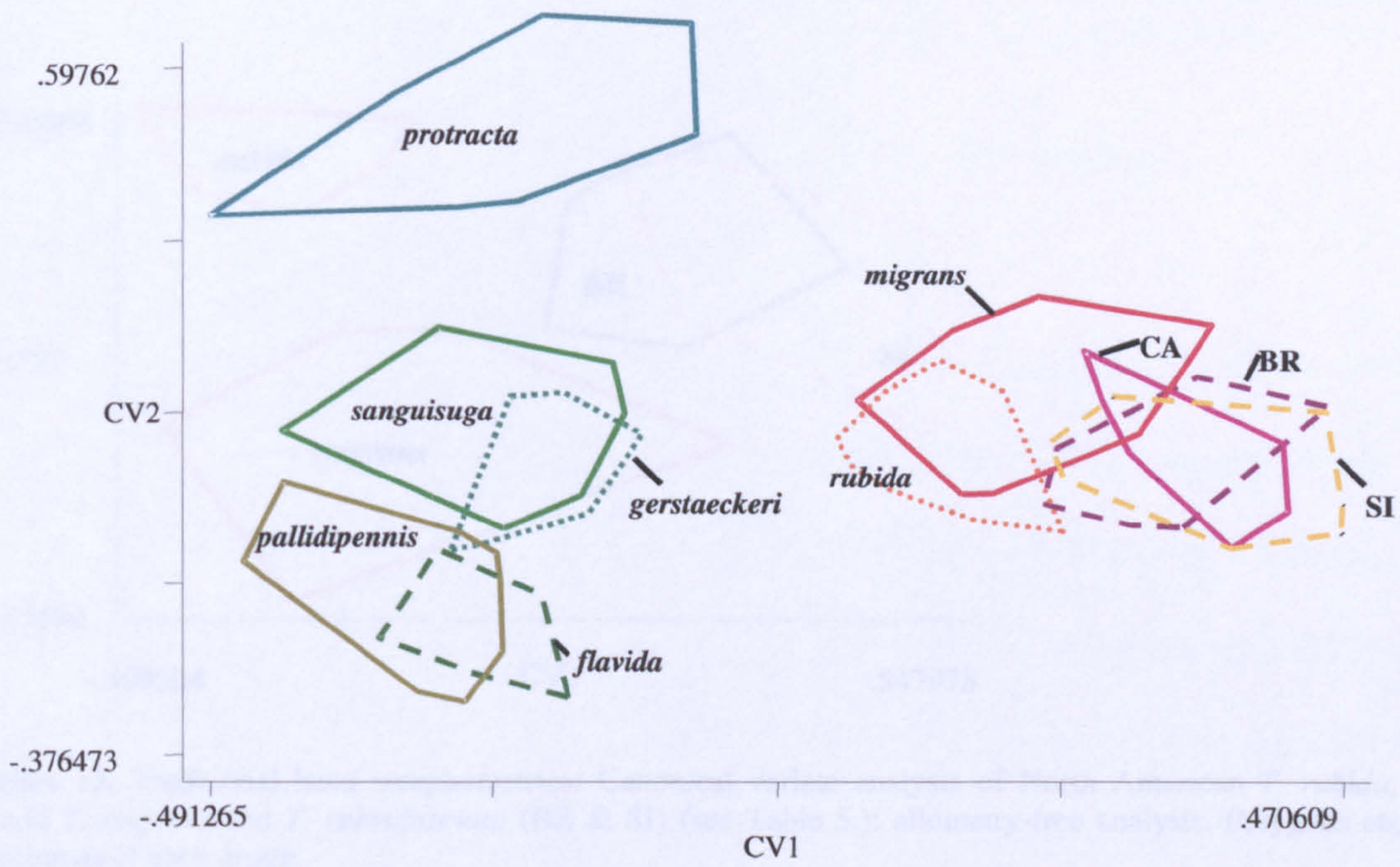

Figure 11. Traditional head morphometrics: Canonical variate analysis of North/Central American groups, Old World *T. migrans* and *T. rubrofasciata* (CA, BR & SI) (see Table 5.): isometry-free analysis. Polygons enclose specimens of each group.

4.1.2.1.1.3 Allometry-free analysis

The CPC approach (Materials and methods) was used to elucidate the intraspecific relationships between allopatric populations of *T. rubrofasciata* and interspecific relationships between *T. rubrofasciata*, Old World *T. migrans* and New World *T. rubida.* To validate the outcome of CPC analysis it was first necessary to test the data for a common

allometric axis (common principal component). Both intraspecific and interspecific analyses seemed to fit the CPC model (P= 0.08 and P= 0.09 respectively) so the CPC analyses were carried out using subsets of six variables (A, C, D, E, G & R3) and groups of 15 specimens (see Patterson *et al.* 2001).

Allometry-free analysis of *T. rubida, T. rubrofasciata* and *T. migrans* served to elucidate the relationships between these groups. The CVA was significant (Table 5), reflected by 86.7% correct reclassification. CV1 and CV2 accounted for 97.4% of the variance and separated the groups in the discriminant space (Fig. 12), with *T. rubrofasciata* and *T. migrans* having closest proximity.

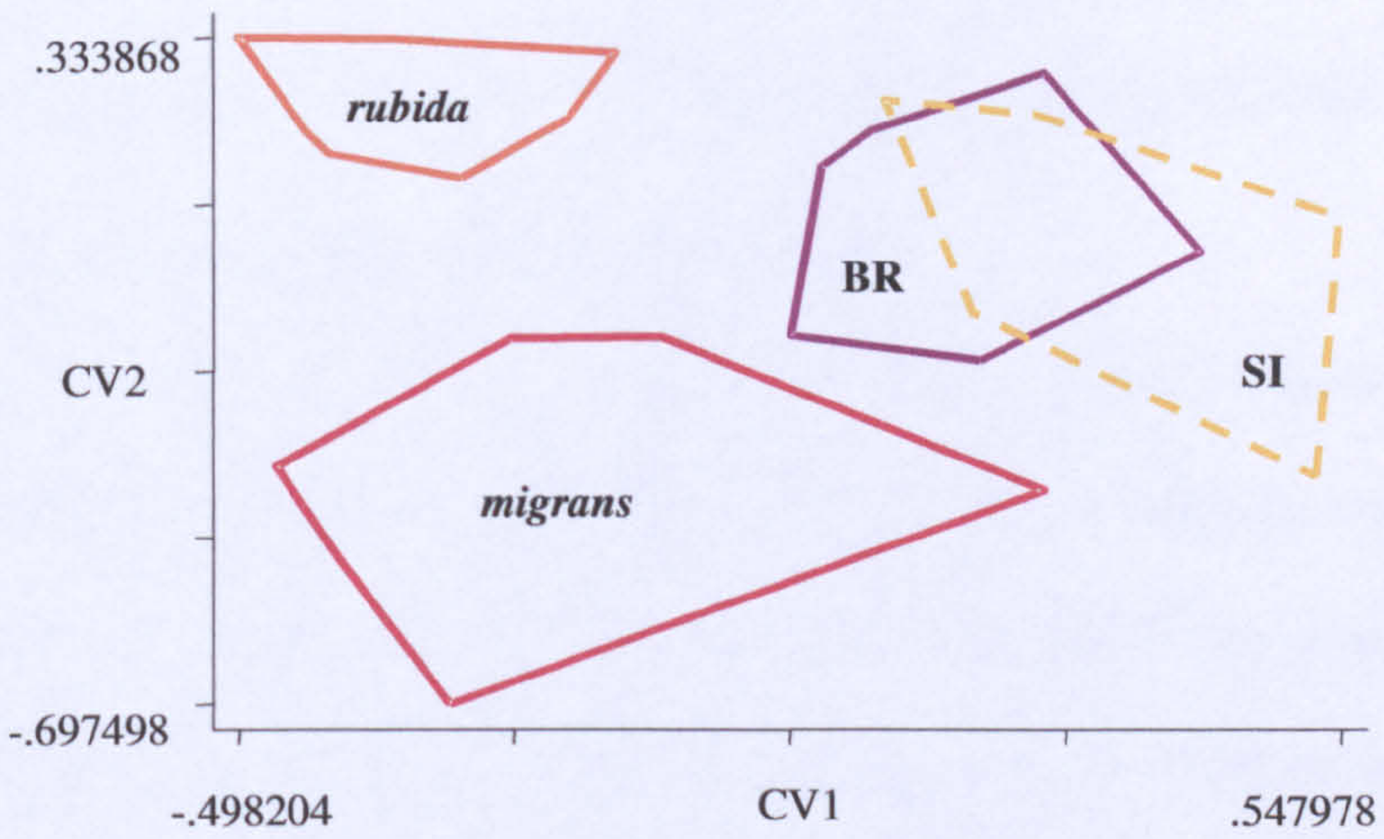

Figure 12. Traditional head morphometrics: Canonical variate analysis of North American *T. rubida*, Old World *T. migrans* and *T. rubrofasciata* (BR & SI) (see Table 5.): allometry-free analysis. Polygons enclose specimens of each group.

Allometry-free analysis of *T. rubrofasciata* allopatric populations was significant (Table 5), however the Wilk's Lambda statistic was relatively high (0.47) and only 44.4% of original cases were correctly reclassified by the CVA. The plot of CV1 and CV2 (Fig. 13) shows the allopatric populations of *T. rubrofasciata* to be generally homogeneous without any clear separation of the groups.

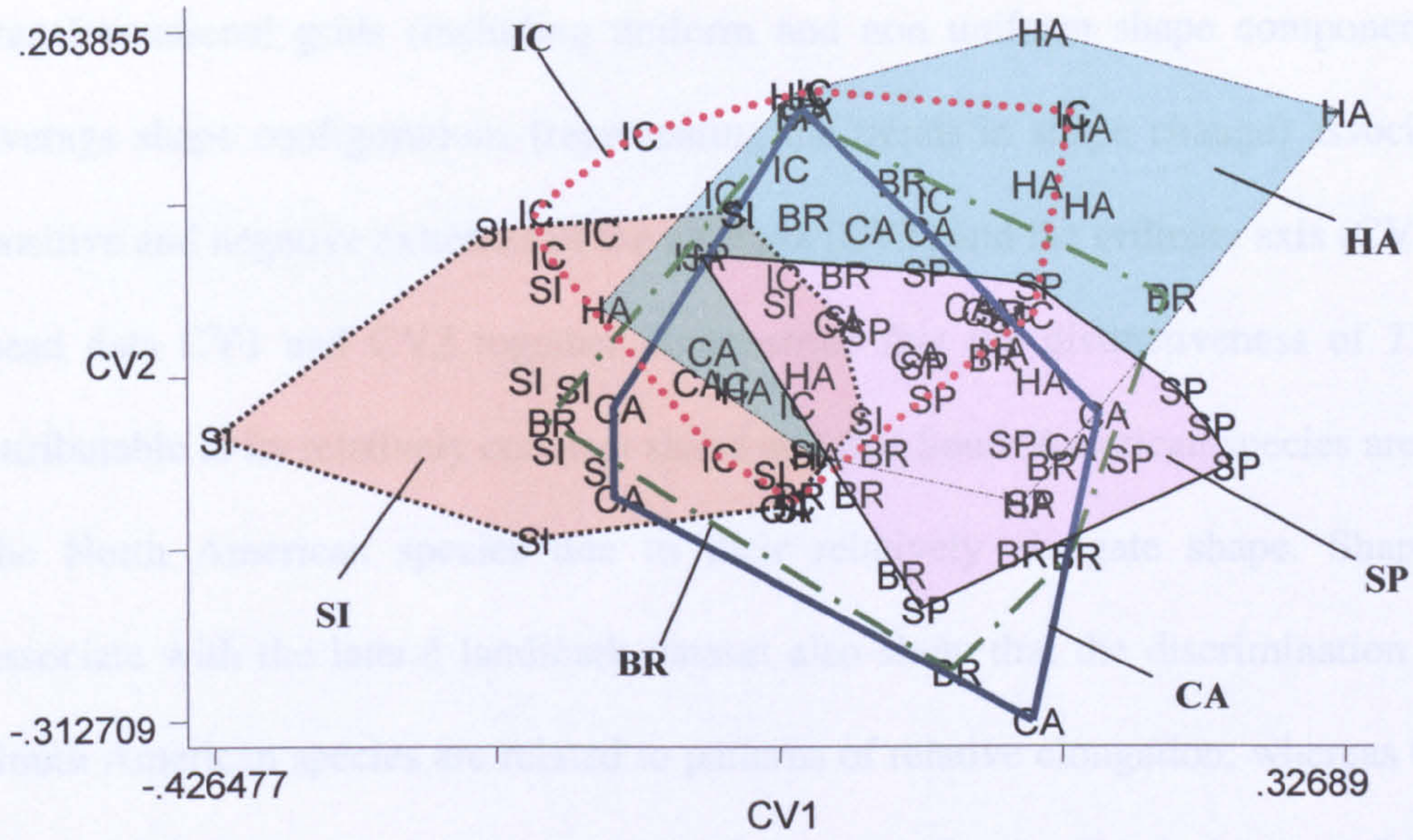

Fig. 13. Traditional head morphometrics: Canonical variate analysis of allopatric populations of *T. rubrofasciata* (HA, SP, CA & SI) (see Table. 5) allometry free analysis. Polygons enclose specimens of each group.

4.1.2.1.2 Comparative Geometric morphometrics of head and wing.

4.1.2.1.2.1 Interspecific comparisons

For most of the specimens used previously, shape components (relative warps including affine and non affine components), derived from head (dorsal orientation and lateral view) and wing landmarks (see Fig. 7) were analysed by discriminant CVA. Fig. 14 shows a plot of the first two CVs for head and wing data, accounting for 71%, 88% and 86% of the variance for head-dorsal, head-lateral and wing data sets respectively. The head landmark data sets show similar patterns of interspecific variation (Fig. 14) as demonstrated by the results obtained from traditional morphometric approaches. However, the analysis of wing landmark data seems to give less resolution (Fig. 14), it has a higher Wilk's lambda value (0.04, p=<.0001) compared to values for dorsal head (0.001, p=<.0001) and lateral head (0.006, p=<.0001). Moreover, the wing landmark analysis shows a somewhat different pattern of discrimination, most notably demonstrating a departure of *T. migrans* and *T. rubida* from the two populations of *T. rubrofasciata.*

Plots of the CV1 and CV2 of head and wing data sets (Fig. 14) coupled with TPS transformational grids (including uniform and non uniform shape components) show the average shape configurations (representing the trends in shape change) associated with the positive and negative extremes of the abscissa (CV1) and the ordinate axis (CV2). For dorsal head data CV1 and CV2 together demonstrate that the distinctiveness of *T. protracta* is attributable to its relatively compact shape and that South American species are distinct from the North American species due to their relatively elongate shape. Shape differences associate with the lateral landmark dataset also show that the discrimination of North and South American species are related to patterns of relative elongation, whereas CV2 seems to particularly relate to relative eye size and accounts for the discrimination of the Old World species and *T. rubida* from the North American species. The main difference in wing shape associated with CV1 & CV2 relate to patterns of relatively elongated wing shapes being more associated with the South American species. In particular, CV1 for wing shape separates *T. rubrofasciata, T. migrans* and *T. rubida* from the other *Triatoma*: This pattern of discrimination relates to a different position for landmark 5 (basal vein junction on border of corium); i.e. it is basally placed in relation to the position of landmarks 4 & 6, whereas the *T. rubrofasciata* have landmark 5 either linear to 4 and 6 or positioned distally.

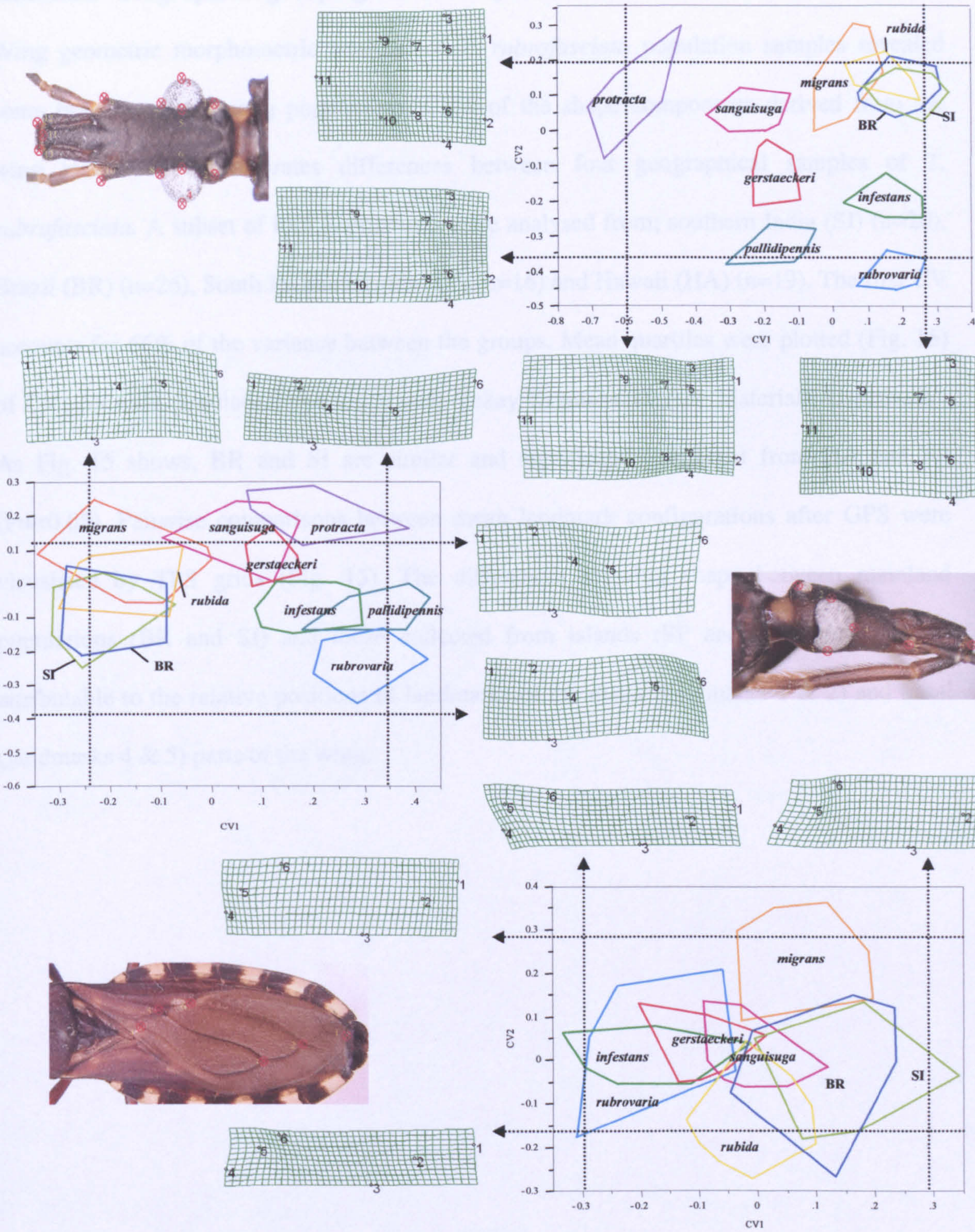

Figure. 14 Geometric morphometric analysis: Canonical variate analysis of shape components from head (dorsal; upper plot, lateral middle plot) and wing (lower plot) landmark data. Polygons enclose specimens in each group The following species/population samples were used: *T. gerstaeckeri* (n=15); *T. infestans* (n=18); *T. migrans* (n=27); *T. pallidipennis* (n=16); *T. protracta* (n=18); *T. rubida* (n=34); *T. rubrovaria* (n=22); *T. sanguisuga* (n=36); *T. rubrofasciata* from South India (SI) (n=26); *T. rubrofasciata* from Brazil (BR) (n=26). (Wing landmark analysis does not include *T. pallidipennis* and *T. protracta*). For the dorsal landmarks of the heads CV1 accounts for 43% of the total variance and CV2 accounts for 28% (∑ =71 %). For the lateral view of head CV1 63%, CV2 25% (∑ 88%). For the wings CV1 58%, CV2 28% (∑ 86%). Thin plate spline grids have been interpolated and correspond to values of the respective CVs, as indicated by arrows.

4.1.2.1.2.2 Geographical groupings of *T. rubrofasciata*

Wing geometric morphometric analysis of *T. rubrofasciata* population samples revealed some heterogeneity among populations. CVA of the shape components derived from the wing landmarks demonstrates differences between four geographical samples of *T. rubrofasciata.* A subset of four populations were analysed from; southern India (SI) (n=20), Brazil (BR) (n=26), South Pacific islands (SP) (n=16) and Hawaii (HA) (n=19). The first CV accounts for 66% of the variance between the groups. Mean quartiles were plotted (Fig. 15) of CV1 for each population and tested with Tukey-Kramer tests (see Materials & methods). As Fig. 15 shows, BR and SI are similar and significantly different from HA and SP ($P=<0.05$). Pairwise comparisons between mean landmark configurations after GPS were visualised by TPS grids (Fig. 15). The differences in wing shape between mainland populations (BR and SI) and those collected from islands (SP and HA) appear to be attributable to the relative positions of landmarks of the distal (landmarks 1 & 2) and basal (landmarks 4 & 5) parts of the wing.

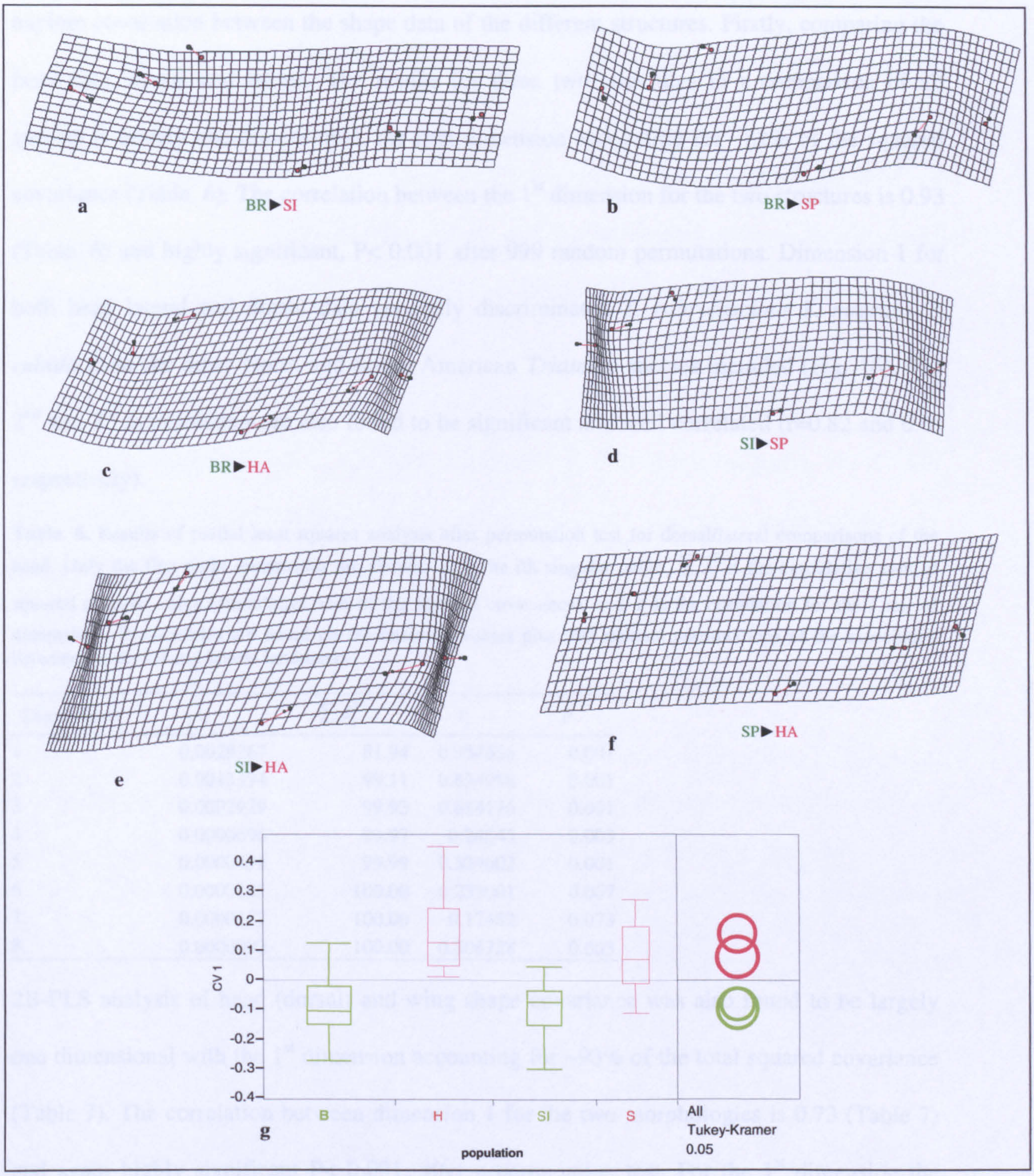

Figure 15. Comparisons of wing shape between populations of *Triatoma rubrofasciata* from mainland locations; Brazil (BR) and southern India (SI) and island locations; Hawaii (HA) and south Pacific islands (SP) (see Table 3). A series of pairwise comparisons, **a-f** by least squares superimposition of consensus configurations from each location. The displacement vectors (red lines) and thin plate spline grids show the deformation exaggerated by a factor of five. **g;** Plot of mean quantiles of CV1 for each location derived from CVA of wing shape components. Results of Tukey–Kramer tests are shown graphically, separation of circles indicates a significant difference (P=<0.05)

4.1.2.1.2.3 Covariation of shape

The two block- partial least squares (2B- PLS) analysis (Material and Methods) was used to explore covariation between the shape data of the different structures. Firstly, comparing the head data, dorsal and lateral. The results for these two structures in a comparison of all species is largely one-dimensional, the first dimension accounting for ~82% of the squared covariance (Table. 6). The correlation between the 1st dimension for the two structures is 0.93 (Table. 6) and highly significant, P< 0.001 after 999 random permutations. Dimension 1 for both head lateral and dorsal data generally discriminated *T. rubrofasciata T. migrans T. rubida* from the other North and South American *Triatoma* species included (Fig. 16). The 2nd and 3rd dimensions were also found to be significant and well correlated (r=0.82 and 0.61 respectively).

Table. 6. Results of partial least squares analysis after permutation test for dorsal/lateral comparisons of the head. Only the first eight dimensions are shown. λ_i is the *i*th singular value, $\sum \lambda_i^2$ is the cumulative sum of squared singular value (cumulative sum of the squared covariance), and r_i is the correlation for the *i* pair of dimensions. Probabilities are based on the observed values plus 999 random permutations of the association between the dorsal and lateral landmarks.

Dimensions	λ_i	$\sum \lambda_i^2$	r_i	P
1	0.0029267	81.94	0.934636	0.001
2	0.0013394	99.11	0.834998	0.001
3	0.0002929	99.93	0.614176	0.001
4	0.0000696	99.97	0.24543	0.003
5	0.0000436	99.99	0.324602	0.001
6	0.0000242	100.00	0.239001	0.007
7	0.0000187	100.00	0.17482	0.073
8	0.0000092	100.00	0.206728	0.003

2B-PLS analysis of head (dorsal) and wing shape covariance was also found to be largely one dimensional with the 1st dimension accounting for ~93% of the total squared covariance (Table 7). The correlation between dimension 1 for the two morphologies is 0.73 (Table 7) and again highly significant P< 0.001, after a permutation test. For the 1st dimension the results show a similar pattern to the PLS analysis of dorsal and lateral head landmarks (Fig.

16) The 2nd and 3rd dimensions were also found to be significant and reasonably well correlated (r=0.42 and 0.43 respectively).

Plots of the first three dimension for both PLS analyses (Fig. 16) (accounting for >99% of the variance in both cases) show varying patterns of discriminating the groups. The correlations between the two sets of head landmark data are more highly correlated, as clearly evident in the paired plots (Fig. 16) and also the strong correlation of their centroid sizes (Table. 8). This demonstrates the integration of these two datasets, which represent two aspects of the same functionally integrated morphology. The wing and dorsal-head landmark data are less strongly correlated and only strongly for the 1st dimension, which seems largely attributable to size covariation (See Table 8. for centroid size correlation tests). The 2nd and 3rd dimensions are relatively free from size effects and reveal latent components of the head shape that covary with wing shape to discriminate *T. rubrofasciata* from *T. rubida* and *T. migrans,* whereas the relationships between the other species remain relatively constant through the dimensions.

Table. 7. Results of partial least squares analysis after permutation test for head-dorsal and wing comparisons. Only the first eight dimensions are shown. λ_i is the *i*th singular value, $\sum \lambda_i^2$ is the cumulative sum of squared singular value (cumulative sum of the squared covariance), and r_i is the correlation for the *i* pair of dimensions. Probabilities are based on the observed values plus 999 random permutations of the association between the head-dorsal and wing landmarks

Dimensions	λ_i	$\sum \lambda_i^2$	r_i	P
1	0.0009075	93.187	0.729012	0.0010
2	0.0001847	97.0468	0.421696	0.0010
3	0.0001419	99.3262	0.439775	0.0010
4	0.0000681	99.8517	0.397804	0.0010
5	0.0000308	99.959	0.268764	0.0090
6	0.0000143	99.9822	0.15552	0.5340
7	0.0000102	99.9941	0.180126	0.1820
8	0.0000072	100	0.121824	0.5150

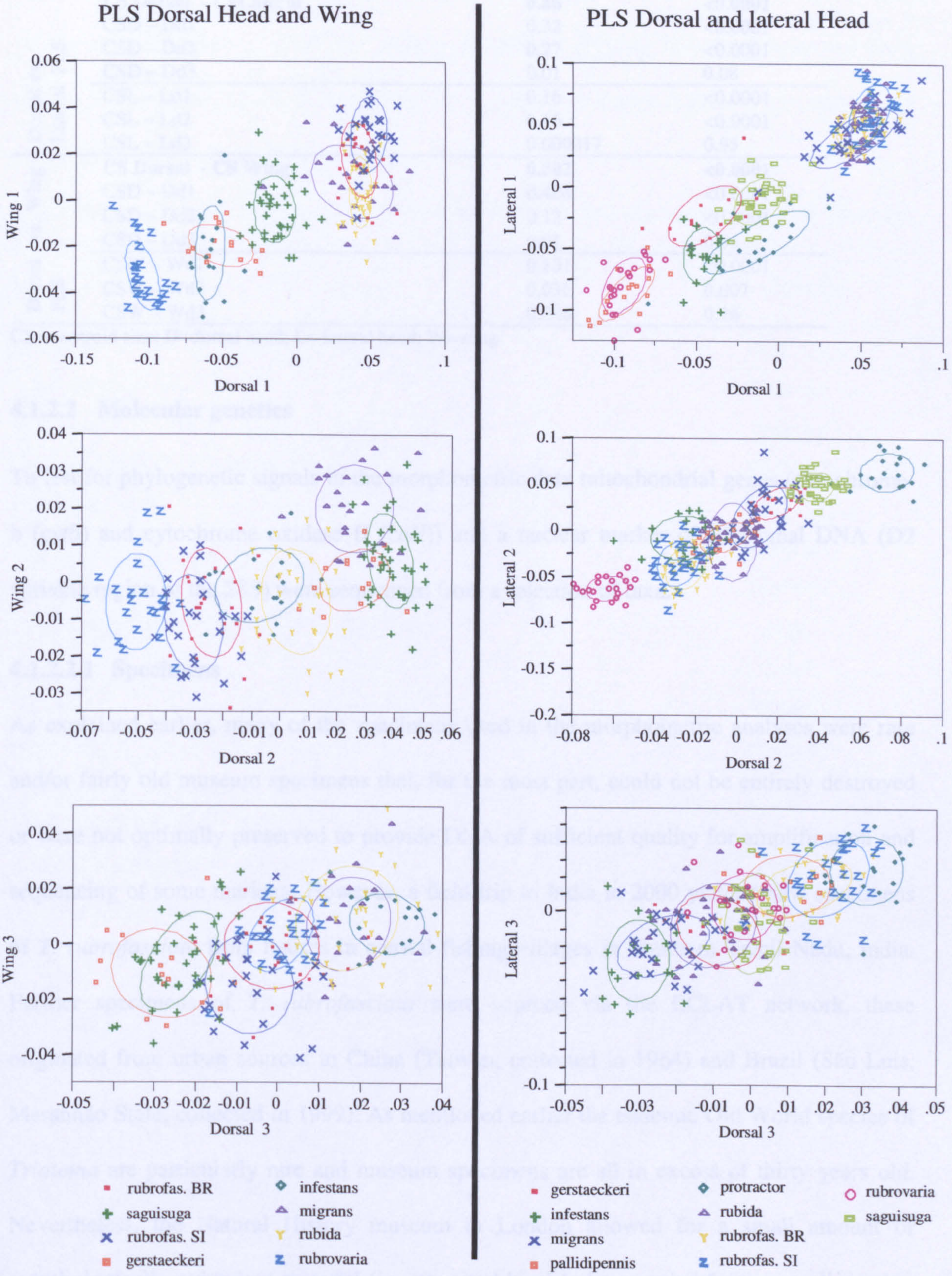

Figure 16. Analysis of shape covariation among *Triatoma* species. Plots of dimensions 1, 2 & 3 for head-dorsal vs wing landmark data (left plots) and head-dorsal vs head-lateral landmark data (right plots) after partial least squares analysis. Ellipses enclose 50% of the distribution of specimens in each group.

Table. 8 Analysis of shape covariation in relation to size among *Triatoma* species: Correlation tests of partial least squares dimensions and centroid size.

	Regression – centroid size vs PLS dimension (d)	r^2	p
Dorsal vs. Lateral PLS	**CS Dorsal - CSLateral**	**0.86**	**<0.0001**
	CSD – Dd1	0.32	<0.0001
	CSD – Dd2	0.27	<0.0001
	CSD – Dd3	0.01	0.08
	CSL – Ld1	0.16	<0.0001
	CSL – Ld2	0.16	<0.0001
	CSL – Ld3	0.000017	0.95
Dorsal vs. Wing PLS	**CS Dorsal - CS Wing**	**0.502**	**<0.0001**
	CSD – Dd1	0.408	<0.0001
	CSD – Dd2	0.12	<0.0001
	CSD – Dd3	0.01	0.06
	CSW – Wd1	0.101	<0.0001
	CSW – Wd2	0.036	0.007
	CSW – Wd3	0.006	0.26

CS= centroid size; D=dorsal head; L= lateral head; W=wing

4.1.2.2 Molecular genetics

To test for phylogenetic signals in the morphometric data mitochondrial genes (cytochrome-b (*cytb*) and cytochrome oxidase II (*coII*)) and a nuclear marker of ribosomal DNA (D2 variable region of the 28S) were sequenced from a selection of taxa.

4.1.2.2.1 Specimens

As explained earlier, many of the specimens used in the morphometric analyses were rare and/or fairly old museum specimens that, for the most part, could not be entirely destroyed or were not optimally preserved to provide DNA of sufficient quality for amplification and sequencing of some markers. However, a field trip to India in 2000 yielded new specimens of *T. rubrofasciata* from houses in coastal fishing villages in Southern Tamil Nadu, India. Further specimens of *T. rubrofasciata* were sourced via the ECLAT network, these originated from urban sources in China (Taiwan, collected in 1964) and Brazil (São Luis, Maranhão State, collected in 1999). As mentioned earlier the endemic Old World species of *Triatoma* are particularly rare and museum specimens are all in excess of thirty years old. Nevertheless, the Natural History museum in London allowed for a small amount of morphologically redundant material (i.e. unpaired legs) to be sampled from a small number

of *T. migrans* (the best represented species in collections), giving rise to two fruitful DNA extracts, one from Sarawak and the other from Brunei. All New World material was sourced via the ECLAT network, FIOCRUZ reference cultures (Rio de Janeiro, Brazil) and from various field collections made during the course of my research. Table 9. summarises the specimens used and fragments amplified.

Table 9. DNA sequences obtained for Old and New World *Triatoma* (*Rhodnius* species included as outgroups).

Species	Origin	Marker			Source of material
		coII	*cytb*	*D2*	
P. megistus	SA	*	*		FIOCRUZ
R. ecuadoriensis	SA	*			Collected
R. prolixus	SA	*	*	*	Collected
T. brasiliensis	SA			*	FIOCRUZ
T. dimidiata	NA		*		ECLAT
T. infestans	SA		*	*	Collected
T. matogrossensis	SA			*	FIOCRUZ
T. migrans Brunei	OW				NHM
T. migrans Sarawak	OW	*	*		NHM
T. platensis	SA			*	FIOCRUZ
T. protracta	NA		*		FIOCRUZ
T. rubida	NA	*	*	*	ECLAT
T. rubrofasciata Brazil	SA	*	*	*	ECLAT
T. rubrofasciata China	OW	*			ECLAT
T. rubrofasciata India	OW	*	*		Collected
T. sanguisuga	NA		*	*	ECLAT
T. sordida	SA		*		Genbank#

see appendix for accession number. Origin code: SA= South American; NA= North American (including Central American origin); OW= Old World. * indicates that a sequence was obtained For photographs of representative specimens of species used in this chapter see Fig. 93 in the appendix

4.1.2.2.2 Molecular markers

4.1.2.2.2.1 Mitochondrial genes

Attempts were made to amplify the two mitochondrial targets; *cytb* and *COII*. Due to the varying age and state of preservation of the specimens large fragments could not be

amplified from some. A panel of primer sets were designed and evaluated for regions of COI and *COII* genes. A 400bp fragment of *COII* could be amplified and sequenced for some of the less optimal samples. In addition the established 700bp fragment of *cytb* gene was also amplified where possible and sequenced (see Materials and Methods). Table 9. summarises the fragments obtained from the range of taxa examined.

For *COII*, alignments of sequences amounted to 307bp and for *cytb* 358bp, neither contained any gaps identity of the amplicons sequenced was confirmed by BLAST search and direct alignments to the complete *COII* and *cytb* genes of *T. dimidiata* (Dotson and Beard 2001; GenBank accession AF301594)

4.1.2.2.2.2 D2 region of 28S rDNA.

A ~700bp fragment of the D2 region of the 28S rDNA was successfully amplified and sequenced for some of the taxa sampled (see Table. 9) (see Materials and Methods). Alignments were 640bp and indels were disregarded in the analyses giving a consensus alignment of 528bp

4.1.2.2.3 Analysis of sequences

For comparative analysis of the sequences obtained and subsequent phylogenetic analyses nucleotide differences and distance matrices were calculated. For these data sets several models of base substitution were used in comparison (p distances, kimura 2 parameter (K2p), Jukes Cantor, Tajima-Nei, Tamura 3 parameter, Tamura-Nei). All models assessed here, for this data set gave comparable results without any significant differences in the results of the eventual phylogenetic analyses. For this reason, only K2p distances were used and percentages of sequence divergence among operational taxonomic units (OTUs) are shown here (Tables 10 & 11).

4.1.2.2.3.1 Phylogenetic analyses

4.1.2.2.3.1.1 Distance based

Neighbour joining trees were generated using the various models of base substitution, and statistical support was evaluated by bootstrap resampling with 1000 replicates and a random seed number. All models of base substitution investigated yielded essentially equivalent results, all trees having identical topologies and similar bootstrap supports.

4.1.2.2.3.1.2 Maximum parsimony

To support the phylogeny reported by the neighbour joining analysis the haplotypes were also subjected to a maximum parsimony analysis. The branch and bound algorithm was used to recover three equally parsimonious trees, from which strict consensus trees were produced with bootstrap supports.

4.1.2.2.4 *T. rubrofasciata* and *T. migrans* populations

4.1.2.2.4.1 *COII* sequences

The *COII* target was successfully sequenced for three geographically disparate samples of *T. rubrofasciata*; India China and Brazil (see Tables. 9 & 12). Alignments of sequences revealed 11 variable sites (0 parsimony-informative) each geographical location represented by a unique haplotype. Of the 11 variable sites 0 corresponded to third codon position substitutions (silent), 10 to first codon positions and only one to the second. Translation to amino acid sequence revealed that among the three haplotypes there are 8 amino acid differences.

Among haplotype differences for the *T. rubrofasciata* samples range from 6 to 9 nucleotides (a sequence divergence of 1.9% - 2.9%) see Table. 12. For among each of the species

geographic samples/populations within group differences were assessed by absolute nucleotide differences (Table 12)

The parsimony network constructed for the three specimens of *T. rubrofasciata* using TCS software (figure 17) shows the number of mutational steps separating any two of the haplotypes and the number and position of all inferred haplotypes that could conceivably be found with further sampling.

The *COII* target was successfully sequenced for *T. migrans* Sarawak and Brunei (see Table. 9 & 12). Alignments of the two haplotype sequences obtained revealed 10 variable sites (a sequence divergence of 3.26%), of which 1 corresponded to a third codon position substitutions (silent), 6 the first codon positions and 3 to the second. Translation to amino acid sequence revealed that among the three haplotypes there are 8 amino acid differences.

The NJ trees (Figs. 17 & 19) demonstrate that both species are well supported and that the level of intraspecific variation is comparable (Table 12).

4.1.2.2.4.2 *Cytb* sequences

The *cytb* target was successfully sequenced for two *T. rubrofasciata* geographically disparate samples; India and Brazil (see Table. 9 & 11). Alignments of the two haplotype sequences revealed 19 variable sites, of which, 16 corresponded to third codon positions substitutions (silent), 3 the first codon positions and 0 to the second. Translation to amino acid sequence revealed that among the three haplotypes there is only one amino acid difference.

Neighbour-joining (NJ) trees for *cytb* and *COII* sequences (Figs. 19 and 20) demonstrate good bootstrap support for the Old World species, *T. migrans* falling with all *T. rubrofasciata* samples.

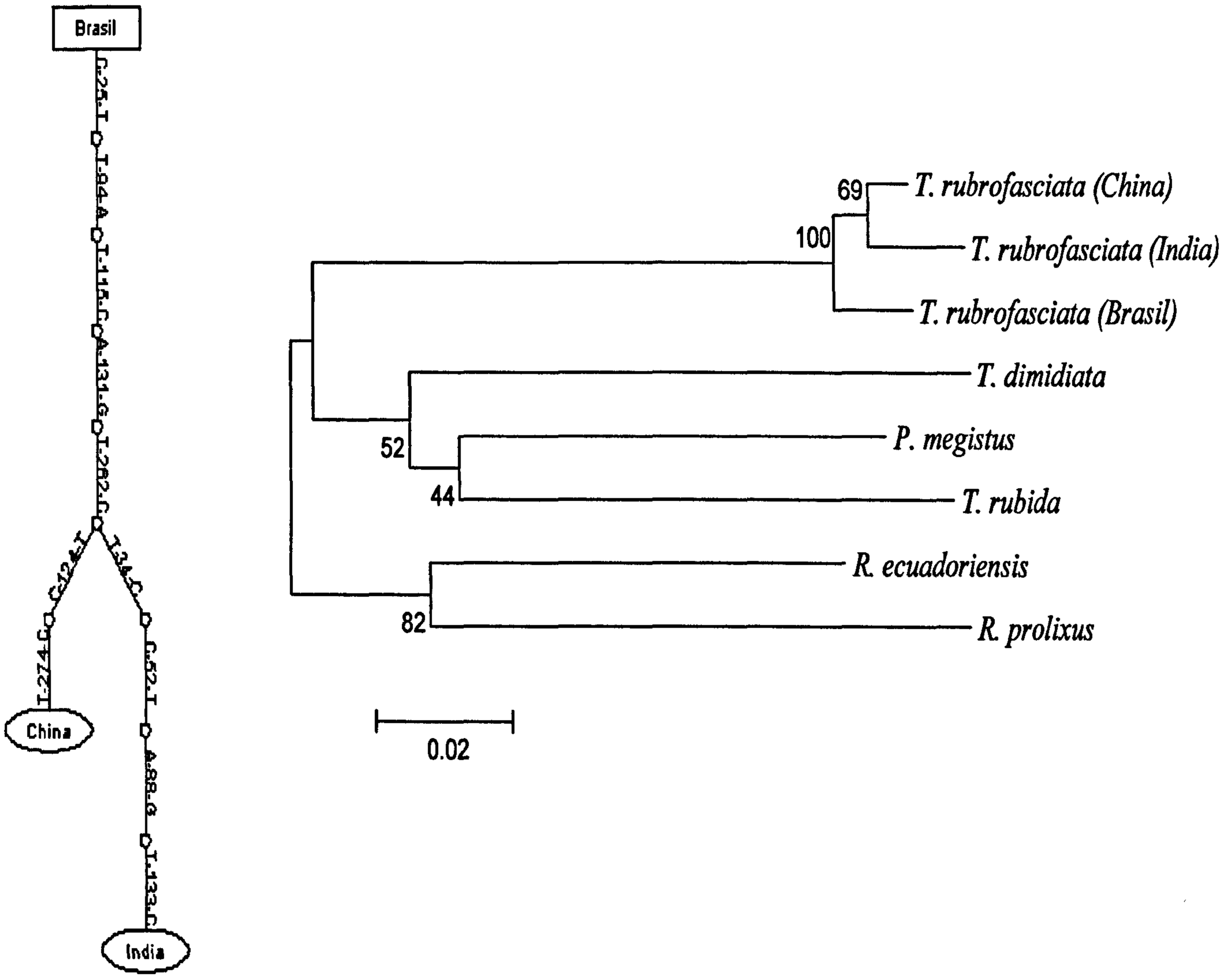

Figure. 17. Analysis of *COII* sequences To the left a network of *T. rubrofasciata* haplotypes, the maximum number of steps connecting parsimoniously two haplotypes is indicated; one step is indicated by a single line between two haplotypes and each additional base substitution by a small circle. The haplotype with the highest ancestral probability is displayed as a rectangle, while other haplotypes are displayed as ovals. The size of the square or oval corresponds to the haplotype frequency. To the right a Neighbour- joining tree constructed form k2p distances, with 1000 bootstrap replicates sum of branch lengths = 0.517, scale: substitutions/site

4.1.2.2.5 Old World – New World *Triatoma* phylogeny

The markers examined here unambiguously group *T. rubrofasciata* and *T. migrans* and separate them with strong bootstrap supports in both MP and NJ distance trees from the New World species of *Triatoma* examined (Figs. 19, 20, 21 and 22). The *cytb* fragment suggests a closer relationship to the North/Central American species (Fig.. 20). However, the D2-28S analysis including only Brazilian *T. rubrofasciata* indicates that the Old World group is equally distant from all American *Triatoma* included (see Table. 10 & 11)

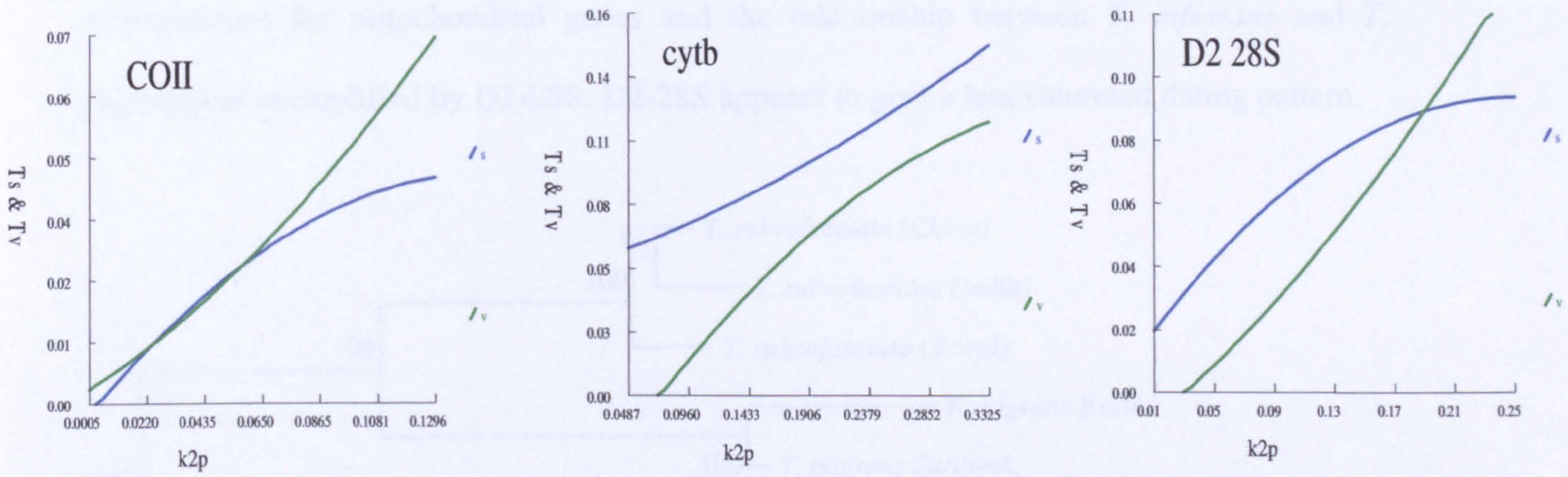

Figure. 18. Plots of transition and transversions against k2p distances for markers used in analyses (blue lines = transitions; green = transversions) (calculated using all sequences listed in Table 9)

The plots of transitions and transversions against k2p distances (Fig. 18) indicate that some saturation of transitions occurs at higher genetic distances and accounts for the lack of support for the basal nodes of the tree presented here. Saturation is also evident due to low transition to transversion ratios for the two mitochondrial targets (*COII*; R= 1.1 and *cytb*; R= 1.3). This observation, considered together with p distances being > 0.09-0.1 (the saturation threshold for the *cytb* gene, as recommended by Meyer (1994) suggests that the models of base substitution used to calculate the genetic distances may have been biased by saturation of transitions.

Despite the possiblility of back-substitutions, as suggested by the observation of saturated levels of transitions, I have estimated divergence times based on the estimate of 2.3% pairwise sequence divergence per million years for mitochondrial genes (see Brower 1994). For the D2-28S a rate of 0.5% per million years (see Whitfield 2002) was considered but a rate of 0.17% per million years gives dates of divergence in line with those estimated by Bargues *et. al.*, (2000) for ITS-2 rDNA. The saturation of substitution rates clearly causes the dating estimates of mitochondrial genes to saturate quickly at ~2 Million years ago (Mya) at around which date both mitochondrial estimates correspond to the D2-28S in dating closely related species/populations (see Tables. 10, 11 & 12) e.g. populations of *T. rubrofasciata* for mitochondrial genes and the relationship between *T. infestans* and *T. platensis* as exemplified by D2-28S. D2-28S appears to give a less saturated dating pattern.

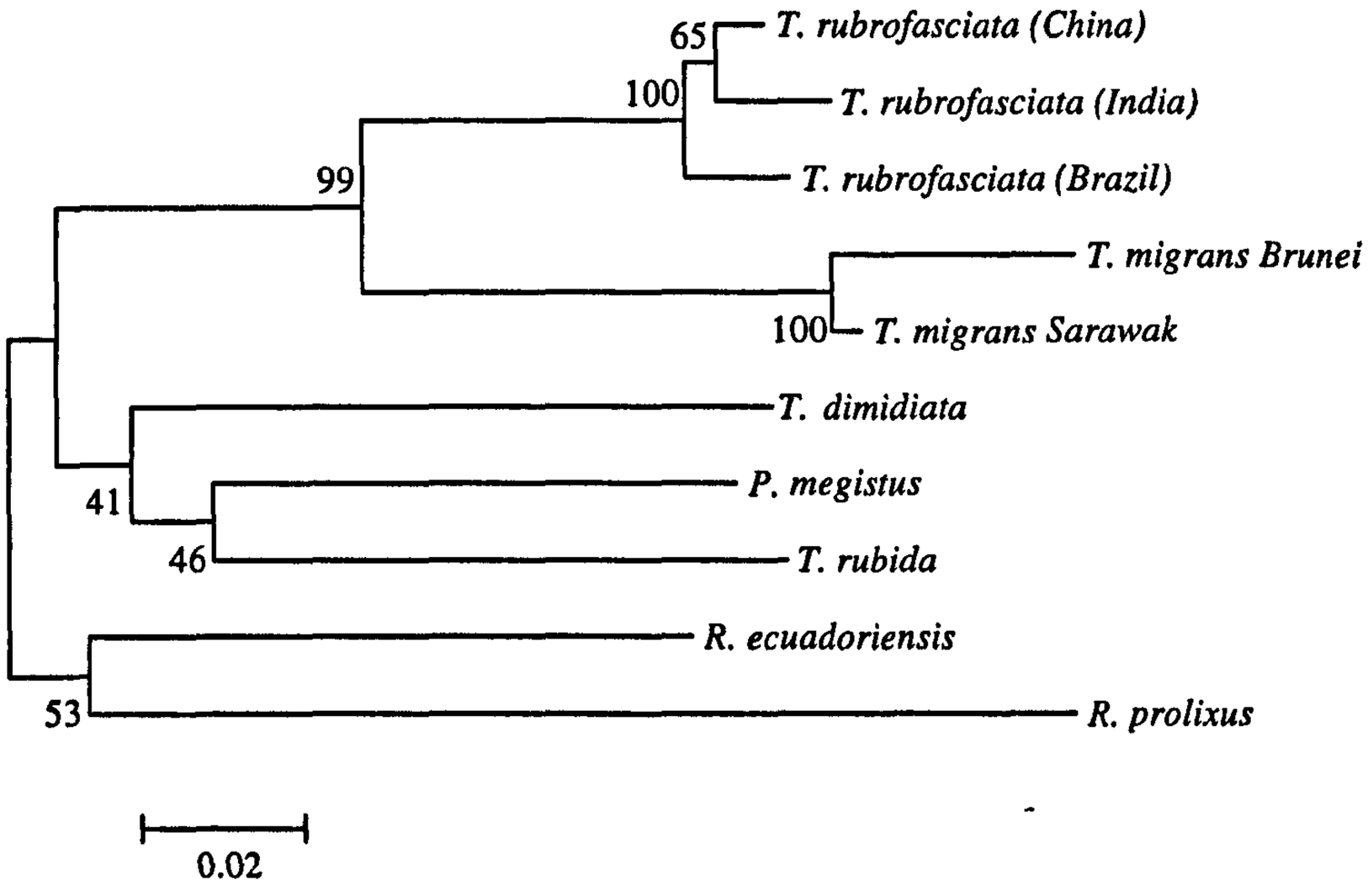

Figure 19. *Neighbour*-joining phylogenetic tree of *COII* sequences including *R. prolixus* and *R. ecuadoriensis* as outgroups. Constructed using k2p model, with 1000 bootstrap replicates sum of branch lengths = 0.653, scale: substitutions/site

It may be underestimating some older divergences because the estimate of ~60Mya for the divergence of *Rhodnius* and *Triatoma* is considerably less than the estimate of ~90 Mya

estimated with greater support by Gaunt and Miles (2002), but concurs with the estimate of ~50-60 Mya (Bargues *et al.* 2000).

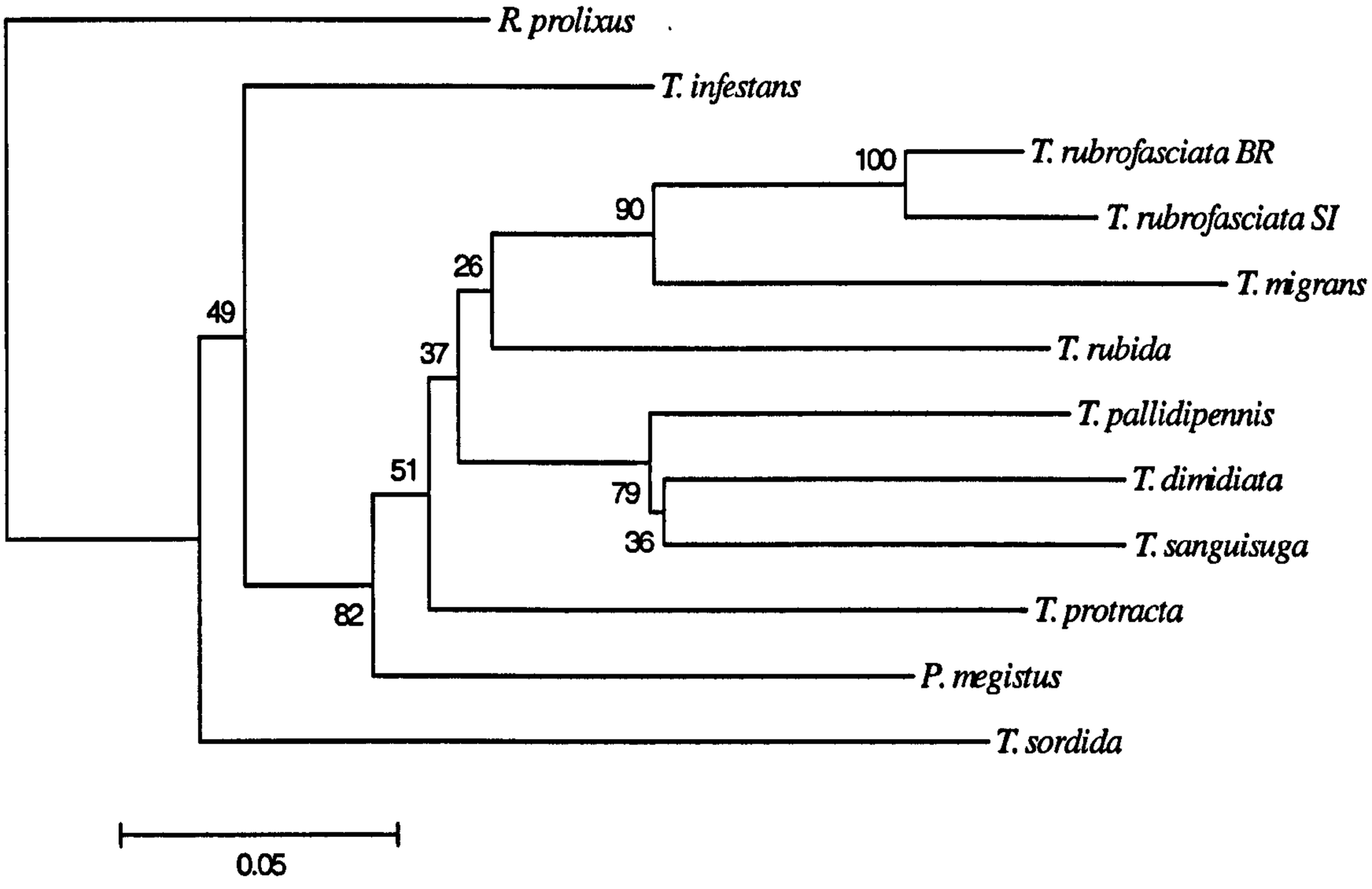

Figure 20. *Neighbour*-joining phylogenetic tree of *cytb* sequences including *R. prolixus* as an outgroup. Constructed using k2p model, with 1000 bootstrap replicates sum of branch lengths = 1.210, scale: substitutions/site.

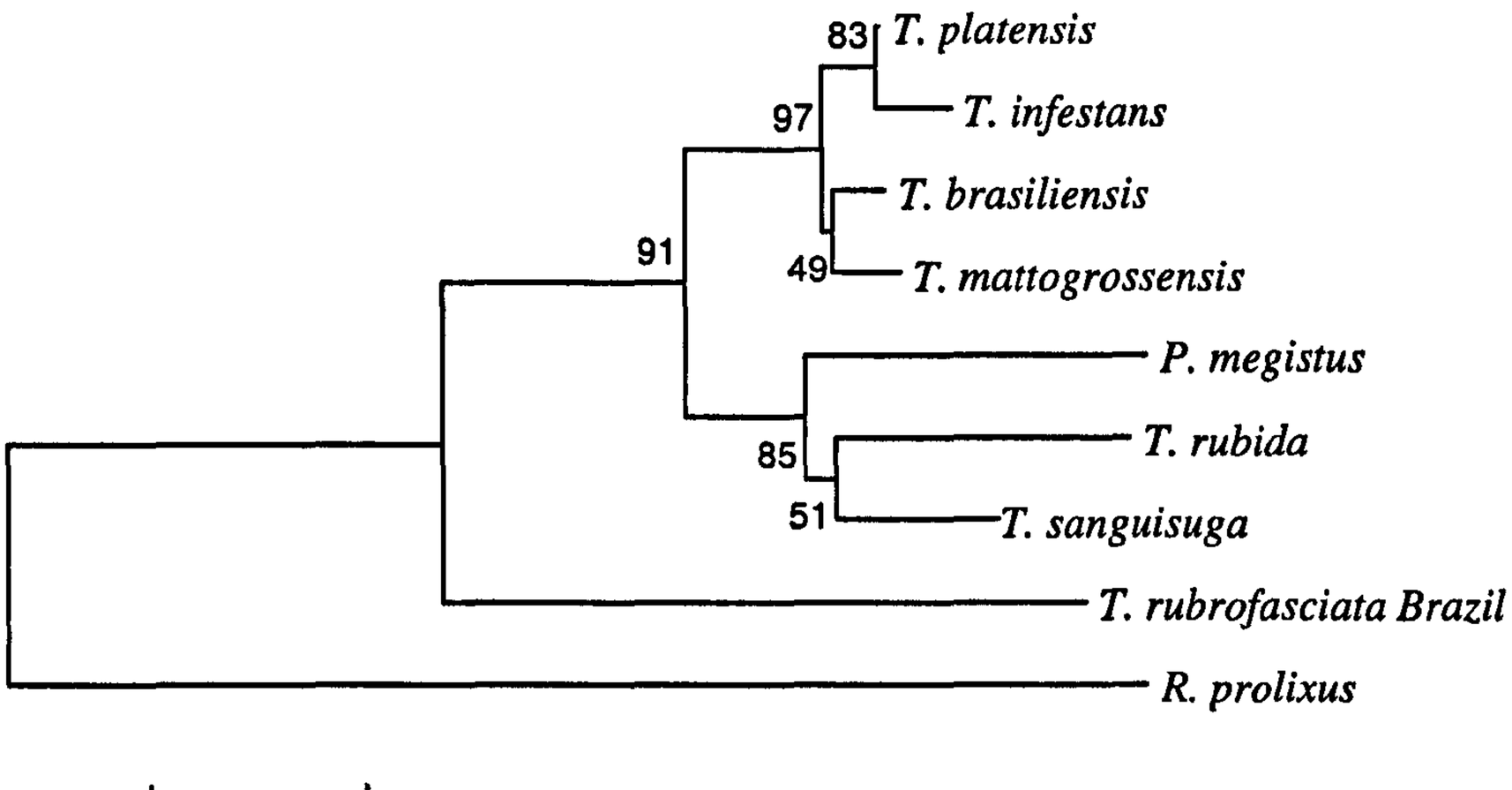

Figure 21 *Neighbour*-joining phylogenetic tree of D2 28S sequences including *R. prolixus* as an outgroup. Constructed using k2p model, with 1000 bootstrap replicates sum of branch lengths = 0.168, scale: substitutions/site

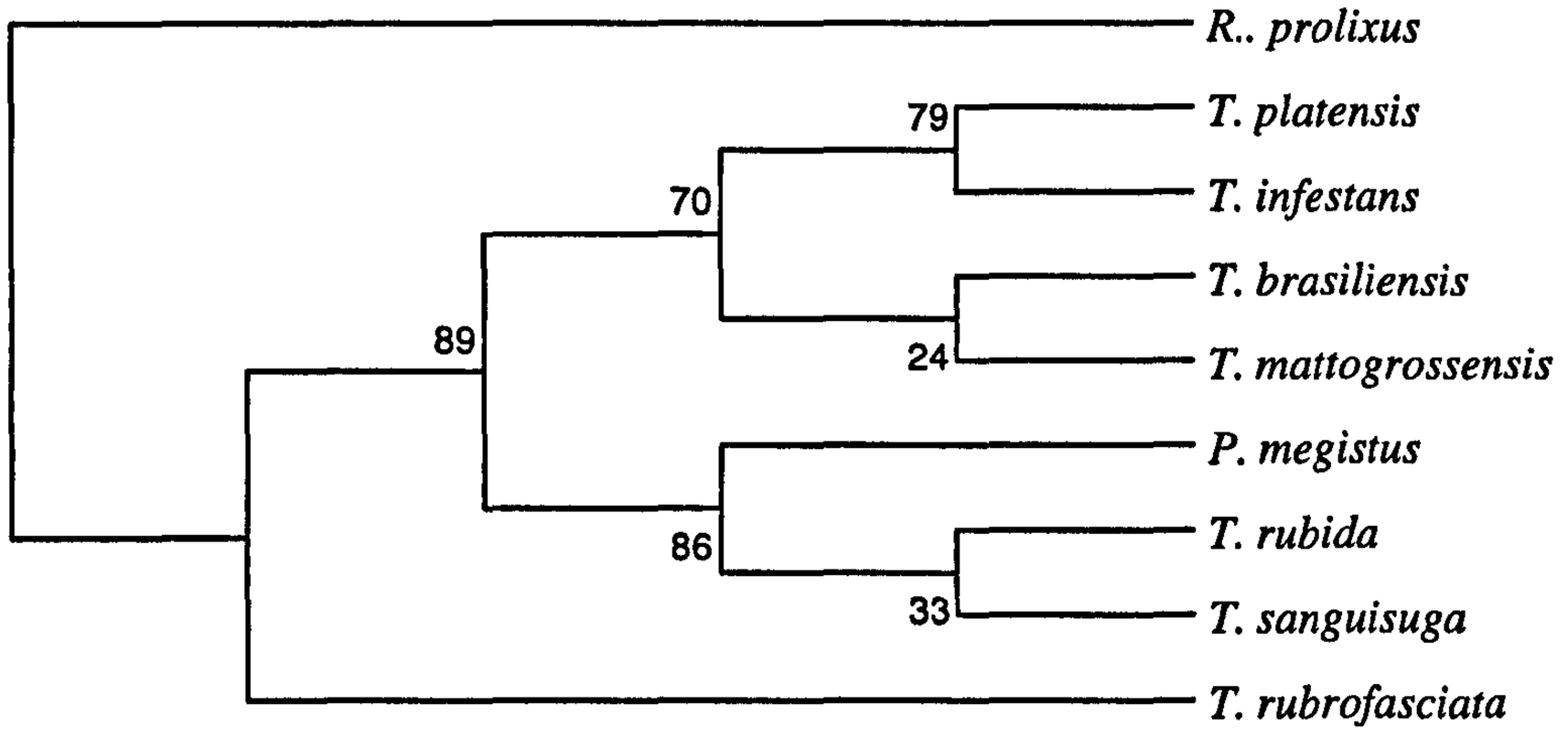

Figure 22 Maximum parsimony strict consensus phylogeny of D2 28S sequences constructed using branch-and-bound algorithm with 1000 bootstrap replicates CI = 0.894 RI = 0.696 RCI = 0.623 (for all sites) and iCI = 0.736 iRI = 0.696 iRCI = 0.513 (for parsimony informative sites).

Table.10. D2- 28S rDNA pairwise percentages of sequence divergence (lower matrix), estimated divergence time in millions of years (upper matrix)

	1	2	3	4	5	6	7	8	9
R. prolixus (1)		55.81	53.58	56.93	52.46	53.58	53.58	54.69	56.93
P. megistus (2)	9.49		16.74	17.86	18.98	18.98	14.51	17.86	39.07
T. platensis (3)	9.11	2.85		17.86	3.35	3.35	14.51	2.23	27.90
T. rubida (4)	9.68	3.04	3.04		16.74	17.86	12.28	18.98	35.72
T. brasiliensis (5)	8.92	3.23	0.57	2.85		3.35	13.39	5.58	26.79
T. matogrossensis (6)	9.11	3.23	0.57	3.04	0.57		14.51	5.58	27.90
T. sanguisuga (7)	9.11	2.47	2.47	2.09	2.28	2.47		15.63	31.25
T. infestans (8)	9.30	3.04	0.38	3.23	0.95	0.95	2.66		30.14
T. rubrofasciata BR (9)	9.68	6.64	4.74	6.07	4.55	4.74	5.31	5.12	

Table 11 Cytochrome b pairwise percentages of sequence divergence (lower matrix), estimated divergence time in millions of years (upper matrix)

	1	2	3	4	5	6	7	8	9	10	11	12
T. dimidiata (1)		8.26	8.50	6.07	10.81	9.11	6.32	9.84	8.02	8.74	9.59	8.38
T. infestans (2)	18.99		7.41	7.89	8.02	8.50	8.87	7.89	8.38	8.14	8.87	8.02
P. megistus (3)	19.55	17.04		8.74	8.87	7.89	9.11	9.96	8.14	8.26	9.96	7.65
T. pallidipennis (4)	13.97	18.16	20.11		10.32	7.53	6.19	10.44	8.38	8.74	9.23	8.38
R. prolixus (5)	24.86	18.44	20.39	23.74		9.72	9.59	9.59	9.84	10.57	10.57	9.72
T. protracta (6)	20.95	19.55	18.16	17.32	22.35		9.23	10.20	8.14	8.50	8.62	8.50
T. sanguisuga (7)	14.53	20.39	20.95	14.25	22.07	21.23		11.05	8.14	8.50	9.84	7.04
T. sordida (8)	22.63	18.16	22.91	24.02	22.07	23.46	25.42		9.84	10.93	10.93	11.42
T. rubrofasciata BR (9)	18.44	19.27	18.72	19.27	22.63	18.72	18.72	22.63		2.31	6.56	7.29
T. rubrofasciata SI (10)	20.11	18.72	18.99	20.11	24.30	19.55	19.55	25.14	5.31		6.92	7.53
T. migrans (11)	22.07	20.39	22.91	21.23	24.30	19.83	22.63	25.14	15.08	15.92		8.87
T. rubida (12)	19.27	18.44	17.60	19.27	22.35	19.55	16.20	26.26	16.76	17.32	20.39	

Table 12. *COII* pairwise percentages of sequence divergence (lower matrix), estimated divergence time in millions of years (upper matrix)

	1	2	3	4	5	6	7	8	9	10
T. migrans Brunei (1)		1.42	5.38	8.64	7.93	9.35	8.36	5.38	5.52	7.79
T. migrans Sarawak (2)	3.26		4.39	7.65	6.80	8.50	7.65	4.53	4.67	7.22
T. rubrofasciata China (3)	12.38	10.10		7.08	6.80	8.07	7.51	0.85	0.99	6.37
R. ecuadoriensis (4)	19.87	17.59	16.29		5.81	7.51	6.80	7.22	7.08	7.51
P. megistus (5)	18.24	15.64	15.64	13.36		8.92	5.38	7.08	6.80	6.23
R. prolixus (6)	21.50	19.54	18.57	17.26	20.52		8.21	8.50	8.36	8.21
T. rubida (7)	19.22	17.59	17.26	15.64	12.38	18.89		7.93	7.22	6.09
T. rubrofasciata India(8)	12.38	10.42	1.95	16.61	16.29	19.54	18.24		1.27	6.66
T. rubrofasciata Brazil (9)	12.70	10.75	2.28	16.29	15.64	19.22	16.61	2.93		6.80
T. dimidiata (10)	17.92	16.61	14.66	17.26	14.33	18.89	14.01	15.31	15.64	

4.1.2.3 Morphometric/ genetic comparisons

Comparisons of corresponding subsets of morphometric and genetic datasets were conducted to assess the morphometric data for phylogenetic signals. Using the Mahalanobis distances calculated during the canonical variate analyses dendrograms were drawn by UPGMA cluster analysis to facilitate direct comparisons of head and wing morphometrics to the phylogenetic trees derived from the *cytb* and D2-28S sequence data (Fig. 23). The topology of the dendrogram representing the geometric morphometrics of the wings is the most congruent with both of the molecular phylogenetic trees (Fig. 23), whereas the head data demonstrate a stronger affiliation between *T. rubida* and *T. rubrofasciata*. To further assess the relationship between the genetic and phenotypic data pairwise Mantel tests were used to assess correlation of distance matrices. Mahalanobis distances for head, wing and genetic distance were included. Only the correlation between aspects of head shape themselves, and not with wing shape or genetic markers, was significant (Table. 13). Despite some congruence among tree topologies, the wing and genetic marker matrices are not significantly correlated (Table 13 and Fig. 23).

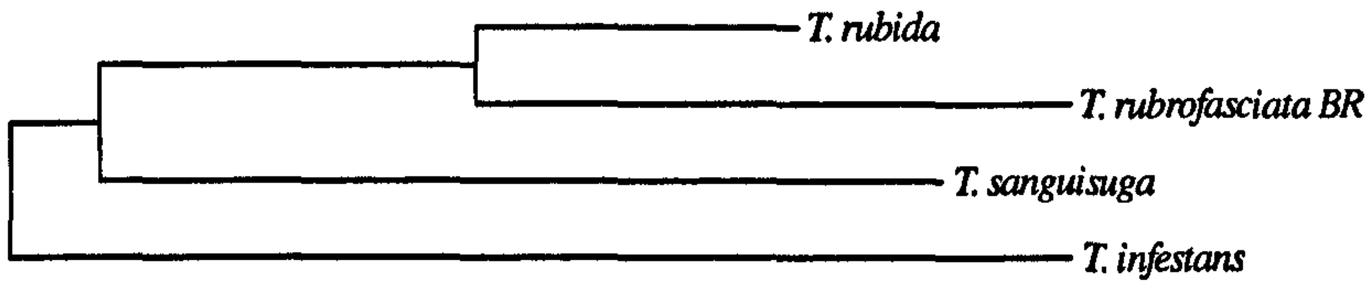

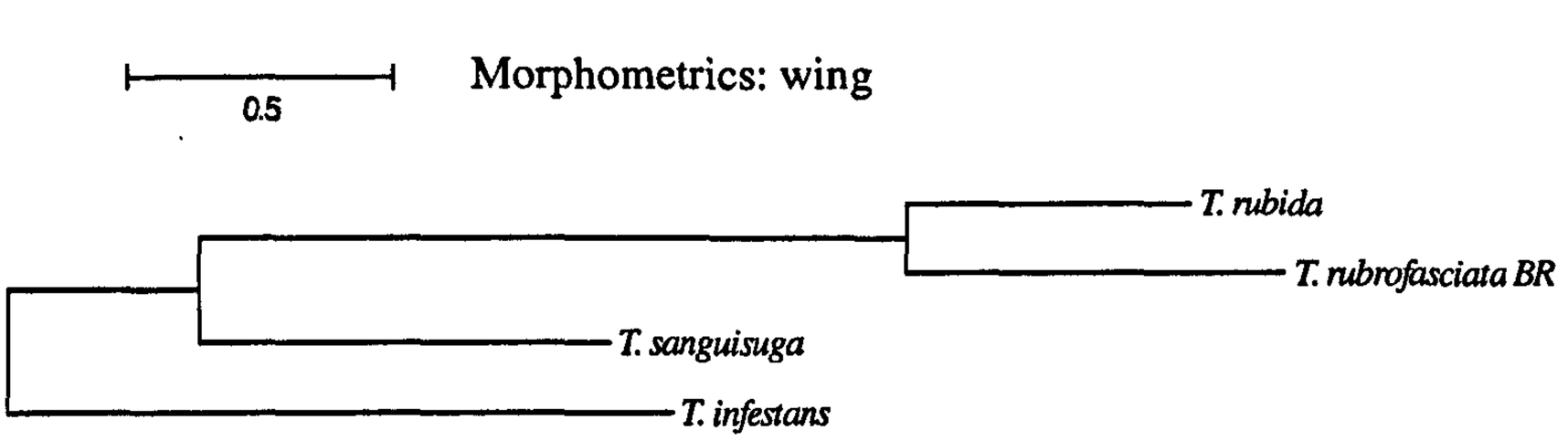

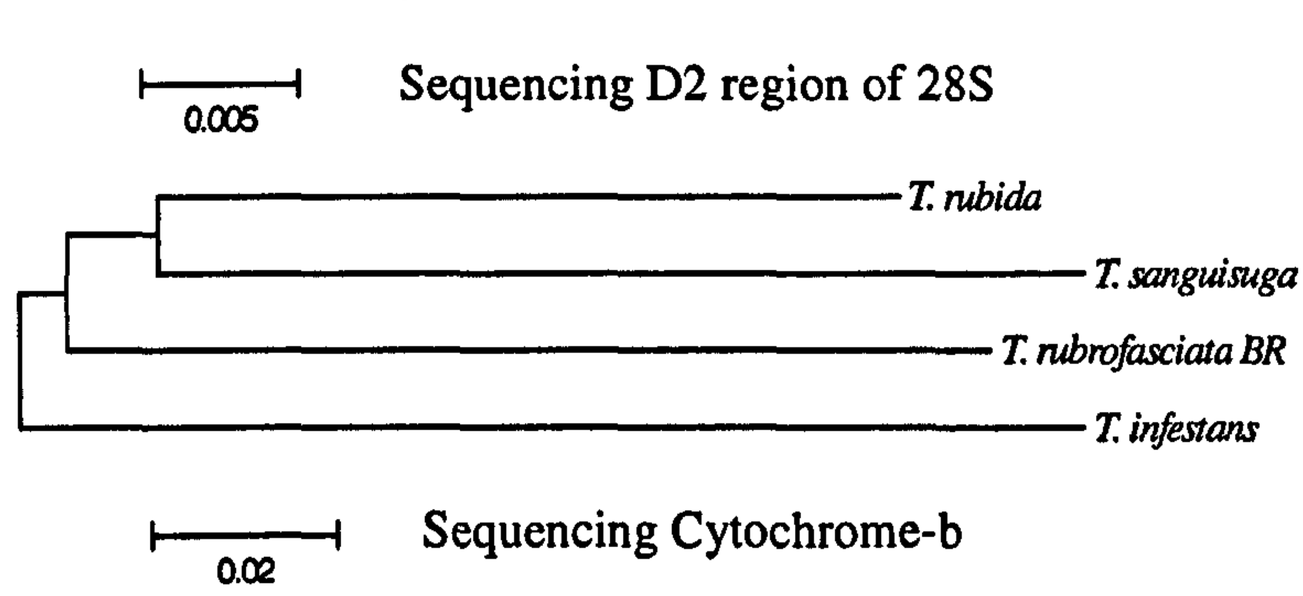

Figure 23. Comparative Neighbour-joining cluster analysis of Mahalanobis distances (derived from morphometric analysis)and genetic distances (k2p) Upper= wing shape, Middle= head shade, lower 2= genetic distance.

Table. 13 Analysis of correlation between data sets for Old and New World *Triatoma* (see Fig 24): Results of pair-wise Mantel tests between morphometric (head and wing), geographical and genetic distance matices (K2p distances).

	Dorsal	Lateral	Wing	*Cytb*
Dorsal				
Lateral	0.845 **			
Wing	0.281 NS	0.4 NS		
Cytb	0.76 NS	0.433 NS	0.36 NS	
D2	0.316 NS	-0.279 NS	0.43 NS	0.05 NS

Values = rxy, NS= not significant; ** <0.05, P values are calculated after 10000 permutations.

Morphometrics and phylogeny of the Old World and New World Triatominae: patterns of parallel and divergent morphological evolution

4.2 Part II: The Indian genus *Linshcosteus* reveals cryptic monophyly of the Old World Triatominae.

4.2.1 Introduction

The genus *Linshcosteus* Distant, 1904 is the only genus of the Triatominae endemic to the Old World, specifically the Indian subcontinent. Only one species, *Linshcosteus carnifex* Distant, 1904 was known until Ghauri (1976) described two further species, *L. confumus* and *L. costalis*. Later, Lent and Wygodzinsky (1979) described another two species, *L. chota* and *L. kali*. The genus is well characterised and can be easily differentiated from the other Triatominae by the absence of the stridulatory sulcus and by a short rostrum, not reaching the prosternum. These characteristics were designated by Lent and Wygodzinsky (1979) as apomorphic characteristics of the genera of the tribe Triatomini. Gorla *et al.*, (1997), based on morphometric analysis, demonstrated that all species of *Linshcosteus* are distinct from the species of *Triatoma* recorded from the Old World and infer that they are not closely related and suggest an independent Old World origin for *Linshcosteus,* a view emphasised by Schofield (2000). Schaefer (1998) commented on the divergent opinions of several authors as to the taxonomic position of *Linshcosteus* within the subfamily Triatominae, concluding that studies on the phylogenetic relationships of *Linshcosteus* with other Triatominae should be based not only on morphology, but also on biological and behavioural data. In response to these arguments and the morphological distinctiveness of the genus, Carcavallo *et al.*, (2000) made an adjustment to the taxonomy of the Triatominae by removing *Linshcosteus* from the tribe Triatomini to create the new tribe, Linshcosteini.

4.2.2 New species of *Linshcosteus*

4.2.2.1 Ecology

In August 2000 approximately 30 specimens of the genus *Linshcosteus* were collected close to Kalakkadu, Tamil Nadu state, south India (77° 29' 21.6" E 8° 35' 66" N, 143 m.o.s.l.). The insects were found at a single locality; an exfoliated sedimentary rock formation, approximately 10 meters high and 40 meters in length, situated on an expanse of semi-arid scrub, sparsely populated by xerophytic vegetation (Fig. 24). The bugs were captured from deep fissures and crevices in the rock (Fig. 24). Examination of the specimens revealed a new species which is described below. A pair of adults and seven nymphs were maintained alive and introduced to the colony of the insectary of the *Laboratório Nacional e Internacional de Referência em Taxonomia de Triatomíneos do Departamento de Entomologia,* Oswaldo Cruz Institute, FIOCRUZ, Rio de Janeiro, where the development of the species was studied. (Galvao *et al.,* 2004). Preliminary observations have shown that the new species is able to feed on pigeons (*Columba livia*), mice (*Mus musculus*) and humans. Preliminary analysis of blood meals by ELISA and precipitin tests from specimens subsequently collected from the same site identify a variety of prey species including canines, avians, rodents and ungulates. Indeed this species appears to exploit an opportunistic predatory feeding strategy, as opposed to close host/nest associations most typically exhibited by triatomines. More specifically their niche seems to be defined by their exploiting a refuge positioned in an otherwise exposed landscape. Further observations of the collection site include sightings of reptiles and bats secreted between the fissures of the rock. Also, consistent with the blood meal analyses, large amounts of rodent faeces were observed

A

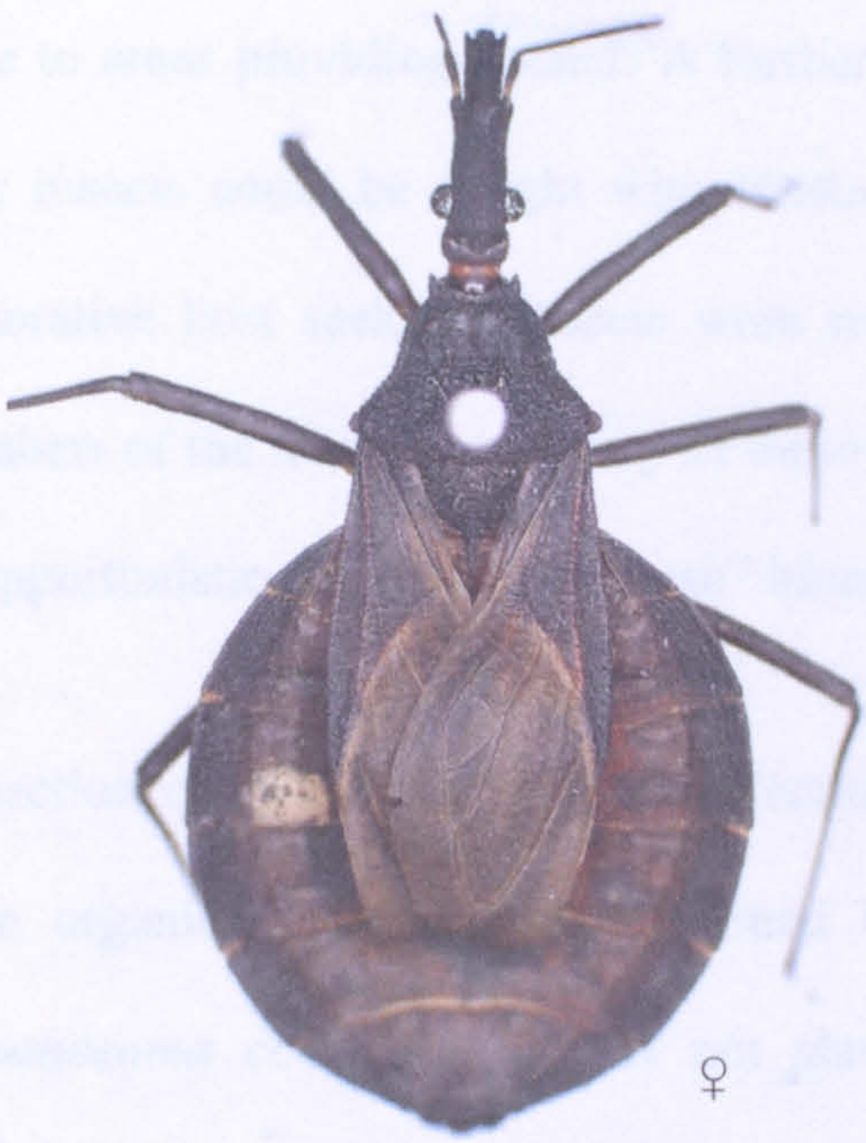

♀

♂

B

C

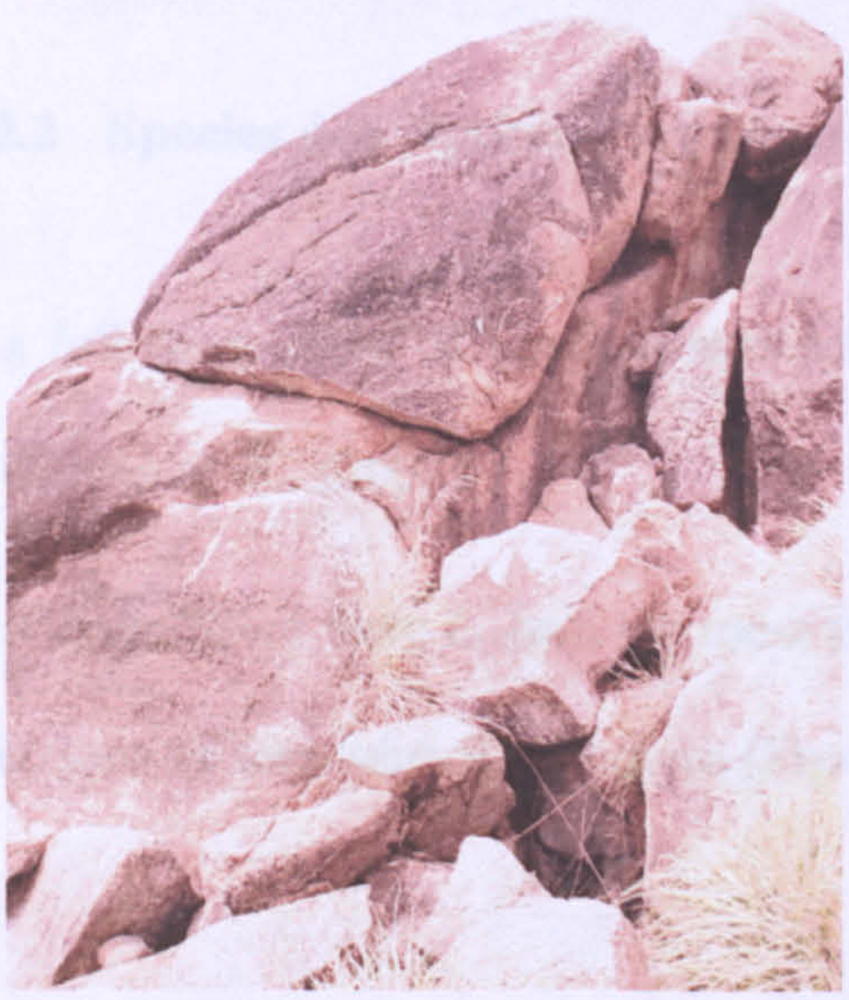

D

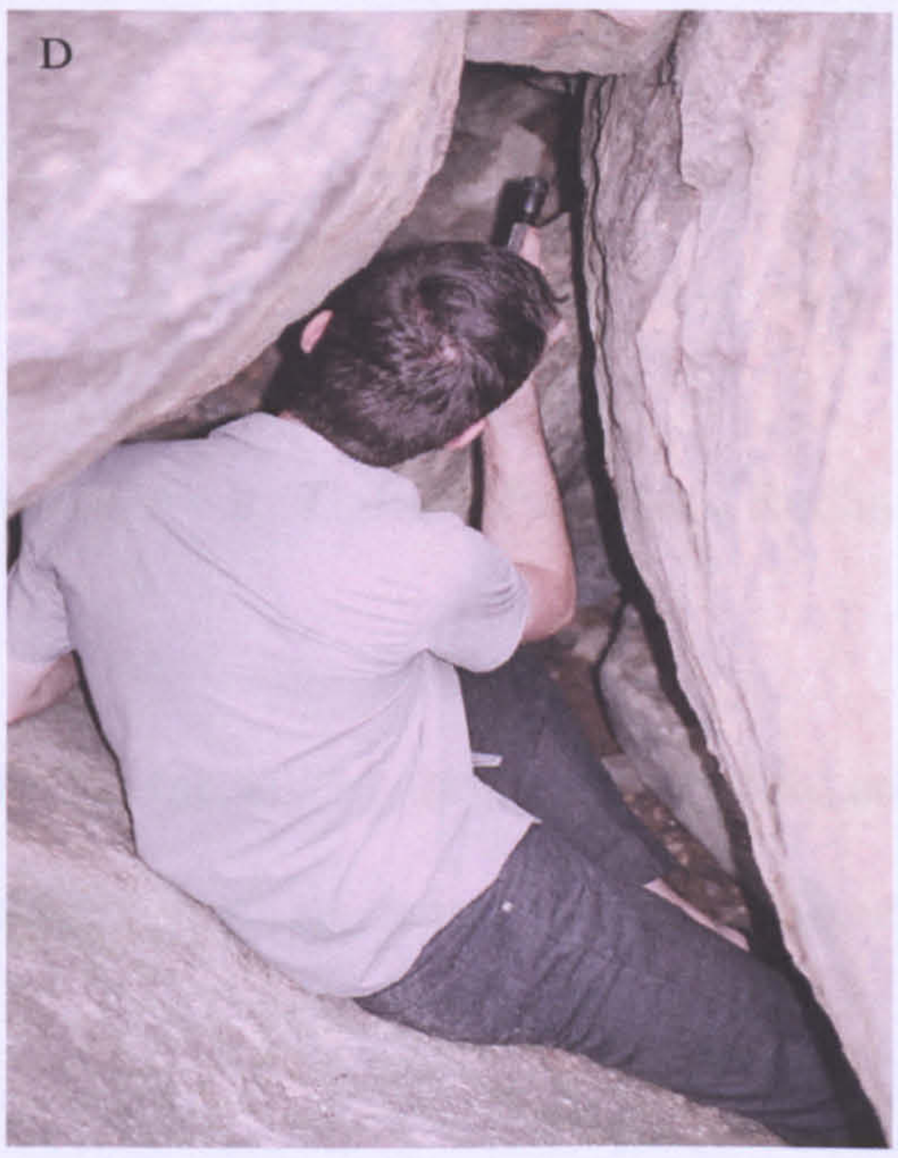

Figure 24, (previous page) A *Linshcosteus karupus sp.n.* **Female and male adults. B, collection locality near kalakkadu, Tamil Nadu, southern India. C, detail of collection site. D, bugs were collected from between rocks**

within crevices, and what appeared to be wild dog faeces accumulated around the periphery, close to areas providing shelter. A further pertinent observation is that during collection at dusk insects could be caught with limited searching since the bugs exhibited aggressive/ explorative host seeking. Insects were readily drawn from cover by the cues exuded by members of the team. A corollary of these observations supports the view that this species is an opportunistic, generalist "ambush" blood feeder.

Dissection of specimens revealed infections of flagellates in the hind gut. The identity of these organisms were later confirmed by Matthew Yeo using RAPD analysis to be *Trypanosoma conorhini* (details not shown). This species of trypanosome is a known parasite of rats (*Rattus rattus*) which is consistent with the observed prey of the insects. Furthermore, *T. conorhini* is known to be carried by *T. rubrofasciata,* which also has a distribution in India.

This constitutes the first report of the susceptibility of *Linshcosteus spp.* (and the first Old World triatomine with known natural ecology) to infections with trypanosomes also infective to mammals.

4.2.2.2 Species description

For a full description of *Linshcosteus karupus sp. n.*, Galvão, Patterson, Rocha & Jurberg. See Galvão *et al.,* (2002)

L. karupus differs from *L. kali,* the most similar species, by the very prominent anterolateral projections of fore lobe of pronotum (Figs. 25; 7 & 8), the length to width ratio of the

pronotum: 1:1.35. (*L. kali* 1:1.41), by the pilosity of the head, and many other characteristics (see Galvão *et al.*, 2002). The male genitalia of the new species has five structures which can help to separate it from *L. kali*: articulatory apparatus, parameres, endosome process, vesica and phallosome, differing in either shape, size or bristle arrangement (see Galvão *et al.*, 2002).

4.2.2.3 Traditional morphometrics of Linshcosteus

To add credence to the diagnosis of this species by discrete characters a morphometric analysis of the *Linshcosteus* including *L. karupus sp. n.* was conducted.

Nine linear distances were measured from the head capsule of 29 bugs:

Linshcosteus karupus sp. n. – *Holotype,* ♂, nº 5655, one *Paratype,* ♀, nº 5656 of the Rodolfo Carcavallo Collection, *Paratypes*, 9♂, 1♀, deposited in the Collection of the Natural History Museum, London, UK (NHM); *L carnifex – Holotype,* ♀ (NHM); *L chota – Holotype,* ♂ (NHM); *L confumus – Holotype,* ♂ *Paratypes*, 1♂, 2♀ (NHM); *L. costalis – Holotype,* ♂ *Paratypes*, 2♂, 6♀ (NHM) *L. kali – Paratype*, 1♂ (NHM). A second specimen of *L. kali* was kindly provided by Dr C. J. Schofield.

(For photographs of representative specimens of *Linshcosteus spp.* see Fig. 93 in the appendix.)

Measurements (Figs. 25, 2 &4) were obtained from calibrated digital photographs (see methods section). The isometric size free data were then subjected to covariance-matrix based principal component (PC) analysis. The first three PCs were then used to plot the relative positions of specimens, representing the six species (Fig. 26).

The first three PCs respectively accounted for 42.9% 30.3% and 8.5% (Σ= 81.8%) of the total variance in the data set. A matrix of the first eight PCs (cumulatively accounting for 100% of variance) was subjected to an Unweighted Pair-Group Method with Arithmetic mean (UPGMA) cluster analysis, from which a dendrogram was constructed (Fig. 27). The

analysis clearly demonstrates the distinctiveness of this new species, separated by PC analysis from all other species (Fig. 26).

The relationships suggested by cluster analysis (Fig. 27) agree with those observed by Gorla *et. al.*, (1997) and demonstrates that *L. karupus sp. nov.* is most similar to *L. kali* and the closely related *L. costalis*.

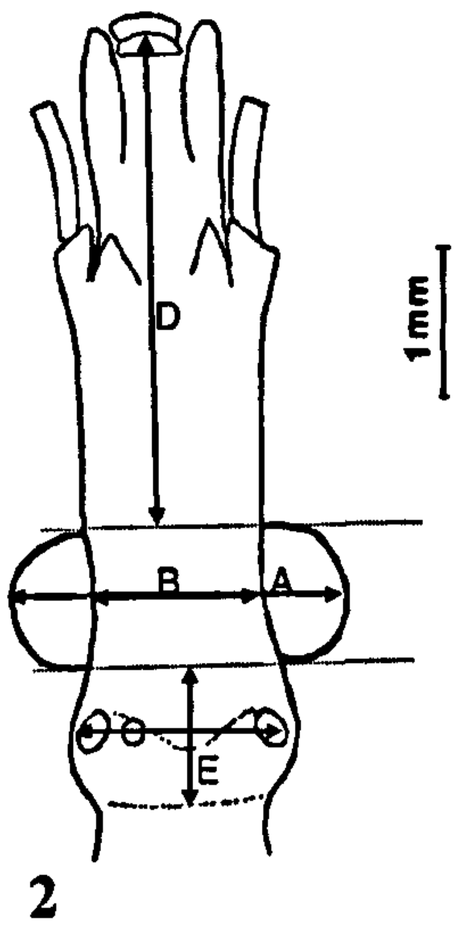

2

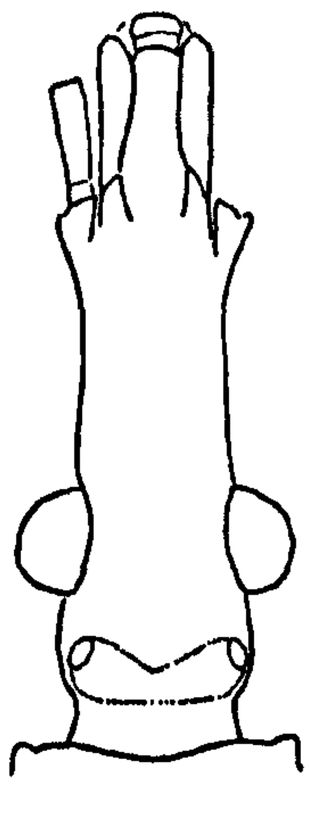

3

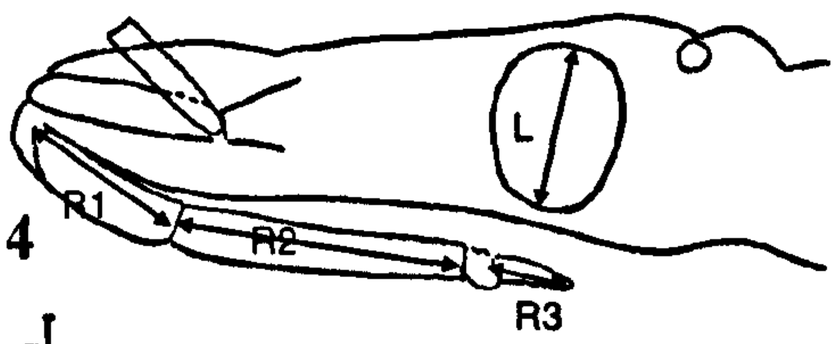

4

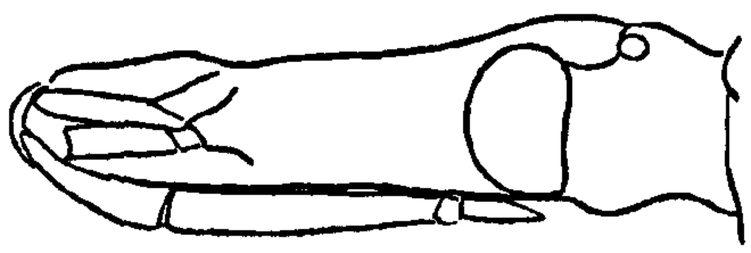

5

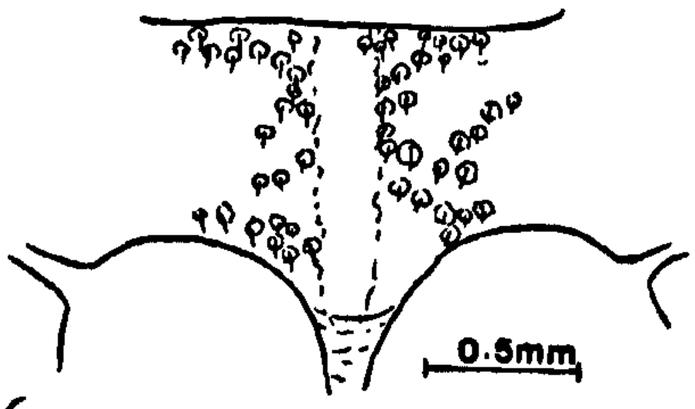

6

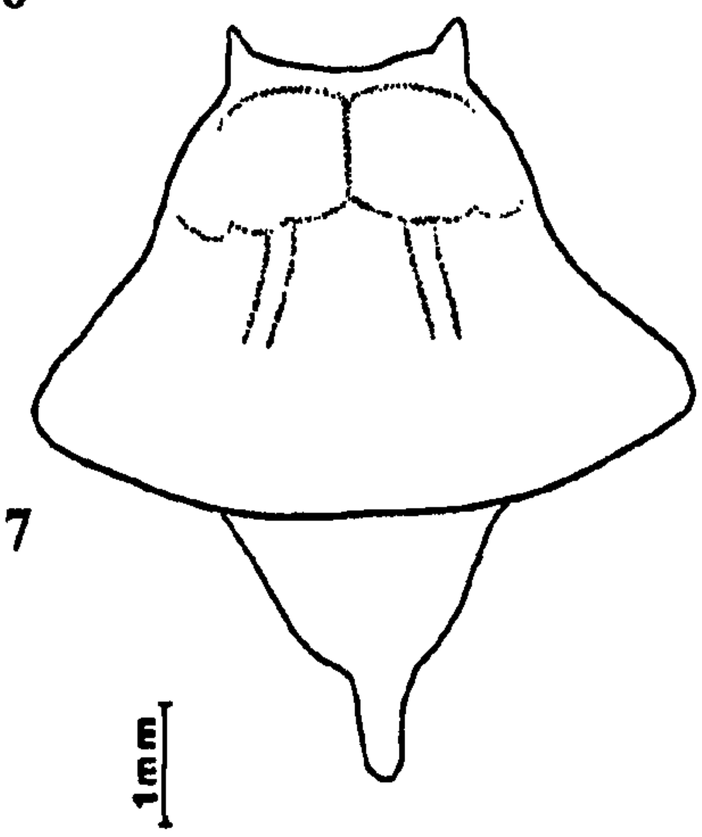

7

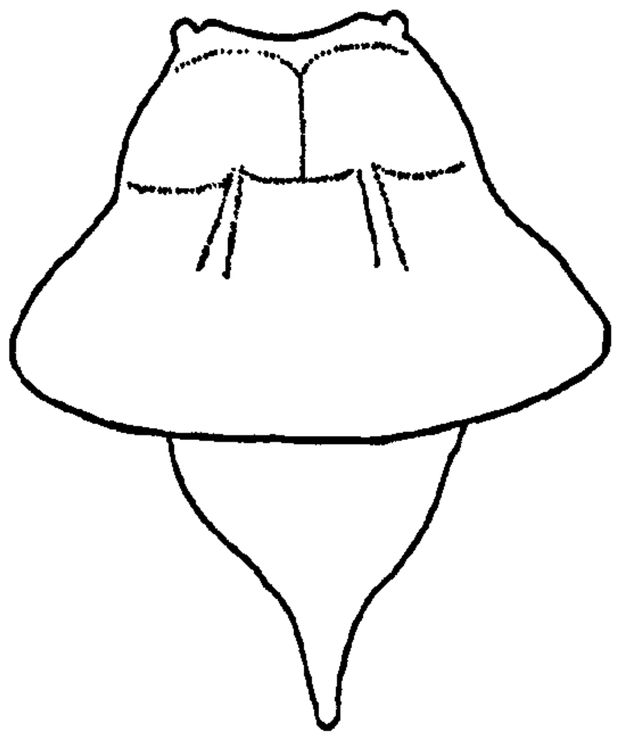

8

Figure 25. Comparative morphology: Head dorsal and lateral views: 2 and 4, *Linshcosteus. karupus*; 3 and 5, *L. kali* Lent & Wygodzinsky, 1979. Prosternum, *L. karupus*, 6. Pronotum: 7, *L. karupus*; 8, *L. kali* Lent & Wygodzinsky, 1979. 2 & 4 indicate the 9 measurements used in the morphometric analysis.

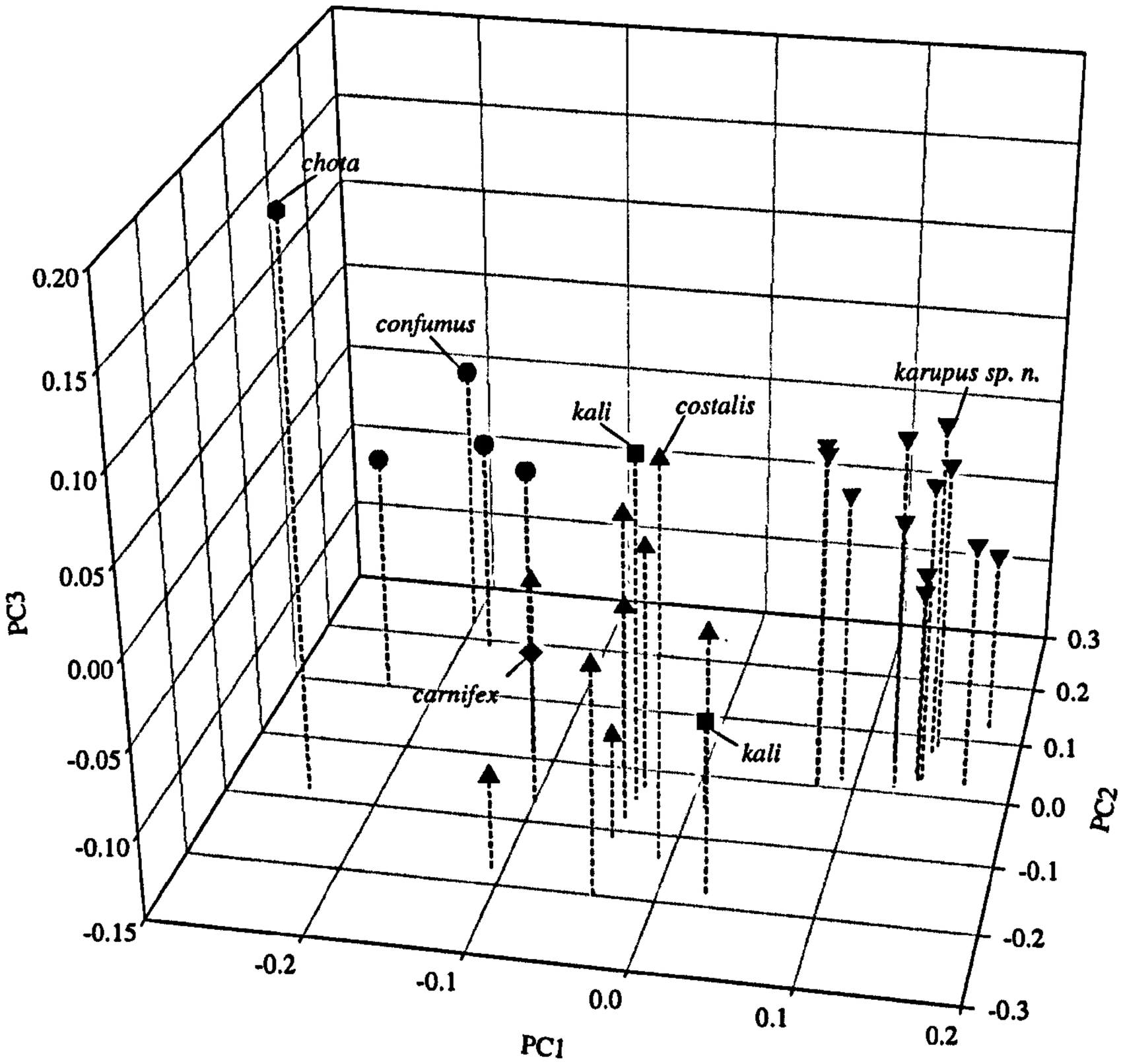

Figure 26 Morphometrics of head shape: 3D plot of *Linshcosteus spp.*, symbols indicate the relative position of each specimen in space defined by the first three principal components. PC1 accounts for 42.9% of the total variance in the data set, and PC2 & PC3 respectively account for 30.3% and 8.5%.

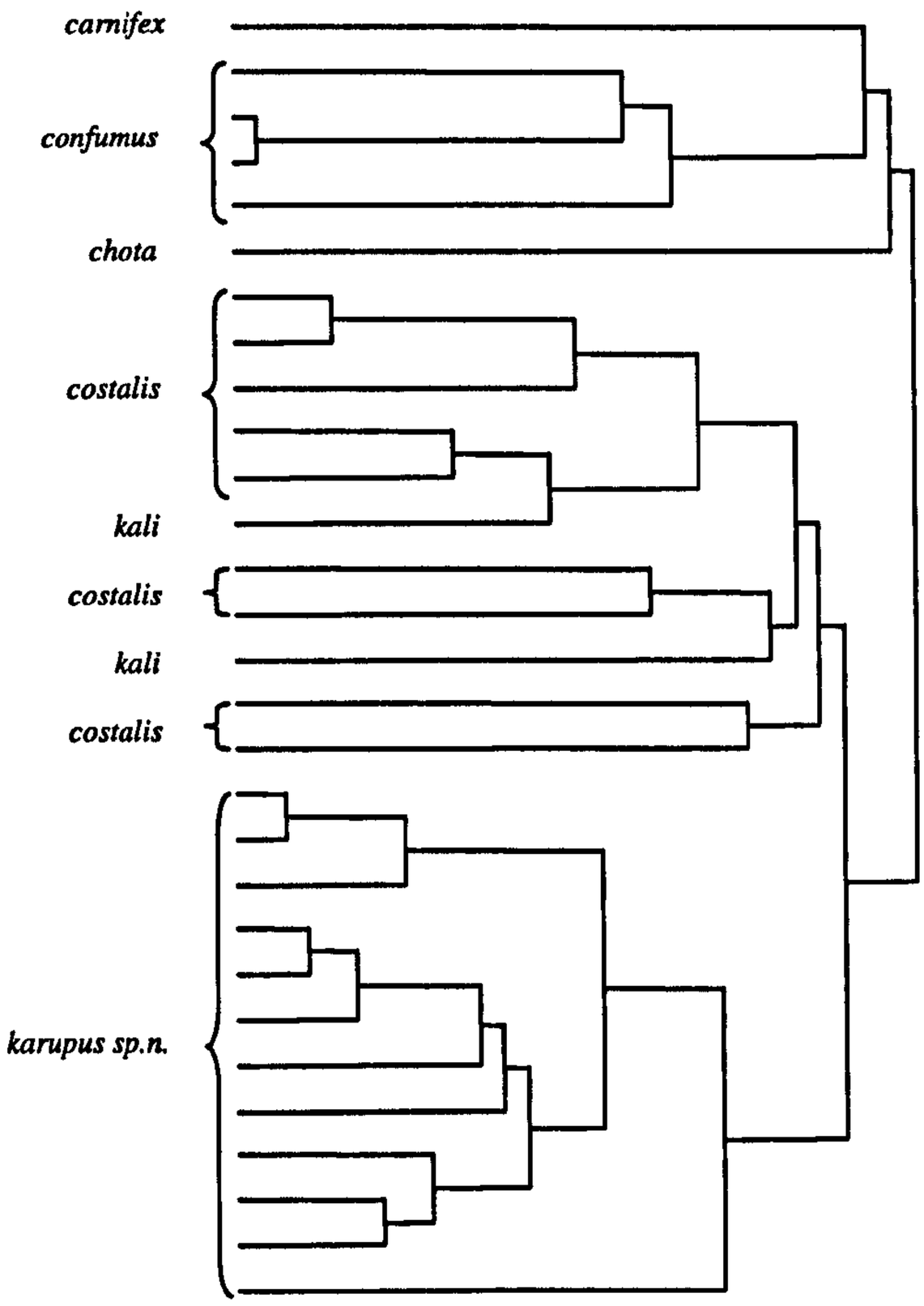

Figure 27 Morphometrics of head shape: dendrogram of *Linshcosteus spp.* constructed by UPGMA cluster analysis of the principal component matrix. Each terminus represents a single specimen.

4.2.3 Relationships among *Linshcosteus*, Old World *Triatoma* and New World Triatominae

4.2.3.1 Geometric morphometrics

The geometric morphometric analysis of dorsal head and wing shape presented in the previous section was extended to include *L. karupus* and some out groups of *Rhodnius spp.* (see Fig. 28). Fig 28 shows a plot of the first two CVs for head and wing data, accounting for 96.6% and 85.6% of the variance for head- dorsal, head and wing data sets respectively. Plots of the CV1 and CV2 of head and wing data sets (Fig. 28) coupled with TPS transformational grids (including uniform and non uniform shape components) show the

average shape configurations (representing the trends in shape change) associated with the positive and negative extremes of the abscissa (CV1) and the ordinate axis (CV2). Focusing on the placement of *L. karupus* there is a noticeable difference in the pattern of species affinities suggested by head shape in comparison to those indicated by wing shape. A long narrow head shape places it close to *T. rubrovaria* in the discriminant space defined by CV1 and CV2 for head shape (Fig. 28). However, wing shape places *L. karupus* more ambiguously with the North American and Old World species (Fig. 28).

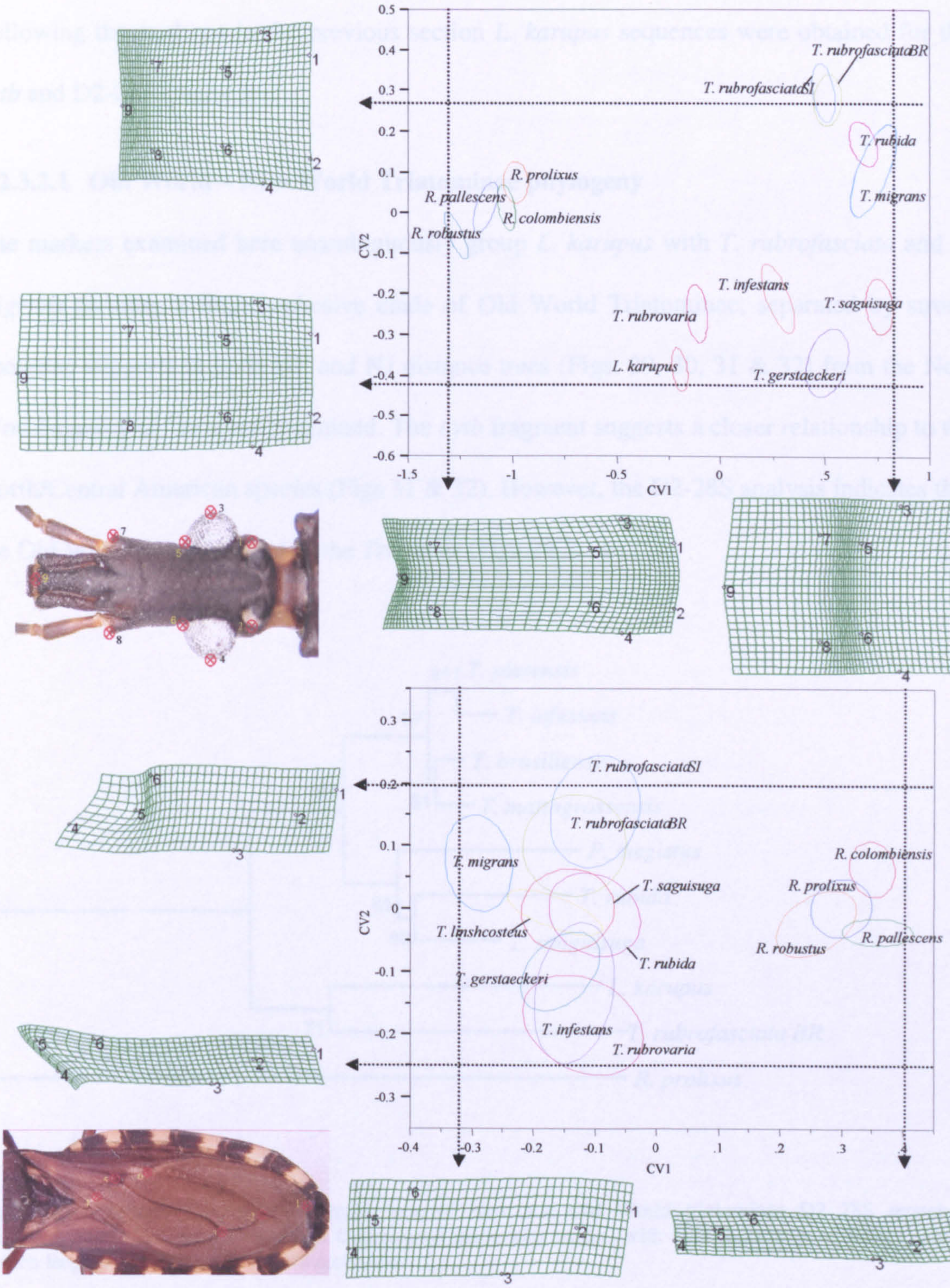

Figure 28. Geometric morphometric analysis of New and Old World triatominae: Canonical variate analysis of shape components from dorsal view of head (upper plot), and wing, (lower plot) landmark data. Polygons enclose specimens in each group The following species/population samples were used: *T. gerstaeckeri* (n=15); *T. infestans* (n=18); *T. migrans* (n=23); *T. rubida* (n=34); *T. rubrovaria* (n=22); *T. sanguisuga* (n=36); *T. rubrofasciata* from south India (SI) (n=25); *T. rubrofasciata* from Brazil (BR) (n=25); *L. karupus* (n=12); *R. colombiensis* (n=12); *R. pallescens* (n=10); *R. prolixus* (n=66); *R. robustus* (n=10); Total n =308. For the dorsal landmarks of the heads CV1 accounts for 89.6% of the total variance and CV2 accounts for 7% ($\sum$ =96.6 %). For the wings CV1 73.9%, CV2 11.7% ($\sum$ 85.6%). Thin plate splines are included showing, shape differences of the wing that correspond to the CV axes.

4.2.3.2 Molecular genetics

Following the analyses in the previous section *L. karupus* sequences were obtained for the *cytb* and D2-28S fragments.

4.2.3.2.1 Old World – New World Triatominae phylogeny

The markers examined here unambiguously group *L. karupus* with *T. rubrofasciata* and *T. migrans* forming a single cohesive clade of Old World Triatominae, separated by strong bootstrap supports in both MP and NJ distance trees (Figs. 29, 30, 31 & 32) from the New World species of *Triatoma* examined. The *cytb* fragment suggests a closer relationship to the North/Central American species (Figs 31 & 32). However, the D2-28S analysis indicates that the Old World group is basal to the *Triatoma* (Figs 29 & 30).

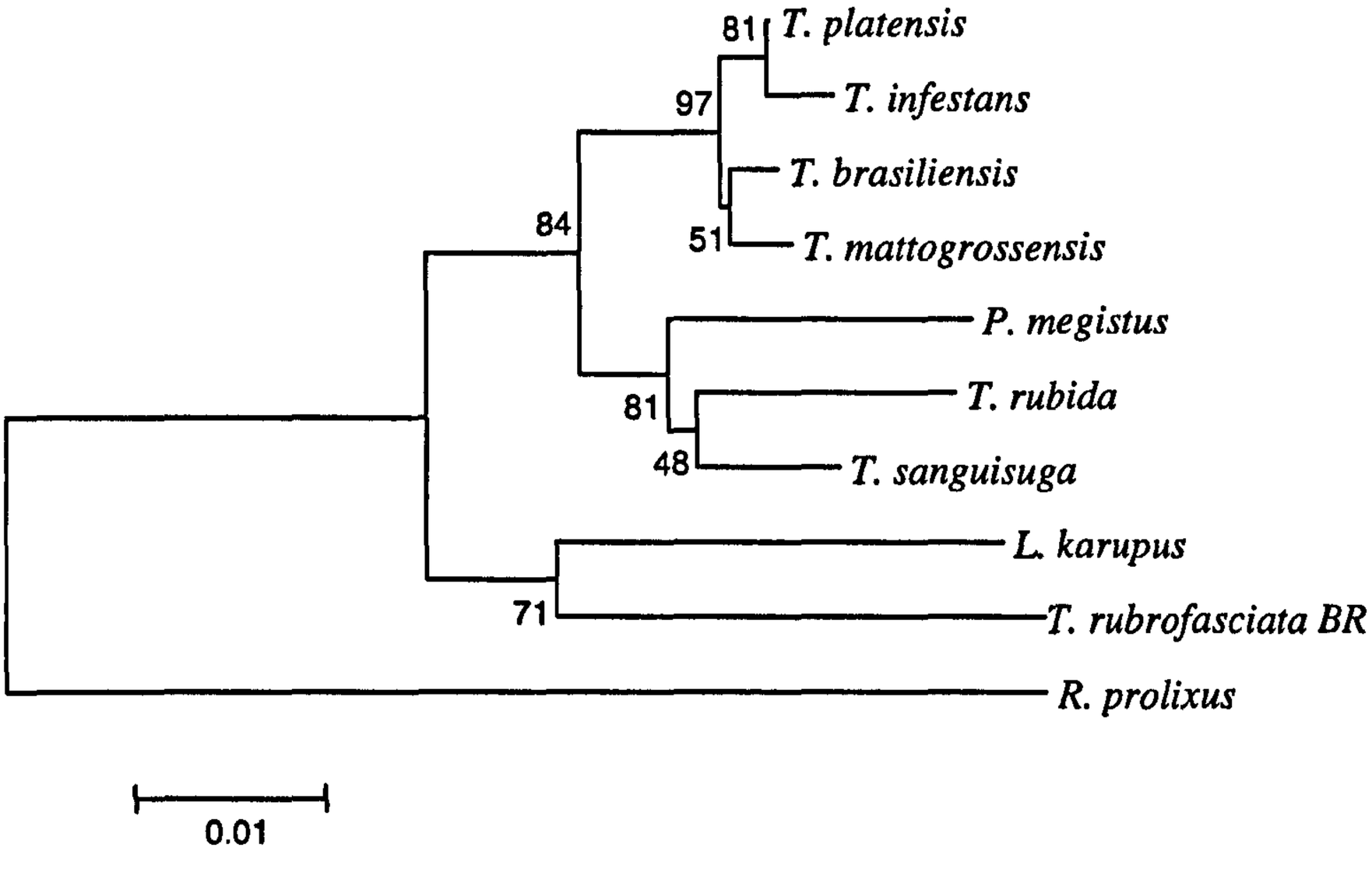

Figure29. Neighbour-joining phylogenetic tree of New and Old World triatominae D2 28S sequences including *R. prolixus* as an outgroup. Constructed using k2p model, with 1000 bootstrap replicates sum of branch lengths = 0.203, scale: substitutions/site

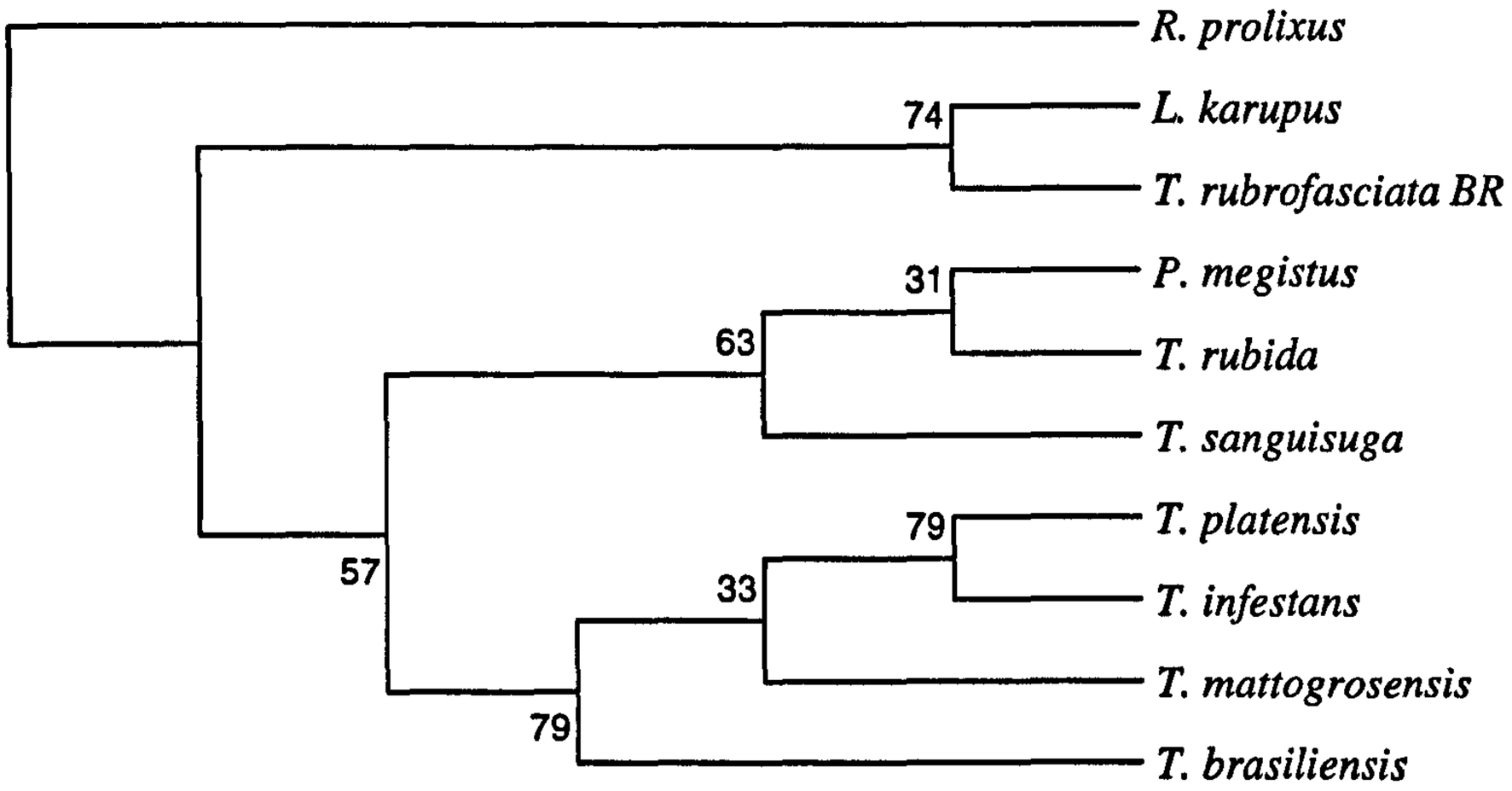

Figure 30. Maximum parsimony strict consensus phylogeny of New and Old World triatominae D2 28S sequences constructed using branch-and-bound algorithm with 1000 bootstrap replicates CI = 0.855 RI = 0.644 RCI = 0.551 (for all sites) and iCI = 0.686 iRI = 0.644 iRCI = 0.442 (for parsimony informative sites).

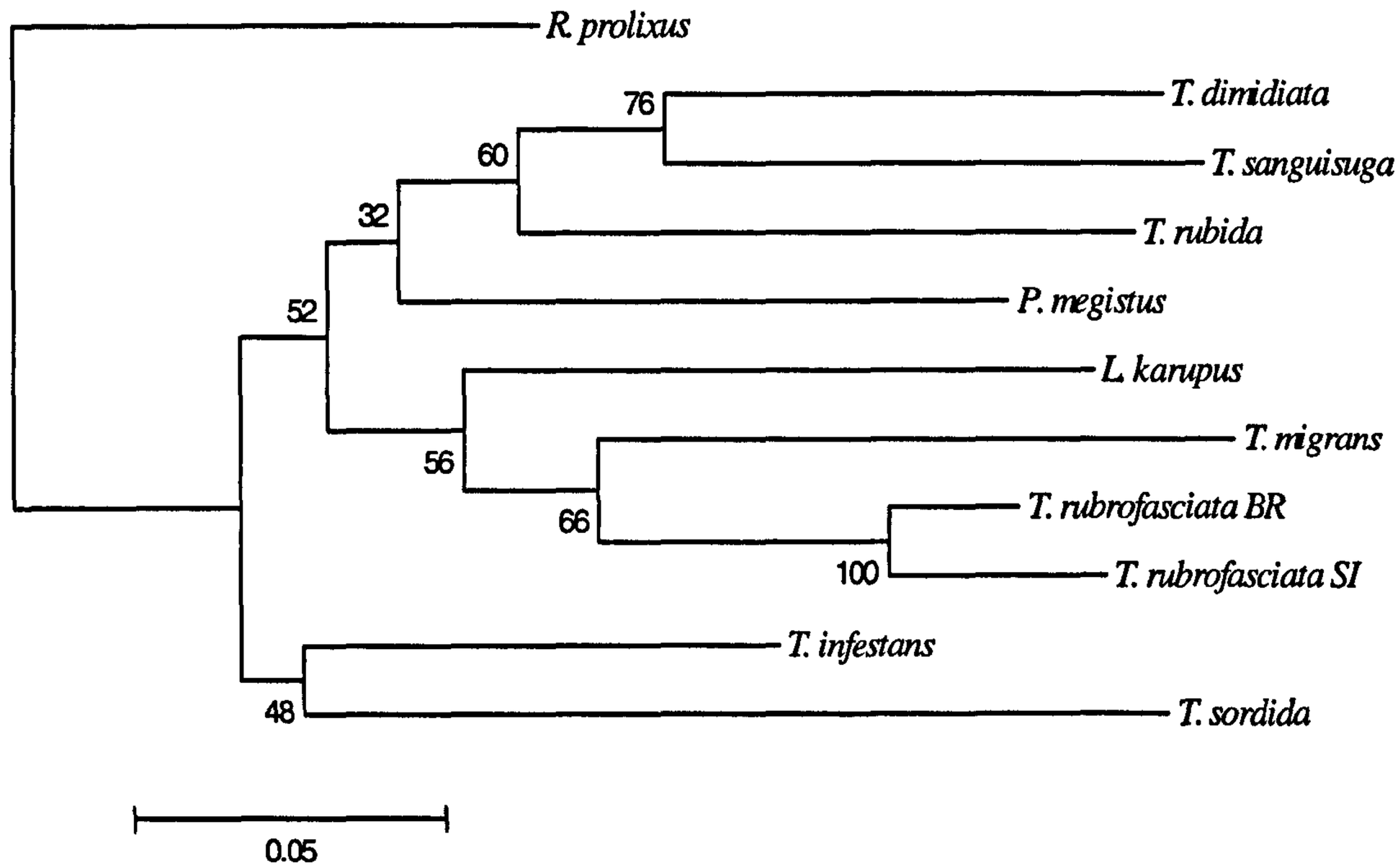

Figure 31. Neighbour-joining phylogenetic tree of New and Old World triatominae *cytb* sequences including *R. prolixus* as an outgroup. Constructed using k2p model, with 1000 bootstrap replicates sum of branch lengths = 1.13, scale: substitutions/site.

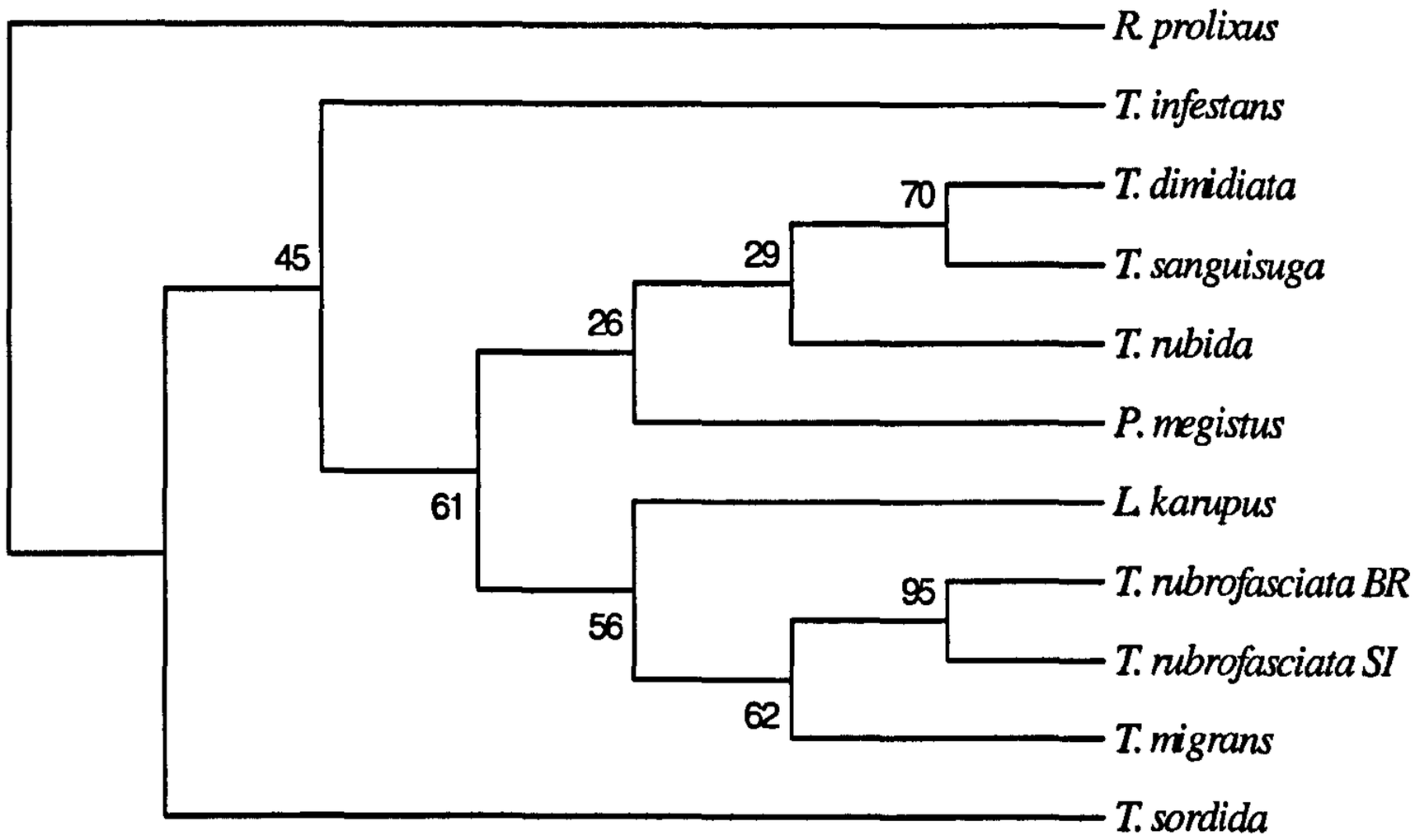

Figure 32. Maximum parsimony strict consensus phylogeny of New and Old World triatominae *cytb* sequences constructed using branch-and-bound algorithm with 1000 bootstrap replicates.

The 0.17% per million year rate of sequence divergence for D2 28S (see previous section) was applied again, as a tentative measure of divergence times. The results (Table 14) suggest that the divergence of New World from Old Triatominae occurred ~30 Mya,.

Table.14. New and Old World triatominae D2- 28S rDNA pairwise comparisons. percentages of sequence divergence (lower matrix); estimated divergence time in millions of years ago (upper matrix)

	1	2	3	4	5	6	7	8	9	10
L. karupus (1)		61.39	34.60	27.90	31.25	26.79	27.90	26.79	29.02	27.90
R. prolixus (2)	10.44		55.81	53.58	56.93	52.46	53.58	53.58	54.69	56.93
P. megistus (3)	5.88	9.49		16.74	17.86	18.98	18.98	14.51	17.86	39.07
T. platensis (4)	4.74	9.11	2.85		17.86	3.35	3.35	14.51	2.23	27.90
T. rubida (5)	5.31	9.68	3.04	3.04		16.74	17.86	12.28	18.98	35.72
T. brasiliensis (6)	4.55	8.92	3.23	0.57	2.85		3.35	13.39	5.58	26.79
T. matogrossensis (7)	4.74	9.11	3.23	0.57	3.04	0.57		14.51	5.58	27.90
T. sanguisuga (8)	4.55	9.11	2.47	2.47	2.09	2.28	2.47		15.63	31.25
T. infestans (9)	4.93	9.30	3.04	0.38	3.23	0.95	0.95	2.66		30.14
T. rubrofasciata BR (10)	4.74	9.68	6.64	4.74	6.07	4.55	4.74	5.31	5.12	

4.2.3.3 Morphometric/ genetic comparisons

With the inclusion of *L. karupus* and subsequent addition of *R. prolixus* as an out group further comparisons of corresponding subsets of morphometric and genetic datasets were conducted to assess the morphometric data for phylogenetic signals. Using the Mahalanobis

distances calculated during the canonical variate analyses, dendrograms were drawn by UPGMA cluster analysis to facilitate direct comparisons of head and wing morphometrics to the phylogenetic trees derived from the *cytb* and D2-28S sequence data (Figs. 33 & 34). Again, the topology of the dendrograms representing the geometric morphometrics of the wings is the most congruent with both the molecular phylogenetic trees (Figs. 33 & 34), whereas the head data demonstrate a stronger affiliation between *T. rubida* and *T. rubrofasciata* and show *L. karupus* as least similar, grouping more closely to *Rhodnius.* Pairwise Mantel tests were used to assess correlation of distance matrices. Mahalanobis distances for head, wing and genetic distance were included. Only the correlation between wing shape and genetic distance matrices were significant (Table. 15 and 16). From this we can infer an apparent phylogenetic signal in the morphometric data of wing shape corresponding to mt-DNA and n-DNA.

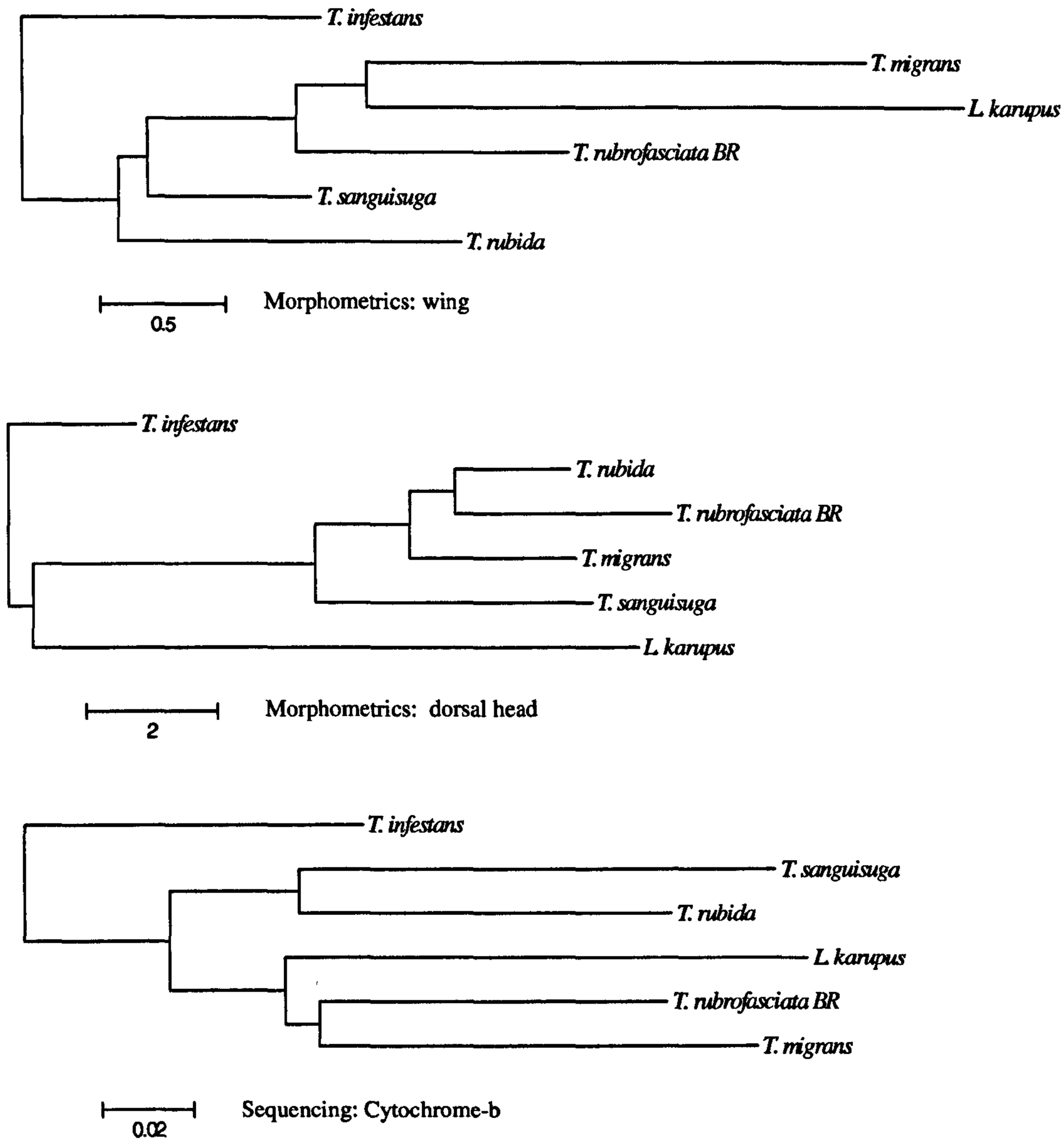

Figure 33. Comparative Neighbour-joining cluster analysis of Mahalanobis distances (derived from morphometric analysis) and genetic distances (k2p *cytb*) for New and Old World triatominae. Upper= wing shape, Middle= head shade, lower= genetic distance.

Table. 15. Analysis of correlation between data sets for New and Old World triatominae (see Fig 33): Results of pair-wise Mantel tests between morphometric (head and wing), geographical and genetic distance matices (K2p *cytb*).

xy	Matrix correlation (rxy)	p
Head Dorsal vs. Wing	0.44	0.120
Head Dorsal vs. *Cytb*	0.328	0.101
Wing vs. *Cytb*	0.502	0.027

P values are calculated after 10000 permutations (significant correlations in red)

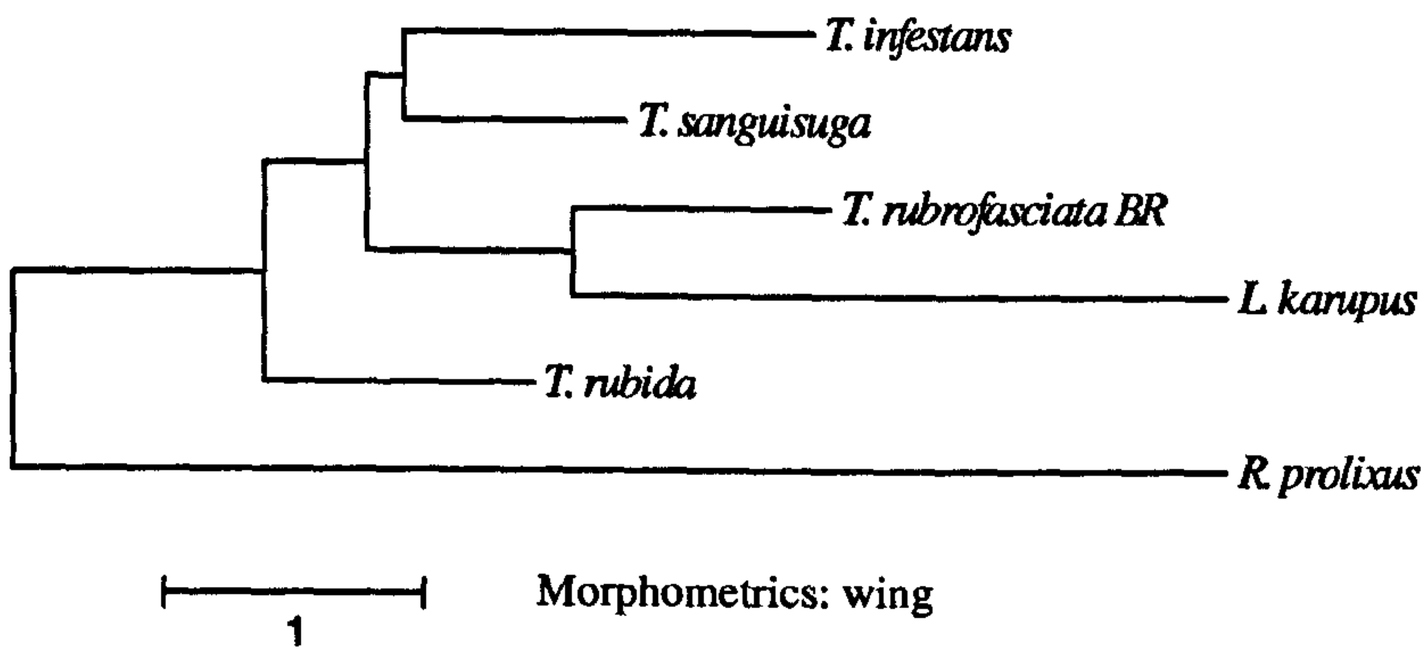

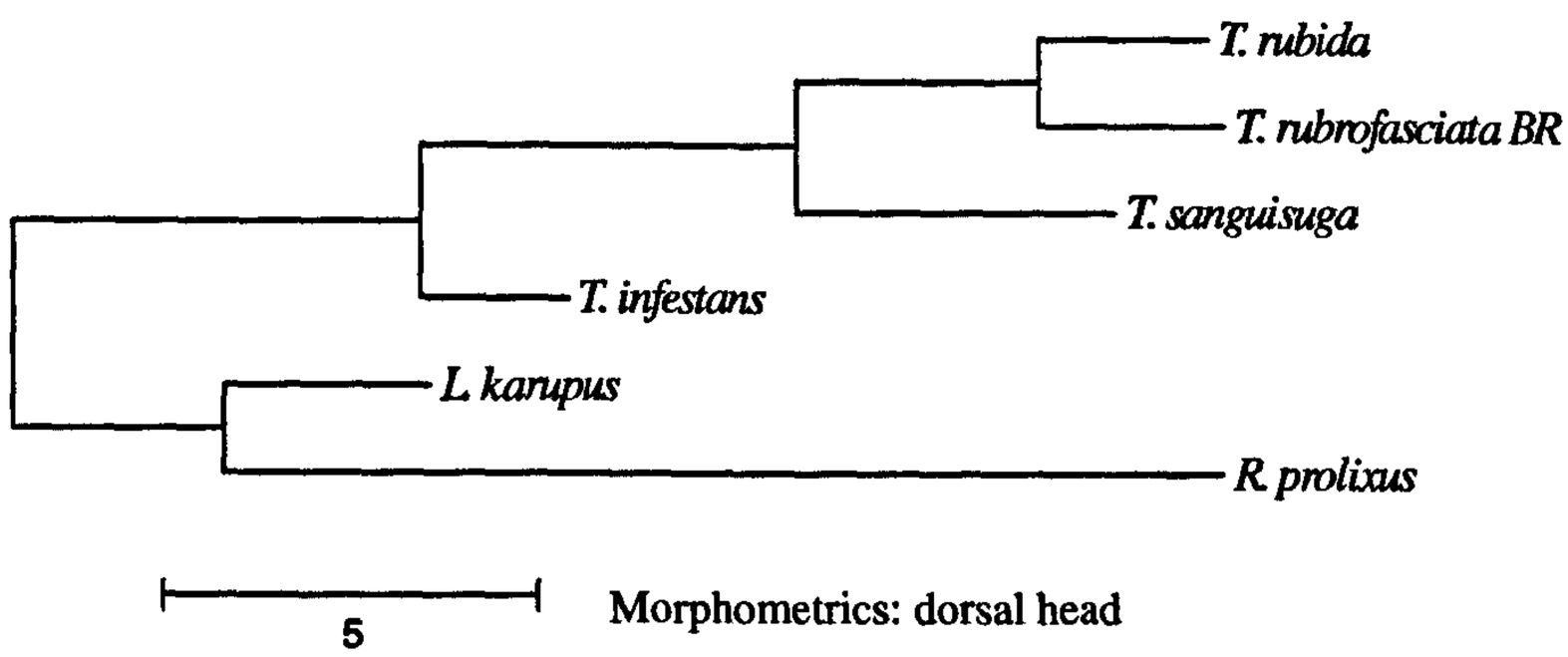

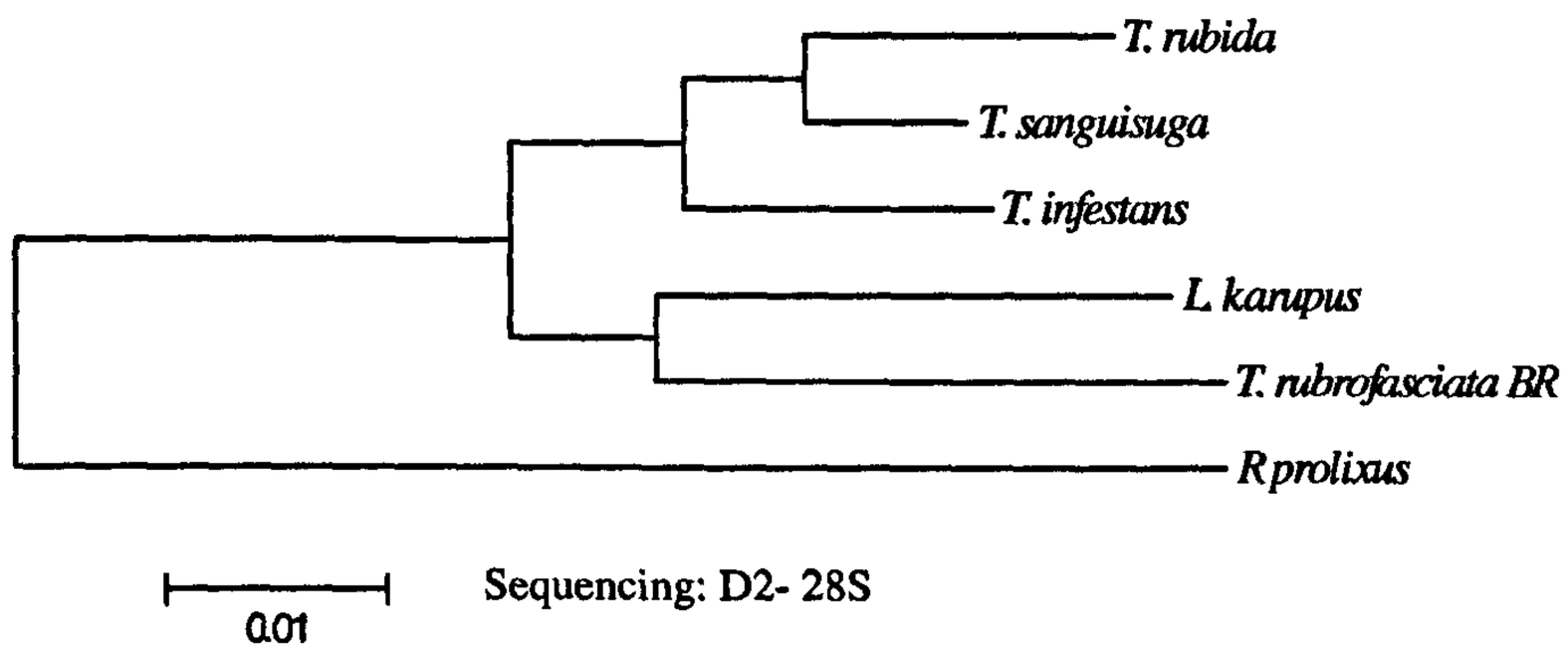

Figure 34. Comparative Neighbour-joining cluster analysis of Mahalanobis distances (derived from morphometric analysis) and genetic distances (k2p D2-28S) for New and Old World triatominae. Upper= wing shape, Middle= head shade, lower= genetic distance.

Table 16. Analysis of correlation between data sets for New and Old World triatominae (see Fig 33): Results of pair-wise Mantel tests between morphometric (head and wing), geographical and genetic distance matices (K2p D2-28S).

xy	Matrix correlation (rxy)	p
Head Dorsal vs. Wing	0.72	0.06
Head Dorsal vs. D2 28S	0.69	0.11
Wing vs. D2-28S	0.923	0.01

P values are calculated after 10000 permutations (significant correlations in red)

4.3 Discussion

4.3.1 *Triatoma rubrofasciata* populations

Morphometric comparisons of allopatric populations of *T. rubrofasciata*, representing much of its worldwide distribution, showed a high level of homogeneity by morphometric analysis (Fig. 10, 11, 12 & 13). This reinforces the concept of single species in spite of its known morphological variation. However, no evidence for a clinal series was seen, except for the larger size of specimens from South India (see Patterson *et al.* 2001). Studies of two other highly domesticated and widely dispersed species of Triatominae, *R. prolixus* and *T. infestans*, have shown that the largest specimens are usually associated with the putative geographical origin (Dujardin *et al.* 1998b). In the case of *T. rubrofasciata* however, the working hypothesis of dispersal by association with man and shipping (Gorla *et al.* 1997) presents the possibility that populations could be transferred relatively frequently from one location to another, distorting any clinal series. Such an idea could also explain the relative homogeneity of the various allopatric populations. However the differences established by geometric morphometrics of wings (Fig. 15), comparing two mainland samples with two from islands may indicate subtle founder effects.

The diversity among the haplotypes of mitochondrial genes from geographically disparate populations of *T. rubrofasciata* are within the level of intraspecific variation observed for other triatomine species (see other chapters of this thesis). Indeed, the studies of *R. ecuadoriensis* and *R. prolixus* populations in relative sympatry revealed levels of intraspecific variation in the range of 4-7% sequence divergence, whereas the range observed among *T. rubrofasciata* samples from Brazil, China and India is only 1.9-2.9%. This adds credence to the single species concept for *T. rubrofasciata* and as a snapshot of population structure suggests that the global population is relatively panmictic, again

supporting the hypotheses that they have dispersed passively and recently in association with shipping.

4.3.2 Origin of *T. rubrofasciata* and the Old World *Triatoma*

The aim here is to investigate the evolutionary history of *T. rubrofasciata* in relation to its seven Old World relatives, particularly *T. migrans* and representatives of several of the New World species groups of *Triatoma*.

In relation to other Old World species of *Triatoma*, my findings endorse the conclusions of other authors that group these species with *T. rubrofasciata* as the *rubrofasciata* complex, characterised by the microstructure of the adult venter and inferring monophyly from this apomorphic character (Lent & Wygodzinsky, 1979; Schofield, 1988). This conclusion was endorsed by Gorla *et al.*, (1997) from a morphometric study using characters of head, thorax and abdomen. Gorla *et al.*, (1997) proposed a Brazilian origin for *T. rubrofasciata*, recalling that parts of north-eastern Brazil had at one time been colonised by Dutch planters and so implying a maritime link with the then Dutch East Indies.

In contrast, our studies would suggest a North American ancestral origin, but not at all as recently as previously speculated based on the morphometric assessment alone (Patterson *et al.* 2001). The morphometric similarities between *T. rubrofasciata* and the North and Central American species, particularly *T. rubida*, with less similarity to South American species of *Triatoma.* (Fig. 11 & 12) have been revealed by the molecular analyses of mt-DNA and n-DNA to be affected by processes of parallel evolution by allopatric convergence. The particular similarity of head shape between *T. rubrofasciata* and *T. rubida* is perhaps attributable to their shared ecology of rodent host association. The lesser similarity observed for wing shape supports a theory of host–responsive morphological adaptation leading to convergence because the convergent morphology pertains to those structures involved in feeding behaviour specifically (i.e. head and mouthparts). In the partial least squares analysis

of head and wing shape the disassociation of *T. rubida* and *T. rubrofasciata* is more variable through the dimensions of shape covariation compared to species that are closely related, e.g. *T. sanguisuga* and *T. gerstaeckeri*, their association remaining relatively constant through the dimensions (Fig. 16). This reveals the power of the partial least squares method for detecting discontinuous patterns of morphological evolution in morphometric studies, particularly when coupled with phylogenetic data.

There is increasing evidence that the genus *Triatoma* is polyphyletic. Such an idea was indicated from morphological characters by Lent & Wygodzinsky (1979), and has received support from morphometric studies (Dujardin *et al.*, 2000) and comparison of ITS-2 rDNA sequences (Marcilla *et al.*, 2001). Two major clades are inferred within the genus, representing species of South America and those of Central and North America north of the Isthmus of Panama. Our studies are in line with this idea, showing a clear and consistent separation between representatives of the South American species and those of Central and North America (Figs. 20 & 21).

As observed in other sections here, particularly in the case of *R. prolixus* (see also Fitzpatrick *et al.* submitted) mitochondrial DNA markers can give misleading representations of intraspecific relationships due to introgression. It has also been observed that incongruence between mt-DNA and n-DNA reveal that interspecific hybridisation can render speciation histories based on mt-DNA alone as extremely misleading (Shaw 2002).

Whereas, we previously speculated that the Old World *Triatoma* arose very recently by a rapid process of speciation (Patterson *et al.* 2001). Given the molecular evidence subsequently presented here and estimates of divergence dates (see Table 10 and 14) it seems likely that the Old World Triatominae originated as a result of American ancestral stock migrating across the Bering land bridge (BLB) in the warm Eocene ~30 Mya. This

period corresponds to the appearance of the first modern mammals (including bats) and with the formation of the Himalayas. It is possible that the Old World lineage represents the remnants of a process of expansion and subsequent extinction (see Fig. 35). Extinction could, at least in part, have been due to competition. Schofield (2000) suggests that the extant Polyctenidae are the dominant haematophagous Hemipterans in Asia and have impeded the establishment of the Cimicidae and Triatominae. Isolation in India gave rise to *Linshcosteus* and subsequent limited dispersal of the Old World lineage from the Indian subcontinent gave rise to the Old World *Triatoma*. It is likely that cooling during the Oligocene and late Miocene prevented further migration across the BLB which opened ~ 7.5 – 5 Mya (Marinovich and Gladenknov, 1999).

Previous to this, the *Triatoma* had diverged from the *Rhodnius* up to 90Mya (Gaunt and Miles, 2002). The divergence date between North and South American *Triatoma* (~20Mya) corresponds to the earliest (only) occurrence of a member of the Triatominae in the fossil record, from Dominican amber and apparently *Triatoma* (Poinar 2005). Therefore, migration prior to the formation of the Isthmus of Panama, which occurred no earlier than 3.5 Mya (Coates and Obando, 1996, Haug and Tideman, 1998) must have been by passive dispersal with birds and mammals. Occurrences of endemic Caribbean triatomines, both extant (e.g. *T. flavida*), and extinct (represented by the fossil mentioned above), support a theory that bugs could have dispersed from South to North America by "stepping stones" between islands that later constituted the Isthmus or via the Proto-Antillean landmass. Such a process would account for the apparent early radiation and dispersal, prior to the final formation of the Isthmus. A mode of passive dispersal is evidenced in the amber fossil (Poinar 2005), where hairs, deduced to be those of a bat, were also found. I speculate that other triatomine groups could have spread from South to North America with perhaps subsequent extinction events

(see Fig. 35), resulting in the small specialised extant group of mainly rodent associated North American *Triatoma.*

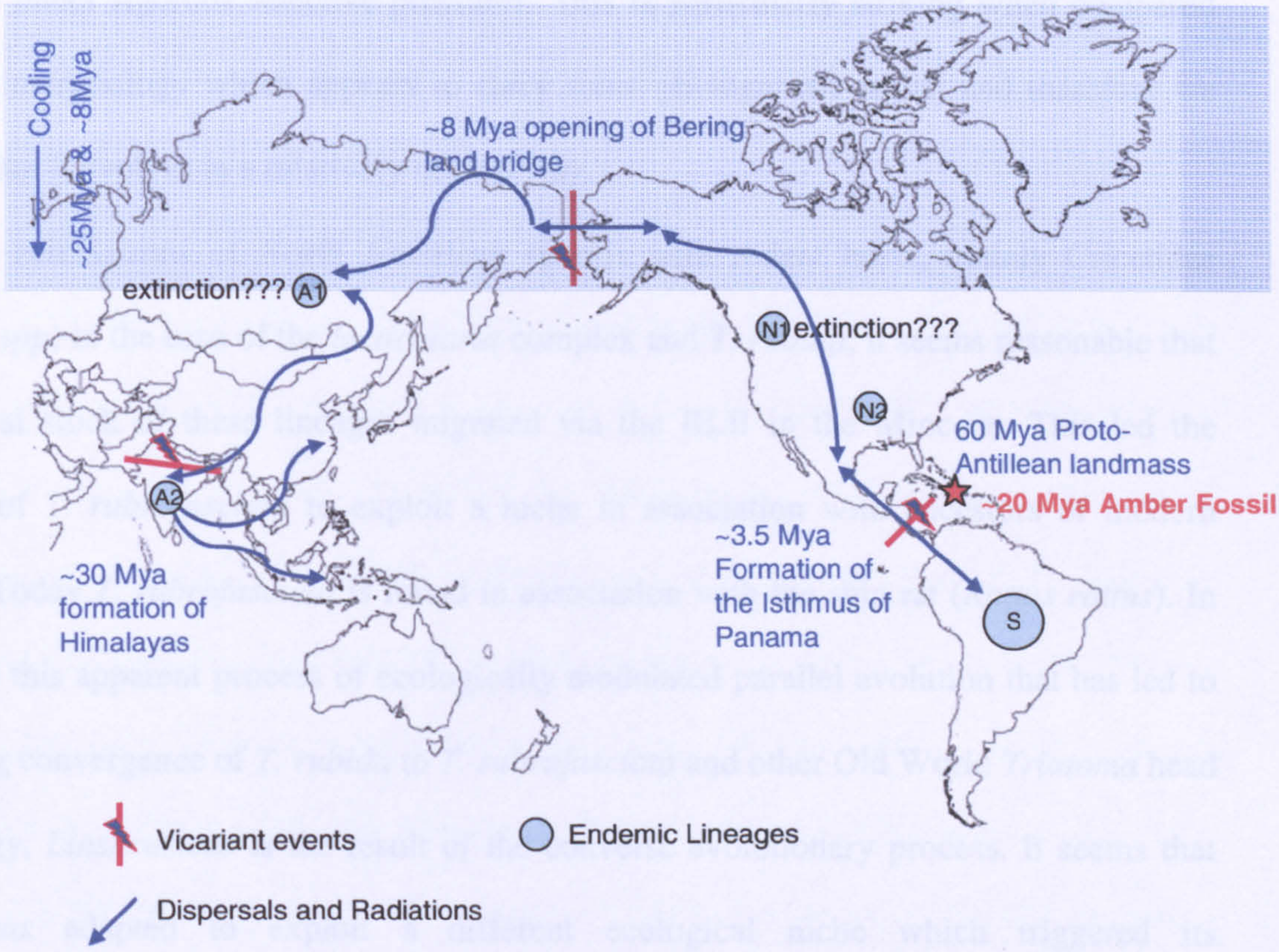

Figure 35. Hypothesised scheme of the radiation and formation of the Old and New World *Triatoma* lineages. Showing vicariant events and dates and routes of dispersal. A1 represents lineages that possibly became extinct in Asia, A2 represents the extant lineages of Old World *Triatoma.* N1 represents a possibly extinct lineages of Triatominae and N2 the extant group. S represent extant South American *Triatoma.*

4.3.3 Old World divergence; host switching and convergent parallel evolution

Our relative estimates of the date of divergence from New World lineages are similar for Old World *Triatoma,* including *Triatoma rubrofasciata* and *Linshcosteus*. This has concurrently been demonstrated during the course of this work by other authors (Hypsa *et al.* 2002; Paula *et al.* 2005). The striking diversification and adaptation of *Linshcosteus* is discussed at greater length in a subsequent section of this thesis (Head shape evolution). Suffice is to say, this genus has adapted so acutely and strikingly, that it is described as a separate tribe from the Triatomini (Carcavallo *et al.*, 2000; Galvao *et al.,* 2004). However, considering that the

weight of cladistic and taxonomic work focuses on head morphology (Schaefer & Coscaron, 2001), the discontinuity of head morphology with phylogeny can be reconciled with the working hypotheses arising from this work, i.e. that head morphology, and head shape in general, is under rigorous selective pressures. This is particularly striking when compared with wing morphology which appears to carry some phylogenetic signal and therefore we postulate that it evolves in a relatively neutral way.

Given the associations of North American species with rodent hosts, mainly Cricetidae (*Neotoma spp*) in the case of the *lecticularia* complex and *T. rubida*, it seems reasonable that an ancestral stock of these lineages migrated via the BLB in the Miocene. This led the ancestors of *T. rubrofasciata* to exploit a niche in association with ancestors of modern Muridae. Today *T. rubrofasciata* is found in association with the ship rat (*Rattus rattus*). In contrast to this apparent process of ecologically modulated parallel evolution that has led to the striking convergence of *T. rubida* to *T. rubrofasciata* and other Old World *Triatoma* head morphology, *Linshcosteus* is the result of the converse evolutionary process. It seems that *Linshcosteus* adapted to exploit a different ecological niche which triggered its morphological diversification. Such processes of discontinuous morphological evolution, or type switching, are often only detectable by molecular methods, for example in the case of Carabid ground beetles (Osawa *et al.* 2004). The demonstration of the phylogenetic signal in wing landmark data by correlation to genetic distances highlights the facility of morphometrics in detecting conserved morphology that has evolved relatively neutrally.

5 Higher taxonomic relationships within the Triatominae and to other reduviid subfamilies: support for a polyphyletic origin of haematophagy within the Reduviidae.

5.1 Introduction

5.1.1 Biosystematics of the Reduviidae

The predatory assassin bugs (Hemiptera: Heteroptera: Cimicomorpha: Reduviidae) are one the largest and most morphologically diverse families of the true bugs, composed of approximately 23-32 subfamilies with some 6000 species (Maldonado Capriles 1990). With the exception of a few aberrant plant-feeding members (Bérenger & Pluot-Sigwalt 1997) and the blood-sucking triatomines all reduviids are predators on other invertebrates. The Reduviidae have a worldwide distribution. The subfamily composition and relationship of Reduviidae with other heteropteran families remain unsettled (Ambrose 1999). As for the phylogentics of the whole Reduviidae family, very little is clear. A simple phylogenetic arrangement was postulated by Usinger (1943) (Fig. 36) with almost no subsequent investigations. Ambrose (1999) presented a rather speculative evolutionary hypothesis for the derivation of entomophagous and haematophagous behaviour from cimicoid herbivorous stock for a selection of subfamilies. This hypothesis is based on a few morphological observations and requires affirmation by robust phylogenetic analysis. Ambrose (1999) states that "Family Reduviidae still contains the highest number of subfamilies among all heteropterus families and there is an absolute need for its comprehensive reassessment". Moreover without a valid systematic structure based on robust

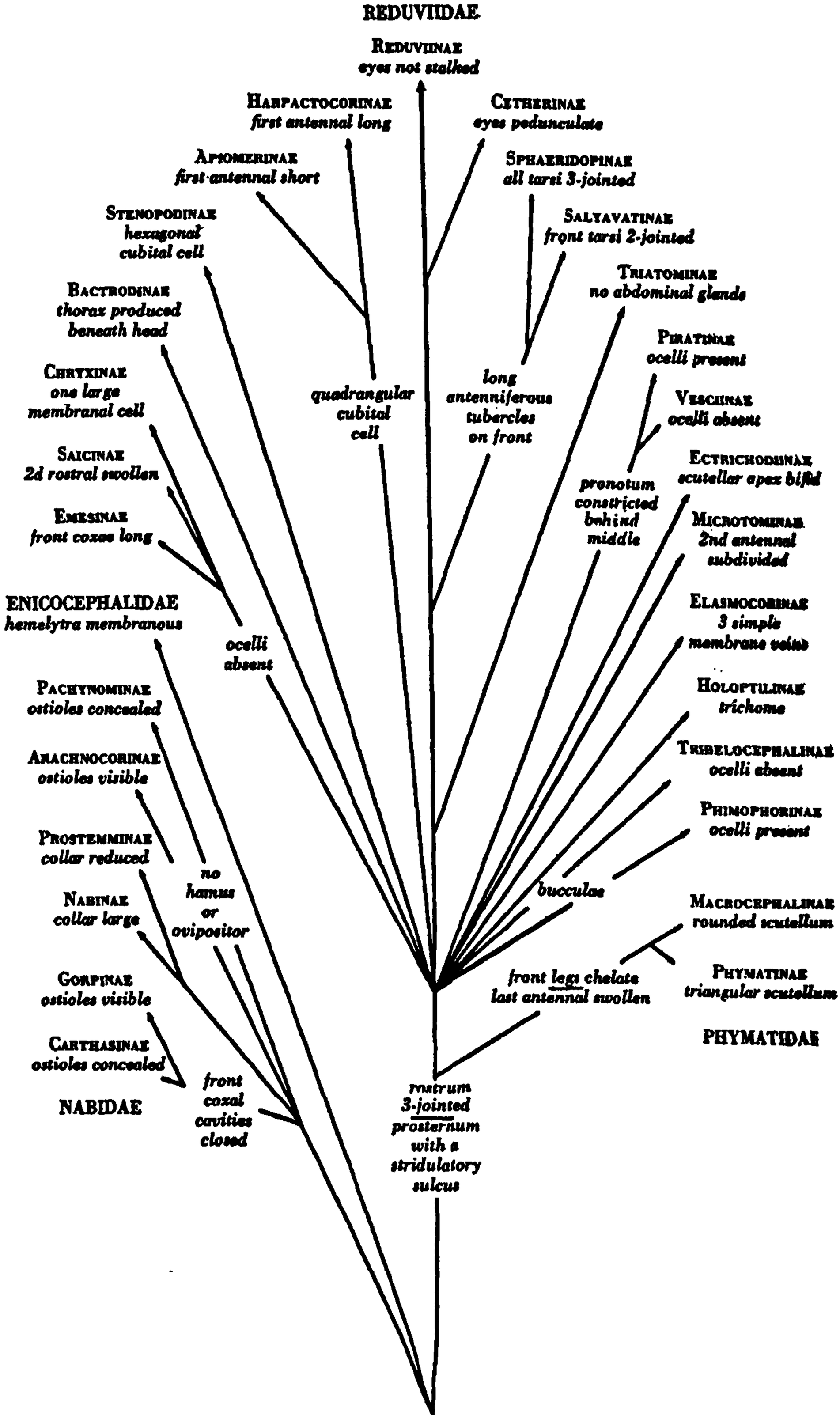

Figure 36. Simple phylogenetic key to the families and subfamilies of Reduvioidea, after Usinger (1943)

phylogenies, evolutionary processes cannot be examined.

In addition to the Medical importance of the Reduviidae, due to the Triatominae, several reduviid subfamilies are beneficial, with obvious socio-economic relevance. In East Africa *Tinna wagneri* preys on mosquitoes in houses. Many Reduviidae are natural predators of crop pests, such as *Phonoctonus spp.*, which feed on cotton stainer bugs (*Dysdercus spp.*) and *Sycanus collaris,* which preys on slug moth caterpillars (Limacoridae larvae). *Amphibolus venator* and *Peregrinator biannulipes* are predators on stored-product pests. Indeed, there is mounting research into the feasibility of exploiting the natural host preferences of reduviids as biological control agents. Candidate species (with special attention to Indian species) are reviewed by Ambrose (2003, 1999). Experimentation on culturing, bioassays and studies of population dynamics towards ascertaining the potential of various reduviids as biological control agents are current in groups around the world e.g. Egypt (El-Sebaey *et al.* 2002), Brazil (Jahnke *et al.* 2002), Australia (Grundy & Maelzer 2000, 2002). Furthermore, the Triatominae are of great interest evolutionarily because it is one of the few major groups of heteropterans that feed on vertebrate blood. The only other major blood-feeding heteropteran groups are Cimicidae (bed bugs) and related Polyctenidae, which are true ectoparasites of bats.

The majority of hemipteran groups are plant feeding and it is likely that reduviids evolved from phytophagous ancestors. Evidence for this has been found by considering the type of proteinase digestive enzymes used by triatomines. Most haematophagous insects predominantly use trypsin, whereas, bloodfeeding hemipterans are exceptional in using cathepsin-like proteinases. This is consistent with a proposed plant-feeding ancestry (Lehane 2005). Evolution by this route is likely to have occurred either by descent from sap-sucking ancestors that did not use trypsins and lost them, or from seed-feeding ancestors that adapted to overcome serine proteinase inhibitors. In either case, cathepsins

occur within the lysosomes of all cells and it is proposed that hemipterans co-opted them for extracellular digestion (Billingsley & Downe, 1988). In line with the proposed descent of triatomines from predatory reduviids (see below and general introduction), cathepsins would have initially been used by predatory reduviids to digest insect haemolymph and later for blood as the triatomine lineages arose.

5.1.2 Ecology of the predatory Reduviidae

Species of the largest recognised reduviid subfamily, the Harpactorinae, have a preference for soft-bodied insects, such as lepidopterous and coleopterous caterpillars. However, different tribes of Harpactorinae exhibit a variety of host preferences, for example the Apiomerini (Apiomerinae of some authors) mainly hunt bees and other Hymenoptera, and the Tegeini feed on termites. The Harpactorinae may be an assemblage of convergent lineages. Some predatory subfamilies of the Reduviidae exhibit specialisation for particular prey. The Ectrichodinae, for example, are typically heavy-bodied and are obligate predators of millipedes, rejecting other arthropods even when starved (Louis 1974). Emesinae, which are spindly with mantid-like raptorial fore-legs, typically prey on Diptera (and some ingest vertebrate blood through predation on blood-engorged mosquitoes), although one genus appears to comprise obligate predators on spiders (Cobben 1978). The Phymatidae, or ambush bugs, lie in wait, often beautifully camouflaged, in flower heads and prey on nectar-feeders. Despite such specialisations, some of which may also be convergent, many subfamilies of Reduviidae have unknown feeding behaviour, although they may share habitat preference (Table 17). A reconstructed phylogeny of a group permits one to hypothesise about the evolutionary history of biological and ecological traits through an approach referred to as ecological phylogenetics (Spence & Anderson, 1994). This considers biological and ecological data

of extant species in the framework of the inferred phylogeny to reveal probable patterns of evolution.

Table 17. Ecology and diversity of the Reduviidae: (subfamilies according to Schuh & Slater, 1995).

Subfamily	Prey/host	Habitat	Species	Genera
Bactrodinae	?	?	1	1
Centrocneminae	?	Bark of trees	33	4
Cetherinae	Termites	Terrestrial	22	6
Chryxinae	?	?	3	3
Ectrichodiinae	Millipedes	Terrestrial	643	111
Elasmodeminae	?	Under bark of trees	-	-
Emesinae	Flies/spiders	Various	918	92
Hammacerinae	?	Under bark of trees	18	2
Harpactorinae	Generally soft bodied insect larvae	Various	2059	288
Holoptilinae	Ants	Under bark of tree / Terrestrial	76	15
Manangocorinae	?	?	1	1
Phimophorinae	?	?	3	2
Phymatinae	Plant and nectar feeders	Vegetation		
Physoderinae	?	Leaf litter/debris	60	13
Pieratinae	Hard-bodied arthropods	Terrestrial	47	31
Reduviinae	Various/ social insects	Various	47	31
Saicinae	?	?	139	24
Salyavatinae	?	Terrestrial	98	15
Spaeridopinae	?	?	4	4
Stenopodainae	?	Terrestrial	724	114
Triatominae	Vertebrates (blood feeders)	Nest and burrows of vertebrates	137	15
Tribelocephalinae	?	Leaf-litter	123	14
Vesciinae	?	?	18	5

5.1.3 Polyphyly versus monophyly of the Triatominae

As stated in the general introduction; it is reasonably proposed that the Triatominae are derived from vertebrate nest dwelling predatory ancestors, which adapted and evolved to exploit the niche of blood feeding on birds and mammals. However, it is by no means clear whether there was a single divergent event (monophyletic origin) or, as is hypothesised by some, a polyphyletic or diphyletic origin. Despite the growing presumption of polyphyly amongst many authors (see general introduction) nowhere is it evident that these differences are sufficient to indicate separate reduviid origins for the tribes of the Triatominae. Monophyly has been incorrectly supported by Hypsa *et al.* (2002) and alluded to by Gaunt & Miles (2000) in which they comment on a molecular clock that dates divergence between the two main genera/tribes; *Triatoma* and *Rhodnius*

at ~ 40Mya, before the arrival of bats and rodents to South America and suggest that the ancestor of the two lineages would most likely already have adapted to exploit the marsupials and edentates extant 65 Mya. However, Gaunt & Miles (2002) later estimated the same divergence at ~95 Mya and correlated it with the emergence of palm trees with which extant *Rhodnius* have a close association. Clearly ancient divergence does not preclude the possibility that the divergent ancestors were predatory reduviids, separated by ecological specialisation and later adapting to haematophagy in parallel. Moreover, the numerous molecular phylogenetic studies to date (Stothard, *et al.* 1998 García & Powell, 1998, García, 1999 Lyman, *et al.* 1999, Monteiro, *et al.* 1999a,b, 2000, 2001 Bargues *et al.* 2000, Marcilla *et al.* 2001, Gaunt & Miles 2000, Hypša *et al.* 2002) have failed to represent all of the triatomine tribes in a single analysis, and only one or two representatives of other reduviid subfamilies have been included. To begin resolving the controversy of monophyly vs. di-polyphyly Schaefer (2003) highlighted two questions that need to be answered:

1) Do the two main tribes differ more greatly from each other than either does from other triatomine groups?

2) Do the triatomine tribes differ at least as greatly from each other as do separate subfamilies of the Reduviidae?

In summary Schaefer (2003) makes the following statement, "Answering these questions is of more than academic interest, for if triatomines had more than one non-triatomine ancestor, and therefore are not phylogenetically close, it is impossible to generalise what is known about one group to others, and this inability may hinder control of these disease vectors. It is therefore vital (literally!) to determine if Triatominae is a holophyletic group and, if not, to determine which groups now classified as triatomines are related to which others".

Concurrent with this work Paula *et al.* (2005) have produced preliminary evidence for polyphyly by including several other reduviid subfamilies in a meta-analysis of mitochondrial rDNA sequences. Again only the Triatomini and Rhodniini were included. In an attempt to elucidate the phylogenetic relationships among reduviid taxa, I present here further analysis of a broader range of taxa utilising both nuclear and mitochondrial markers, with an assessment of phylogenetic signals in morphometric data.

5.2 Morphometric exploration of the higher taxonomy of the Triatominae

5.2.1 Head morphometrics

To test for the presence of phylogenetic signals in morphometric data a morphometric analysis of the Triatominae at the level of genera and tribes was conducted. Seven head measurements were taken from samples of 29 species, representing 11 genera and 4 tribes (see Fig. 5, Material and Methods page28). A dendrogram was constructed by UPGMA cluster analysis using a matrix of principal components (Fig.37). Paraphyly of *Triatoma* has previously been suggested by sequence data (Marcilla *et al.* 2001). However, the sequence data and morphometric data presented here in the Old World/New World *Triatoma* chapter suggest that North American and South American lineages are separate. The analysis of traditional morphometrics of head morphology from an extended sample of taxa presented here (fig. 37) shows some mixture of the two putative lineages. It seems that as more species are included morphometric analysis of the head becomes increasingly vulnerable to being confounded by homoplasies or divergences, due to ecologically modulated morphological specialisation; these issues are highlighted by Dujardin *et al.* (1999c). The obvious disruption to the phylogenetic signal in the morphometrics of head shape is attributable to homoplasy of head shape, particularly in elongate head shape versus compact head shape. A morphometric investigation into head

shape differences among reduviid subfamilies would require a different morphometric approach, probably one in three dimensions. The reason for this is, that the two dimensional orthogonal projection captured by photographing the dorsal view of the head would cease to capture consistently the full set of homologous landmarks. Fig 38 shows the variation in head shape among reduviid subfamilies, and the loss of homology in images would largely be due to the variable ventral curvature of the anterior region of the head (clypeus and gena). This would result in foreshortening of the anterior region as viewed dorsally, and obstruction of the view of the anti-clypeus. Fig.38 shows representatives of three tribes of the Triatominae, demonstrating the consistency of having a straight, elongated postocular region across the diversity of the bloodfeeding group. This "cone-nose" configuration is one of the key diagnostic characters of the Triatominae, and as such, represents either a homoplasy in response to optimising head shape for blood-feeding, or it is an autapomorphy of the group. Constructing a molecular phylogeny will identify which is most likely to be the case.

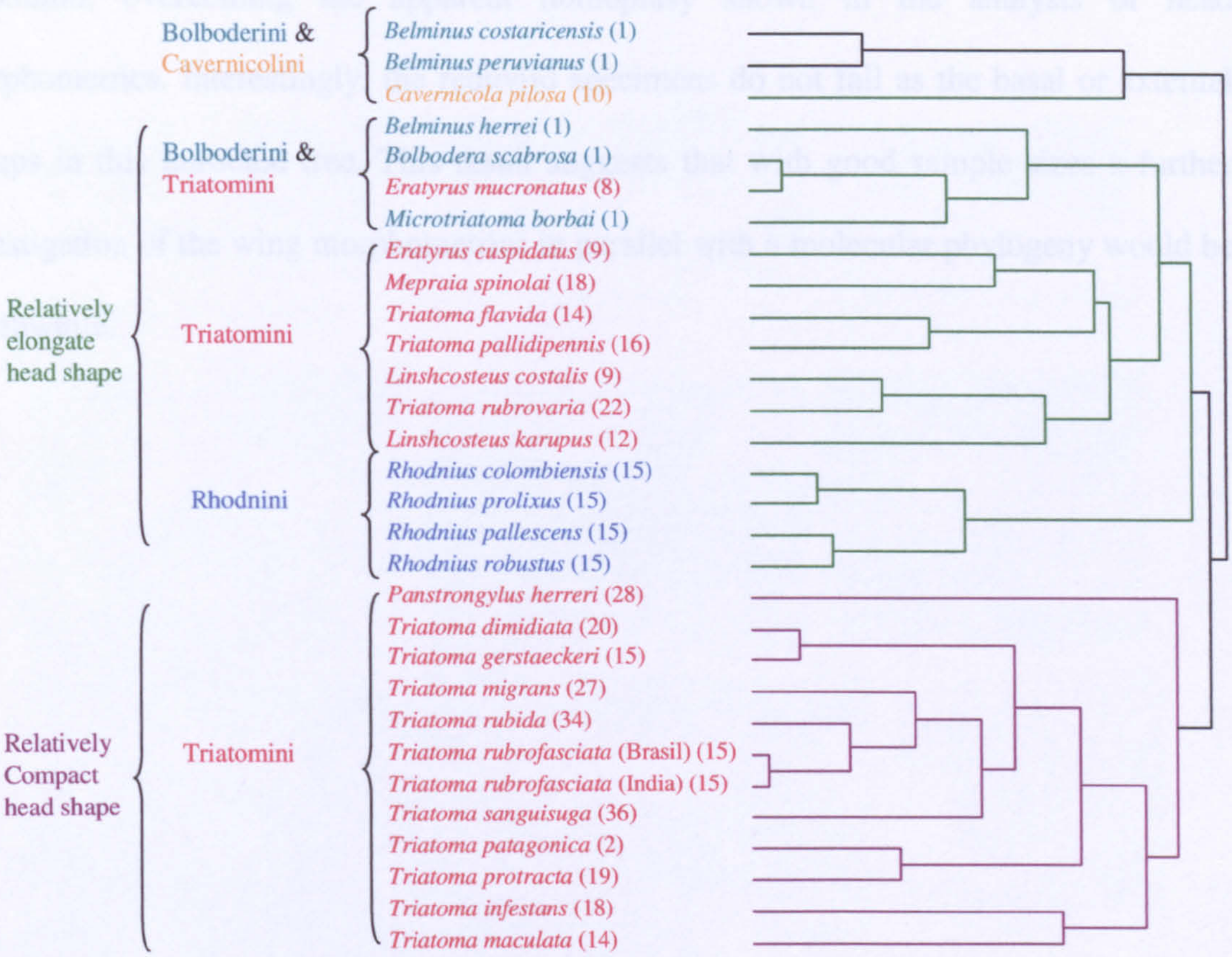

Figure 37. . Tribal analysis of Triatominae by traditional head morphometrics. Dendrogram derived from UPGMA cluster analysis of principal components. Measurements used: A, Outer distance between eyes (dorsal view) B, Inner distance between eyes (dorsal view) (synthlipsis) D, Anteocular distance (dorsal view) E, Postocular distance; from the posterior edge of the eye to the beginning of the neck. (dorsal view) G, Length of antenniferous tubercle; anterior edge of eye to furthest lateral extremity of antenniferous tubercle. (dorsal view) L, Maximum diameter of the eye (lateral view). Numbers in brackets represent sample size, Total N=425.

5.2.2 Wing morphometrics

In contrast to head morphology, homology of wing morphomtrics across sub-families is consistent. However, given the small numbers of available reduviid specimens and some triatomines only a cursory analysis could be conducted here.

Fig. 39. shows a geometric morphometric analysis of single wings including representatives of 4 out of the five tribes of the Triatominae and two predatory reduviids, representing the Reduviinae and Ectrichodinae. Again, a dendrogram was constructed by UPGMA cluster analysis using a matrix of principal components. The result should be

considered tentatively, but it does show a clear separation of the Triatomini from the Rhodniini, overcoming the apparent homoplasy shown in the analysis of head morphometrics. Interestingly, the reduviid specimens do not fall as the basal or external groups in this unrooted tree. This result suggests that with good sample sizes a further investigation of the wing morphometrics in parallel with a molecular phylogeny would be worthwhile.

Triatomini: *Triatoma rubrofasciata*

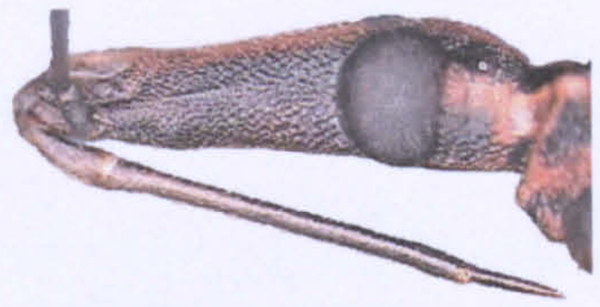

Rhodniini: *Rhodnius prolixus*

Bolboderini: *Microtriatoma trinidadensis*

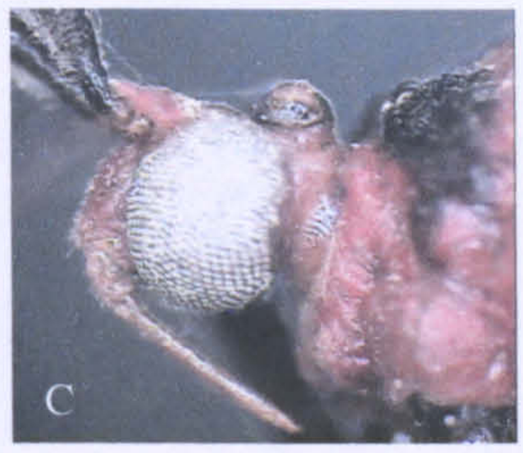

Figure 38.. Variation in head morphology among reduviid.subfamilies. The uppermost three lateral head views represent the variation within the Triatominae. A-L show lateral head views of 11 other reduviid subfamilies: **A**. Centrcneminae (CNS); **B**. Ectrichodiinae (ECD); **C.** Sphaeridopinae (SSA); **D**. Stenopodinae (SSC); **E**. Ecrichodiinae (ECT) **F**. Salyavatinae (SVH); **G.** Reduviinae (RTS); **H**. Vesciinae (VPA); **I**. Peiratinae (PMA); **J.** Saicinae (SSF); **K**. Physoderinae (PPB) **L**. Salyavatinae (SSV). (codes in brackets refer to the genus and species, as summarised in Table 19)

Figure 39. . Tribal analysis of Triatominae by geometric morphometrics of the wings. Dendrogram derived from UPGMA cluster analysis of shape components. Actual wings are shown and the scheme of landmarks used is shown bottom left. *Reduviinae, **Ectrichodinae, Triatomini in green, Rhodniini in blue, *Microtriatoma* representing the Bolboderini and *Cavernicola pilosa* the Cavernicolini.

5.3 Molecular phylogenetics of the Reduviidae

5.3.1 Material examined

The specimens representing the diversity of the Triatominae were the same as those described previously, with further specimens that were either collected, obtained from the reference collections of FIOCRUZ (Rio de Janeiro, Brazil) or sourced from the ECLAT collaborative network (see Table 18)

To obtain a broad representation of reduviid diversity museum specimens from the Natural History Museum, London were surveyed by sampling redundant morphology, ie. unpaired legs. However, due to age and/or sub-optimal preservation, many museum specimens surveyed failed to provide DNA of sufficient quality for amplification and sequencing of some/all markers. For this reason further specimens were obtained from field collections incidental to other field work conducted in Venezuela and Paraguay. Table 18. summarises the reduviid specimens used. For out-groups sequences were obtained from some other haematophagous cimicomorphans; *Cimex hemipterus* (Cimicidae) and *Clerada apicicornis* (Lygaeidae)

For photographs of representative specimens of some reduviid subfamilies used in this chapter see Fig. 94 & 95 in the appendix.

Table 18. Triatominae: specimens and markers sequenced.

Tribe	Genus	species	origin	source	*cytb*	*COII* 1st	*COII* 2nd	*COII* whole	D2-28S
Bolboderini	*Microtriatoma*	*trinidadensis*	NA	ECLAT					*
Rhodniini	*Psammolestes*	*arturi*	SA	collected			*		*
Rhodniini	*Psammolestes*	*coreodes*	SA	Genbank#	*				
Rhodniini	*Rhodnius*	*ecuadoriensis*	SA	Collected		*	*	*	
Rhodniini	*Rhodnius*	*ecuadoriensis*	SA	†					*
Rhodniini	*Rhodnius*	*pallescens*	SA	†					*
Rhodniini	*Rhodnius*	*pallescens*	SA	Genbank#	*				
Rhodniini	*Rhodnius*	*prolixus*	SA	Collected					
Rhodniini	*Rhodnius*	*prolixus*	SA	collected	*		*		*
Rhodniini	*Rhodnius*	*robustus*	SA	†					*
Triatomini	*Dipetalogaster*	*maximus*	NA	Genbank#	*				
Triatomini	*Dipetalogaster*	*maximus*	NA	†					*
Triatomini	*Eratyrus*	*mucronatus*	SA	ECLAT		*			
Triatomini	*Eratyrus*	*mucronatus*	SA	†					*
Triatomini	*Mepraia*	*spinolai*	SA	ECLAT		*			
Triatomini	*Mepraia*	*spinolai*	SA	†					*
Triatomini	*Panstrongylus*	*megistus*	SA	FIOCRUZ	*	*	*	*	*
Triatomini	*Paratriatoma*	*hirsuta*	NA	†					*
Triatomini	*Triatoma*	*brasiliensis*	SA	FIOCRUZ					*
Triatomini	*Triatoma*	*delpontei*	SA	†					*
Triatomini	*Triatoma*	*dimidiata*	NA	ECLAT	*		*	*	
Triatomini	*Triatoma*	*gerstaeckeri*	NA	†					*
Triatomini	*Triatoma*	*infestans*	SA	Collected					
Triatomini	*Triatoma*	*infestans*	SA	collected	*	*			*
Triatomini	*Triatoma*	*lecticularia*	NA	FIOCRUZ	*	*			*
Triatomini	*Triatoma*	*matogrossensis*	SA	FIOCRUZ					
Triatomini	*Triatoma*	*matogrossensis*	SA	†					*
Triatomini	*Triatoma*	*migrans* Brunei	OW	NHM	*		*		
Triatomini	*Triatoma*	*migrans* Sarawak	OW	NHM	*				
Triatomini	*Triatoma*	*nitida*	NA	†	*				
Triatomini	*Triatoma*	*platensis*	SA	FIOCRUZ					
Triatomini	*Triatoma*	*platensis*	SA	collected					*
Triatomini	*Triatoma*	*protracta*	NA	FIOCRUZ	*				*
Triatomini	*Triatoma*	*rubida a*	NA	ECLAT	*		*	*	*
Triatomini	*Triatoma*	*rubida b*	NA	ECLAT	*				
Triatomini	*Triatoma*	*rubrofasciata* Brazil	SA	ECLAT	*		*	*	*
Triatomini	*Triatoma*	*rubrofasciata* India	OW	Collected	*	*	*		
Triatomini	*Triatoma*	*sanguisuga*	NA	ECLAT	*				*
Triatomini	*Triatoma*	*sordida*	SA	Genbank#	*				
Triatomini	*Triatoma+*	*pallidipennis*	NA	†					*
Triatomini	*Triatoma+*	*pallidipennis*	NA	ECLAT	*				
Triatomini++	*Linshcosteus*	*karupus*	OW	Collected	*	*	*	*	*

Origin code: SA= South American; NA= North American (including Central American origin); OW= Old World. ;† Refers to D2-28S sequences provided by Fernando Monteiro. * indicates that a sequence was obtained "Collected" refers to our own field caught specimens, FIOCRUZ refers to specimens supplied by the reference collection of FIOCRUZ, Rio de Janeiro, Brazil and ECLAT refers to those field caught specimens provided by collaborators via the ECLAT network. # Genbank accession numbers: Genbank accession numbers: *Triatoma sordida:* AF045730; *Psammolestes coreodes:* AF045719; *Rhodnius pallescens:* AF045720; *Dipetalogaster maximus:* AF045728

Table 19. Other subfamilies of Reduviidae: specimens and markers sequenced.

code	Year collected	Origin	source	Sub-family	Genus	species	*cytb*	*COII* 1st	*COII* 2nd	*COII* whole	D2-28S
CNS	1947	Sarawak	NHM	Centrcneminae	*Neocentrocnemis*	*signoreti*					
CNF+	1980	Sarawak: Batu Niah	NHM	Centrcneminae	*Neocentrocnemis*	*formosana*					
CCM	1972	Angola	NHM	Cetherinae	*Cethera*	*musiva*					
ECD	1975	N. Nigeria	NHM	Ectrichodiinae	*Decoratus*						
ECT	1992	Temburrong, Brunei	NHM	Ectrichodiinae	*Cimbus*	*tenax*		*	*		
ELT+	1990	South India: Tamil Nadu,	NHM	Ectrichodiinae	*Labidocoris*	*tuberculatus*					
VEB	2004	Venezuela, Potuguesa State	Collected	Ectrichodiinae	*Brontostoma*	*sp*			*		
VE	2003	Venezuela	Collected	Ectrichodiinae	*?*						*
PER	2002	Paraguay, Chaco	Collected	Ectrichodiinae	*Rhiginia*		*		*		*
PEE	2003	Paraguay, mbaracyu	Collected	Emesinae	*Emesaya*	*sp*					
VEE	2001	Venezuela, Portuguesa state	Collected	Emesinae	*Emesaya*						*
EEH		V. de Chiriqui	NHM	Eupheninae	*Eupheno*	*histionicus*					
PH	2003	Paraguay, Chaco	Collected	Hammaceriinae	*?*			*	*		*
PH+	2002	Paraguay, Chaco	Collected	Hammaceriinae	*?*						
HHG	1967	Costa Osorno, Chile	NHM	Hammacerinae	*Hammatocerus*	*gayi*					
HAV	1997	Roncesvalles, Colombia	NHM	Harpactorinae	*Ambastus*	*villosus*	*	*			
HAV+	1997	Colombia, Roncesvalles,	NHM	Harpactorinae	*Ambastus*	*villosus*			*		
HCA+1	1991	Brazil P. Alegre, RS	NHM	Harpactorinae	*Cosmoclopius*	*annulosus*					
HCA+2	1991	Brazil P. Alegre, RS	NHM	Harpactorinae	*Cosmoclopius*	*annulosus*					
VHA	2001	Venezuela, Potuguesa State	Collected	Harpactorinae	*Apiomerus*	*sp*		*	*		
VH	2001	Venezuela, Portuguesa state	Collected	Harpactorinae	*?*		*				
HP	1953		NHM	Holoptilinae	*Ptilocenemis*						
PTC	1981	Mexico: Campeche,	NHM	Peiratinae	*Thymberus*	*pyrrhopterus*					
PM	?	?	†	Peiratinae	*Melanolestes*	*sp.*					*
PMA	1952	Rio Grande do sul, Brazil	NHM	Peiratinae	*Melanolestes*	*argebtinus*					
PPF	1967	Rio Grande do Sul	NHM	Phymatinae	*Phymatipsa*	*fortificata*					
PMA+	1981	Costa Rica, Braulio Carillo	NHM	Phymatinae	*Macrocephalus*	*attenuatus*					
PPB	1914	N. Luzon	NHM	Physoderinae	*Physoderoides*	*browni*					
PPBS	1965	Solomon Island	NHM	Physoderinae	*Physoderoides*	*browni*					
PPB+1	1965	Solomon Island	NHM	Physoderinae	*Physoderoides*	*browni*			*		
PPB+2	1965	Solomon Island	NHM	Physoderinae	*Physoderoides*	*browni*					
RTS	1920	Indo-China	NHM	Reduviinae	*Tiarodes*	*selangorensis*					
RTS+	1977	Sabah: S. Mt Trus Madi	NHM	Reduviinae	*Tiarodes*	*selangorensis*			*		
RZ+	2002	BELIZE: Cayo, Chiquibul.	NHM	Reduviinae	*Zelurus*	*sp.*	*				
PRZ	2003	Paraguay, Chaco	Collected	Reduviinae	*Zelurus*	*sp*					*
PRZ+	2003	Paraguay, Chaco	Collected	Reduviinae	*Zelurus*	*sp*		*	*		
PRO	2003	Paraguay, Chaco	Collected	Reduviinae	*Opithacidus*	*sp*			*		*
VRL	2001	Venezuela, Guarico State	Collected	Reduviinae	*Leogorrus*	*sp*	*	*	*	*	
PRL	2002	Paraguay, Chaco	Collected	Reduviinae	*Leogorrus*	*sp*	*		*		*
PRO+	2002	Paraguay, Chaco	Collected	Reduviinae	*Opithacidus*	*sp*					
BOP	?	Bolivia*	Collected	Reduviinae	*Opithacidus*	*pertinax*		*			*
RPB	2003	Commercial supply	Collected	Reduviinae	*Platymerus*	*bigutata*	*	*	*	*	*
SSF	1979	Union camp, Belize	NHM	Saicinae	*Saica*	*fuscipes*					
SSV	1937	British Honduras	NHM	Salyavatinae	*Salyavanta*	*variagata*					
SVH+	1992	Brunei: Temburong District,	NHM	Salyavatinae	*Valentia*	*hoffmanni*					
SSI+	1994	W. Malaysia, Gombak	NHM	Salyavatinae	*Syberena*	*izzardi*	*	*	*	*	*
SSA	1907	Parana Brazil	NHM	Sphaeridopinae	*Shaeridops*	*amoenus*					

code	Year collected	Origin	source	Sub-family	Genus	species	*cytb*	*COII* 1st	*COII* 2nd	*COII* whole	D2-28S
SSC	1967	Missiones, Argentina	NHM	Stenopodinae	*Stenopoda*	*cinerea*					
SSC+	2002	Belize: Cayo, Chiquibul.	NHM	Stenopodinae	*Stenopoda*	*cinerea*	*	*	*	*	
VS	2003	Venezuela	Collected	Stenopodinae	*?*						*
PS	2003	Paraguay	Collected	Stenopodinae	*?*						*
TTT	1970	Nigeria	NHM	Tribelocephalinae	*Tribelocephala*	*tchadensis*					
TTN+	1973	Nigeria, Enugu.	NHM	Tribelocephalinae	*Tribelocephala*	*noctivaga*					
VPA	1948	Colombia	NHM	Vesciinae	*Pessoaia*	*argentina*					
PVP	2003	Paraguay, Chaco	Collected	Vesciinae	*Pessoaia*	*sp*			*		*

Source code: # see appendix for Genbank accession number;† refers to D2-28S sequences provided by Fernando Monteiro, ? refers to unknown data, * indicates that a sequence was obtained., "Collected" refers to our own field caught specimens and NHM refers to material sourced form the collections of the Natural History Museum, London.

5.3.2 Molecular genetics

5.3.2.1 Mitochondrial gene amplification and sequencing

Attempts were made to amplify three mitochondrial targets; *cytb* and two contiguous fragments covering the whole of Cytochrome Oxidase II (*coII*) (*coII* 1st and *coII* 2nd). Due to the varying age and state of preservation of the specimens large fragments could not be amplified from some. Degenerate primers were also designed but this still failed to give amplification of a single marker for all specimens (see materials and methods) The smaller ~400bp fragments of *coII* could be amplified and sequenced for some of the less optimal samples. In addition the established 700bp fragment of cytochrome b (*cytb*) gene was also amplified where possible and sequenced (see materials and methods). Tables 18 & 19. summarises the fragments obtained from the range of taxa examined.

For *COII*, alignments of sequences amounted to 356 bp for *COII* 1st , 297bp for *COII* 2nd and 358bp for *cytb*, none contained any gaps. Identity of the amplicons sequenced was confirmed by BLAST search and direct alignments to the complete *COII* and *cytb* genes of *T. dimidiata* (Dotson and Beard 2001; GenBank accession AF301594). Where both

coII fragments were obtained the contiguous fragments were aligned to give a complete *coII* sequence for those specimens.

5.3.2.2 D2 region of 28S rDNA amplification and sequencing

A ~700bp fragment of the D2 region of the 28S rDNA was successfully amplified and sequenced for some of the taxa sampled (see Tables. 18 & 19). (see materials and methods). Alignments were 658bp and indels were disregarded in the analyses giving a consensus alignment of 449bp

5.3.2.3 Analysis of sequences

For comparative analysis of the sequences obtained and subsequent phylogenetic analyses nucleotide differences and distance matrices were calculated. For these data sets several models of base substitution were used in comparison (p distances, kimura 2 parameter (K2p), Jukes Cantor, Tajima-Nei, Tamura 3 parameter, Tamura-Nei). All models assessed here, for this data set gave comparable results without any significant differences in the results of the eventual phylogenetic analyses. For this reason, only K2p distances were used and percentages of sequence divergence among OTUs are shown here (Table 20).

5.3.2.3.1 Phylogenetic analyses

5.3.2.3.1.1 Distance based

Neighbour-joining trees were generated using the various models of base substitution, and statistical support was evaluated by bootstrap resampling with 1000 replicates and a random seed number. All models of base substitution investigated yielded essentially equivalent results, all trees having identical topologies and similar bootstrap supports.

5.3.2.3.1.2 Maximum parsimony

To re-assess the phylogeny reported by the neighbour-joining analysis the haplotypes were also subjected to a maximum parsimony analysis. The branch and bound algorithm was used to recover three equally parsimonious trees, from which a strict consensus trees were produced with bootstrap supports.

5.3.2.3.1.3 Maximum likelihood

A heuristic search was conducted on the D2-28S sequences by stepwise additions using the tree-bisection-reconnection (TBR) branch-swapping algorithm (see materials and methods) the resulting tree was submitted to 200 bootstrap replicates and the 50% Majority-rule tree was calculated.

5.3.2.4 *COII* & *Cytb* sequences

The NJ trees for *COII* fragments and *cytb* (Figs. 41 , 42, 43 & 44) demonstrate that at this taxonomic level there is too much variation among the sequences of these taxa, so that the phylogenetic signal is lost for these sequences, very few of the nodes have any degree of bootstrap support. The sequences obtained are all quite short and heavily diverged, the effect is a high degree of saturation (see Fig. 40) and to a large extent they are effectively randomised. For this reason it is extremely difficult to discern the long branch attraction among the taxa. For this reason unrooted NJ trees were drawn in parallel. for *cytb* and *coII* sequences (Figs. 41, 42, 43 & 44). All mitochondrial fragments essentially portray polytomy, star phylogenies without any direction. Only the tree drawn from *COII* 1st (Fig. 43) appears to offer any informative phylogenetic structure. However, this is simply a division of the Triatomini from the Rhodnini, each with some reduviids associated by long branch attraction.

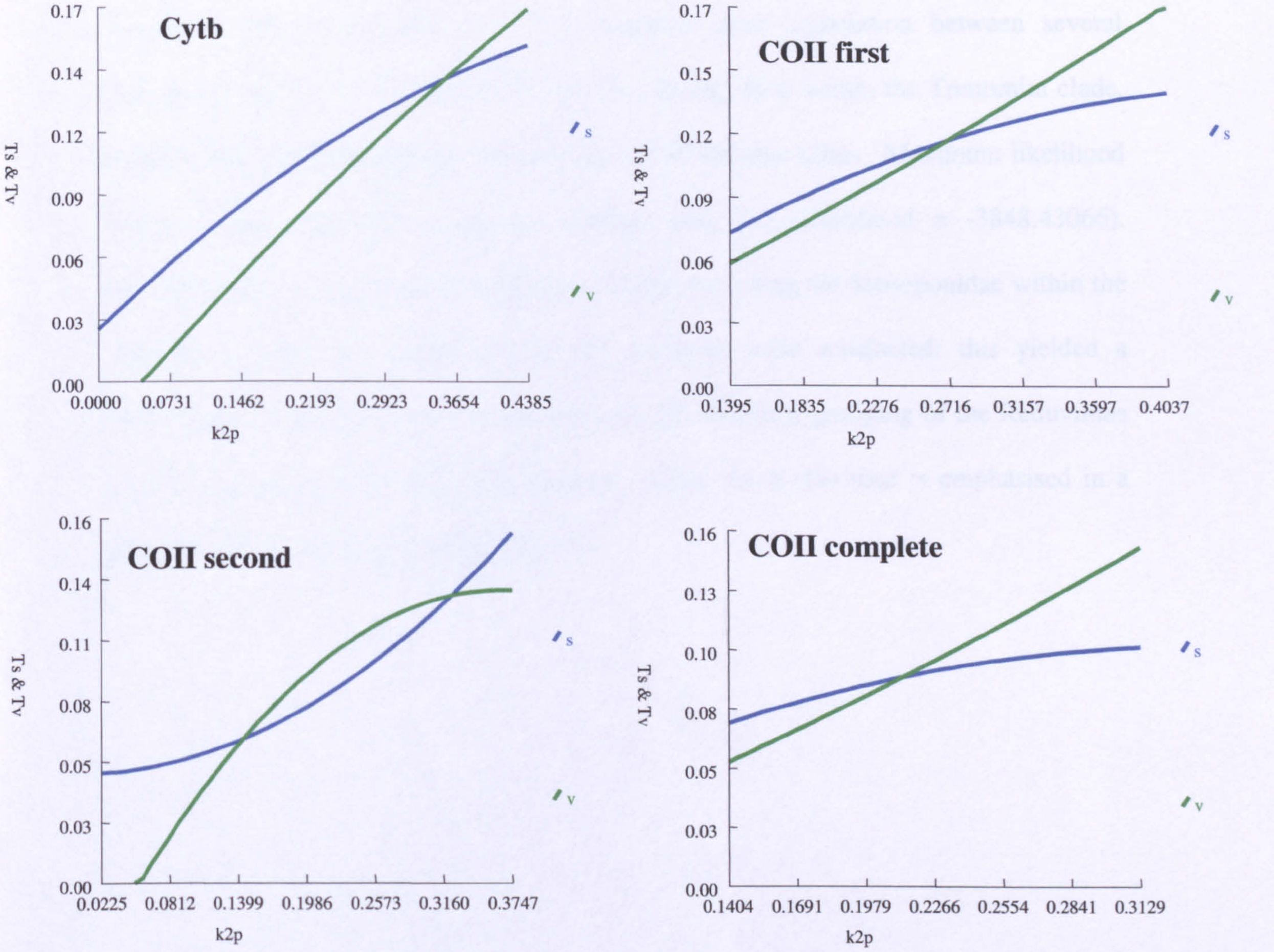

Figure. 40. Plots of transition and transversions against k2p distances for mitochondrial gene markers used in analyses (blue lines = transitions; green = transversions)

The plots of transitions and transversions for mitochondrial gene fragments against k2p distances (Fig. 40) indicate that saturation of transitions occurs, particularly at higher genetic distances and contributes to the lack of support for the basal nodes of the tree presented here.

5.3.2.5 D2 region of 28S rDNA

NJ and MP trees were generated for a group of 39 taxa (Fig. 45) these trees were congruent in their topology and bootstrap supports were calculated for the NJ tree. Many

of the reduviid taxa form a polytomy by long branch attraction close to the base of the tree. There is good bootstrap support at the node that separates the Rhodniini from the Triatomini. The same same node also supports close association between several Reduviinae (BOP, PRO & PRZ see Table 19), placing them within the Triatomini clade, whereby establishing polyphyly between the two triatomine tribes. Maximum likelihood (ML) analysis supports the general topology (Fig 47) (likelihood = -3848.43066). However, the ML topology differs slightly by also including the Stenoponidae within the Triatomini clade. Two hundred bootstrap replicates were conducted; this yielded a Majority consensus tree (Fig. 48) that supports the observed grouping of the Reduviinae with the Triatomini. The striking polyphyly among the Reduviinae is emphasised in a collapsed unrooted NJ phylogeny (Fig. 46).

Table 20 D2- 28S rDNA pairwise percentages of sequence divergence (upper matrix), estimated divergence time in millions of years (lower matrix)

	1	2	3	4	5	6	7	8	9	10	11	12	13	14	15	16	17	18	19	20	21	22	23	24	25	26	27	28	29	30	31	32	33	34	35	36	37	38	39
1 Triatoma platensis		10.1	3.4	39.5	20.1	18.0	2.8	7.8	3.4	13.9	3.4	5.3	3 8	35.1	19.9	19.2	18.2	3.4	3.2	11.0	18 6	0.6	0.4	0.6	6.6	10.2	12.7	7.8	8.0	8.5	8.3	4.9	3.4	3.4	3.0	3.8	2.1	0.0	17.3
2 Linshcosteus karupus	36.8		6.1	41.0	22.4	20.5	4.7	10.2	6.8	16.9	5.1	8.3	6.1	36.6	21.4	21.6	21.3	5.7	4.9	14.6	20.3	6.1	6.6	5.9	7.6	13.3	15.4	9.3	9.5	10.6	10.4	7.2	5.1	5.1	4.6	5.3	5.5	6.3	19.5
3 Reduviinae BOP	20.1	35.7		40.6	21.4	17.8	2.7	8.0	4.0	13.9	3.2	4.2	1.5	35.1	19.5	19.5	19.4	3.0	3.2	11.4	17.5	3.2	3.8	3.4	8.0	10.8	13.3	7.8	8.0	8.3	8.2	4.4	3.4	3.4	2.8	3.6	2.5	3.4	16.9
4 Cimex	232	241	239		38.9	39.3	40.2	41.4	40.6	38.5	40.0	39.8	40 8	28.1	37.2	38.9	43.1	39.3	40.4	40.6	40.8	39.3	39.7	39.5	41.4	40.8	41.0	41.7	41.7	41.6	41.7	39.7	40.4	40.2	40.2	40.2	40.4	39.5	36.4
5 Emesinae VEE	118	132	126	229		23.3	20.5	21.4	21.3	21.1	20.5	20.1	21.4	36.4	22.2	22.0	23.0	20.3	21.1	21.6	23.0	20.1	20.3	19.7	22.0	22.6	23.5	21.6	21.8	22.4	22.2	21.1	20.7	20.7	20.5	19 9	21.1	20.1	22.0
6 Harpactorinae VH	106	121	105	231	137		17.5	19.7	19.0	19.7	17.8	17.1	18.4	37.0	22.4	21.1	22.4	16.7	17.6	21.1	23.0	17.8	17.8	18.0	22.0	21.1	21.1	19.5	19.7	19.7	19.9	17.8	17.5	17.5	17.6	17.6	17.8	18.0	22.6
7 Triatoma lecticularia	16.7	27.9	15.6	237	121	103		7.4	2.3	14.0	0.8	5.1	2.7	34.9	19.7	19.5	19.7	1.3	1.1	11.8	18.2	2.7	3.2	2.8	6.8	9.9	13.7	6.8	7.0	7.8	7.6	3.4	1.1	1.1	0.2	0.9	2.1	2.8	16.9
8 Psammolestes arturi	45.8	60.3	46.9	243	126	116	43.5		7.4	17.1	8.0	8.0	8.3	37.2	21.4	20.9	21.6	8.0	7.6	13.5	20.5	7.6	7.8	7.8	12.3	12.1	15.2	1.3	1.5	1.7	1.5	8.5	7.6	7.6	7.6	8.3	7.4	7.8	18.2
9 Panstrongylus megistus	20.1	40.2	23.4	239	125	112	13.4	43.5		15.6	2.7	6.1	4.2	34.3	19.5	20 7	20.3	3.2	2.7	11.6	18.2	3.6	3.6	3.4	7.6	10.1	13.5	6.6	6.8	7.6	7.4	4.7	2.8	2.8	2.1	3.0	3.2	3.4	17.6
10 Reduviinae RPB	81.5	99.3	81.5	227	124	116	82.6	100	91.5		14.6	12.9	13.9	34.9	19.2	21.8	16.1	14.4	13.9	18.0	19.9	13.9	14.0	14.0	18.4	18.8	18.6	17.6	17.8	17.3	17.3	14.8	13.9	13.9	14.2	14.2	13.5	13.9	18.2
11 Triatoma protracta	20.1	30.1	19	236	121	105	4.46	46 9	15.6	85.9		5.5	3.2	34.9	19.7	19.9	19 9	2.1	1.7	12.3	18.4	3.2	3.8	3.4	7.0	10.2	14.2	7.4	7.6	8.3	8.2	3.6	1.9	1.9	0.9	1.3	2.7	3.4	17.1
12 Reduviinae PRZ	31.3	49.1	24.6	234	118	100	30.1	46.9	35.7	75.9	32.4		3.6	35.5	18.2	17.8	18.2	5.3	5.5	11.0	17.6	5.1	5.3	5.3	9.1	11.4	13.7	8.2	8.3	8.7	8.5	6.3	5.7	5.7	5.3	6.1	4.4	5.3	16.9
13 Reduviinae PRO	22.3	35.7	8.93	240	126	108	15.6	49.1	24.6	81.5	19	21.2		35.5	19.7	19.5	19.2	2.8	3.2	11.2	18.0	3.6	4.2	3.8	8.2	11.0	13.5	7.8	8.0	8.7	8.5	4.7	3.4	3.4	2.8	3.6	3.0	3.8	16.9
14 Hammaceriinae PH	206	215	206	165	214	218	205	219	202	205	205	209	209		35.3	38.7	39.8	34.3	35.1	37.0	35.9	35.1	35.1	35.1	37.0	36.4	37.8	37.2	37.2	36.8	37.0	34.7	34.7	34.5	34.9	34.7	35.3	35.1	32.1
15 Vesciinae PVP	117	126	115	219	131	132	116	126	115	113	116	107	116	208		20.9	17.5	19.4	19.9	21.1	17.8	19.9	19 9	19.5	23.5	23.1	22.2	21.6	21.8	21.6	21.4	19.7	19.5	19.9	19.5	19.9	19.2	19.9	21.4
16 Ectrichodiinae VE	113	127	115	229	129	124	115	123	122	128	117	105	115	228	123		20.5	19.4	19.9	21.8	20.7	19.0	19.2	19.5	23.5	22.8	22.0	20.9	21.1	20.7	20.9	20.3	20.3	20.3	19.7	19.7	19.0	19.2	23.0
17 Salyavatinae SSI+	107	125	114	253	135	132	116	127	119	94.9	117	107	113	234	103	121		19.5	19.7	20.7	21.1	18.2	18.4	18.0	23.1	22.0	20.1	21.4	21.3	21.8	21.6	19.9	19.7	19.7	19.7	19.9	19.2	18.2	20.7
18 Triatoma rubida	20.1	33.5	17.9	231	119	98.2	7.81	46.9	19	84.8	12 3	31.3	16.7	202	114	114	115		1.9	12.1	18.8	3.2	3.8	3.4	7.6	10.4	13.5	7.6	7.8	8.7	8.5	3.8	2.1	1.7	1.5	1.7	2.5	3.4	16.7
19 Triatoma sanguisuga	19	29	19	238	124	104	6.7	44 6	15.6	81.5	10	32.4	19	206	117	117	116	11.2		12.1	18.6	3.0	3.6	3.2	6.8	9.9	13.9	7.2	7.4	8.0	7.8	3.6	1.3	0.9	1.3	1.9	2.5	3.2	16.7
20 Stenopodinae PS	64.7	85.9	67	239	127	124	69.2	79.2	68.1	106	72.6	64.7	65.9	218	124	128	122	71.4	71.4		20.5	11.0	11.0	10.6	13.5	15.9	10.2	13.7	13.5	13.9	13.9	12.7	11.8	12.0	11.6	12.7	11.4	11.0	19.0
21 Reduviinae PRL	109	119	103	240	135	135	107	121	107	117	108	104	106	211	105	122	124	111	109	121		18.8	18.6	18.6	21.8	21.8	20.9	20.3	20.5	20.1	20.1	18.4	18.4	18.8	18.2	18.6	17.8	18.6	22.0
22 Triatoma brasiliensis	3.35	35.7	19	231	118	105	15.6	44.6	21.2	81.5	19	30.1	21.2	206	117	112	107	19	17.9	64.7	111		0.9	0.6	6.5	10.2	12.7	7.6	7.8	8.3	8.2	4.7	3.2	3.2	2 8	3.6	1.9	0.6	16.9
23 Triatoma infestans	2.23	39.1	22.3	233	119	105	19	45.8	21.2	82.6	22.3	31.3	24.6	206	117	113	108	22.3	21.2	64.7	109	5.58		0.9	6.6	10.4	12.9	7.8	8.0	8.5	8.3	5.3	3.8	3.8	3.4	4.2	2.5	0.4	17.5
24 Triatoma matogrossensis	3.35	34.6	20.1	232	116	106	16.7	45.8	20.1	82.6	20.1	31.3	22.3	206	115	115	106	20.1	19	62.5	109	3.35	5.58		6.3	10.2	12.3	7.8	8.0	8.5	8.3	4.9	3.4	3.4	2.7	3.8	2.1	0.6	17.3
25 Triatoma rubrofasciataBrazil	39.1	44.6	46.9	243	129	129	40.2	72.6	44.6	108	41.3	53.6	48	218	138	138	136	44.6	40.2	79.2	128	38	39.1	36.8		14.6	14.8	11.6	11.4	11.8	12.0	8 9	7.0	7.0	6.6	7.4	6.8	6.6	20.7
26 Microtriatoma trinidadensis	60.3	78.1	63.6	240	133	124	58	71.4	59.2	111	60.3	67	64.7	214	136	134	129	61.4	58	93.8	128	60.3	61.4	60.3	85.9		16.9	11.2	11.4	12.5	12.3	11.8	9.5	9.5	10.1	11.0	9.9	10.2	20.9
27 Stenopodinae VS	74.8	90.4	78.1	241	138	124	80.4	89.3	79.2	109	83.7	80.4	79.2	222	131	129	118	79.2	81.5	60.3	123	74.8	75.9	72.6	87.1	99.3		15.4	15.2	15.6	15.6	14.4	13.9	13.9	13.5	14.6	12.1	12.7	22.0
28 Rhodnius pallescens	45.8	54.7	45.8	246	127	115	40.2	7.81	39.1	104	43.5	48	45.8	219	127	123	126	44.6	42.4	80.4	119	44.6	45.8	45.8	68.1	65.9	90.4		0.2	1.5	1.3	8.0	7.0	7.0	7.0	7.8	7.0	7.8	19.2
29 Rhodnius ecuadoriensis	46.9	55.8	46.9	246	128	116	41.3	8.93	40.2	105	44.6	49.1	46 9	219	128	124	125	45.8	43.5	79.2	121	45.8	46.9	46 9	67	67	89.3	1.12		1.3	1.1	8.2	7.2	7.2	7.2	8.0	7.2	8.0	19.4
30 Rhodnius prolixus	50.2	62.5	49.1	244	132	116	45.8	10	44.6	102	49.1	51.3	51.3	217	127	122	128	51.3	46.9	81.5	118	49.1	50.2	50.2	69.2	73.7	91.5	8.93	7.81		0.2	8.9	8.2	8.2	8 0	8.7	8.2	8.5	19.4
31 Rhodnius robustus	49.1	61.4	48	246	131	117	44.6	8 93	43.5	102	48	50.2	50.2	218	126	123	127	50.2	45 8	81.5	118	48	49.1	49.1	70.3	72.6	91.5	7.81	6.7	1.12		8.7	8.0	8.0	7.8	8.5	8.0	8.3	19.2
32 Eratyrus mucronatus	29	42.4	25.7	233	124	105	20.1	50.2	27.9	87.1	21.2	36.8	27.9	204	116	119	117	22.3	21.2	74.8	108	27.9	31.3	29	52.5	69.2	84.8	46.9	48	52.5	51.3		3.6	4.0	3.6	4.0	4.4	4.9	17.1
33 Triatoma pallidipennis	20.1	30.1	20.1	238	122	103	6.7	44.6	16.7	81.5	11.2	33.5	20.1	204	115	119	116	12.3	7.81	69.2	108	19	22.3	20.1	41.3	55.8	81.5	41.3	42.4	48	46.9	21.2		0.4	1.3	2.3	2.7	3.4	17.1
34 Triatoma gerstaeckeri	20.1	30.1	20 1	237	122	103	6.7	44.6	16.7	81.5	11.2	33.5	20.1	203	117	119	116	10	5.58	70.3	111	19	22.3	20.1	41.3	55.8	81.5	41.3	42.4	48	46.9	23.4	2.23		1.3	2.1	2.7	3.4	17.1
35 Paratriatoma hirsuta	17.9	26.8	16 7	237	121	104	1.12	44.6	12.3	83.7	5.58	31.3	16.7	205	115	116	116	8.93	7.81	68.1	107	16.7	20.1	15.6	39.1	59.2	79.2	41.3	42.4	46.9	45.8	21.2	7.81	7.81		1.1	2.3	3.0	17.1
36 Dipetalogaster Maximus	22.3	31.3	21.2	237	117	104	5.58	49.1	17.9	83.7	7.81	35.7	21.2	204	117	116	117	10	11.2	74.8	109	21.2	24.6	22.3	43.5	64.7	85.9	45.8	46.9	51.3	50.2	23.4	13.4	12.3	6.7		3.0	3.8	17.3
37 Mepraia spinolai	12.3	32.4	14.5	238	124	105	12.3	43.5	19	79.2	15.6	25.7	17.9	208	113	112	113	14.5	14.5	67	105	11.2	14.5	12.3	40.2	58	71.4	41.3	42.4	48	46.9	25.7	15.6	15.6	13.4	17.9		2.1	16.9
38 Triatoma delpontei	0	36.8	20.1	232	118	106	16.7	45.8	20.1	81.5	20.1	31.3	22.3	206	117	113	107	20.1	19	64.7	109	3.35	2.23	3.35	39.1	60.3	74.8	45.8	46.9	50.2	49.1	29	20.1	20.1	17.9	22.3	12.3		17.3
39 Peiratinae PM	102	115	99 3	214	129	133	99 3	107	104	107	100	99.3	99 3	189	126	135	122	98 2	98 2	112	129	99.3	103	102	122	123	129	113	114	114	113	100	100	100	100	102	99.3	102	

5.3.2.6 Dating divergences

As in the Old World/New World *Triatoma* chapter for the D2-28S a rate of 0.5% sequence divergence per million years (see Whitfield 2002) was considered. However, a rate of 0.17% per million years gives dates of divergence in line with those estimated by Bargues *et. al.*, (2000) for ITS-2 rDNA. The estimate of ~60Mya for the divergence of Rhodniini and Triatomini using 0.17% per million years concurs with the estimate of ~50-60 Mya of Bargues *et al.* (2000). Table 20 summarises the % pairwise sequence divergence among the 39 taxa examined and also shows estimated dates of divergence in millions of years.

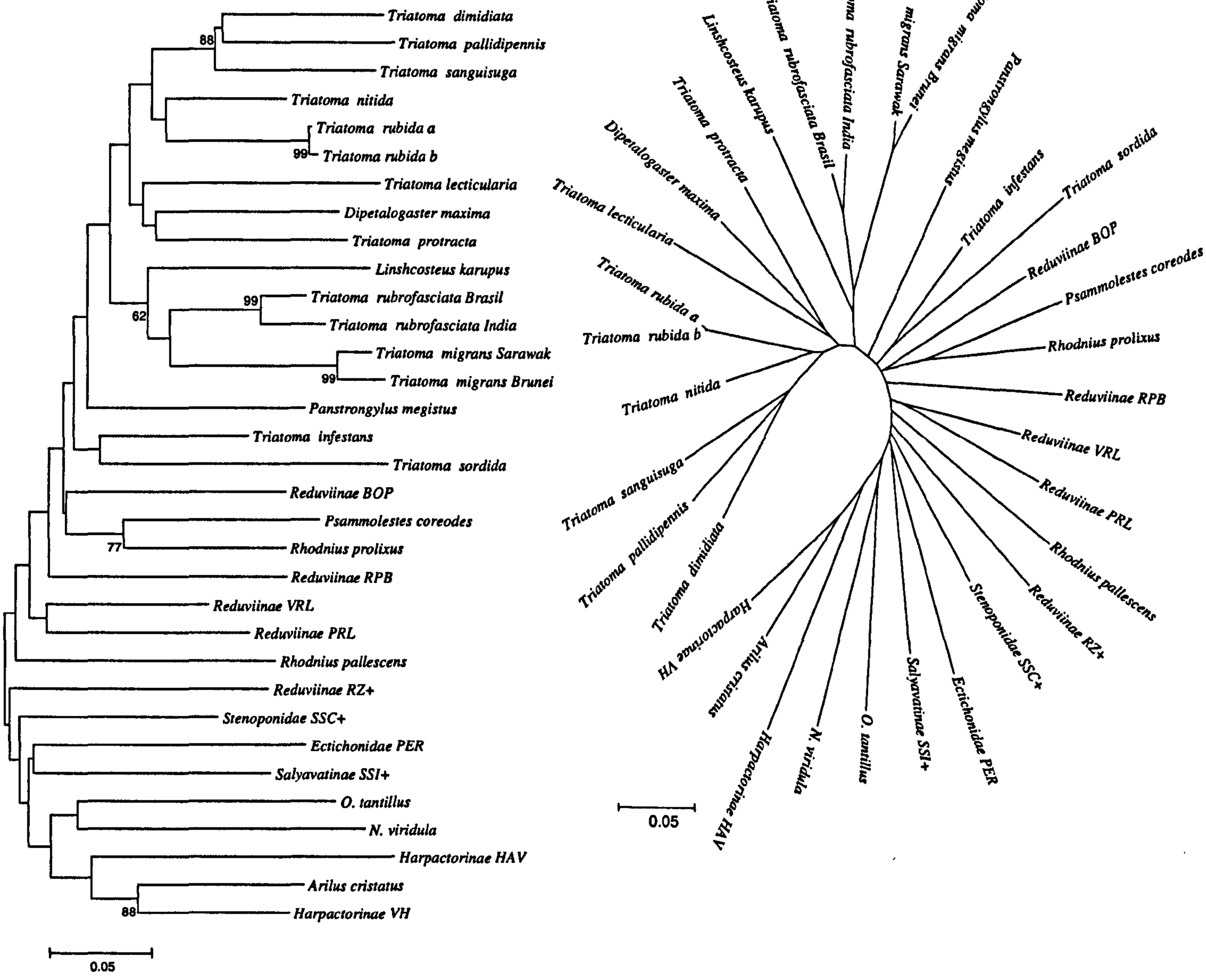

Figure 41. Neighbour-joining phylogenetic tree (rooted and unrooted) of *cytb* sequences of reduviid tata. Constructed using k2p model, with 1000 bootstrap replicates sum of branch lengths = 3.38, scale: substitutions/site
The tree is unresolved and shows a polytomy

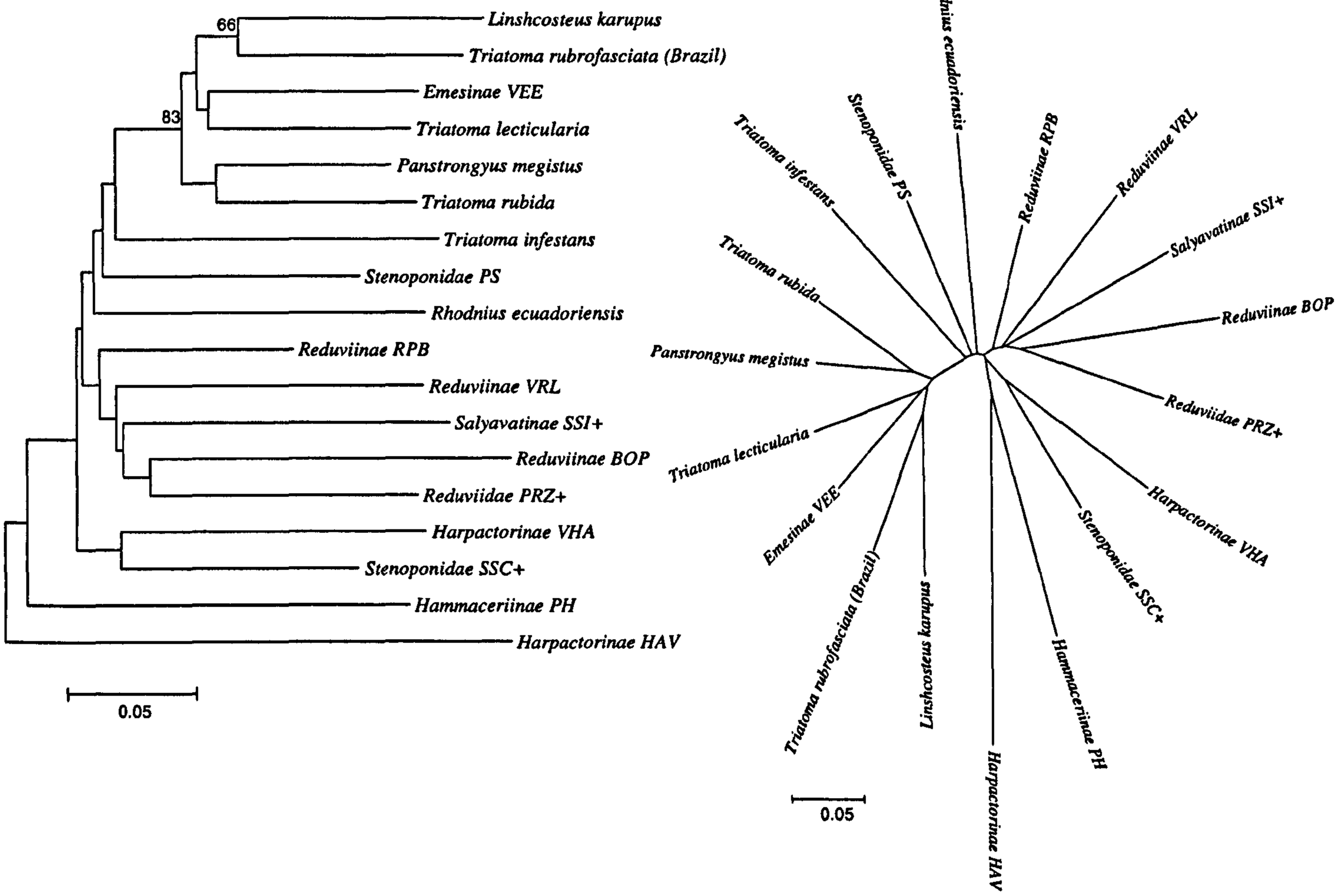

Figure 42. Neighbour-joining phylogenetic tree (rooted and unrooted) of *COII*-1st segment sequences of reduviid taxa. Constructed using k2p model, with 1000 bootstrap replicates sum of branch lengths = 2.11, scale: substitutions/site. The tree is unresolved and shows a polytomy

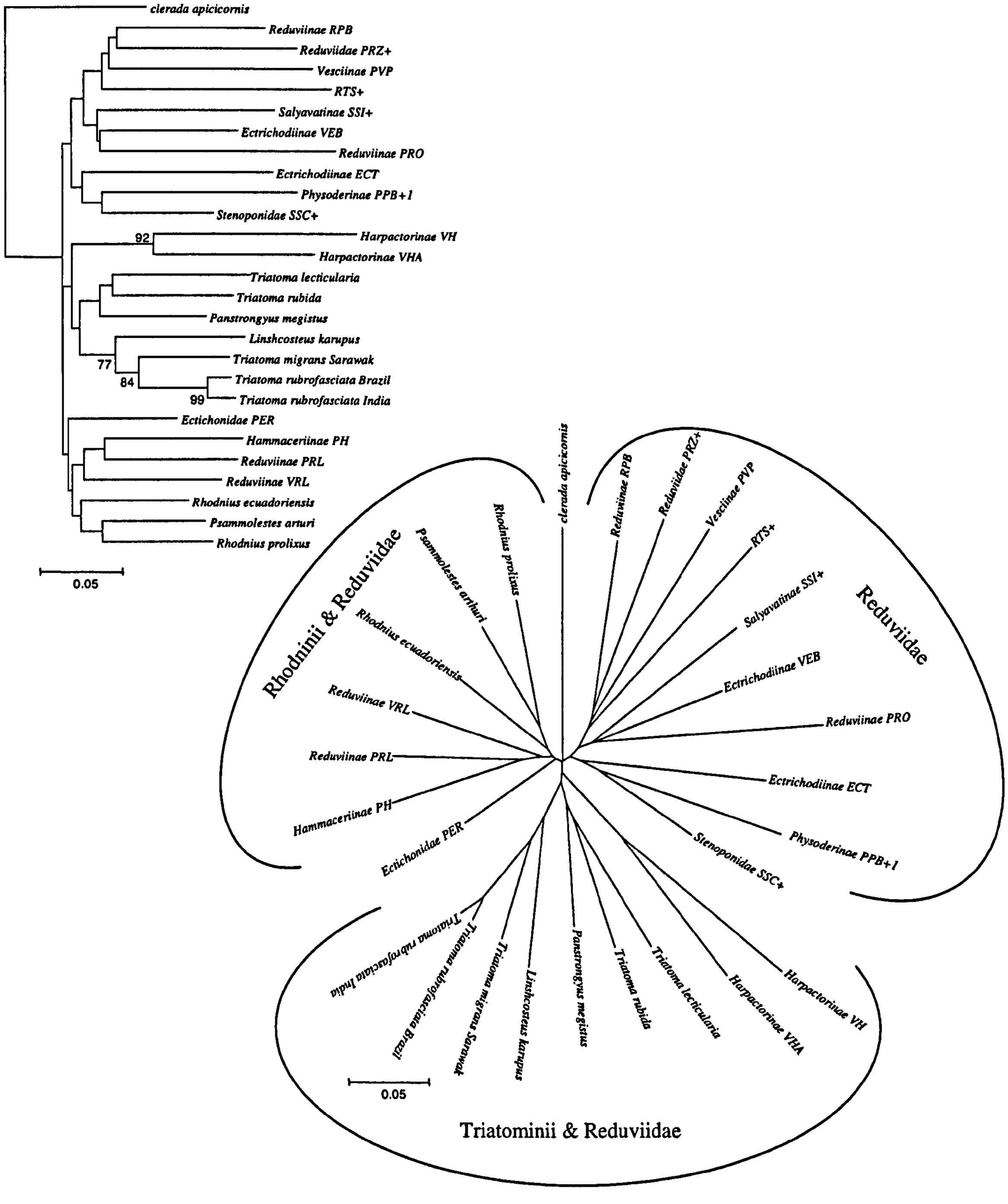

Figure 43. Neighbour-joining phylogenetic tree (rooted and unrooted) of *COII*-2nd segment sequences of reduviid taxa. Constructed using k2p model, with 1000 bootstrap replicates sum of branch lengths = 2.61, scale: substitutions/site

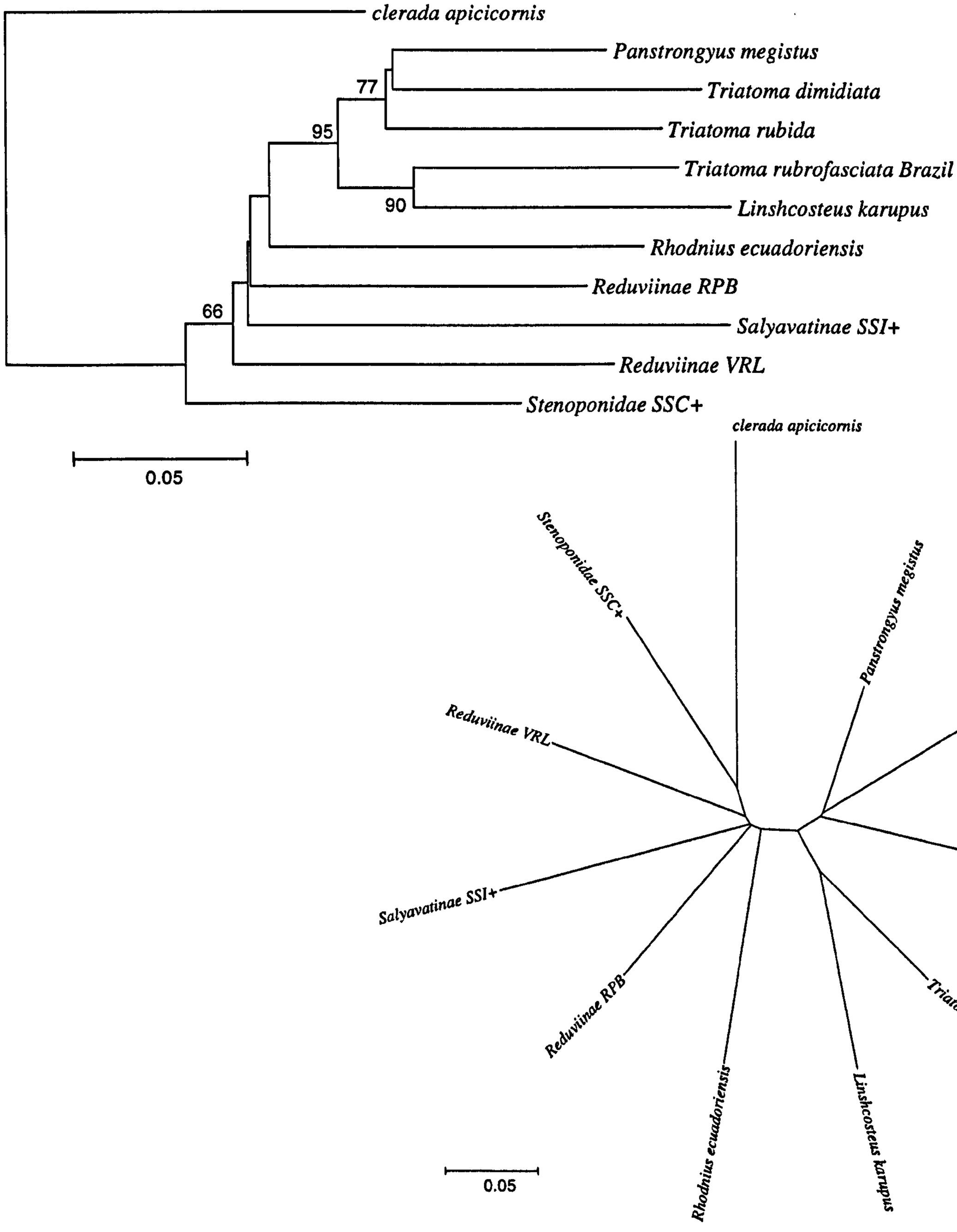

Figure 44. Neighbour-joining phylogenetic tree (rooted and unrooted) of *COII*-complete sequences of reduviid taxa. Constructed using k2p model, with 1000 bootstrap replicates sum of branch lengths = 1.18, scale: substitutions/site. The tree is unresolved and shows a polytomy.

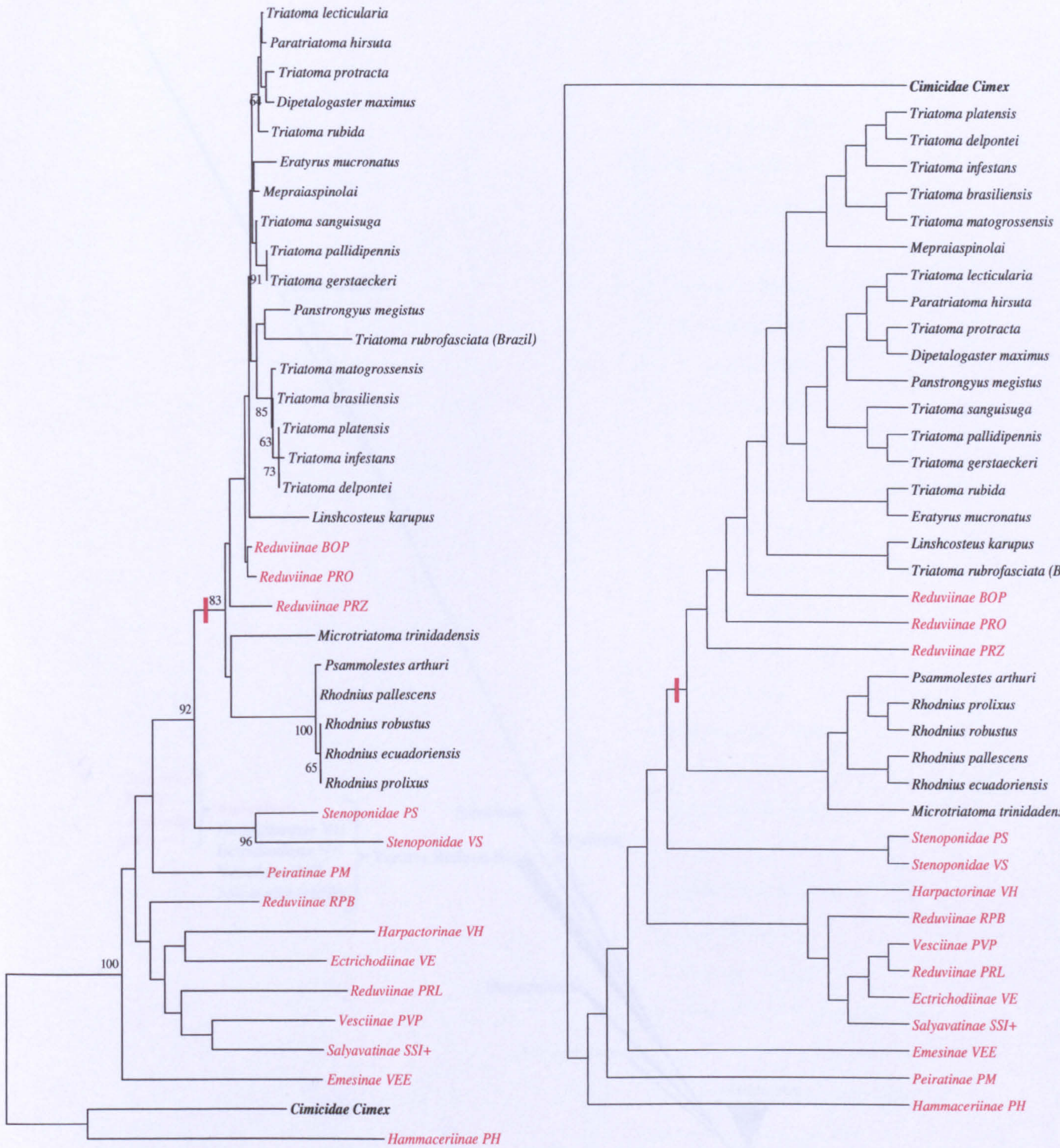

Figure 45. Left: Neighbour-joining phylogenetic tree of D2 28S sequences of reduviid taxa with *Cimex* as an outgroup. Constructed using k2p model, with 1000 bootstrap replicates sum of branch lengths = 0.93, scale: substitutions/site
Right: Maximum parsimony strict consensus phylogeny of D2 28S sequences constructed using branch-and-bound algorithm CI = 0.575 RI = 0.573 RCI = 0.329 (for all sites) and iCI = 0.503 iRI = 0.573 iRCI = 0.289 (for parsimony informative sites).

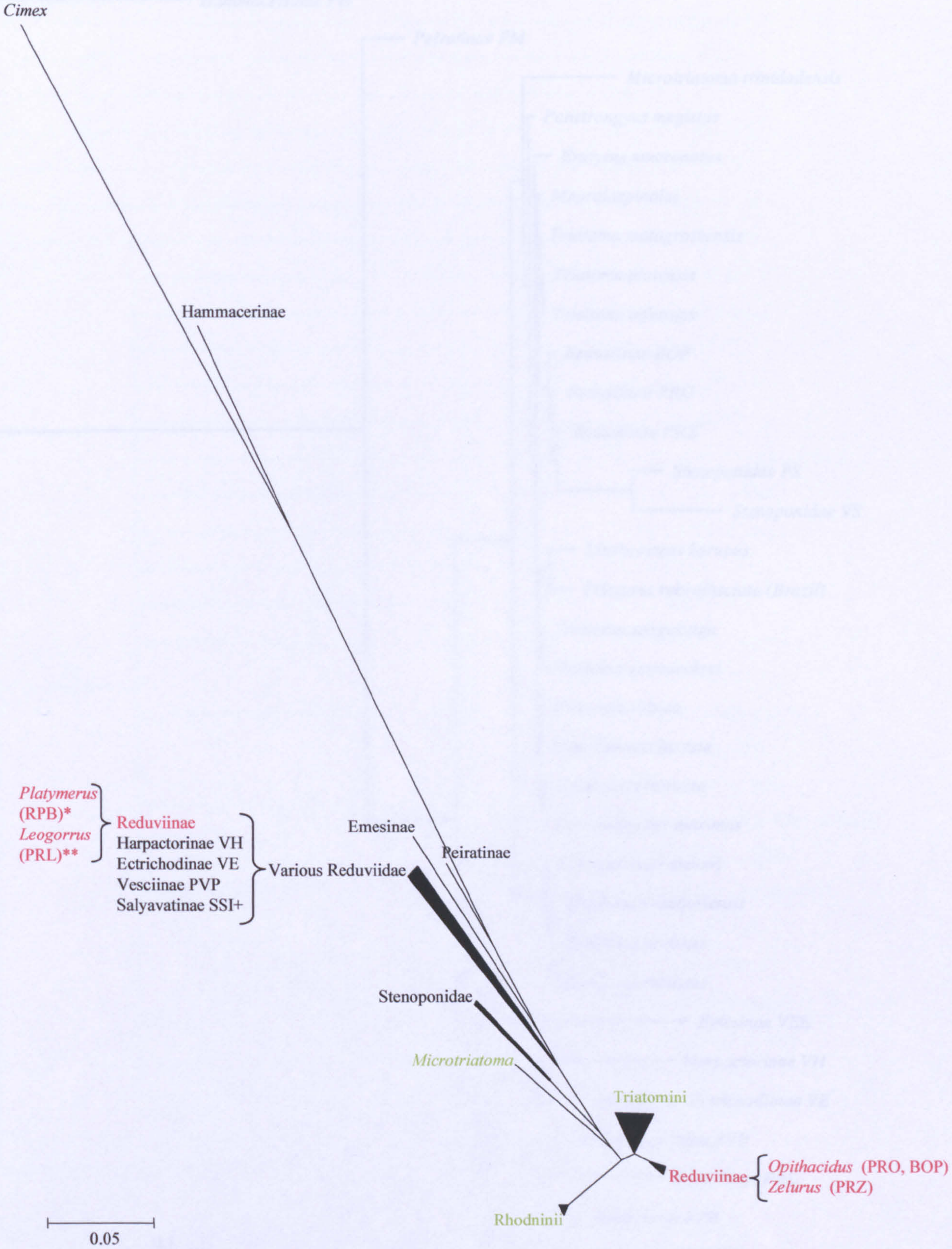

Figure 46. Collapsed Neighbour-joining phylogenetic tree of D2 28S sequences of reduviid taxa with *Cimex* as an outgroup. Constructed using k2p model, with 1000 bootstrap replicates sum of branch lengths = 0.93, scale: substitutions/site Groups of taxa are collapsed emphasising the relationships among Triatominae (green) and Reduviinae (Red). *Microtriatoma* represents the Bolboderini.

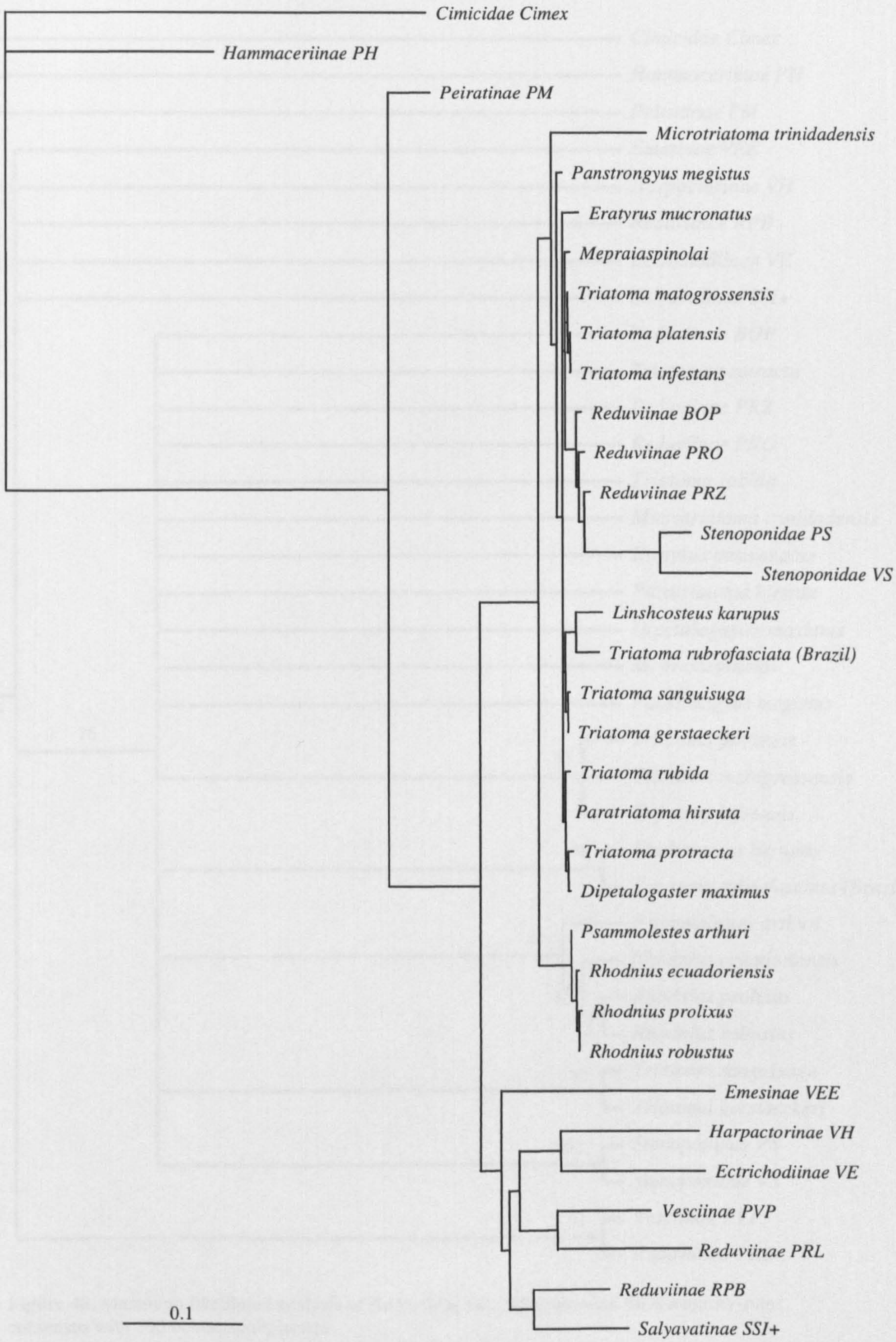

Figure 47. Maximum likelihood analysis of D2-28S of reduviid taxa with *Cimex* as an outgroup.. scale indicates the number of substitutions per sequence position.

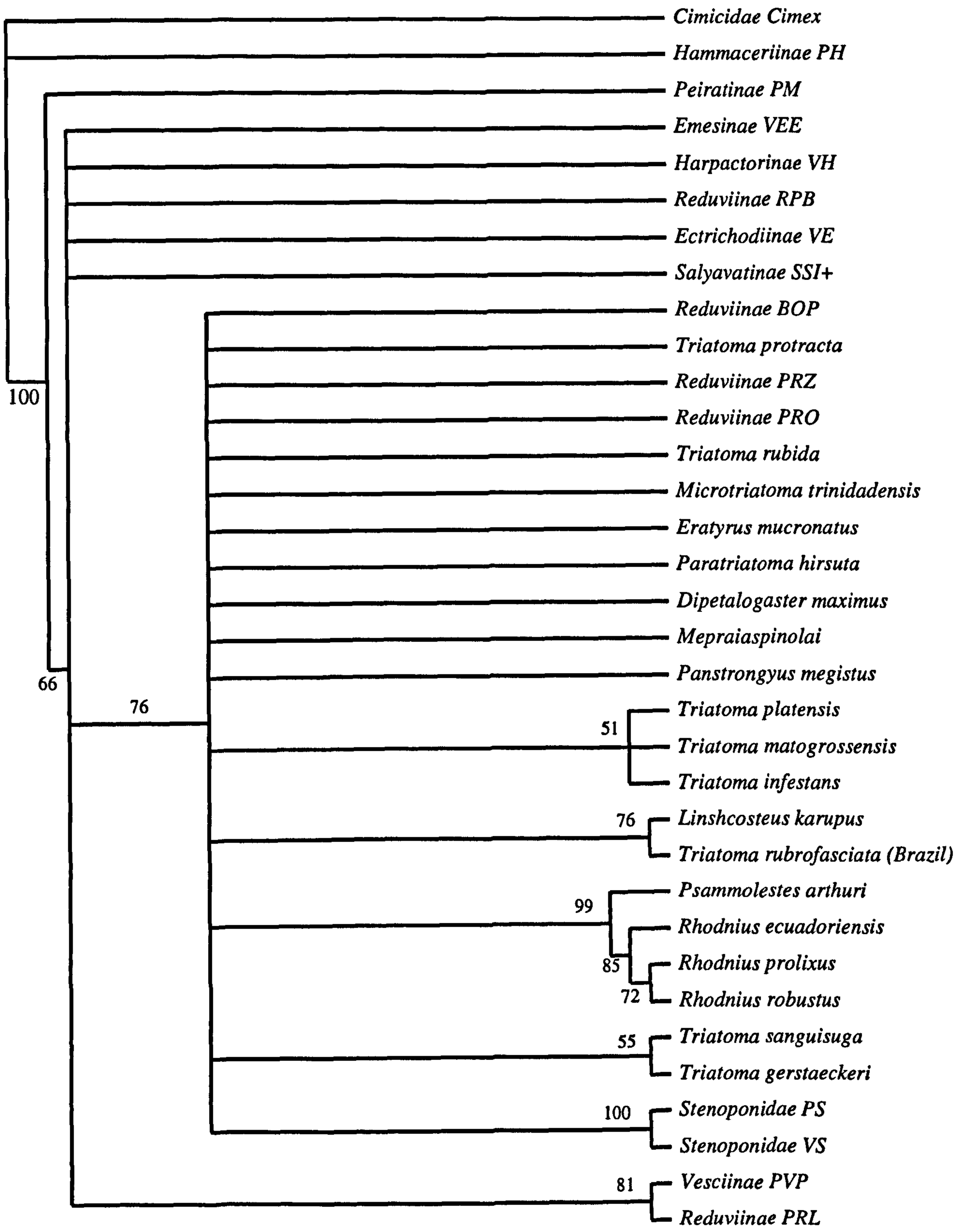

Figure 48. Maximum likelihood analysis of Reduviidae D2-28S sequences. 50% majority-rule consensus with 200 bootstrap replicates.

5.4 Discussion

5.4.1 Morphometrics

The investigative morphometric analysis of head shape among triatomine taxa suggests that head shape is vulnerable to the effects of homoplasy due to convergence. The evolutionary processes involved in head shape variation are discussed in a later section of this thesis.

The cursory analysis of wings (Fig. 39) demonstrates that Triatomini and Rhodniini are cohesive and equally similar/dissimilar to representatives of other reduviid subfamilies. This preliminary assessment with scant material highlights a potential approach for investigating phylogeny of reduviid groups in comparison with molecular methods.

5.4.2 Polyphyly of the Triatominae

Evidence has been acculmulating for a polyphyletic origin for the Triatominae, more precisely the evidence is for di-phyly between the Triatomini and the Rhodninii. see Paula *et al.* (2005). The analysis of D2-28S r-DNA presented here is also evidence for this, but goes further by demonstrating that the group is probably truly polyphyletic by observing that the Bolboderini represent an early offshoot of the Triatominae lineage.

Molecular phylogenetics has become the modern taxonomist's principal approach and gold standard and at the same time revealing the failings and possible inadequacies of past taxonomy. Using robust molecular phylogenetics, a false monophyly might never

be undermined if the relevant related taxa are not surveyed and/or extant. In other words monophyly is not demonstrated, only polyphyly, by accumulation of evidence. A caveat is that recent divergence among taxa can lead to speculation that a group is monophyletic. Conversely, observing ancient divergence among superficially similar lineages can lead to assumptions that homoplasy due to convergence has occurred. Clearly, in these circumstances neither case is necessarily proven.

Through random sampling of reduviid taxa I have been fortunate enough to include what has been revealed to be a sister group to the Triatomini, i.e. representatives of South American Reduviinae (specifically, species of the genera *Opisthacidus* and *Zelurus*). This supports the close relationship between Reduviinae species and Triatomini indicated by Paula *et al.* (2005) and is strong evidence for polyphyly of the haematophagous triatomine lineages. However, this rests on the assumption that the Reduviinae observed to be closely related to the Triatomini represent the ancestral feeding behaviour. It is possible, although counterintuitive, that these predatory Reduviinae descend from a lineage of haematophagous ancestry that has reverted to invertebrate predation.

5.4.3 Polyphyly of the Reduviinae

The close relationship observed between the Triatomini and some Reduviinae (*Opisthcidus* and *Zelurus*) simultaneously demonstrates a polyphyly of the Reduviinae far more striking than that observed for the Triatominae. The other Reduviinae included in the 28S r-DNA phylogeny; *Leogorrus* sp and *Platymerus biguttata* are both very separate from each other and the *Opisthacidus/Zelurus* clade (Fig. 45)

5.4.4 Phylogeography

The taxa from which 28S r-DNA sequences were obtained are mostly of American origin. This is mainly due to our sampling bias and the low success in obtaining good DNA from the limited material available from museum specimens (see Table. 19). The only Old World taxa used were *Platymerus biguttata* (African origin), representing the Reduviinae, and *Syberena izzardi* (Malaysian origin), representing the Salyavatinae. The Cretaceous dates of divergence and radiation discussed above include these Old World reduviids. The Cretaceous period also corresponds to the time when Africa separated from South America, therefore the divergence date of these Old World Reduviidae correspond to the vicariance.

5.4.5 Dating divergences and the fossil record

The dating employed in the previous chapter on the evolution of Old World and New World *Triatoma,* based on the percentage of sequence divergence of the D2 region of 28S r-DNA has been applied at these higher taxonomic levels. The rate of sequence divergence seems to remain constant as the dates given have continued to be compatible with the geological time scale, vicariant events and fossil record (see Fig. 49).

The Hemiptera arose in the Permian (Wootton 1981, Grimaldi & Engel 2005), ~ 286-245 Mya. The earliest divergence estimated by the 28S molecular clock is between the outgroup (*Cimex*) and all reduviid ingroup taxa; this indicates that the cimicid and reduviid lineages diverged ~ 250 – 230 Mya in the Triassic period. This is consistent with the occurrence of the oldest known fossil representing the cimicomophan lineage; *Pterocimex* (Popov *et. al.* 1994), from the upper Triassic/lower Triassic period ~200 Mya.

The earliest divergence estimated within the Reduviidae is of the Hammacerinae, which diverged 200-220 Mya from all other modern reduviid subfamilies examined here. This is ~100 million years before the next observed divergences among reduviid subfamilies. There is apparently little known of the Hammacerinae's ecology (Table.17). However, through my own observations when collecting them, they occur under the bark of trees together with large numbers of arachnids. If the arachnids are their prey, and if this is a persistent specialisation that the lineage has followed, then this might explain their ancient divergence. Since spiders occur earlier in the fossil record (table 41, appendix) than the largest groups of modern insects, then the specialisation of feeding on spiders allowed this ancient lineage of reduviids to arise and persist.

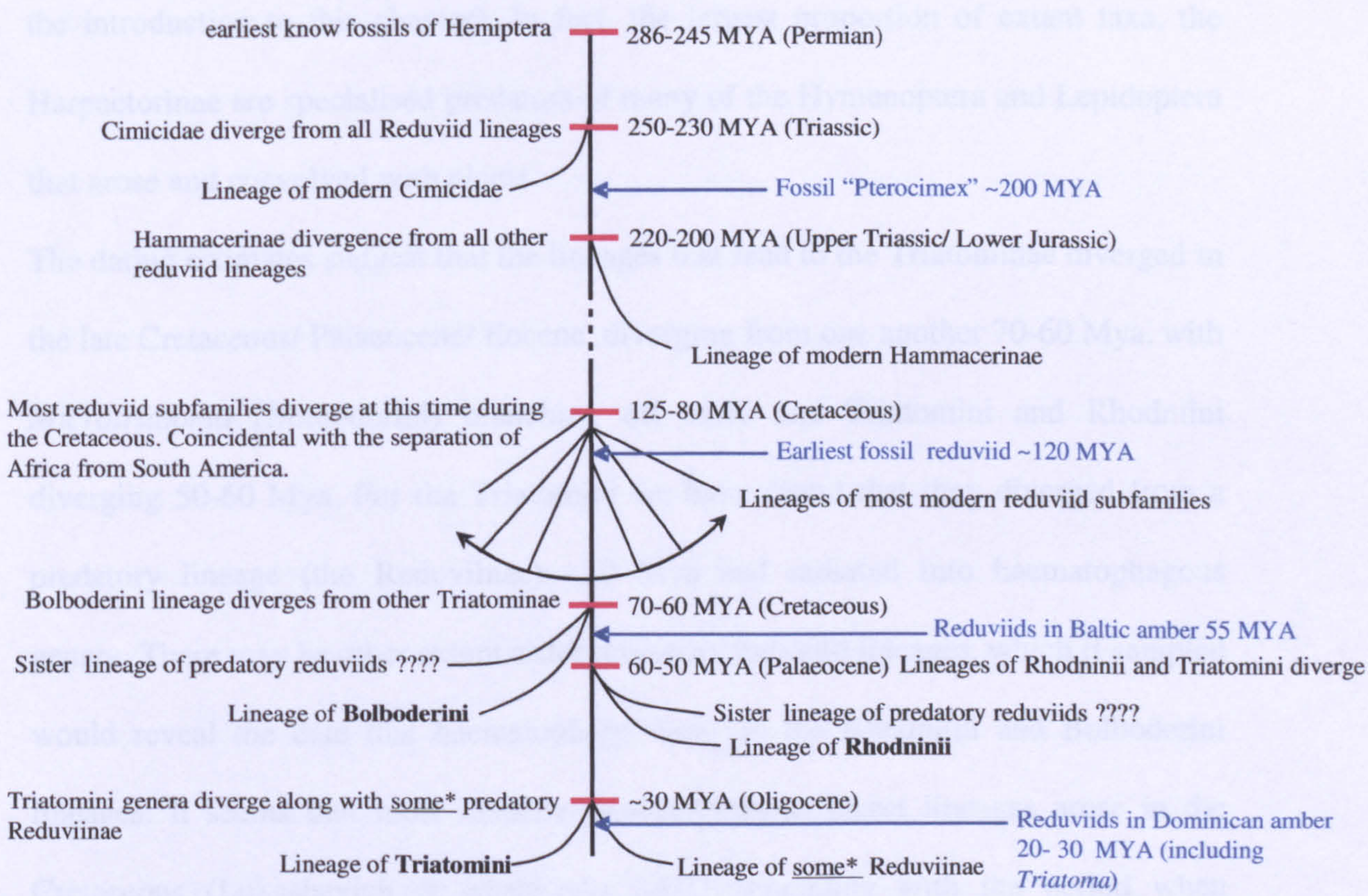

Figure 49. Time line of reduviid evolution based on dating estimates from D2 region of 28S r-DNA sequence divergence. Relevant fossil record entries are indicated. * refers to representatives of the genera *Opisthacidus* and *Zelurus*.

The rest of the reduviid subfamilies assessed here appear to have diverged at around the same time, from 125-80 Mya. This corresponds to the date of the earliest known reduviid fossil from the lower Cretaceous (Hong 1987). The Cretaceous saw the advent of the angiosperms (flowering plants), which, rapidly bolstered by a warm tropical period, became the predominant life forms on land, defining most biomes up to the present day. The radiation of the angiosperms was the cause/effect of contemporaneous radiation and of the emergence of many insect groups that coevolved mainly as pollinators or phytophages (Grimaldi & Engel 2005). In the case of the Reduviidae their response was at the next trophic level, apparently diversifying to exploit the predatory niches defined by the new plant-insect associations. Indeed, the most exquisite examples of reduviid predatory specialisation are observed in those groups that have adapted to prey on plant associated insects (see examples given in the introduction to this chapter). In fact, the largest proportion of extant taxa, the Harpactorinae are specialised predators of many of the Hymenoptera and Lepidoptera that arose and coevolved with plants.

The dating estimates suggest that the lineages that lead to the Triatominae diverged in the late Cretaceous/ Palaeocene/ Eocene, diverging from one another 70-60 Mya, with *Microtriatoma* (Bolboderini) branching off early and Triatomini and Rhodniini diverging 50-60 Mya. For the Triatomini we have found that they diverged from a predatory lineage (the Reduviinae) ~30 Mya and radiated into haematophagous genera. There may be other extant sister predatory reduviid lineages, which if sampled would reveal the date that haematophagy arose in the Rhodniini and Bolboderini lineages. It seems that most modern haematophagous insect lineages arose in the Cretaceous (Lukashevich & Mostovski 2001) coinciding with the period when mammals and birds first became diverse. This raises the question why the reduviids

did not develop haematophagy sooner. The relatively recent development of blood feeding in the Reduviidae is inferred and discussed by Schofield (1999). In general, it seems that at least some triatomines arose ~30 Mya, coinciding with the emergence of modern mammals, such as bats and other nest building mammals. It seems that this was the optimal time for the comparatively sedentary reduviids to adapt to haematophagy in some lineages. This is also the time period put forward as a possible date of divergence for lineages of *T. cruzi* (Kawasshita 2001). Therefore, isolation and diversification of the principal *T. cruzi* lineages could have occured by association with particular triatomine species that channelled parasites to specific hosts and ecologies, see Gaunt & Miles (2000) and Yeo *et al* (2005) for further discussion on this theme.

Baltic amber has yielded representatives of a few of the reduviid subfamilies, as summarised by Weitschat & Wichard, (2002). These include *Collarhamphus mixtus* (Emesinae) (Putshkov and Popov 1995), *Redubitus centrocnemarius* (Centrocnemidinae) (Putshkov & Popov 1993), *Redubinotus liedtkei* (Centrocnemidinae) (Popov & Putshkov 1998) and *Plymerus insignis* (Reduviinae) (Germar & Berendt 1856). Baltic amber dates from only ~55Mya, sometime after the apparent radiation of the group. In the absence of older fossils we can look tentatively to the Hammacerinae as "living fossils"; assuming their niche has been relatively constant they may have changed little from their ancestors, the common ancestors to all modern reduviids ~200 Mya. Furthermore, the Hammacerinae are fairly archetypal large and powerful ruduviids that might well represent the ancestral stock of all reduviids. Support to the basal position of the Hammacerinae is given by Usinger's

phylogeny (Usiinger 1966) see (Fig. 36, NB Usinger uses Microtominae, later synonymised).

Later fossil reduviids are more common from Dominican amber (Poinar 1999). At least ten genera are described, half of which are extant, including an occurrence of *Triatoma* (Poinar 2005). This is discussed in the Old World /New World chapter of this thesis and correlates with the radiation of the Triatomini, see above and Fig. 49.

6 Comparative analyses of vector species

6.1 Part I. *Rhodnius prolixus* domestic and silvatic populations from Venezuela

6.1.1 Introduction

Inspired by the success of the southern cone initiative, in 1993 the first phase of the Andean initiative began with the emphasis on screening blood banks for *T. cruzi*. The vector control phase was launched in 1997. Venezuela has had active control programmes since the mid sixties and has had some notable success. In 1965 house infestation rates in the different States ranged between 2% and 80% and by 1997 were reduced to 0%-4% (Weekly Epidemiological Record, 1999). However it is important to consider that unlike *T. infestans* (the main vector in the southern cone) which is solely domestic through most of its range, the main vector in Venezuela, *R. prolixus,* has numerous silvatic populations (Gamboa 1961, 1963 and Gómez Nuñez 1963). Therefore, to gauge correctly the control strategy required to eliminate domestic populations and transmission it is necessary to study the degree of interaction between silvatic and domestic vector populations (Guhl & Vallejo 1999). It is imperative to the success of control to establish whether silvatic populations readily invade houses. The implication being, that sustained long-term control would be required, with perhaps some level of control aimed at silvatic populations of bugs.

Currently the highest infestation rates are found in the states of Portuguesa and Barinas (>2.9%). Within these states it is the rural communities living on the foothills of the Andes (Cordillera Merida) that are worst affected.

There are 17 species of triatomine bug recorded in Venezuela (Carcavallo & Tonn 1976). As stated, by far the most important vector species is *R. prolixus*. However, as outlined (see general introduction) *R. prolixus* is morphologically extremely similar to *R. robustus,* a solely silvatic species restricted to palm tree ecotopes and first recorded

in Venezuela by Lent & Valderrama (1973). Isoenzyme (Harry 1992 1993a) and morphometrics (Harry 1994) studies suggest that *R. robustus* and *R. prolixus* in Venezuela are very closely related and it is inferred that they might represent a single species. However recent studies with RAPDs (Feliciangeli *et al.* 2002) and DNA sequence data (Monteiro *et al.*, 2000, 2001 2003) suggest that *R. robustus* through its range is a paraphyletic assemblage of several haplotypes, which could be considered as several cryptic species. Furthermore, these studies suggest that Venezuelan *R. robustus* and *R. prolixus* are closely related yet separate species. As more sensitive markers of genetic diversity are applied, the complexity of the relationships between *R. prolixus* and *R. robustus* are gradually being revealed. The present study applies geometric morphometric approaches in comparison to a molecular genetic marker (cytochrome b sequences) to assess the facility of these approaches in the estimation of population structure. Morphometrics methods are relatively cheap, statistically robust and rapid methods of assessing intraspecific variation. But do they estimate population structure reliably?

6.1.2 Collection sites and sampling methods

For the purposes of this study fieldwork was conducted in three states of Venezuela; Portuguesa, Lara and Guarico (see Fig. 50 for collection site locations). Silvatic and domestic ecotopes were surveyed at each location. The Lara and Portuguesa collection sites were located in areas of premountain humid forest, interrupted by small scale cultivation of maize, coffee and bananas. Triatomine bugs were collected from houses and nearby palm trees, the predominant species being *Attalea butyracea*. The samples collected from Lara and Portuguesa were in close proximity. Both domestic and silvatic palm tree samples were collected in Portuguesa, whereas only domestic samples were found in Lara. The ecology of the collection site in Guarico

was dry lowland savannah, situated on the vast flat plains of the Llanos. At this location a different species of palm tree was predominant (*Copernicia tectorum*). The housing in Lara and Portuguesa collection localities was low quality, constructed from wattle and daub with palm or corrugated iron roofs. Whereas at the Guarico site most houses were of higher quality, constructed from cement blocks, improved in the 60s as part of the early control programme.

Figure 50. Maps showing study area in Venezuela from which *Rhodnius prolixus* was collected: upper map shows position within the country; lower shows the locations of collection sites in three Venezuelan states; Guarico 18°18'N, 67°02'W; Portuguesa 9°34'N, 69°21'W; Lara 9°46'N, 69°21'W.

Domestic collections were made by the traditional search and capture method, using forceps and flash lights. Silvatic collections were made using a simple form of baited sticky trap, as exemplified by Noireau (1999), Noireau *et al.* (2002) and Abad-Franch *et al.* (2000). The traps were constructed from small plastic containers approximately 20 X 10 cm, with perforated screw on lids, into which a live mouse was placed with food and bedding. The outer surface of the vessel was then covered with a strongly adhesive double sided tape (the sort used for fixing carpets). Using an adjustable ladder, traps were placed close to the crown of the palm, lodged between the fronds. Typically 4-5 traps were deployed in each palm (~ 5-7 trees per night) shortly before dusk, and then retrieved the following morning. On retrieval of the traps, bugs stuck to the tape were carefully removed with forceps, labelled and preserved. Mature nymphs were kept alive and reared to adults under laboratory conditions.

6.1.3 Results

6.1.3.1 Morphology

Sampling yielded bugs in palm trees at the Guarico and Portuguesa locations and in houses at the Portuguesa and Lara locations. All bugs captured from palm trees and houses were identified as *R. prolixus* Stål, 1859 using the keys of Lent and Wygodzinsky (1979). No obvious consistent morphological differences were observed between the four groups sampled (Fig. 51). However, those bugs collected from palm trees in Guarico were distinctly smaller.

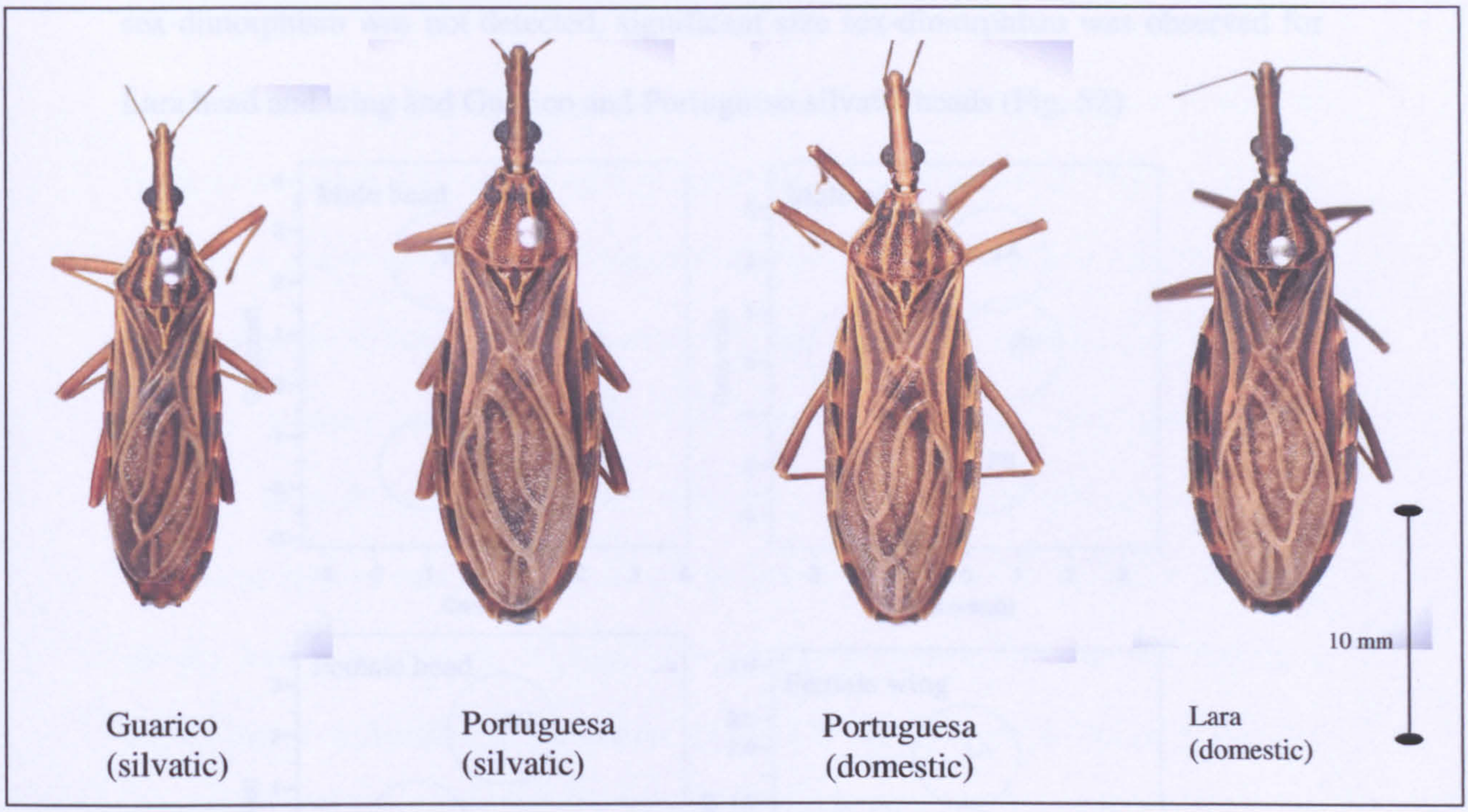

Figure 51 Examples of *Rhodnius prolixus* from each population sampled (all female).

6.1.3.2 Morphometrics

For this morphometric investigation a total of 66 insects were used, composed of 15 to 20 bugs per group (~50/50% males and females). Precise sample sizes were as follows: Guarico 15 (8♂ 7♀), Lara 17 (8♂ 9♀), Portuguesa domestic 16 (8♂ 8♀) and Portuguesa silvatic 18 (10♂ 8♀). From each group sampled 2D landmarks were digitised for dorsal head and wing morphology, as described in the Materials and Methods section.

6.1.3.2.1 Sex

Explorative discriminant analyses of shape variables for both head and wing (Fig. 52) demonstrate that both sexes show the same pattern of group discrimination. Therefore for the remainder of the morphometric analyses sexes were pooled within group to improve statistical power, otherwise weakened by low sample sizes. Although shape

sex-dimorphism was not detected, significant size sex-dimorphism was observed for Lara head and wing and Guarico and Portuguesa silvatic heads (Fig. 52)

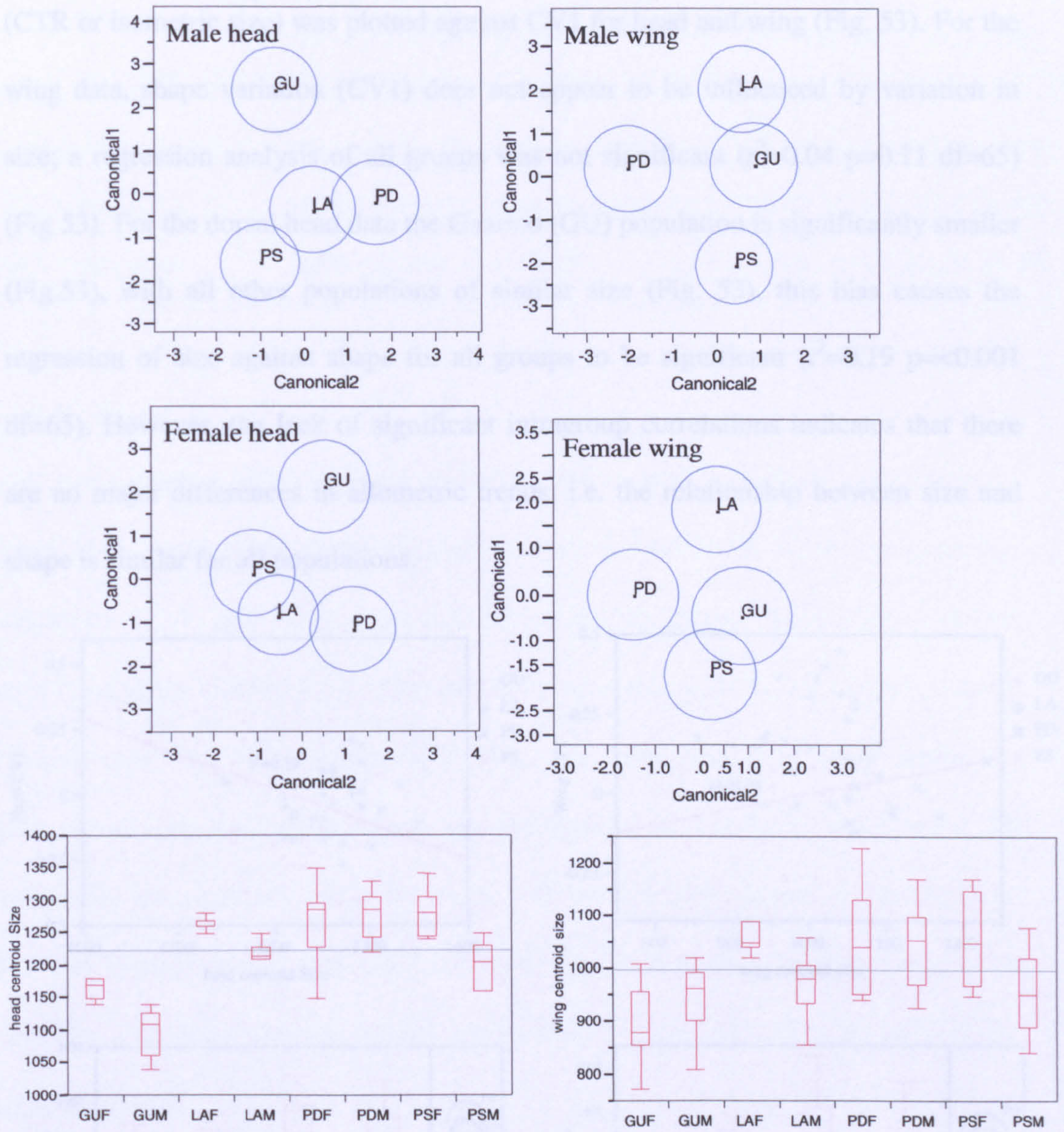

Figure 52. Exploratory analyses of size and shape sexual dimorphism within populations of *Rhodnius prolixus*. The upper four plots are centroid plots after dicriminant analysis of shape variables, head shape plots to the left and wing shape plots on the right. The bar charts below show quartile plots of size variation, again, head size to the left and wing size chart to the right.
Labels on plots and charts refer to the samples: GU- Guarico (silvatic), LA- Lara (domestic), PD Portuguesa (domestic) PS- Portuguesa (silvatic). Suffixes M= Male and F=Female.

6.1.3.2.2 Size

To explore shape differences dependant on size (allometries), respective centroid size (CTR or isometric size) was plotted against CV1 for head and wing (Fig. 53). For the wing data, shape variation (CV1) does not appear to be influenced by variation in size; a regression analysis of all groups was not significant (r^2=0.04 p=0.11 df=65) (Fig 53). For the dorsal head data the Guarico (GU) population is significantly smaller (Fig.53), with all other populations of similar size (Fig. 53), this bias causes the regression of size against shape for all groups to be significant (r^2=0.19 p=<0.001 df=65). However, the lack of significant intragroup correlations indicates that there are no major differences in allometric trends: i.e. the relationship between size and shape is similar for all populations.

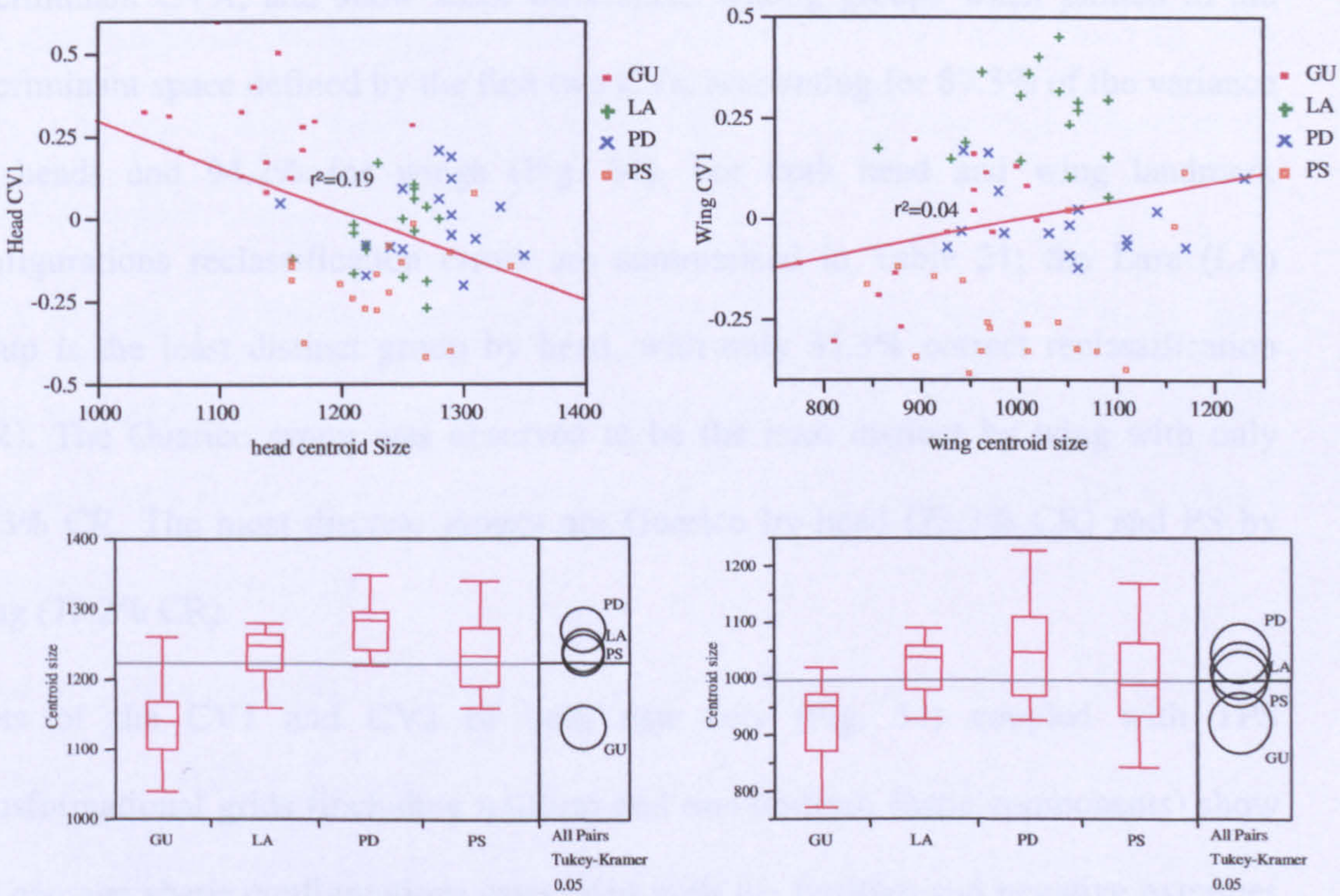

Figure 53. Size differences among population samples of *Rhodnius prolixus*. Upper, scatter plots, head left, wing right, show the relationship between centroid size and CV1 (the main axis of shape variation). Regression lines and respective r^2 values are included. Lower, two charts show mean quartile plots of size for each population, head to the left and wing size in the chart to the right. Tukey-Kramer comparison of means indicate where significant differences occur- Circles for means that are significantly different either do not intersect or intersect slightly.. Labels on plots and charts refer to the samples: GU- Guarico (silvatic), LA- Lara (domestic), PD Portuguesa (domestic) PS- Portuguesa (silvatic)

Table 21. Results of cross checked reclassification after dicriminant analysis of head and wing morphometrics of *Rhodnius prolixus* samples with Wilk's Lambda values and significances. Percentages of correct classification are shown in **bold** and percentages of misclassification as other groups are in parentheses.

Populations	Head , dorsal Wilk's statistic λ =0.156 p=<0.0001	Wings Wilk's statistic λ = 0.145 p=<0.0001
Domestic Portuguesa (PD)	**68.8%** (18.8% LA, 12.5% PS)	**68.8%** (6.3% GU, 12.5%LA, 12.5% PS)
Silvatic Portuguesa (PS)	**72.2%** (5.6% GU, 16.7% LA, 5.6% PD)	**72.2%** (11.1% GU, 16.7% PD)
Domestic Lara (LA)	**35.3%** (29.4% PD, 23.6% PS, 11.8% GU)	**70.6%** (23.5% GU, 5.9% PD)
Silvatic Guarico (GU)	**73.3%** (13.3% LA, 13.3% PD)	**33.3%** (26.7% PD, 26.7% PS, 13.3% LA)

6.1.3.2.3 Shape

Shape components (relative warps including affine and non-affine components), derived from head (dorsal orientation) and wing landmarks were analysed by discriminant CVA, and show some differences among groups when plotted in the discriminant space defined by the first two CVs, accounting for 87.3% of the variance for heads and 94.2% for wings (Fig. 54). For both head and wing landmark configurations reclassification errors are summarised in Table 21; the Lara (LA) group is the least distinct group by head, with only 35.3% correct reclassification (CR). The Guarico group was observed to be the least distinct by wing with only 33.3% CR. The most discrete groups are Guarico by head (73.3% CR) and PS by wing (72.2% CR).

Plots of the CV1 and CV2 of both data sets (Fig. 54) coupled with TPS transformational grids (including uniform and non-uniform shape components) show the average shape configurations associated with the positive and negative extremes of the abscissa (CV1) and the ordinate axis (CV2). Multivariate regression tests demonstrate that CV1 and CV2 for both head and wing data are significantly

associated to the corresponding variation in landmark configurations (Table 22). For head dorsal data CV1 shows that PS PD and LA groups have relatively longer pre-ocular distances (represented by the relative position of landmarks 2, 3, 8, 9) compared to the GU group, with PS and PD having intermediate forms between the two extremes. Shape differences associate with CV2 constitute more subtle differences in the relative elongation and width of the head. The main difference in wing shape associated to CV1 is related to the relative position of the landmarks in the distal part of the wing (landmarks 1, 2, 3 and 4): LA has a least similar wing configuration in comparison to all other groups. CV2, the secondary component of shape relates to differences in the anterior region of the wing (land marks 5, 6, 7 and 8)

Further analysis was conducted including three out-groups: 12 specimens of *R. robustus* (identified according to Lent and Wygodzinsky 1979) collected from palm trees in eastern Ecuador (source Dr F Abad Franch); 10 specimens of *R. colombiensis*, and 10 specimens of *R. pallescens* .

CVA of relative warps (including affine and non-affine components) of dorsal head wind landmarks was performed. Fig 55 shows a plot of the first two CVs for both head and wing data, accounting for 81.5% and 83.7% of the variance for head and wing data sets respectively.

Head CV1 shows clear separation of the *R. prolixus* groups from *R. robustus*, reasonable separation from *R. pallescens* and some overlap with *R. colombiensis.* Head CV2 separates the GU population from all other groups and pertains to the same pattern of shape change (represented by TPS grids) as observed for the CV1 axis of the intraspecifc analysis. The shape changes associated with the CV1 axis represent an exaggerated form of the same pattern of shape variation as observed for CV1 of the

intraspecific analysis, i.e. large differences in the relative ratios of post-ocular to pre-ocular distances and degree of elongation (lengthening and narrowing vs shortening and widening).

Table 22. Fit to the regression model of CV1 and CV2 against head and wing shape components of *R. prolixus* samples was tested using a generalized Goodall F-test with p values after 1000 permutations.

	Head	Wing
CV1	F = 12.587, P =<0.0001, df=14896	F = 12.0922, P = <0.001, df=14896
CV2	F = 8.3341, P =<0.0001, df=14896	F = 26.5277, P = <0.0001, df=14896

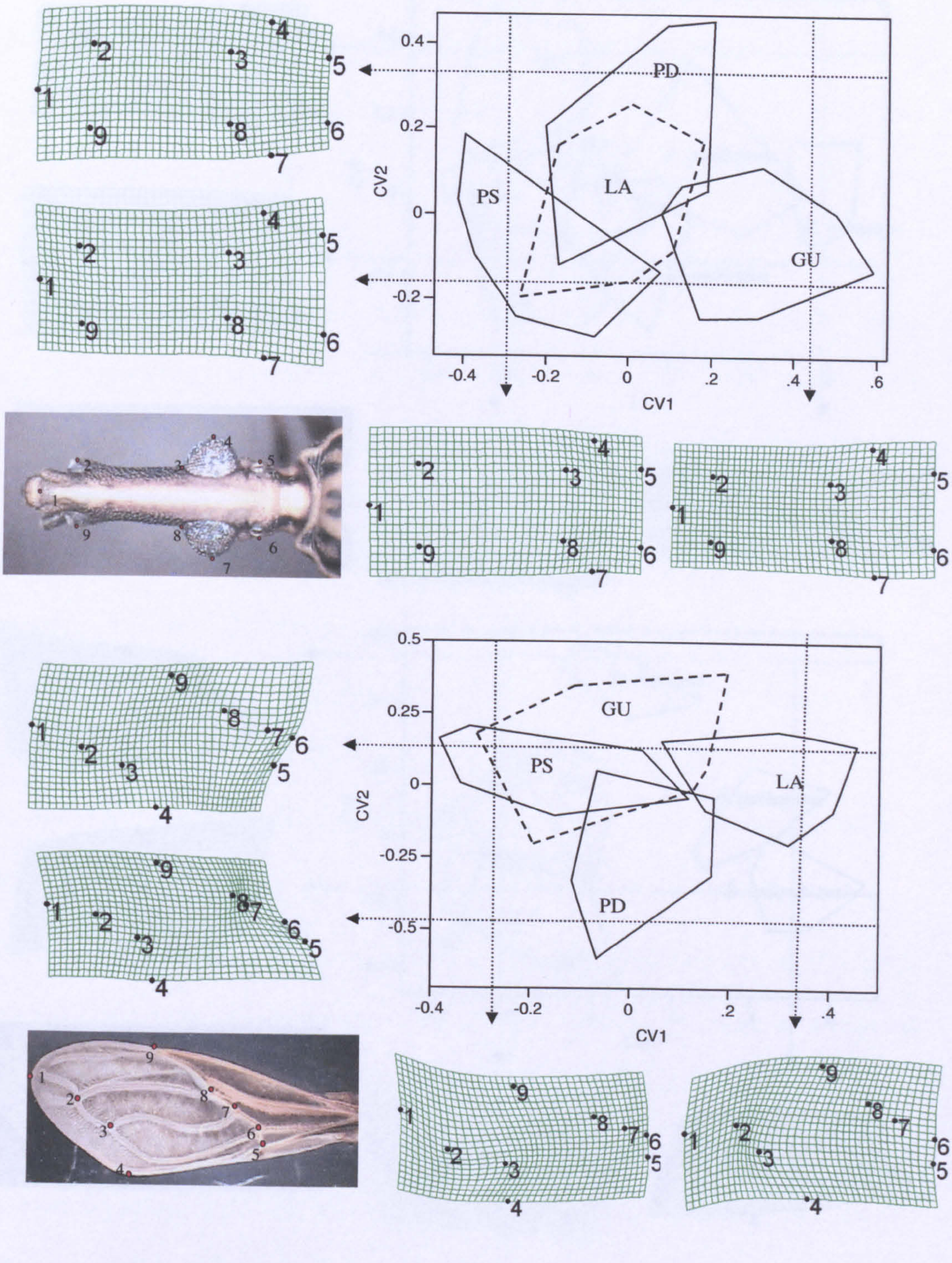

Figure 54.. Morphometric analysis of *Rhodnius. prolixus* intraspecific groups: CVA analysis of shape components after GPA. Polygons enclose distribution of specimens in each group. The upper plot is derived from dorsal head landmarks and the lower from wings. For the heads CV1 accounts for 64.6% of the total variance and CV2 accounts for 22.7% ($\sum$ = 87.3%). For the wings CV1 62.6%, CV2 31.6% ($\sum$94.2 %). Thin plate splines are included showing, shape differences of the head and wing that correspond to the CV axes, as indicated by dashed lines and arrows.. Labels on plots and charts refer to the samples: GU- Guarico (silvatic), LA- Lara (domestic), PD Portuguesa (domestic) PS- Portuguesa (silvatic)

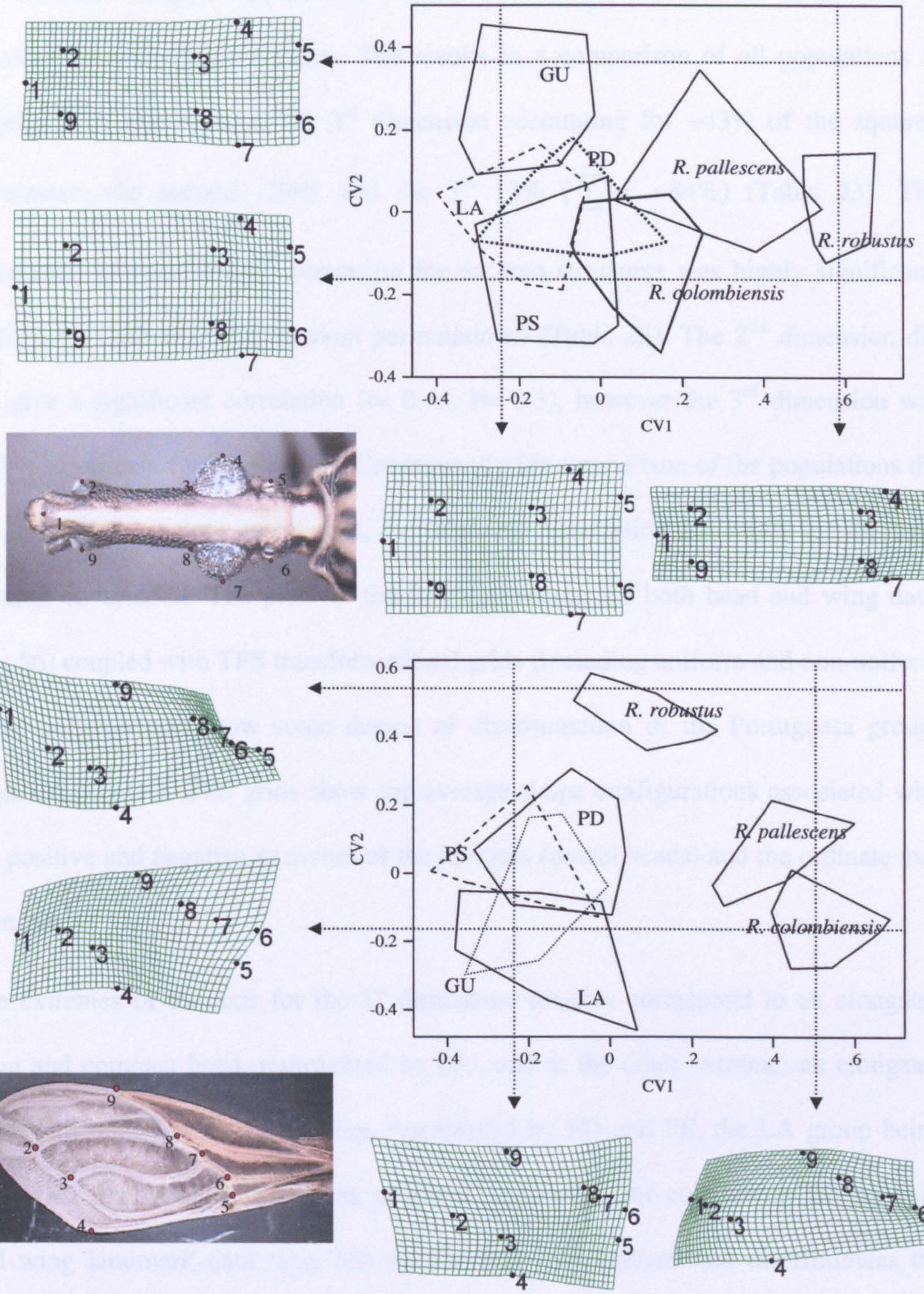

Figure 55..Morphometric analysis of *Rhodnius. prolixus* groups with interspecific out-groups (*R. pallescens* and *R. colombiensis*): CVA analysis of shape components after GPA. Polygons enclose distribution of specimens in each group. The upper plot is derived from dorsal head landmarks and the lower from wings. For the heads CV1 accounts for 67.5% of the total variance and CV2 accounts for 14% ($\sum$ = 81.5%). For the wings CV1 55.5%, CV2 28.2% ($\sum$ 83.7%). Thin plate splines are included showing the shape differences of the head and wing that correspond to the CV axes, as indicated by dashed lines and arrows. Labels on plots and charts refer to the samples: GU- Guarico (silvatic), LA- Lara (domestic), PD Portuguesa (domestic) PS- Portuguesa (silvatic)

6.1.3.2.4 Shape covariation

The 2B-PLS analysis was used to explore covariation between the shape data of dorsal head and wing structures. The results in a comparison of all populations is largely three dimensional, the 1st dimension accounting for ~43% of the squared covariance, the second ~28% and the 3rd 13% ($\sum$ = ~84%) (Table 23). The correlation between the 1st dimension for the two structures was highly significant, (r=0.55 P= 0.02 after 999 random permutations) (Table 23). The 2nd dimension did not give a significant correlation (r= 0.43, P= 0.3), however the 3rd dimension was highly significant (r=0.5 P=0.02). Consequently for comparison of the populations the 1st and 3rd dimensions were used, cumulatively accounting for ~44% of the total squared covariation. The plots of the first dimension, for both head and wing data. (Fig.56) coupled with TPS transformational grids (including uniform and non-uniform shape components) show some degree of discrimination of the Portuguesa groups from LA and GU. TPS grids show the average shape configurations associated with the positive and negative extremes of the abscissa (dorsal heads) and the ordinate axis (wings).

The extremes of the axis for the 1st dimension roughly correspond to an elongated wing and compact head, represented by GU, and at the other extreme; an elongated head with relatively compact wing, represented by PD and PS, the LA group being somewhat intermediate. The plots of the 3rd dimension for covariation among head and wing landmark data (Fig. 56) do not show any pattern that discriminates the groups. However, the variation of correlated head and wing configurations is noticeably higher for the PD group.

Table.23. Results of partial least squares analysis after permutation test for comparisons of the head-dorsal and wing landmarks. Only the first eight dimensions are shown. λ_i is the *i*th singular value, $\sum \lambda_i^2$ is the cumulative sum of squared singular value (cumulative sum of the squared covariance), and r_i is the correlation for the *i* pair of dimensions. Probabilities are based on the observed values plus 999 random permutations of the association between the head-dorsal and wing landmarks

Dimensions	λ_i	$\sum \lambda_i^2$	r_i	P
1	0.000068	0.43553	0.54826	0.0210
2	0.000054	0.71089	0.43178	0.3040
3	0.000037	0.83573	0.49589	0.0210
4	0.000032	0.93334	0.38196	0.2930
5	0.000017	0.959	0.29635	0.7520
6	0.000014	0.9777	0.2812	0.6890
7	0.000010	0.98695	0.21587	0.9180
8	0.000008	0.99302	0.38608	0.0230

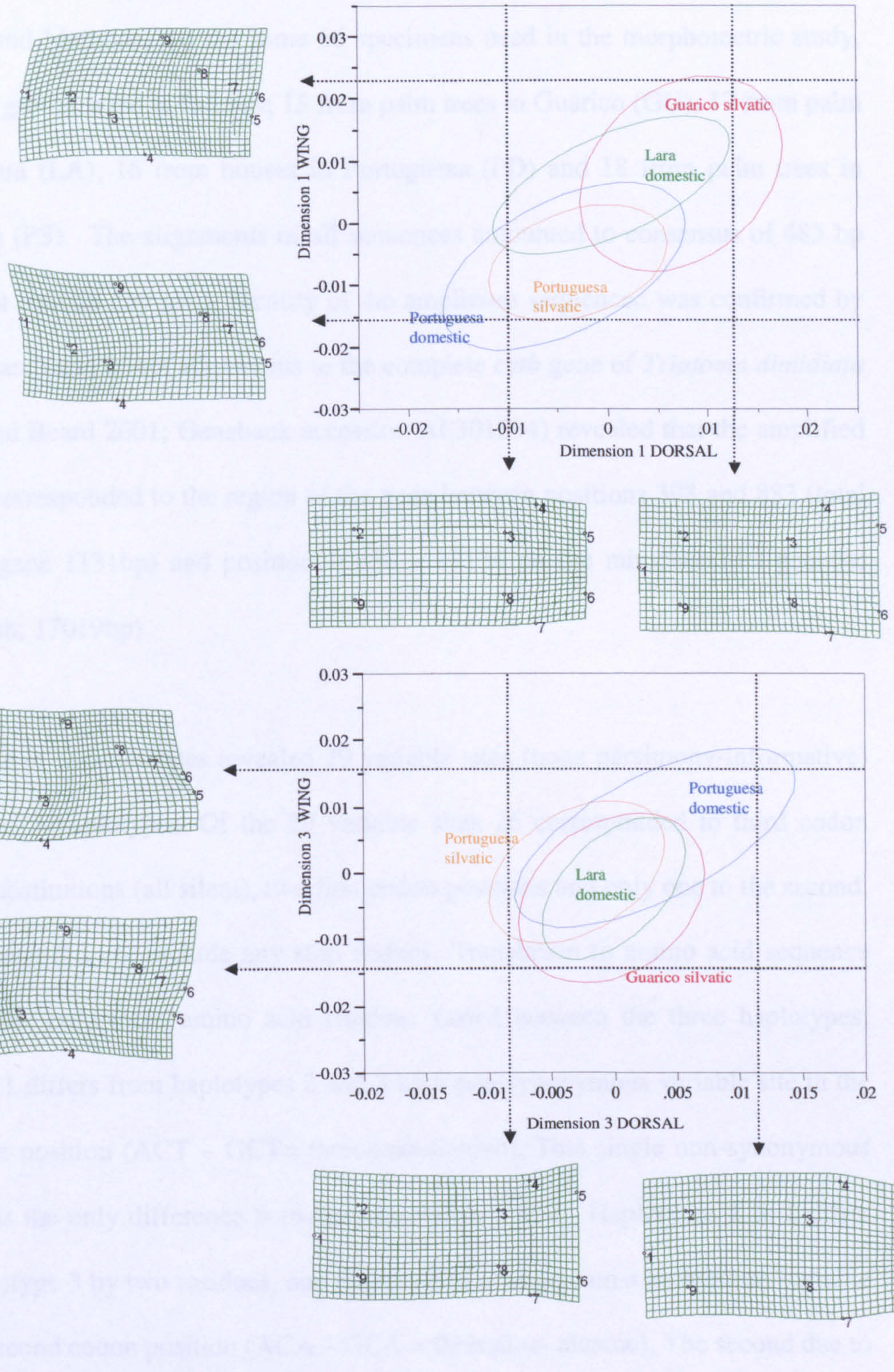

Figure 56. Analysis of shape covariation for head and wing of *Rhodnius prolixus* population samples. Plot of dimensions 1 (upper) and 3 (lower) for head-dorsal (abscissa axes) and wing landmark (ordinate axes) data after Partial least squares analysis. Ellipses enclose 50% of the distribution of specimens in each group. Thin plate spline grids have been interpolated and correspond to values of the respective dimensions, as indicated by dashed lines and arrows.

6.1.3.3 Cytochrome b amplification and sequencing

A 700 bp fragment of the mitochondrial cytochrome b (*cytb*) gene was sequenced (see Materials and Methods) for the same 66 specimens used in the morphometric study. Again, the groups were as follows; 15 from palm trees in Guarico (GU), 17 from palm trees in Lara (LA), 16 from houses in Portuguesa (PD) and 18 from palm trees in Portuguesa (PS). The alignments of all sequences amounted to consensus of 485 bp and did not contain any gaps. Identity of the amplicons sequenced was confirmed by BLAST search and direct alignments to the complete *cytb* gene of *Triatoma dimidiata* (Dotson and Beard 2001; Genebank accession AF301594) revealed that the amplified fragment corresponded to the region of the gene between positions 398 and 883 (total length of gene 1131bp) and position 10650 – 11134 on the mitochondrial genome (total length; 17019bp)

Alignments of all sequences revealed 29 variable sites (none parsimony-informative) and in total 3 haplotypes. Of the 29 variable sites 26 corresponded to third codon position substitutions (all silent), two first codon positions and only one to the second. The sequence did not include any stop codons. Translation to amino acid sequence revealed that only three amino acid residues varied between the three haplotypes; haplotype 1 differs from haplotypes 2 and 3 by a non-synonymous variable site in the first codon position (ACT – GCT= threonine-alanine). This single non-synonymous variation is the only difference between haplotypes 1 & 2. Haplotypes 2 & 1 differ from haplotype 3 by two residues, one the result of a single non-synonymous variable site of a second codon position (ACA – GCA = threonine- alanine). The second due to non-synonymous variation of a first codon position (ATA- ACA methionine-threonine)

6.1.3.3.1 Haplotype distribution

The distribution of the 3 haplotypes amongst the four ecological/geographical groupings are as follows. Out of the 15 bugs sequenced from GU 2 of the 3 haplotypes were found to occur (see Table 24). All the bugs sequenced from LA were haplotype one. Bugs sequenced from PD and PS groups were composed of mixtures of haplotypes 1 & 3 (see table. 24)

Table. 24 Results of *cytb* haplotype analysis of *Rhodnius prolixus* samples: Haplotype composition of the four population samples.

Count	GU	LA	PD	PS	Total
Haplotype 1	5	17	5	12	39
Haplotype 2	10	0	0	0	10
Haplotype 3	0	0	11	6	17
Total (n)	15	17	16	18	66

GU- Guarico (silvatic), LA- Lara (domestic), PD Portuguesa (domestic) PS- Portuguesa (silvatic)

For comparative analysis of the haplotypes and subsequent phylogenetic analyses nucleotide differences and distance matrices were calculated. For this data set several models of base substitution were used in comparison (p distances, Kimura 2 parameter, Jukes Cantor, Tajima-Nei, Tamura 3 parameter, Tamura-Nei). All models assessed, for this data set gave comparable results without any significant differences in the results of the eventual phylogenetic analyses, tree topologies were congruent with good bootstrap support. For this reason, only K2 p distances and nucleotide differences are reported on here. Haplotypes 1 & 2 differed by a single variable site as detailed above. (a sequence divergence of 0.2%) Haplotype 3 occurring in both groups from Portuguesa (PD & PS) differed from haplotypes 1 & 2 by 29 and 28 nucleotides respectively (a sequence divergence of 5.8% – 6%). Differences among groups are very small between geographically disparate Guarico and Lara samples, compared to the very large within-group variation of Portuguesa groups.

For each of the geographic/ecological samples within group differences were assessed by absolute nucleotide differences (Table 25)

Table 25. Absolute number of nucleotide differences (for a 485 bp fragment of *cytb*) within populations of *Rhodnius prolixus*.

Geographical/ecological sample	Within group; absolute nucleotide differences
GU	1
LA	0
PD	29
PS	29

GU- Guarico (silvatic), LA- Lara (domestic), PD Portuguesa (domestic) PS- Portuguesa (silvatic)

The data set of the 3 haplotypes has a high transition to transversion ratio of 13.5. This considered together with all p distances being < 0.09-0.1 (the saturation threshold for the *cytb* gene, as recommended by Meyer (1994) negates the possibility that the models of base substitution used to calculate the genetic distances would be adversely affected by saturation of transitions.

6.1.3.3.2 Phylogenetic analyses

6.1.3.3.2.1 Distance based

Neighbour joining trees were generated using the various models of base substitution, and statistical support was evaluated by bootstrap resampling with 1000 replicates and a random seed number. In the alignment used to construct the trees sequences from two distantly related *Rhodnius* species (*R. pallescens* and *R. colombiensis*) and *T. infestans* were included as outgroups. Reference sequences of *R. prolixus* and *R. robustus* were also included: one *R. prolixus* haplotype from Honduras (domestic). *R. robustus* from Amazonian Brazil (3 haplotypes), one haplotype of *R. robustus* from Trujillo, Venezeuela and one from the Amazonian region of Ecuador. These sequences were provided by Fernando Monteiro (FIOCRUZ) and relate to those described by Monteiro *et al.*, (2003).

All models of base substitution investigated yielded essentially equivalent results, all trees had identical topologies and similar bootstrap supports.

The dissimilarity of haplotype 3 from 1 & 2 is supported by an unambiguous 99% bootstrap support (Fig. 57). Haplotype 3 has identity with a *R. robustus* sequence from Brazil (Fig. 57) and falls in a bootstrap supported clade with other *R. robustus* haplotypes from Brazil and the one from Ecuador. Haplotype 1 has identity with the sample of domestic *R. prolixus* from Honduras, and together with haplotype 2 forms a well supported clade with the Venezuelan *R. robustus* haplotype.

6.1.3.3.3 Maximum parsimony

To support the phylogeny reported by the neighbour joining analysis the haplotypes were also subjected to a maximum parsimony analysis. The branch and bound algorithm was used to recover three equally parsimonious trees, which from which a strict consensus tree was produced with bootstrap supports (Fig. 58).

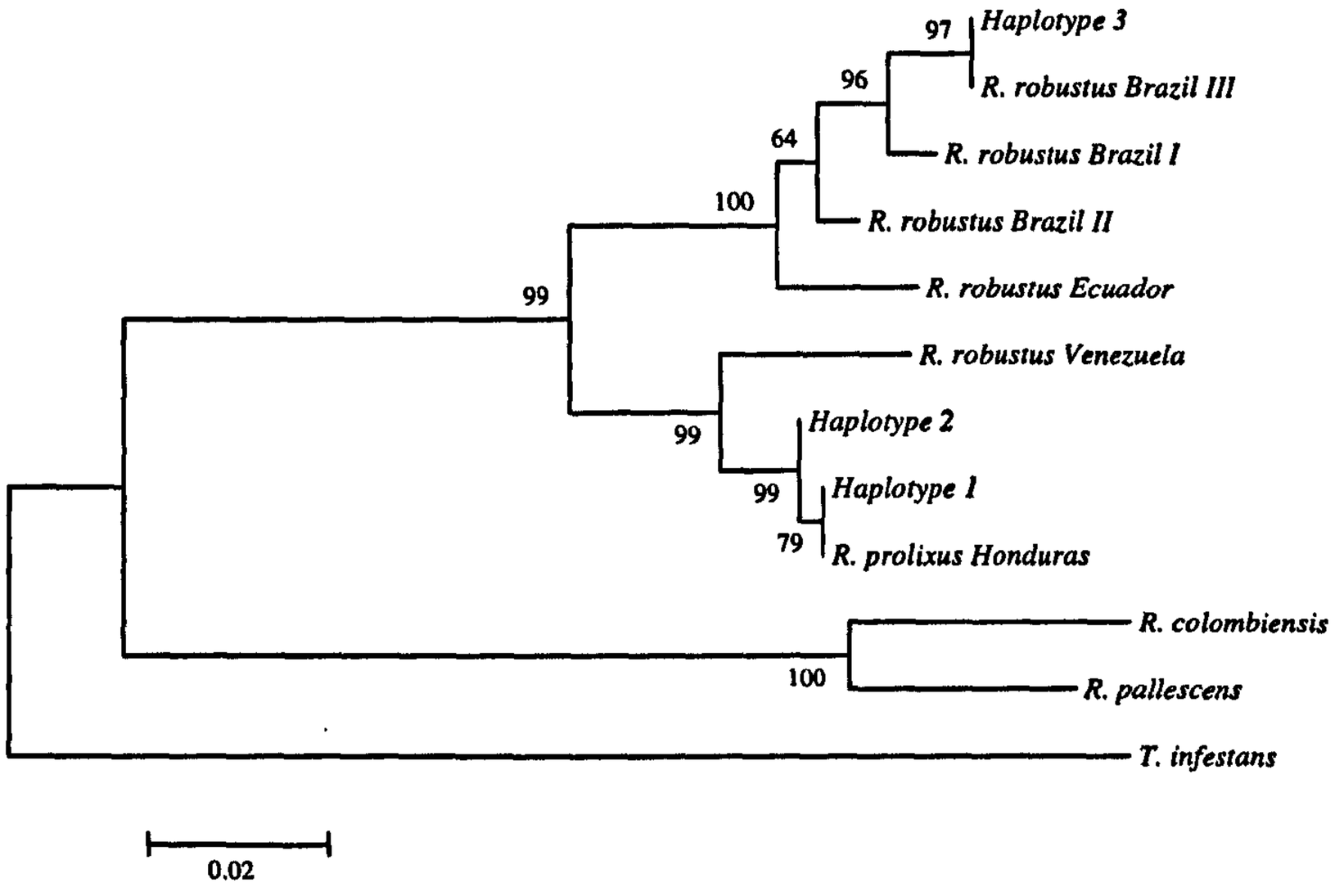

Figure 57. Analysis of *cytb* sequences: Neighbour-joining phylogenetic tree of the 3 *Rhodnius prolixus* haplotypes including reference haplotypes of *R. prolixus, R. robustus* and *R. colombiensis, R. pallescens* and *T.infestans* as outgroups. Constructed using k2p model, with 1000 bootstrap replicates. Sum of branch lengths = 0.444, scale: substitutions/site (refer to Table 24 for distribution of haplotypes).

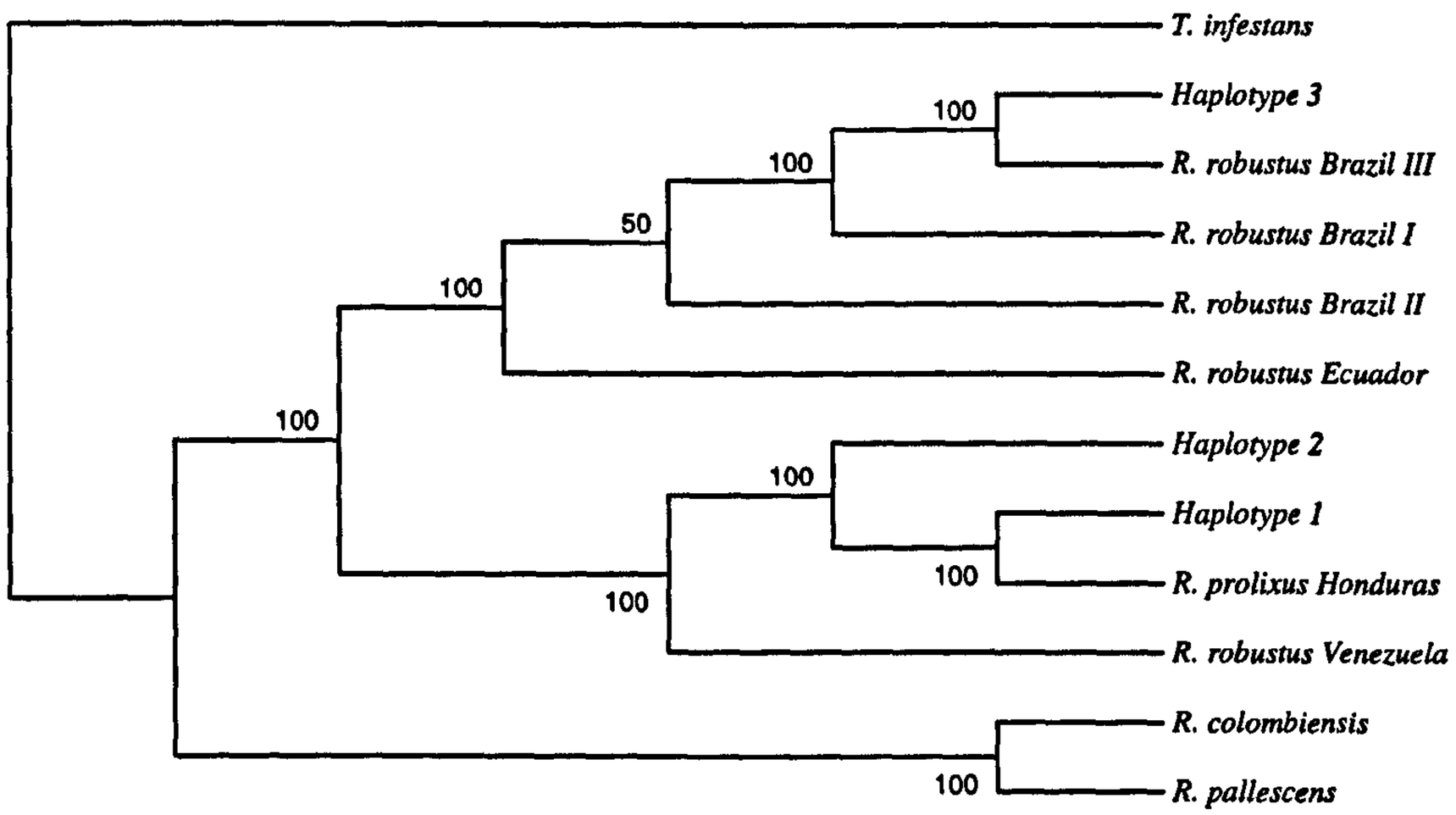

Figure 58. Analysis of *cytb* sequences: Maximum parsimony strict consensus phylogeny of the 3 *Rhodnius prolixus* haplotypes including reference haplotypes of *R. prolixus, R. robustus* and *R. colombiensis, R. pallescens* and *T.infestans* as outgroups constructed using branch-and-bound algorithm with 1000 bootstrap replicates CI = 0.862 RI = 0.860 RCI = 0.741 (for all sites) iCI = 0.796 iRI = 0.860 iRCI = 0.685 (for parsimony informative sites). (refer to Table 24 for distribution of haplotypes).

6.1.3.4 Morphometric/ genetic comparisons

A subset of specimens used in the morphometric studies were matched to samples characterised by mitochondrial haplotype (Fig. 60). In light of the genetic results and phylogenetic analyses it became feasible to assess the morphometric data for phylogenetic signals. Using the Mahalanobis distances calculated during the canonical variate analysis, dendrograms were drawn by UPGMA cluster analysis to facilitate direct comparisons to the phylogenetic trees derived from the mitochondrial sequence data. There is no clear congruence of tree topologies among the datasets (Fig. 59). The only consistent affinity among analyses appears to be between Portuguesa samples (PD & PS). To further assess the relationship between the genetic and phenotypic data pairwise Mantel tests were used to assess correlation of distance matrices. Mahalanobis distances for head and wing, genetic distance and geographical distance

between sampling locations were included. None of the correlations were significant (Table. 26).

Table. 26. Analysis of correlation between data sets for Venezuelan *Rhodnius prolixus* samples: Results of pair-wise Mantel tests between morphometric (head and wing), geographical and genetic distance matices (K2p distances derived from analysis of 485 bp of *cytb*). P values are calculated after 10000 permutations

xy	Matrix correlation (rxy)	p
Head vs. Wing	-0.798	1
Head vs. Geographical distance	0.057	0.502
Head vs. Genetic distance	-0.07	0.624
Wing vs. Geographical distance	0.419	0.337
Wing vs. Genetic distance	0.034	0.622
Geographical vs Genetic distances	0.203	0.507

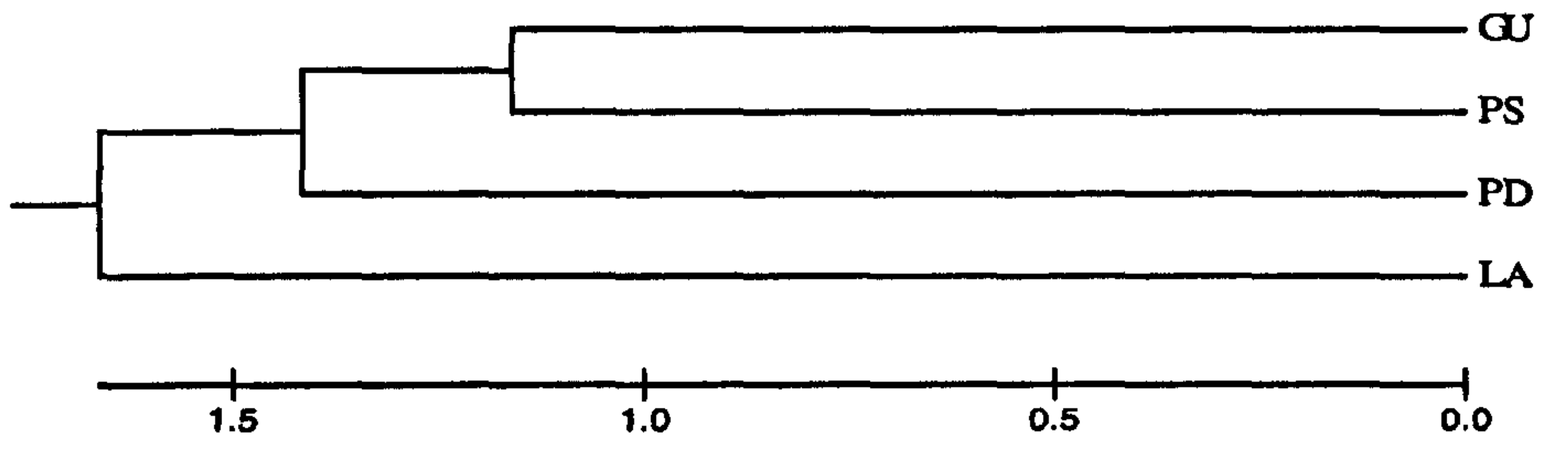

Figure 59. UPGMA cluster analysis of Mahalanobis distances (derived form morphometric analysis) and genetic distances (K2p distances derived from analysis of 485 bp of *cytb*) for Venezuelan *Rhodnius prolixus* samples: Upper= wing shape, Middle= head shape, lower= genetic distance. GU- Guarico (silvatic), LA- Lara (domestic), PD Portuguesa (domestic) PS- Portuguesa (silvatic)

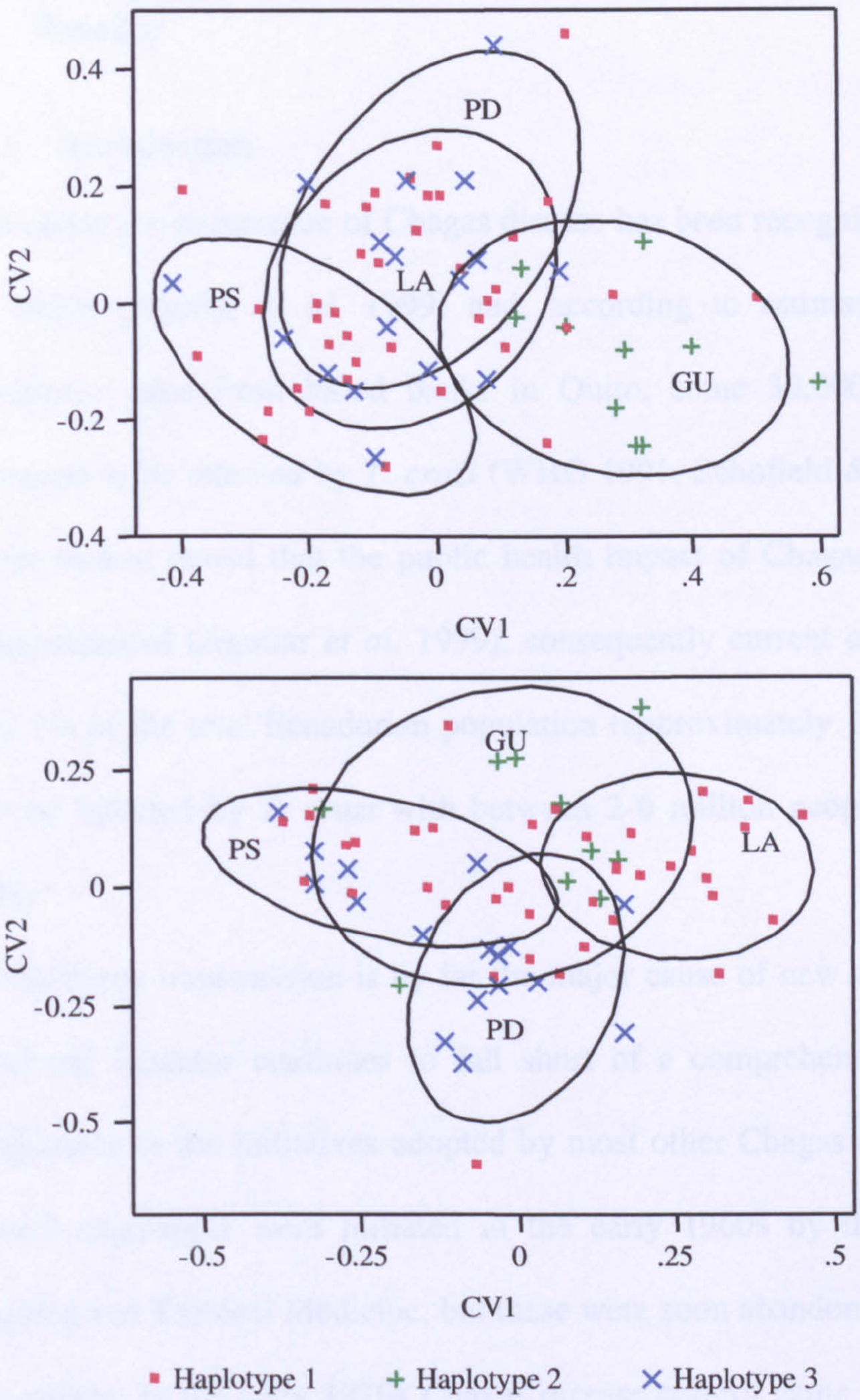

Figure 60. Venezuelan *Rhodnius prolixus cytb* mitochondrial haplotypes matched to morphometrics and superimposed on to CVA plot for wing (upper) and head (lower). Groups are enclosed by 85% density ellipses. GU- Guarico (silvatic), LA- Lara (domestic), PD Portuguesa (domestic) PS-Portuguesa (silvatic)

Comparative analyses of vector species

6.2 Part II. *Rhodnius ecuadoriensis* domestic and silvatic populations from Ecuador

6.2.1 Introduction

In Ecuador the occurrence of Chagas disease has been recognised with certainty since the 1930s (Aguilar *et al.* 1999) and, according to estimates based primarily on prevalence rates from blood banks in Quito, some 30,000 people were recently estimated to be infected by *T. cruzi* (WHO 1991, Schofield & Dias 1996). However, recent studies reveal that the public health impact of Chagas disease has long been underestimated (Aguilar *et al.* 1999), consequently current estimates suggest that at least 1% of the total Ecuadorian population (approximately 125,000-135,000 people) may be infected by *T. cruzi* with between 2-6 million people at risk (Abad-Franch 2003)

Vector-borne transmission is by far the major cause of new cases of Chagas disease. However, Ecuador continues to fall short of a comprehensive control programme comparable to the initiatives adopted by most other Chagas endemic countries. Pilot control campaigns were initiated in the early 1960s by the National Institute of Hygiene and Tropical Medicine, but these were soon abandoned and the coverage was incomplete. In the early 1970s Chagas disease control came under the jurisdiction of the malaria control service, as appointed by the Ministry of Public Health. By the late Seventies house spraying campaigns using malathion were implemented in Guayaquil and the province of Manabí. For the most part, Chagas disease control over the last 25 to 30 years has depended upon coincidental mosquito control activities (Aguilar et al 1999, 2001, Abad-Franch & Aguilar 2002).

Since the recognition of Chagas disease in Ecuador *T. dimidiata* has been implicated as the principal vector. In total, 18 species of Triatominae have been recorded from Ecuador, all are known to occur in natural ecotopes in association with sylvatic vertebrate hosts. After *T. dimidiata* the only other persistently domiciliary species with epidemiological importance is *Rhodnius ecuadoriensis*. *R. ecuadoriensis* Lent & León, 1958 is a vector of Chagas disease on the western side of the Andes of central-southern Ecuador and northern Peru (Abad-Franch *et al.* 2001). Whereas *T. dimidiata* is the only domestic vector in Guayas province and urban/semiurban parts of Manabí province. Sylvatic populations of *R. ecuadoriensis* have only been reported from central Ecuador, where they inhabit *Phytelephas aequatorialis* palm trees (Abad-Franch *et al.* 2001). The species seems to be exclusively associated with human environments in southern Ecuador and over its entire range in Peru.

6.2.2 Collection of material

An extensive evaluation of the ecology and biogeography of *R. ecuadoriensis* (Abad-Franch 2003, Abad-Franch *et al.*, 2002) led in collaboration to the following work. Samples of *R. ecuadoriensis* were obtained from strictly domestic populations in Loja, El Oro and Peru (Chicama), from rural parts of Manabí, where bugs, were collected from both the domestic and sylvatic habitats, and finally a sample of strictly sylvatic bugs from *P. aequatorialis* in Pichincha. The map below (figure 61) indicates the relative positions of the five collection localities. The samples were collected in a comparable manner to that stated previously in the study of *R. prolixus* populations.

In contrast to the previous case study of *R. prolixus*, here we observed clear and obvious phenotypic variation between some of the populations sampled (fig 62.). After conferring, a detailed description of the comparative gross morphology was presented by Abad-Franch (2003). In summary: the forms from Peru and southern Ecuador (Loja and El Oro) are similar to the type specimens held in FIOCRUZ. They

are pale and yellowish, relatively small in size with short stout heads; Manabí forms are yellowish/light brown in colour, intermediate in size and have heads longer than the types; Pichincha forms are the largest, they are dark brown in colour with some reddish markings, the heads are relatively long and narrow.

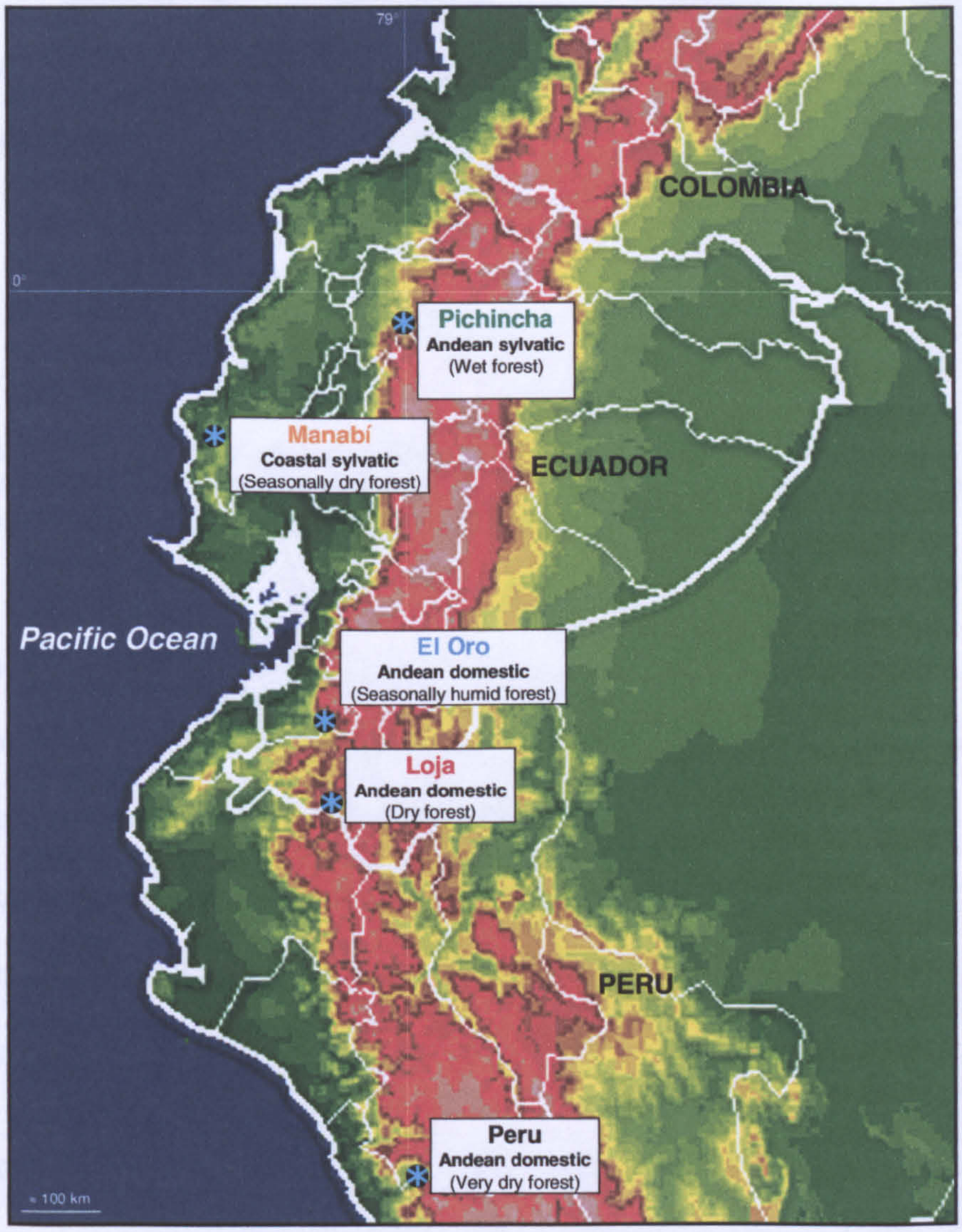

Figure 61. Map of Ecuador and Peru showing the collection site and ecological type for each of the 5 samples of *Rhodnius ecuadoriensis* used in this study. Colours indicate elevation (red- highest i.e. Andes mountain range, yellow- foothills, green- lowlands).

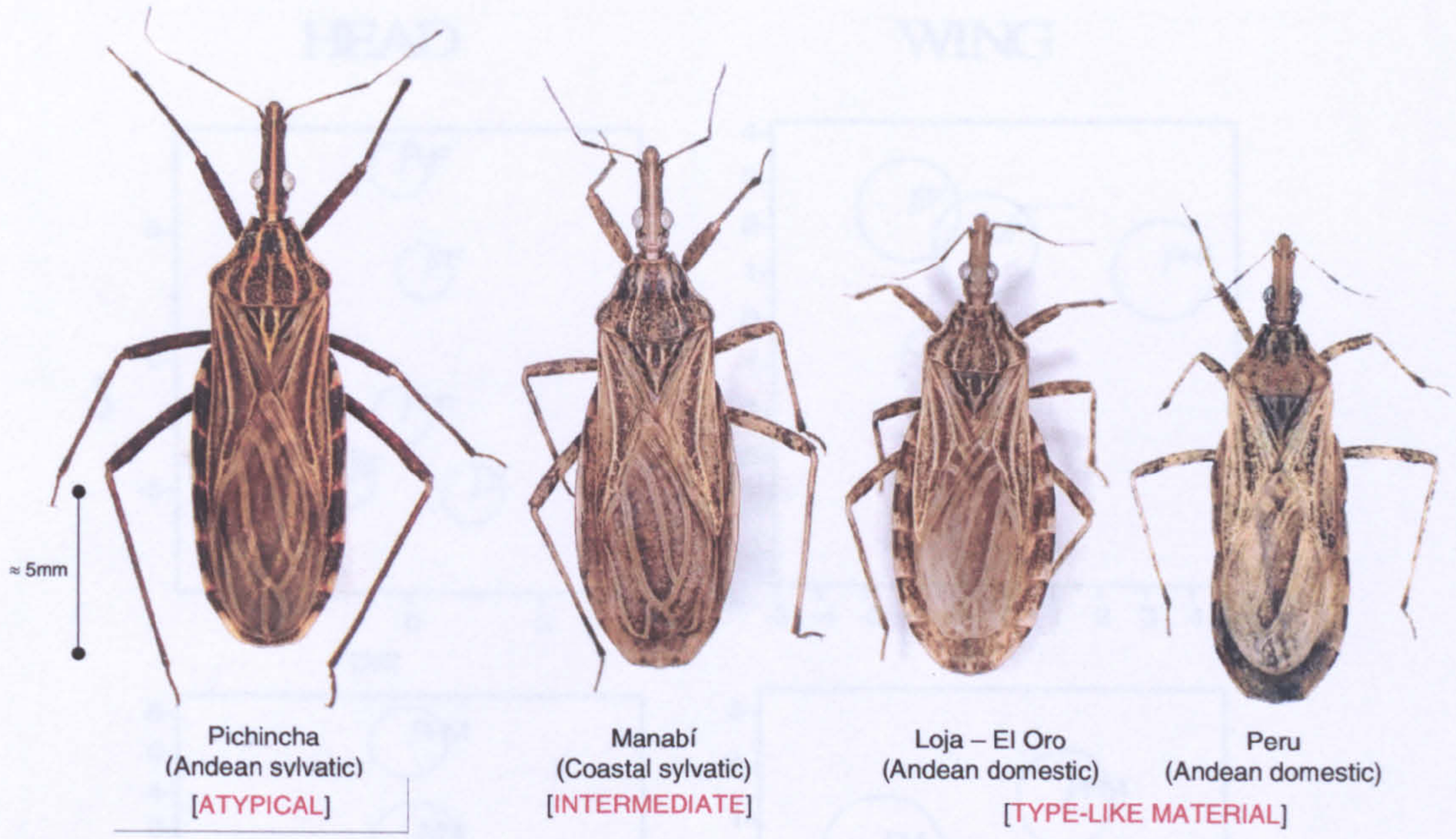

Figure 62. Representative female specimens of the four populations of *R. ecuadoriensis* studied. The small forms from Loja, El Oro and Peru are most similar to the type material of the species; Manabí forms have relatively intermediate morphology compared to the more atypical Pichincha forms.

6.2.3 Morphometrics

In this analysis of intraspecific variation a sample of 15 to 20 bugs were used to represent each of the five geographical populations of *R. ecuadoriensis* (Fig. 62).

Samples sizes were as follows: El Oro 16 (8♀ 8♂), Loja 15 (7♀ 8♂), Manabí 17 (8♀ 9♂), Pichincha 20 (8♀ 12♂), Peru 16 (8♀ 8♂). Refer back to Materials and Methods for details of geometric morphometrics.

6.2.3.1 Sex

Some degree of size-intrapopulational sexual dimorphism was observed, (Fig. 63,) as is usual, females were generally slightly larger. Sexual size-dimorphism was significant for Peru. Explorative discriminant analyses of shape variables for both head and wing (Fig. 63) demonstrate that both sexes show the same pattern of population discrimination. Therefore, for the remainder of the morphometric analyses sexes were pooled within population to improve statistical power, which otherwise would be weakened by low sample sizes.

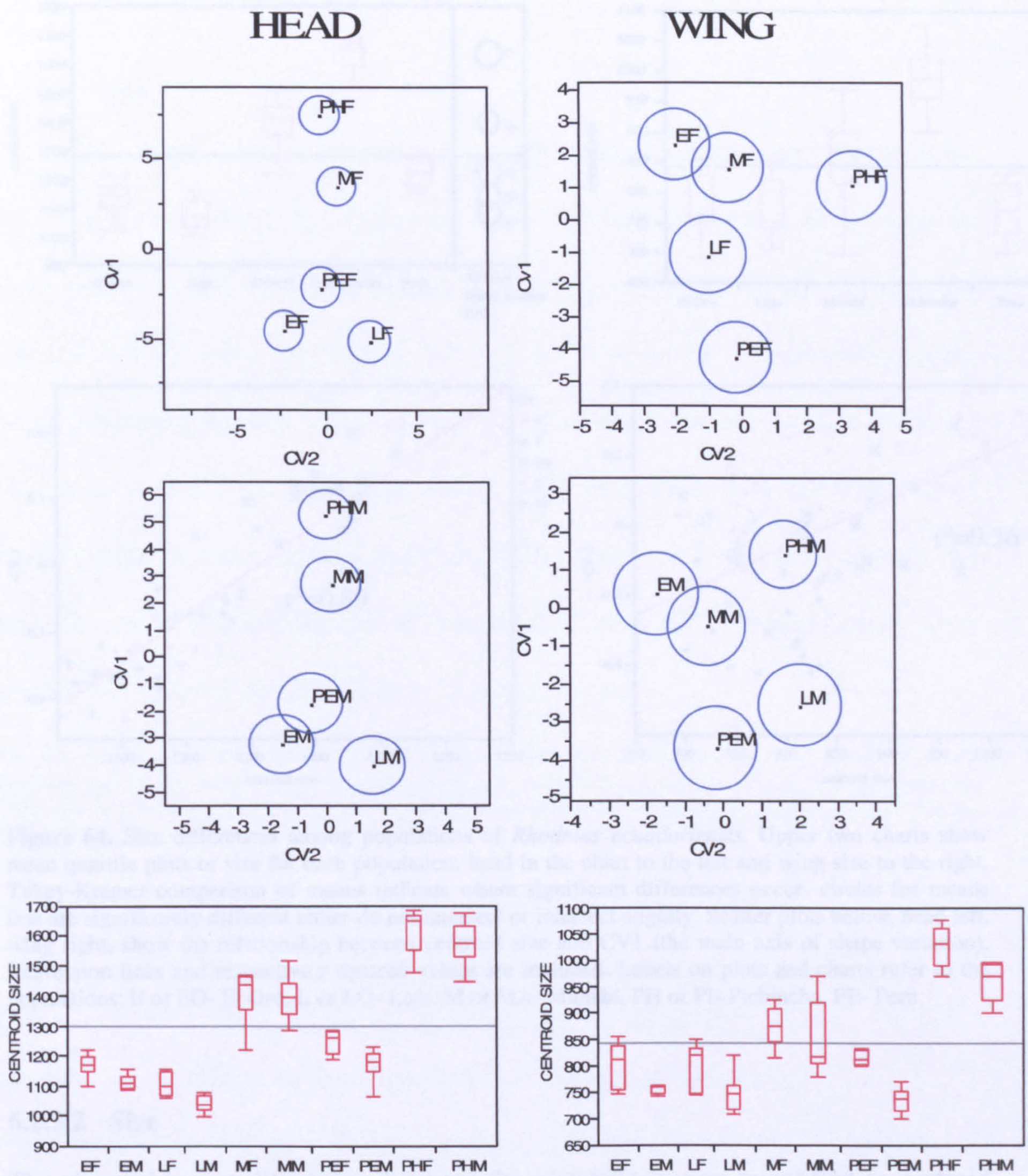

Figure 63. Exploratory analyses of size and shape sexual dimorphism within populations of *Rhodnius ecuadoriensis*. The upper four plots are centroid plots after discriminant anaylsis of shape variables, head shape plots to the left and wing shape plots on the right. The bar charts below show quantile plots of size variation, again, head size to the left and wing size chart to the right.
Labels on plots and charts refer to the populations: E- El Oro, L- Loja, M- Manabí, PH- Pichincha, PE- Peru. Suffixes M= Male and F=Female.

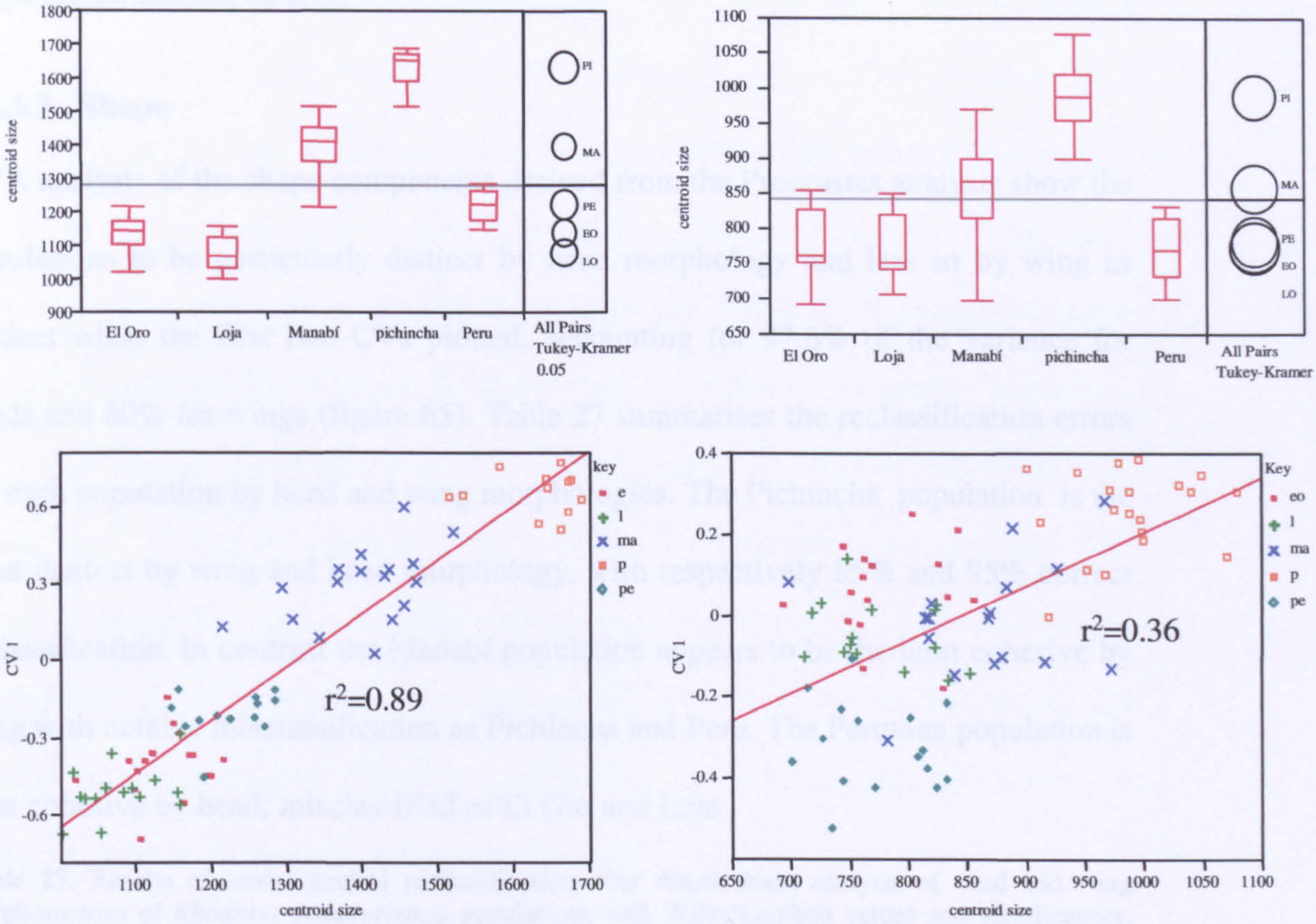

Figure 64. Size differences among populations of *Rhodnius ecuadoriensis*. Upper two charts show mean quartile plots of size for each population, head in the chart to the left and wing size to the right. Tukey-Kramer comparison of means indicate where significant differences occur- circles for means that are significantly different either do not intersect or intersect slightly. Scatter plots below, head left, wing right, show the relationship between centroid size and CV1 (the main axis of shape variation). Regression lines and respective r squared values are included. Labels on plots and charts refer to the populations: E or EO- El Oro, L or LO- Loja, M or MA- Manabí, PH or PI- Pichincha, PE- Peru

6.2.3.2 Size

The observable size differences between the populations were quantified as centroid size (CTR) of head and wing landmark configurations (Fig 64). In summary, El Oro, Loja and Peruvian samples were not clearly distinguishable by size, Manabí samples were significantly distinct and intermediate in size, and finally Pichincha was the largest and significantly distinct from all other populations. Regression of CV1 and CTR within-groups did not reveal any significant correlations, indicating that there are no intrapopulational allometric trends. Among groups there is a strong correlation between CTR and CV1 for the head data (Fig. 64) and a weaker yet significant

correlation for the wing data. This implies that head shape, and to a lesser extent wing shape are influenced by size.

6.2.3.3 Shape

CVA analysis of the shape components derived from the Procrustes analysis show the populations to be particularly distinct by head morphology and less so by wing as evident when the first two CVs plotted, accounting for 97.6% of the variance for heads and 80% for wings (figure 65). Table 27 summarises the reclassification errors for each population by head and wing morphologies. The Pichincha population is the most distinct by wing and head morphology, with respectively 85% and 95% correct reclassification. In contrast the Manabí population appears to be the least cohesive by wing with notable misclassification as Pichincha and Peru. The Peruvian population is least cohesive by head, misclassified as El Oro and Loja .

Table 27. Results of cross checked reclassification after discriminant analysis of head and wing morphometrics of *Rhodnius ecuadoriensis* populations with Wilks'Lambda values and significances. Percentages of correct classification are shown in **bold** and percentages of misclassification as other groups are in parentheses.

Populations	Head Wilk's statistic $\lambda = 0.051$ $p=<0.0001$	Wing Wilk's statistic $\lambda = 0.016$ $p=<0.0001$
Loja (L)	**86.67%** (6.67% EO, 6.67% Pe)	**73.3%** (13.3% M, 13.3% Pe)
El Oro (EO)	**87.5%** (6.25% L, 6.25% Pe)	**81.3%** (12.5% M, 6.3%P)
Manabí (M)	**76.47%** (23.53% P)	**52.9%** (29.4% EO, 11.8% P, 5.9%Pe)
Peru (Pe)	**68.75%** (18.75% EO 12.5% L)	**81.3%** (6.3% EO, 12.5% M)
Pichincha (P)	**95%** (5% M)	**85%** (5% EO, 10% L)

Shape changes associated with CV1 and CV2 for head and wing analyses (Fig. 65) show that most of the variation in head shape as represented by CV1 (accounting for 84% of variance) relates to the relative elongation of head shape in the Pichincha sample as compared to the short compact head as represented by the Loja and El Oro samples. For head CV2 accounts for 11% of the total variance as reflected by

comparatively small differences in the corresponding thin plate line extrapolations. Furthermore, the regression of CV2 against the partial warps matrix does not give a significant correlation (Table. 28). In the analysis of wings, 55% of variance is represented by CV1 and on this axis (Fig 65) shape changes are related to differences in the relative positions of landmarks two and three, two vein junctions of the distal part of the wing. The two landmarks being relatively distant in Peruvian specimens, compared to Pichincha, in which landmarks two and three are in relative proximity. The shape changes associated with CV1 are also represented by the relative position of landmarks 7 and 6; relatively close together in Peru, and comparatively more distant in Pichincha. Secondary shape changes associated with CV2 for wing shape (accounting for 18% of the total variance) again relate somewhat to the relative position of landmarks 2 and 3 and also the relative positions of landmarks seven and eight, proximal in Peru versus separated in Manabí.

Table 28. Fit to the regression model of CV1 and CV2 against head and wing shape components of *Rhodnius ecuadoriensis* populations was tested using a generalized Goodall F-test with 1000 permutations:

	Head	Wing
CV1	F = 435.97, P =<0.001 df =161664	F = 12.0922,: P = <0.001 df=161664
CV2	F = 1.3429, P= 0.1627 df=161664	F = 12.5483, P =<0.001 df=161664

Inclusion of out groups, *R. pallescens* and *R. colombiensis* (Fig. 66) demonstrates that *R. ecuadoriensis* is relatively cohesive by both head and wing analysis supporting the view that it should be considered as a single species in comparison to the two most closely related species. CVA analyses of head and wing both separate the *R. ecuadoriensis* populations from the two outgroups.

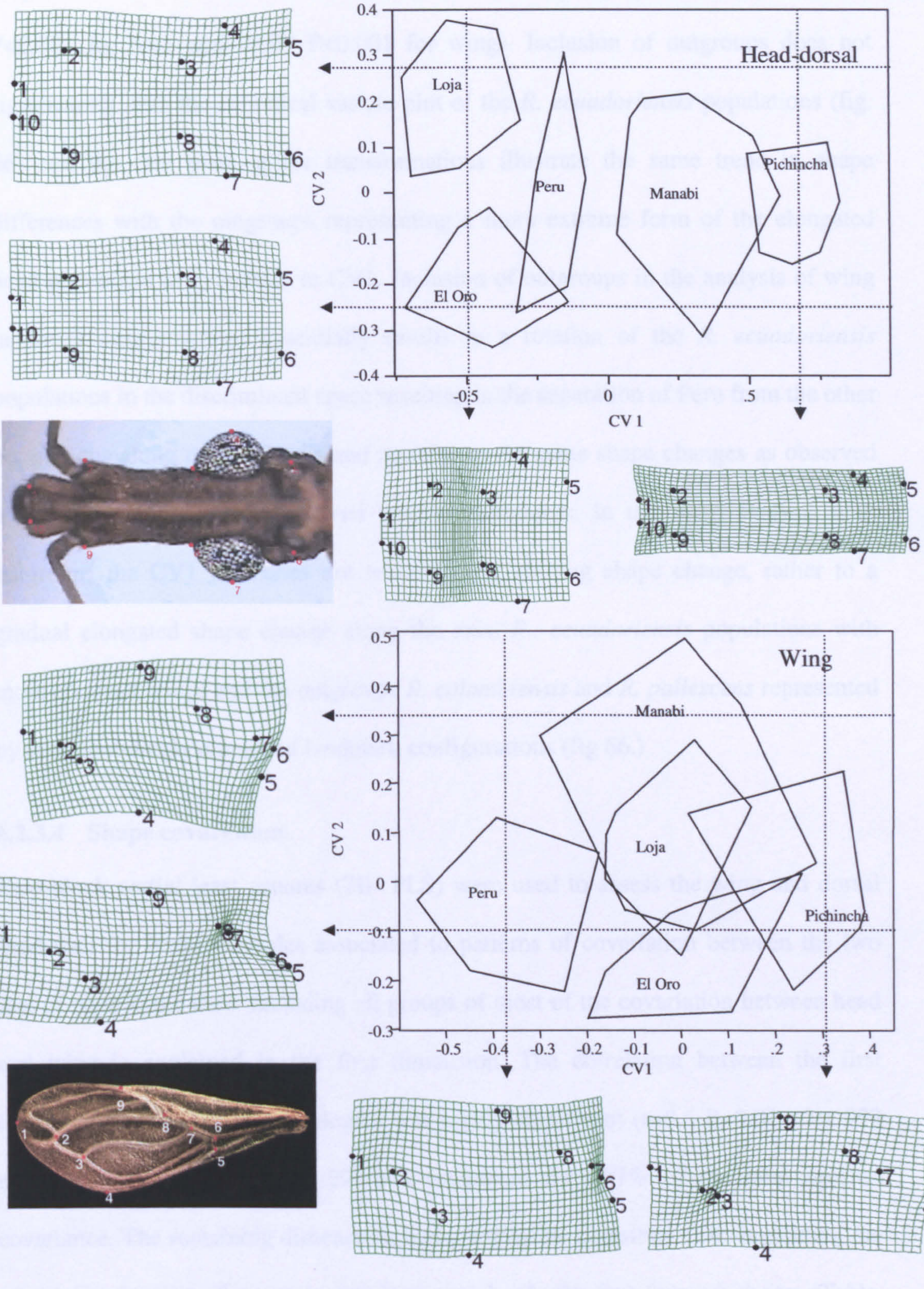

Figure 65. Morphometric analysis of *R. ecuadoriensis* populations: CVA analysis of shape components after GPA. Polygons enclose distribution of specimens in each group. The upper plot is derived from dorsal head landmarks and the lower from wings. For the heads CV1 accounts for 84% of the total variance and CV2 accounts for 11% ($\sum = 95\%$). For the wings CV1 55%, CV2 18% ($\sum$ 73%). Thin plate splines are included showing, shape differences of the wing that correspond to the CV axes, as indicated by dashed lines and arrows.

With outgroups CV1 and CV2 together account for 96% and 76% of the variance in shape differences in head and wing respectively (Wilk's lambda statistic = 0.004, P<0.001 for head and 0.009 P<0.001 for wing). Inclusion of outgroups does not significantly alter the canonical variate plot of the *R. ecuadoriensis* populations (fig. 66) and the thin plate spline transformations illustrate the same trend in shape differences with the outgroups representing a more extreme form of the elongated head phenotype as correlates to CV1. Inclusion of outgroups in the analysis of wing landmark configurations essentially results in a rotation of the *R. ecuadoriensis* populations in the discriminant space resulting in the separation of Peru from the other populations along the CV2 axis and pertains to the same shape changes as observed associated to CV1 in the analysis without outgroups. In the wing analysis with outgroups the CV1 axis does not relate to any striking shape change, rather to a gradual elongated shape change along the axis, *R.. ecuadoriensis* populations with more compact wings and the outgroups *R. colombiensis* and *R. pallescens* represented by correspondingly elongated landmark configurations (fig 66.)

6.2.3.4 Shape covariation

Two-block partial least squares (2B- PLS) were used to assess the wing and dorsal head data for latent variables associated to patterns of covariation between the two sets of phenotypic data. Including all groups of most of the covariation between head and wing is explained in the first dimension. The correlation between the first dimensions of the two morphologies was highly significant (r=0.6 P=0.01 after 999 random permutations) (Table 29) and accounted for ~97% of the total squared covariance. The remaining dimensions had a negligible contribution to explaining the covariation between the two morphologies, and only the first four are shown (Table. 29)

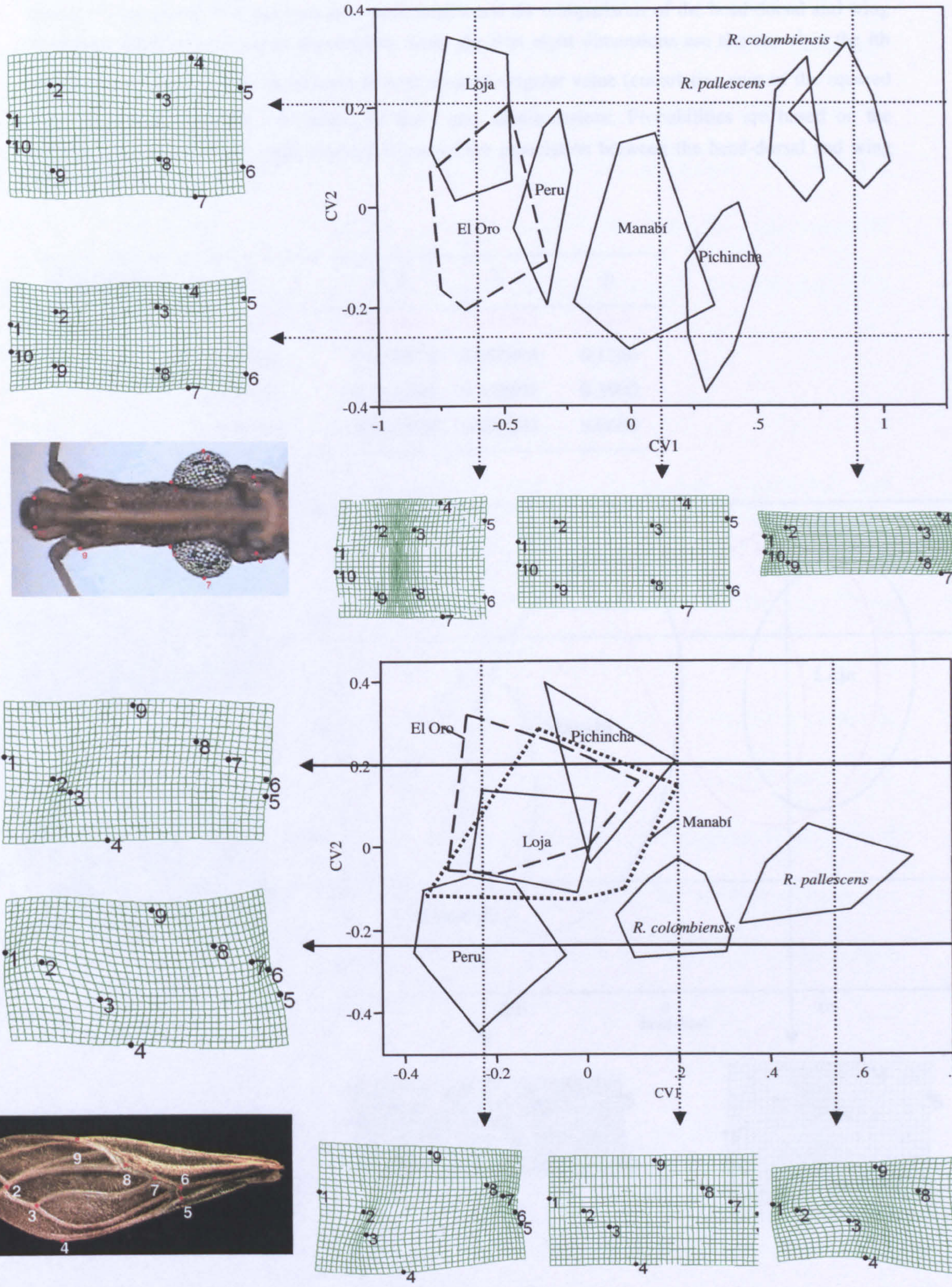

Figure 66.. *R. ecuadoriensis* populations and outgroups: *R. pallescens* and *R. colombiensis*: CVA analysis of shape componmpents after GPA. Polygons enclose distribution of specimens in each group. The upper plot is derived from dorsal head landmarks and the lower from wings. For the heads CV1 accounts for 90% of the total variance and CV2 accounts for 6% ($\sum$ = 96%). For the wings CV1 53%, CV2 23% ($\sum$ 76%). Thin plate splines are included showing the shape differences of the head and wing that correspond to the CV axes, as indicated by dashed lines and arrows.

Table 29. Results of PLS analysis after permutation test for comparisons of the head-dorsal and wing landmarks of *R. ecuadoriensis* populations. Only the first eight dimensions are shown. λ_i is the *i*th singular value, $\sum \lambda_i^2$ is the cumulative sum of squared singular value (cumulative sum of the squared covariance), and r_i is the correlation for the *i* pair of dimensions. Probabilities are based on the observed values plus 999 random permutations of the association between the head-dorsal and wing landmarks

Dimensions	λ_i	$\sum \lambda_i^2$	r_i	P
1	0.00050	0.966994	0.635252	0.0100
2	0.00006	0.978912	0.452994	0.1200
3	0.00005	0.987231	0.359691	0.3900
4	0.00004	0.993096	0.406092	0.0600

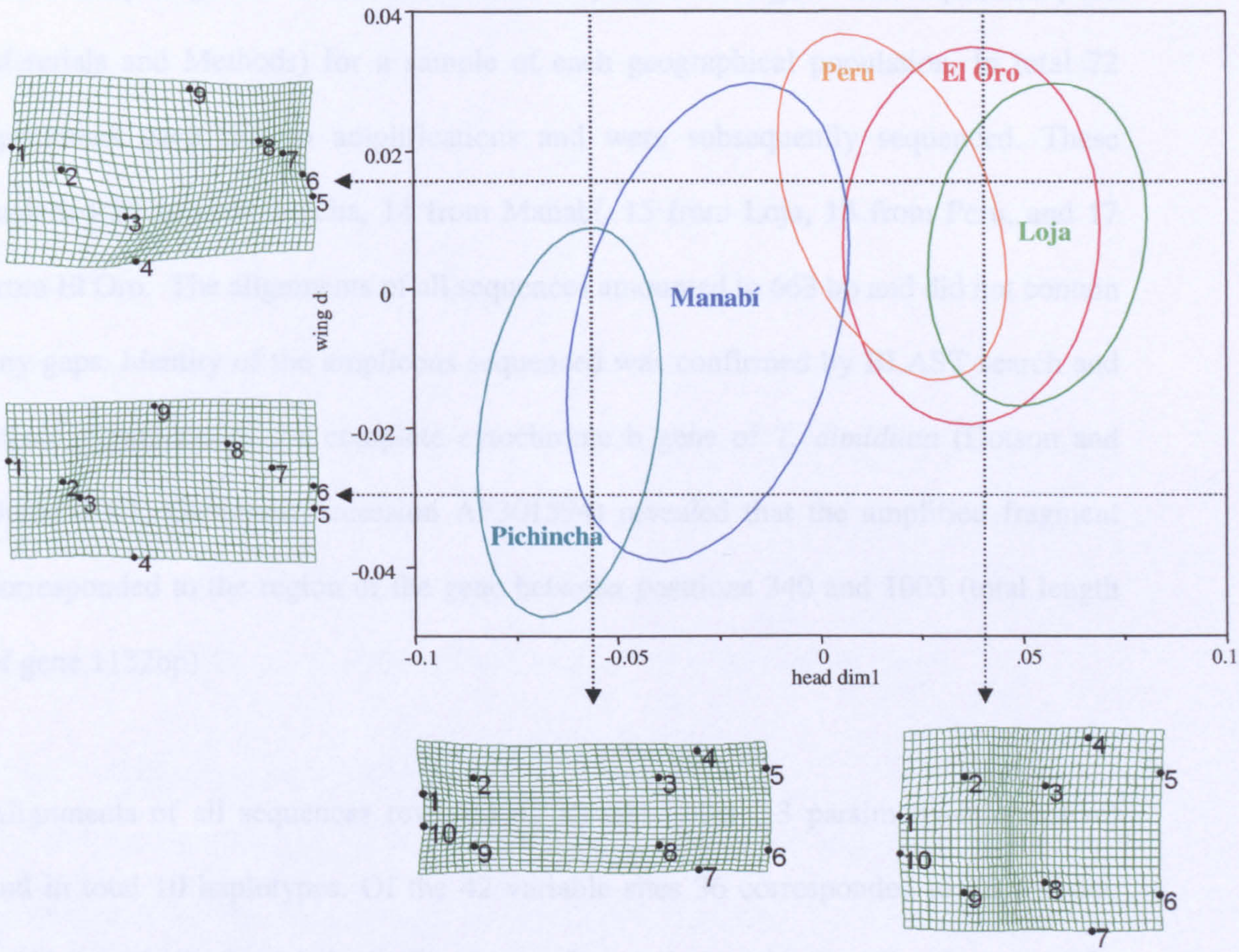

Figure. 67. Analysis shape covariation for head and wing of *Rhodnius ecuadoriensis* population samples. Plot of dimension one for head-dorsal and wing landmark data of *R. ecuadoriensis* populations after partial least squares analysis. Ellipses enclose 85% of the distribution of specimens in each group. Thin plate spline grids have been interpolated and correspond to values of the respective dimensions, as indicated by arrows.

Fig. 67 shows a plot of the first dimension of both head and wing data sets coupled with TPS transformation grids to demonstrate the patterns of shape covariation between head and wing. shape configurations. There is a clear allometric element that appears to account for most of the covariation between morphologies. Size dependant shape covariation is confirmed by regression of each dimension against CTS; r^2=0.55, P=<0.001; r^2=0.55, P=<0.001 for head and wing respectively. The TPS transformation grids in Fig 67 also approximately correspond to the shape changes associated to CV1 axes of head and wing (Fig. 66).

6.2.4 Cytochrome b amplification and sequencing

The 700 bp fragment of this mitochondrial cytochrome b gene was sequenced (see Materials and Methods) for a sample of each geographical population. In total 72 specimens gave rise to amplifications and were subsequently sequenced. These included 20 from Pichincha, 14 from Manabí, 15 from Loja, 13 from Peru, and 17 from El Oro. The alignments of all sequences amounted to 663 bp and did not contain any gaps. Identity of the amplicons sequenced was confirmed by BLAST search and direct alignments to the complete cytochrome b gene of *T. dimidiata* (Dotson and Beard 2001; Genebank accession AF301594) revealed that the amplified fragment corresponded to the region of the gene between positions 340 and 1003 (total length of gene 1132bp)

Alignments of all sequences revealed 42 variable sites (13 parsimony-informative) and in total 10 haplotypes. Of the 42 variable sites 36 corresponded to third codon positions substitutions (silent), five to the first codon positions and only one to the second. The sequence did not include any stop codons. Translation to amino acid sequence revealed that only two of the haplotypes yielded different peptides due to non-synonymous mutations, both only different by a single amino acid, one was from

Manabí, the results of a single non-synonymous variable site in the first codon position (CTT –ATT= leucine-isoleucine), and the other from Peru, the result of non-synonymous variation of first and second codon positions (ACT- GTT = valine-threonine)

6.2.4.1 Haplotype distribution

The distribution of the 10 haplotypes amongst the five geographical populations are as follows. Out of the 14 bugs successfully sequenced from Manabí six of the 10 haplotypes were found to occur; three of these were isolated from only one specimen each and were not found to occur in any other population (MN1. MN3, MN5) haplotype MN6 was also isolated from a single bug in Manabí and all of the specimens from Pichincha. The remaining two haplotypes from Manabí; MN2 and MN4 were isolated from three and five bugs respectively. MN4 was also isolated from all the specimens collected from El Oro. From Loja the sample was found to be composed of bugs represented by three haplotypes, all endemic (LJ 1, LJ 2, LJ 3), LJ 1 represented by a single specimen and LJ 2 and LJ 3 represented by six and eight specimens respectively. All 13 specimens included from the Peruvian population were represented by a single unique haplotype (PE). In summary, intrapopulational variation was observed only in Loja and Manabí, Whereas Manabí was found to share haplotypes with the two localities closest to it i.e. Pichincha and El Oro.

6.2.4.2 Analysis of haplotypes

For comparative analysis of the haplotypes and subsequent phylogenetic analyses, nucleotide differences and distance matrices were calculated. For this data set several models of base substitution were used in comparison (p distances, Kimura 2 parameter, Jukes Cantor, Tajima-Nei, Tamura 3 parameter, Tamura-Nei). All models assessed here, for this data set gave comparable results without any significant

differences in the results of the eventual phylogenetic analyses. For this reason, only K2 p distances and nucleotide differences are represented here. Among group differences are relatively small between haplotypes occurring in Manabí, Pichincha, El Oro and Loja, with differences within the range of 1 to 13 nucleotides (a sequence divergence of 0.15% - ~2%). However, differences between Ecuadorian haplotypes and Peru ranged between 25 to 31 nucleotides i.e. 3.7%-4.7% sequence divergence.

For each of the geographic samples/populations within group differences were assessed by absolute nucleotide differences (Table 30)

Table 30. Absolute number of nucleotide differences (for a 663 bp fragment of cytb) within populations of *Rhodnius ecuadoriensis*.

Geographical sample/ population	Within group; absolute no. of nucleotide differences
Manabí	5.4 +/-1.48
Loja	4.7 +/-1.66
El Oro	0
Pichincha	0
Peru	0

The data set of 10 haplotypes was found to have a relatively high transition to transversion ratio of 8.3. This observation, considered together with all p distances being < 0.09-0.1 (the saturation threshold for the cytochrome b gene, as recommended by Meyer (1994) negates the possibility that the models of base substitution used to calculate the genetic distances would be adversely affected by saturation of transitions.

6.2.4.3 Phylogenetic analyses

6.2.4.3.1 Distance based

Neighbour joining trees were generated using the various models of base substitution, and statistical support was evaluated by bootstrap resampling with 1000 replicates and a random seed number. In the alignment used to construct the trees sequences from two closely related species were also included as outgroups (*R. pallescens* and *R.*

colombiensis). All models of base substitution investigated yielded essentially equivalent results, all trees with identical topologies and similar bootstrap supports.

All models of base substitution demonstrated an unambiguous 97 to 100% bootstrap supported separation of the Peruvian haplotype from all of the Ecuadorian populations. Within the monophyletic Ecuadorian clade a subdivision isolated 4 of the Manabí haplotypes (MN1, MN2, MN3, & MN5) from all remaining sequences from Manabí, Pichincha, El Oro and Loja. See Fig 68.

6.2.4.3.2 Maximum parsimony

To support the phylogeny reported by the neighbour joining analysis the haplotypes were also subjected to a maximum parsimony analysis. The branch and bound algorithm was used to recover three equally parsimonious trees, from which a strict consensus tree was produced with bootstrap supports (Fig. 69).

The parsimony network constructed for all 10 haplotypes using TCS software (figure 70) shows the number of mutational steps separating any two of the haplotypes and the number and position of all inferred haplotypes that could conceivably be found with further sampling. A limitation of the TCS programme prevented the inclusion of steps between the Peruvian haplotype and those from Ecuador. An unrooted neighbour-joining tree was used to illustrate the distance of the Peruvian haplotype from all others (Fig 70).

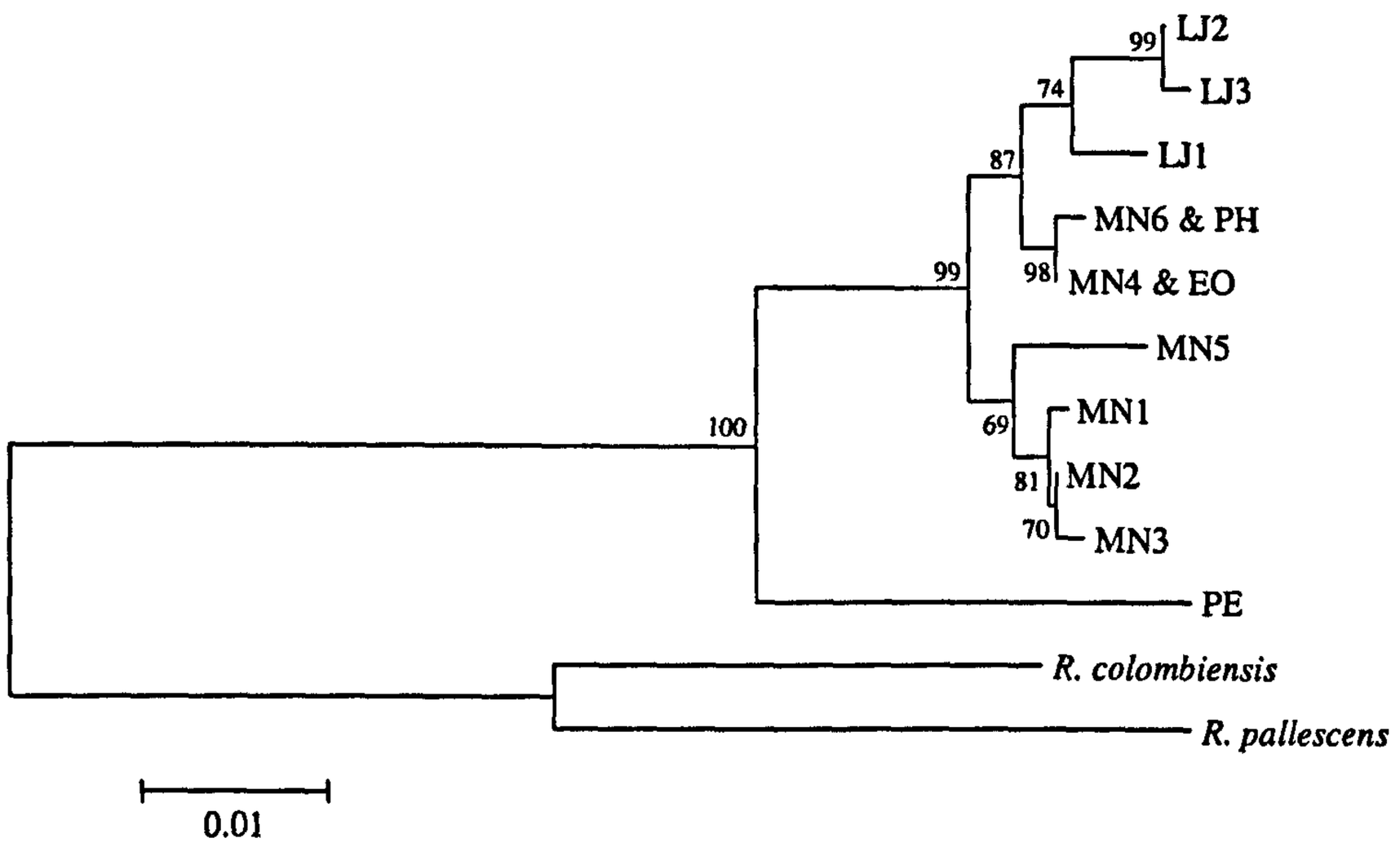

Figure 68. Analysis of *cytb* sequences: Neighbour-joining phylogenetic tree of the 10 *R. ecuadoriensis* haplotypes including *R. colombiensis* and *R. pallescens* as outgroups. Constructed using k2p model, with 1000 bootstrap replicates sum of branch lengths = 0.2152, scale: substitutions/site. See page 164 for haplotype distribution among samples.

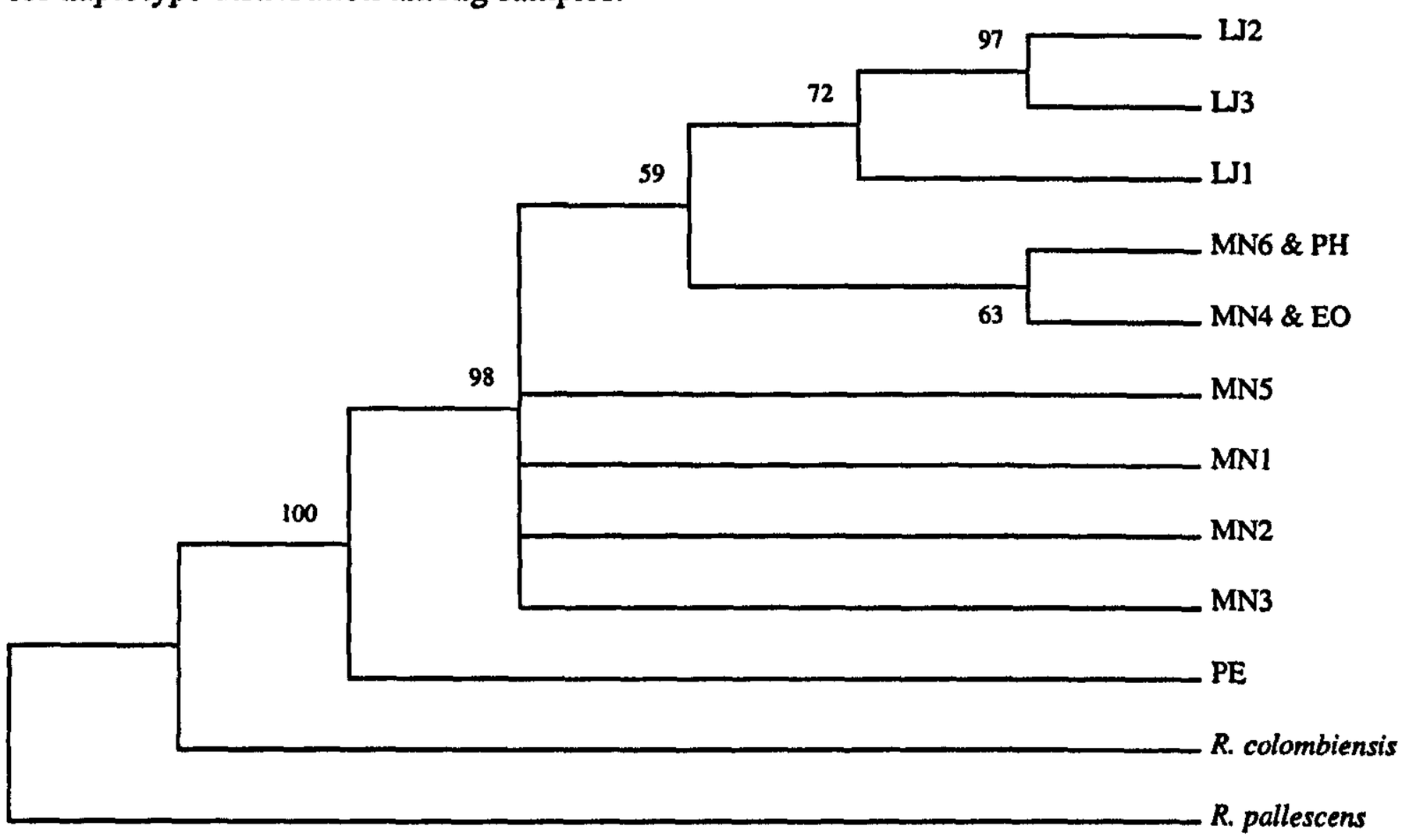

Figure 69 Analysis of *cytb* sequences: Maximum parsimony strict consensus phylogeny of the 10 *R. ecuadoriensis* haplotypes including *R. colombiensis* and *R. pallescens* as outgroups. Constructed using branch-and-bound algorithm with 1000 bootstrap replicates CI = 0.896 RI = 0.821 RCI = 0.7368 (for all sites) and iCI = 0.737iRI = 0.821 iRCI = 0.605 (for parsimony informative sites). See page 164 for haplotype distribution among samples.

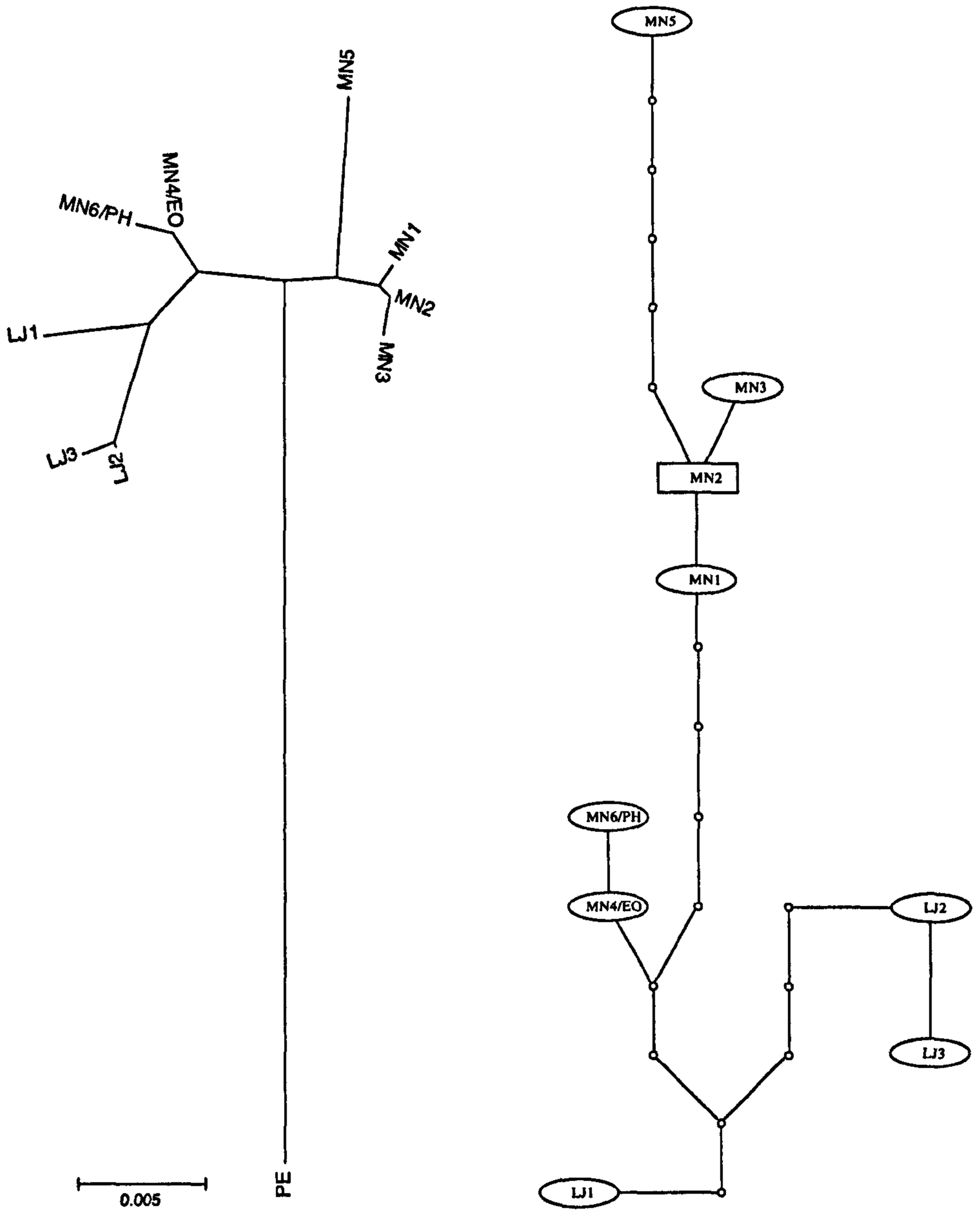

Figure 70.:Analysis of *cytb* sequences: To the right a network of Ecuadorian *R. ecuadoriensis* haplotypes. The maximum number of steps connecting parsimoniously two haplotypes is indicated; one step is indicated by a single line between two haplotypes and each additional base substitution by a small circle. The haplotype with the highest ancestral probability is displayed as a square, while other haplotypes are displayed as ovals. The size of the square or oval corresponds to the haplotype frequency. To the left an unrooted Neighbour- joining tree constructed from k2p distances including the Peruvian haplotype (PE). See page 164 for haplotype distribution among samples.

6.2.5 Morphometric/ genetic comparisons

A subset of specimens used in the morphometric studies were matched to samples characterised by mitochondrial haplotype (Fig.71). In light of the genetic results and phylogenetic analyses it became feasible to assess the morphometric data for

phylogenetic signals. Using the Mahalonobis distances calculated during the canonical variate analysis (Table 31), dendrograms were drawn by UPGMA cluster analysis to facilitate direct comparisons to the phylogenetic trees derived from the mitochondrial sequence data. The topology of the dendrogram representing the geometric morphometrics of the wings is largely congruent with the molecular phylogenetic tree Figure 72, whereas the head data fails to show similar affiliations between the groups. Moreover, the dendrogram derived from wing shape show the same clear separation of Ecuadorian specimens from Peruvian, as unequivocally indicated by the mitochondrial DNA. To test the relationship between the genetic and phenotypic data pairwise Mantel tests were used to assess the significance of the correlation between distance matrices. Mahalonobis distances for head and wing, genetic distance and geographical distance between sampling locations were included. Only the correlation between wing shape and geographical distance was significant (Table 32). Despite the congruence between tree topologies, the wing and genetic matrices are not significantly correlated (Table. 32). However, the frequency histogram of the expected correlation after 10000 permutations (Fig. 73) suggests that the comparatively large genetic distance between Peruvian and Ecuadorian bugs disrupts the expected distribution, as indicated by the bimodal distribution of expected values for the correlation (Fig.74)

Table 31. Pairwise morphometric comparisons: Mean Mahalonobis distances between *R. ecuadoriensis* sample locations after head and wing shape analyses (stardard deviation in bold)

	Wing shape		Head shape	
Between El Oro and Loja:	3.392	**0.072**	4.172	**0.091**
Between El Oro and Manabí:	3.015	**0.069**	6.998	**0.249**
Between El Oro and Pichincha:	3.447	**0.068**	9.644	**0.321**
Between El Oro and Peru:	4.35	**0.08**	3.223	**0.069**
Between Loja and Manabí:	2.955	**0.058**	7.804	**0.282**
Between Loja and Pichincha:	3.672	**0.066**	10.535	**0.345**
Between Loja and Peru:	3.563	**0.091**	3.986	**0.097**
Between Manabí and Pichincha:	3.456	**0.073**	3.362	**0.097**
Between Manabí and Peru:	3.853	**0.086**	5.05	**0.215**
Between Pichincha and Peru:	5.231	**0.119**	7.837	**0.293**
Between El Oro and Loja:	3.392	**0.072**	4.172	**0.091**
Between El Oro and Manabí:	3.015	**0.069**	6.998	**0.249**

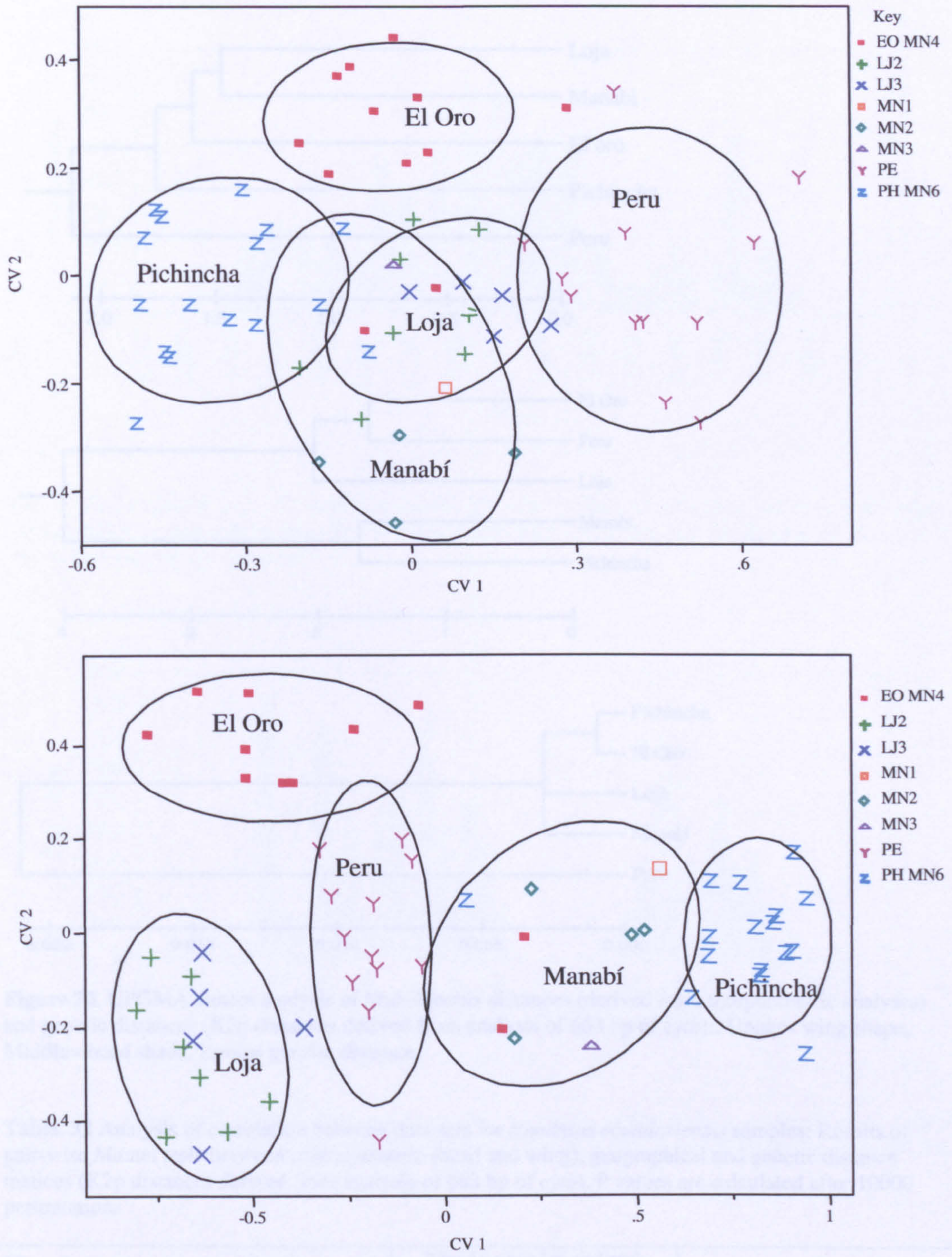

Figure. 71. *Rhodnius ecuadoriensis cytb* mitochondrial haplotypes matched to morphometrics and superimposed on to CVA plot for wing (upper) and head (lower). Groups are enclosed by 85% density ellipses.

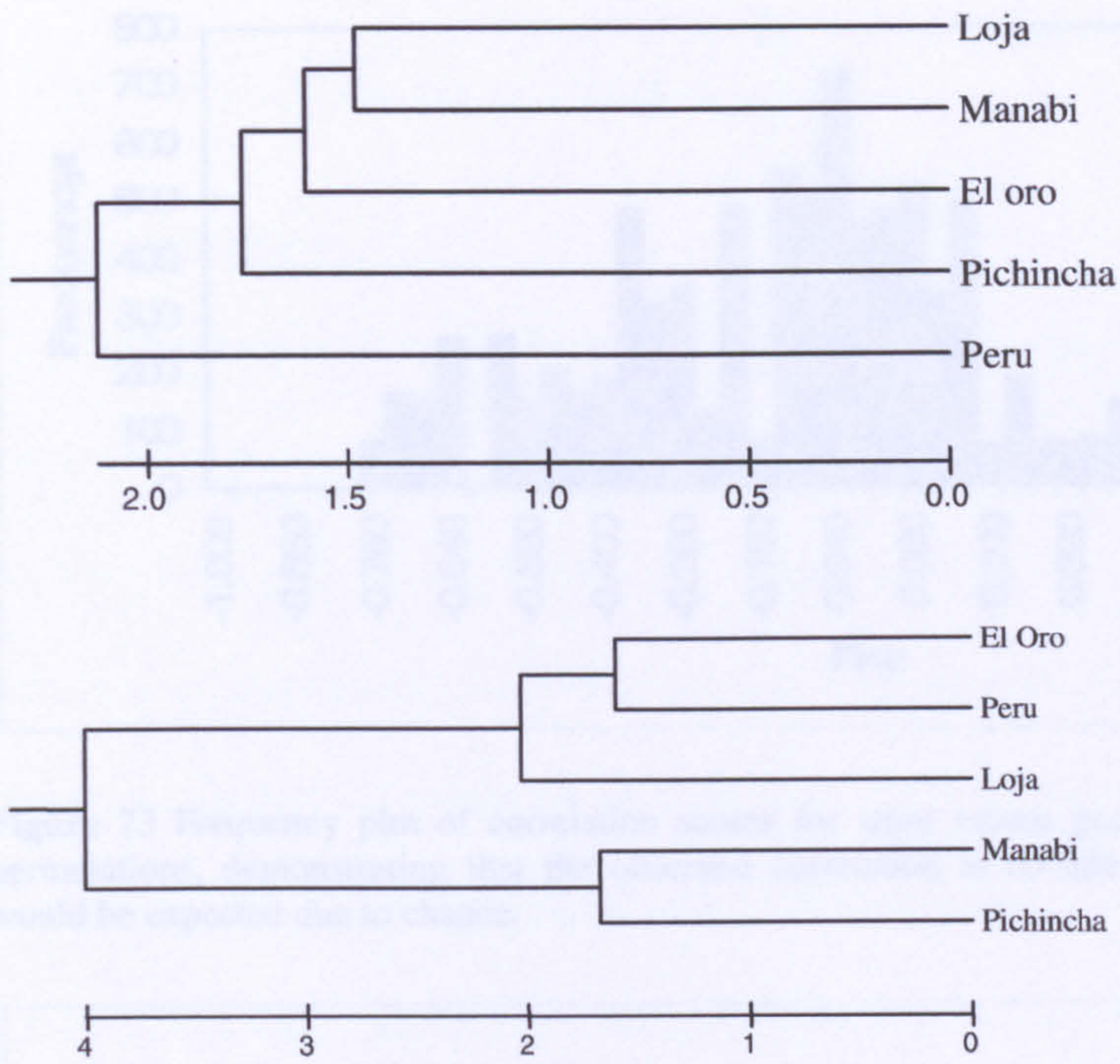

Figure 72. UPGMA cluster analysis of Mahalanobis distances (derived form morphometric analyses) and genetic distances (K2p distances derived from analysis of 663 bp of *cytb*):: Upper= wing shape, Middle= head shade, lower= genetic distance.

Table. 32 Analysis of correlation between data sets for *Rhodnius ecuadoriensis* samples: Results of pair-wise Mantel tests between morphometric (head and wing), geographical and genetic distance matices (K2p distances derived from analysis of 663 bp of *cytb*). P values are calculated after 10000 permutations

xy	Matrix correlation (rxy)	p
Head vs. Wing	0.158	0.180
Head vs. Geographical distance	0.206	0.264
Head vs. Genetic distance	-0.388	0.834
Wing vs. Geographical distance	0.810	0.007
Wing vs. Genetic distance	0.489	0.222
Geographical vs Genetic distances	0.623	0.140

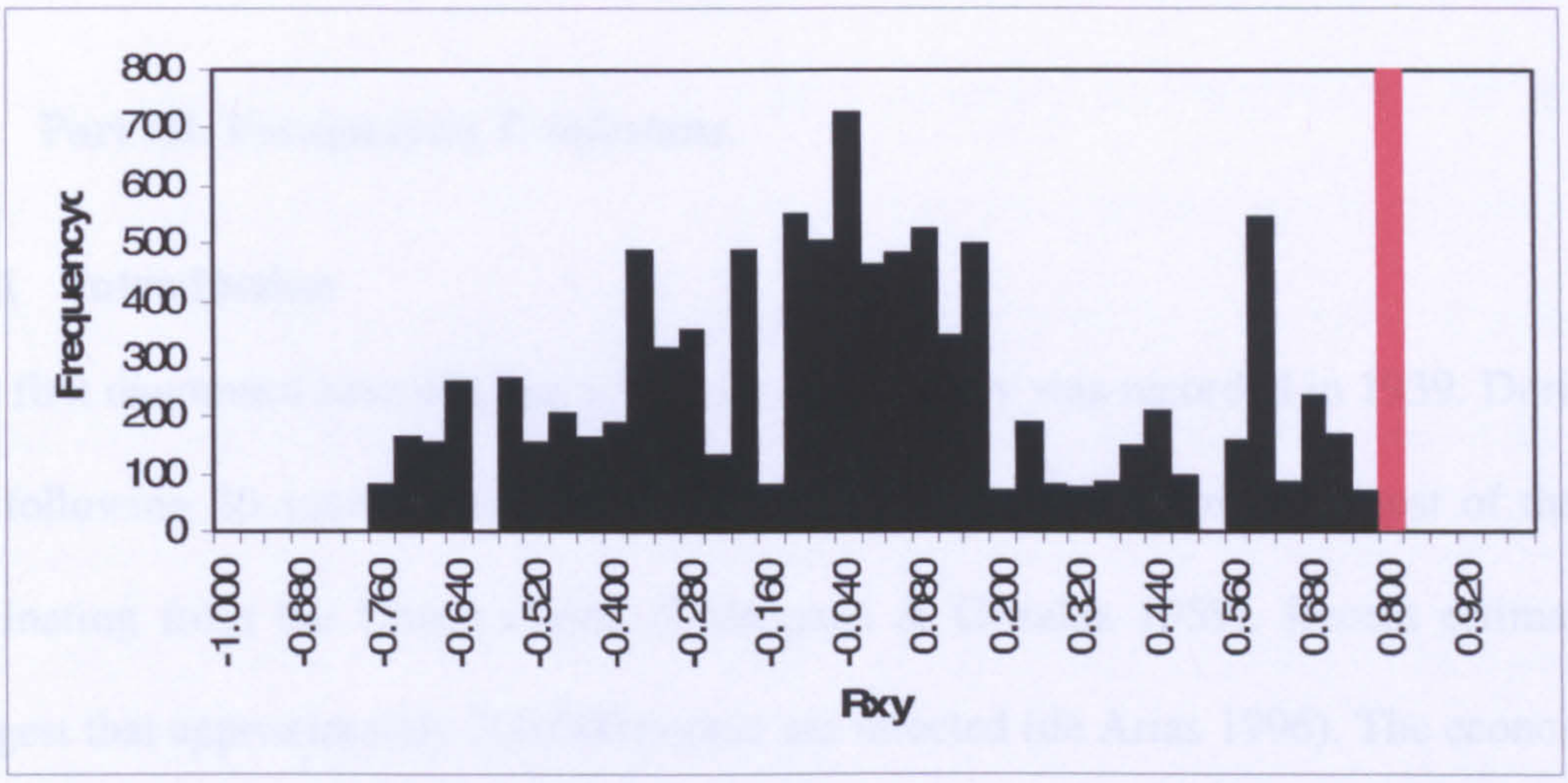

Figure 73 Frequency plot of correlation scores for wing versus geographical distance after 10000 permutations, demonstrating that the observed correlation is outside the distribution of that which would be expected due to chance.

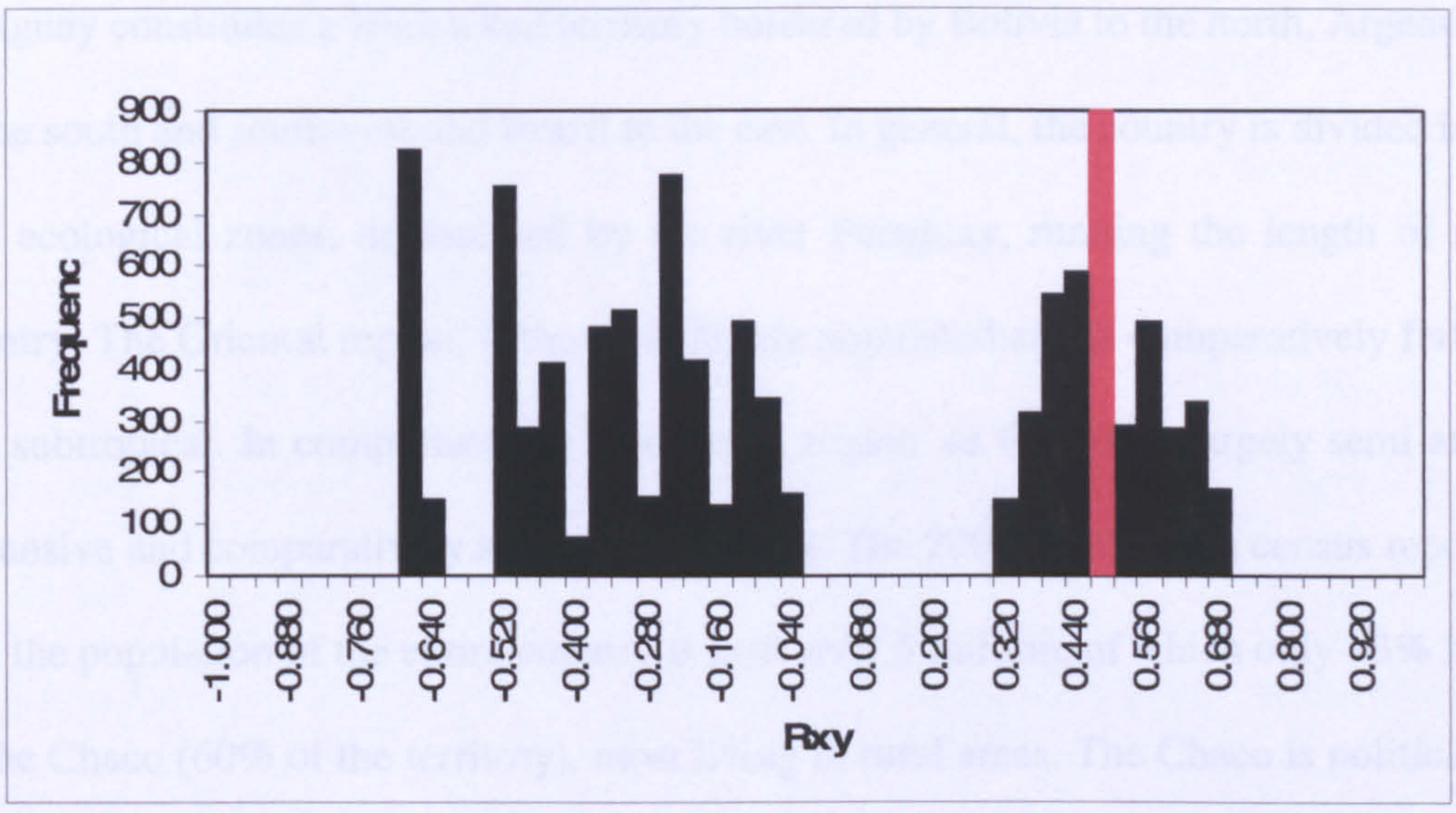

Figure 74. Frequency plot of correlation scores for wing versus genetic distance after 10000 permutations. The observed correlation is within the distribution of that which would be expected due to chance.

Comparative analyses of vector species.

6.3 Part III. Paraguayan *T. infestans*.

6.3.1 Introduction

The first diagnosed case of Chagas disease in Paraguay was recorded in 1939. During the following 20 years a further 50 or so cases were also diagnosed, most of these originating from the Chaco region (Valazquez & Gozalez 1959). Recent estimates suggest that approximately 300,000 people are infected (de Arias 1996). The economy of Paraguay is largely agricultural, with 43% of the population living in rural areas, the poorest of whom being at particular risk to Chagas disease.

Paraguay constitutes a landlocked territory bordered by Bolivia to the north, Argentina to the south and southwest and Brazil to the east. In general, the country is divided into two ecological zones, demarcated by the river Paraguay, running the length of the country; The Oriental region, is the most highly populated and is comparatively fertile and subtropical. In comparison the Occidental region, or Chaco, is largely semi-arid, expansive and comparatively sparsely populated. The 2003 Paraguayan census reports that the population of the entire country is little over 5 million, of which only ~3% live in the Chaco (60% of the territory), most living in rural areas. The Chaco is politically divided into 3 departments, (Pesidente Hayes, Boquerón & Alto Paraguay) with the oriental region composed of a further 14 (Fig. 75). The wilderness of the Chaco is interrupted by cattle ranches, interspersed with a striking contrast of comparatively wealthy Mennonite urban centres and indigenous communities. It is within these indigenous communites (1.4% of the total population) that infection rates of Chagas disease are highest (Chapman *et al.*, 1984)

Since the initiation of the southern cone programme in 1991 Paraguay and five neighbouring countries began the initiative to eliminate *T. infestans*. In Paraguay a campaign of chemical spraying resulted in the treatment of 40,000 dwellings per year. There is continual surveillance and research into the optimization of insecticide application (de Arias *et al.*, 2004, de Arias *et al.*, 2003). In addition to chemical control partnerships were formed to promote house improvement. The National University of Asuncion's Institute of Health Science Research works with the Indigenous Mennonite Association (ASCIM), the Pan American Health Organization (PAHO) and Canada's International Development Research Centre (IDRC) on a programme of Housing Improvement, particularly focusing on houses in the Chaco region. There are also concerted efforts to interrupt transmission by blood transfusion. (Moncayo, 2003). Paraguay and some other southern cone countries have also implemented a national routine of screening pregnant woman for *T. cruzi* infection, so providing diagnostic guidance at childbirth (Dias *et al.*, 2002).

There are about ten triatomine species reported to occur in Paraguay. Three genera are represented, (*Triatoma, Panstrongylus* and *Psammolestes*). Most of these do not enter houses and pose little threat as vectors. *T. infestans* is the primary vector of Chagas disease in Paraguay and *T. sordida* is implicated as a secondary vector in the oriental region.

T. infestans is exclusively domestic through most of its range, and silvatic populations are rare (Lent and Wygodzinsky, 1979). Despite previous reports of silvatic *T. infestans* populations in Paraguay (Velasquez and Gonzalez, 1959), Argentina, and Brazil, for a summary see Noireau *et. al* (1997), it was considered that because most specimens were found in ecotopes relatively close to houses (Usinger et al. 1966) and that they do not represent self-sustainable wild populations. Since then uncertainty has

surrounded the ability of *T. infestans* to occupy silvatic ecotopes. Until recently, the only generally accepted reports of true silvatic *T. infestans* were some Bolivian Andean populations (Usinger *et. al* 1966, Dujardin *et.al.* 1987, Bermudez *et al.* 1993). However, more recently there have been reports of dark morphs of silvatic *T. infestans* occurring in the Bolivian Chaco (Noireau *et al.*, 1997, Noireau *et al.*, 2000, Noireau *et al.*, 2005)

6.3.2 Collection sites and sampling

In Paraguay it is still generally held that silvatic foci of *T. infestans* were not known to occur despite ecological continuity with the other regions of the Chaco, from which silvatic forms have been reported. This position was based on repeated negative surveys of silvatic habitats carried out in parallel to control activities during recent years (A. Rojas de Arias pers. comm.). However, in 2002 *T. infestans* was collected from two foci in close proximity with apparently silvatic ecology (fallen trees and vegetation impacted with soil, so as to resemble wattle and daub), both foci being at least 300m from the closest settlements (Yeo 2003). The foci of collection were both located in Boqueron state (see Fig. 75), one in the vicinity of San Domingo and the other close to San Martin, both small villages, set in the typical semi arid scrub of the Chaco. The villages were inhabited by indigenous populations of subsistence farmers/ hunters occupying simply constructed huts. At the time of collection the houses of these villages were found to be negative for infestation of *T. infestans*. Samples of domestic *T. infestans* were collected from houses of the nearby settlements Campo Loro and Loma Plata (see Fig. 75). Other samples used in the study were obtained from the reference collections compiled during control programme activities and held centrally in Asunción (Instituto de Investigaciones en Ciencias de la Salud, Universidad Nacional de Asunción)

A further sample of domestic *T. infestans* from the same area of the Chaco was included; these were collected several years earlier. In addition, two samples were included from the oriental region (south of Asunción and east of the river Paraguay). One of these samples was from Cordillera state and the other from Paraguarí state (see Fig. 75), both also collected several years prior to the main Boqueron collections of this study.

The putative silvatic samples from Boqueron and those domestic samples described above were analysed by morphometrics and molecular typing, as presented here. Table 33 summarises the details of the groups included.

Table. 33 Details of *T. infestans* groups used in study, see maps for locations (Fig 75)
* Instituto de Investigaciones en Ciencias de la Salud, Universidad Nacional de Asunción
**Chaco samples S= silvatic, D= domestic, PD= "Previous" domestic

Group	Date of collection	Abbreviation
Silvatic Boqueron sample from Chaco (San Domingo & San Martín)	2002	CHA-S**
Domestic, Boqueron sample from Chaco (Campo Loro and Loma Plata)	2002	CHA-D**
Domestic Boqueron sample from Chaco IICS* reference collection	1998-1999	CHA-PD**
Domestic Cordillera sample IICS* reference collection	1998-1999	COR
Domestic Paraguarí sample IICS* reference collection	1998-1999	PAR

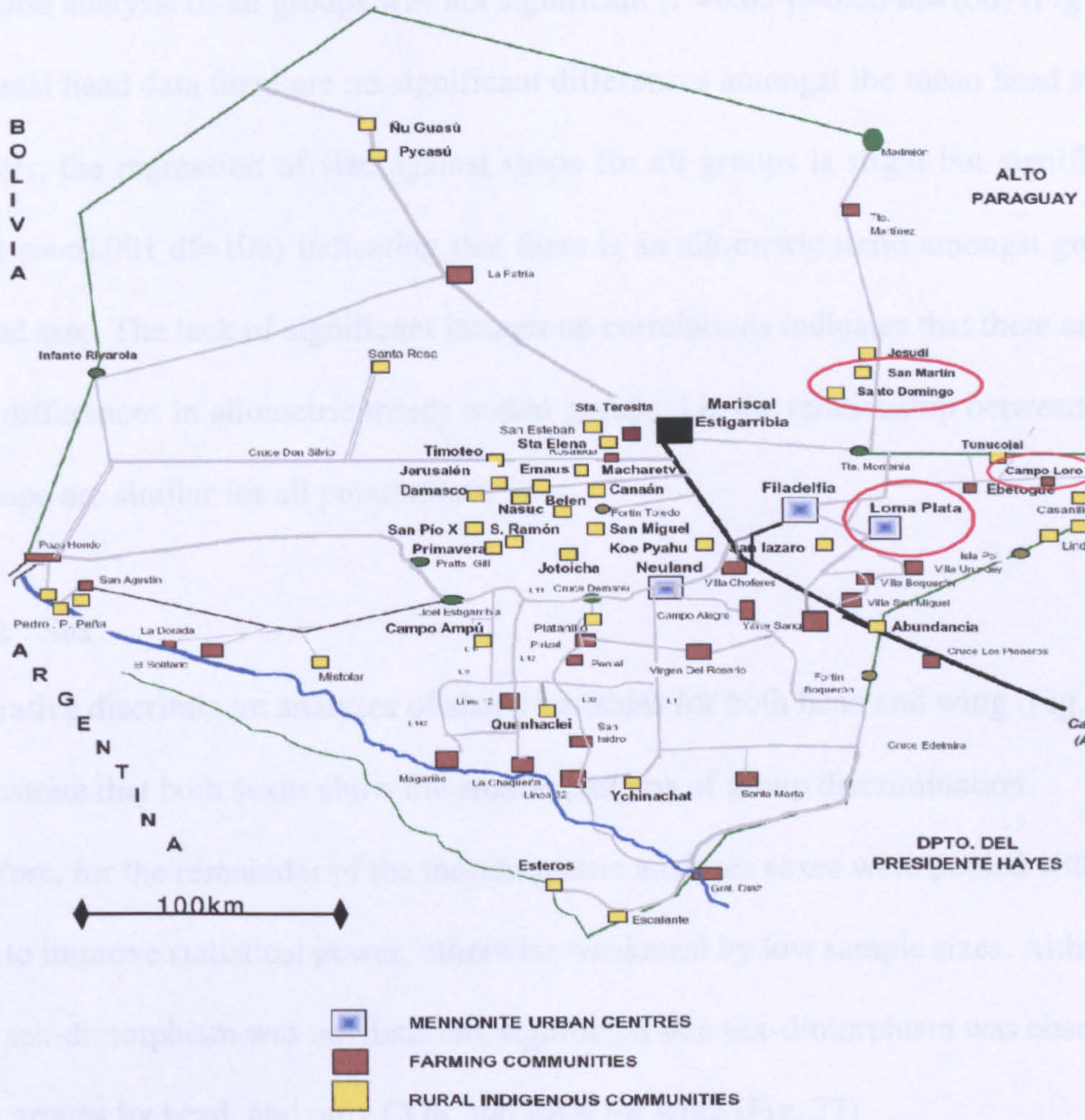

Figure 75. Maps showing study area in Paraguay from which *Triatoma infestans* was collected: The upper map of Paraguay shows collection sites in Boqueron, Cordillera (COR) and Paraguari (PAR) departments (encircled in red). The lower map of Boqueron department below shows community locations (encircled in red) from which samples CHA-S, CHA-D and CHA-PD were collected.

6.3.3 Morphometrics

For this morphometric investigation a total of 107 insects were used, sample sizes were 15-32 specimens per group (~50/50% males and females). Precise sample sizes were as follows: CHA-D 15 (6♂ 9♀), CHA-PD 20(6♂ 14♀), CHA-S 32 (14♂ 18♀) COR 19 (11♂ 8♀) and PAR (13♂ 8♀) from each group sampled. 2D Landmarks were digitised for dorsal head and wing morphology, as described in the Material and Methods section

6.3.3.1 Size

To explore shape differences dependant on size (allometries), respective centroid size (CTR or isometric size) was plotted against CV1 for head and wing (Fig. 76). For wing data, shape variation (CV1) does not appear to be influenced by variation in size; a regression analysis of all groups was not significant (r^2=0.03 p=0.06 df=106) (Fig 76). For dorsal head data there are no significant differences amongst the mean head sizes. However, the regression of size against shape for all groups is slight but significant (r^2=0.1 p=<0.001 df=106) indicating that there is an allometric trend amongst groups for head size. The lack of significant intragroup correlations indicates that there are no major differences in allometric trends within groups: i.e. the relationship between size and shape are similar for all populations.

6.3.3.2 Sex

Explorative discriminant analyses of shape variables for both head and wing (Fig. 77) demonstrate that both sexes show the similar patterns of group discrimination.

Therefore, for the remainder of the morphometric analyses sexes were pooled within group to improve statistical power, otherwise weakened by low sample sizes. Although shape sex-dimorphism was not detected, significant size sex-dimorphism was observed for all groups by head, and only COR and PAR for wing (Fig. 77)

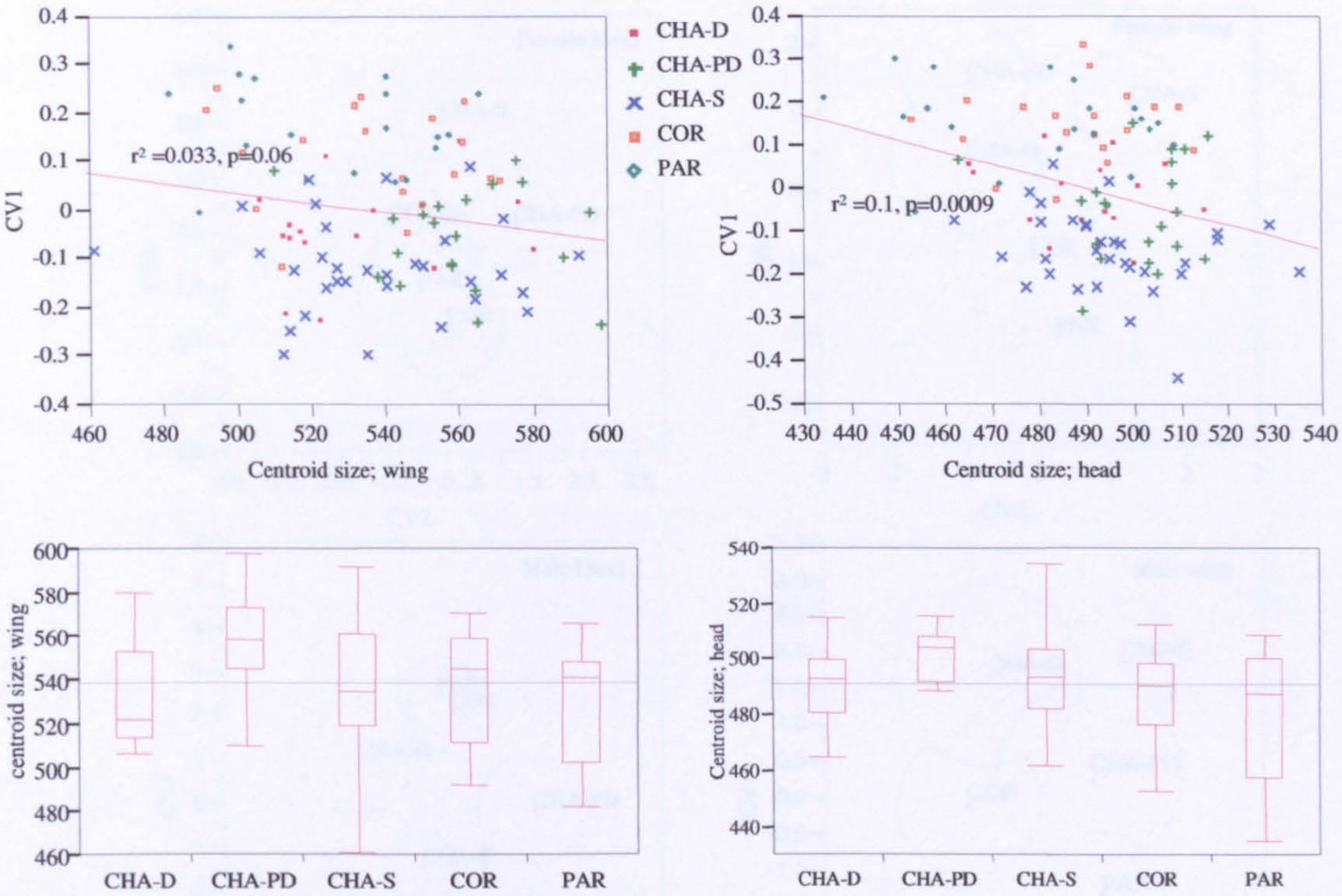

Figure 76. Size differences among *Triatoma infestans* populations. Upper Scatter plots, wing left, head right, show the relationship between centroid size and CV1 (the main axis of shape variation). Regression lines and respective r squared values are included. Labels on plots and charts refer to the groups, CHA-D, CHA-PD and CHA-S from the Chaco, COR from Codillera state, and PAR from Paraguari state (see Table 33 for full details) The lower two charts show mean quartile plots of size for each population, wing to the left and head size in the chart to the right.

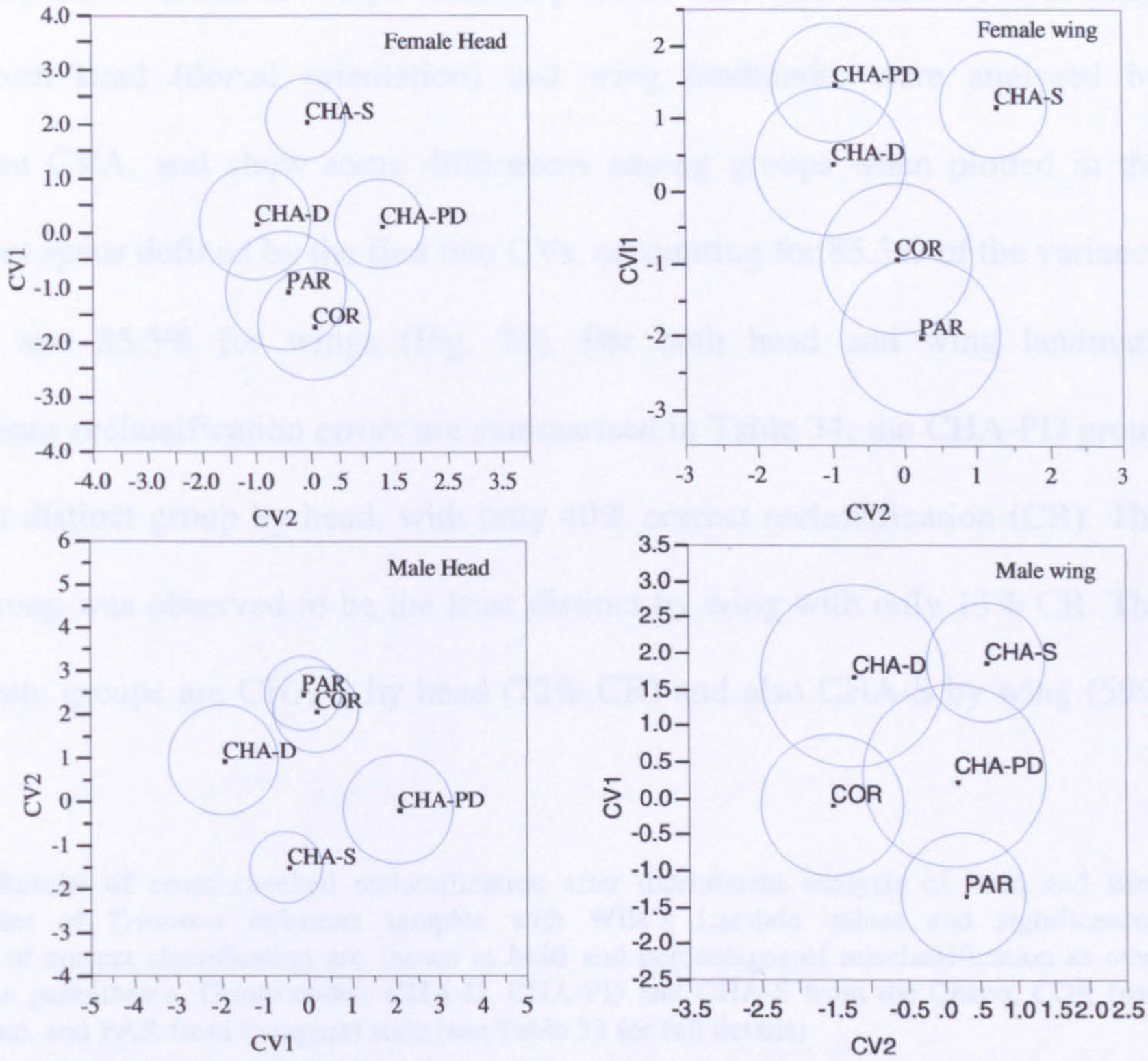

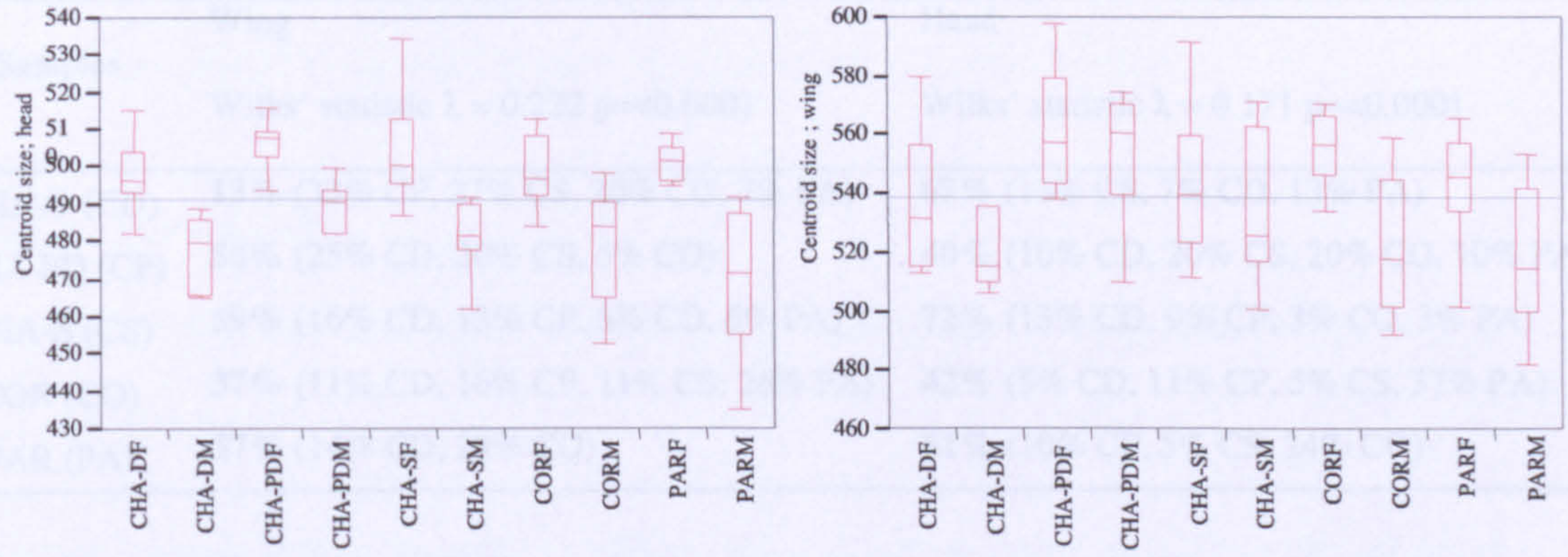

Figure 77. Exploratory analyses of size and shape sexual dimorphism within populations of *Triatoma infestans*. The upper four plots are centroid plots after dicriminant analysis of shape variable, head shape plots to the left and wing shape plots on the right. The bar charts below show quartile plots of size variation, again, head size to the left and wing size chart to the right.
Labels on plots and charts refer to the groups; CHA-D, CHA-PD and CHA-S from the Chaco, COR from Codillera state, and PAR from Paraguari state (see Table 33 for full details), Suffixes M= Male and F=Female.

6.3.3.3 Shape

Shape components (relative warps including affine and non-affine components), derived from head (dorsal orientation) and wing landmarks were analysed by discriminant CVA, and show some differences among groups when plotted in the discriminant space defined by the first two CVs, accounting for 85.3% of the variance for heads and 85.5% for wings (Fig. 78). For both head and wing landmark configurations reclassification errors are summarised in Table 34; the CHA-PD group is the least distinct group by head, with only 40% correct reclassification (CR). The CHA-D group was observed to be the least distinct by wing with only 13% CR. The most discrete groups are CHA-S by head (72% CR) and also CHA-S by wing (59% CR).

Table 34. Results of cross checked reclassification after dicriminant analysis of head and wing morphometrics of *Triatoma infestans* samples with Wilk's Lambda values and significances. Percentages of correct classification are shown in **bold** and percentages of misclassification as other groups are in parentheses. Group codes; CHA-D, CHA-PD and CHA-S from the Chaco, COR from Codillera state, and PAR from Paraguari state (see Table 33 for full details)

Samples	Wing Wilks' statistic $\lambda = 0.222$ p=<0.0001	Head Wilks' statistic $\lambda = 0.171$ p=<0.0001
CHA-D (CD)	**13%** (33% CP, 27% CS, 20% CO, 7% PA)	**67%** (13% CS, 7% CO, 13% PA)
CHA-PD (CP)	**50%** (25% CD, 20% CS, 5% CO)	**40%** (10% CD, 20% CS, 20% CO, 10% PA)
CHA-S (CS)	**59%** (16% CD, 13% CP, 6% CO, 6% PA)	**72%** (13% CD, 9% CP, 3% CO, 3% PA)
COR (CO)	**37%** (11% CD, 16% CP, 11% CS, 26% PA)	**42%** (5% CD, 11% CP, 5% CS, 37% PA)
PAR (PA)	**57%** (14% CD, 29% CO)	**61%** (10% CP, 5% CS, 24% CO)

Plots of the CV1 and CV2 of both data sets (Fig. 78) coupled with TPS transformational grids (including uniform and non-uniform shape components) show the average shape configurations associated with the positive and negative extremes of the abscissa (CV1) and the ordinate axis (CV2). Multivariate regression tests demonstrate that CV1 and CV2 for both head and wing data are significantly associated to the corresponding variation in landmark configurations (Table 35).

Table 35. Fit to the regression model of CV1 and CV2 against head and wing shape components of *T. infestans* samples was tested using a generalized Goodall F-test with p values after 1000 permutations

	Head	Wing
CV1	F = 19.28, P =<0.0001 df=101050	F = 22.63, P = <0.001 df=101050
CV2	F = 24.28, P =<0.0001 df=101050	F = 9.9, P =<0.0001 df=101050

For head dorsal data CV1 shows that the CHA-S group has a relatively elongated head shape compared to the COR and PAR group, with CHA-D and CHA-PD having intermediate forms between the two extremes. Shape differences associated with CV2 constitute more subtle differences in the relative elongation and width of the head. The main difference in wing shape associated to CV1 is again related to the relative elongation of the wing (the relative positions of landmarks 6-7 and 2-3. Chaco populations exhibited more elongated wings in comparison to COR and PAR. CV2, the secondary component of shape also relates to differences in the pattern of elongation, (the relative positions of landmarks 4 - 5 and 1-2). In this respect Chaco domestic populations grouped together as more elongate than the other groups

6.3.3.4 Interspecific

Further analysis was conducted including two out-groups: *T. delpontei* (DEL) and *T. platensis* (PLA).

CVA of relative warps (including affine and non-affine components) of dorsal head wind landmarks was performed. Fig 79 shows a plot of the first two CVs for both head and wing data, accounting for 81.5% and 83.7% of the variance for head and wing data sets respectively.

Head CV1 shows clear separation of the *T. infestans* groups from DEL and PLA, and relates to DEL and PLA having more compact heads relative to the groups of *T.*

infestans (represented by TPS grids). Head CV2 separates the CHA-S population from all other groups and pertains to the same pattern of shape change as observed for the CV1 axis of the intraspecifc analysis.

Wing CV1also shows clear separation of *T. infestans* groups from DEL and PAL. The transformation grids show that the shape differences relate to differences in the landmark configurations of the anterior and posterior regions of the wing.

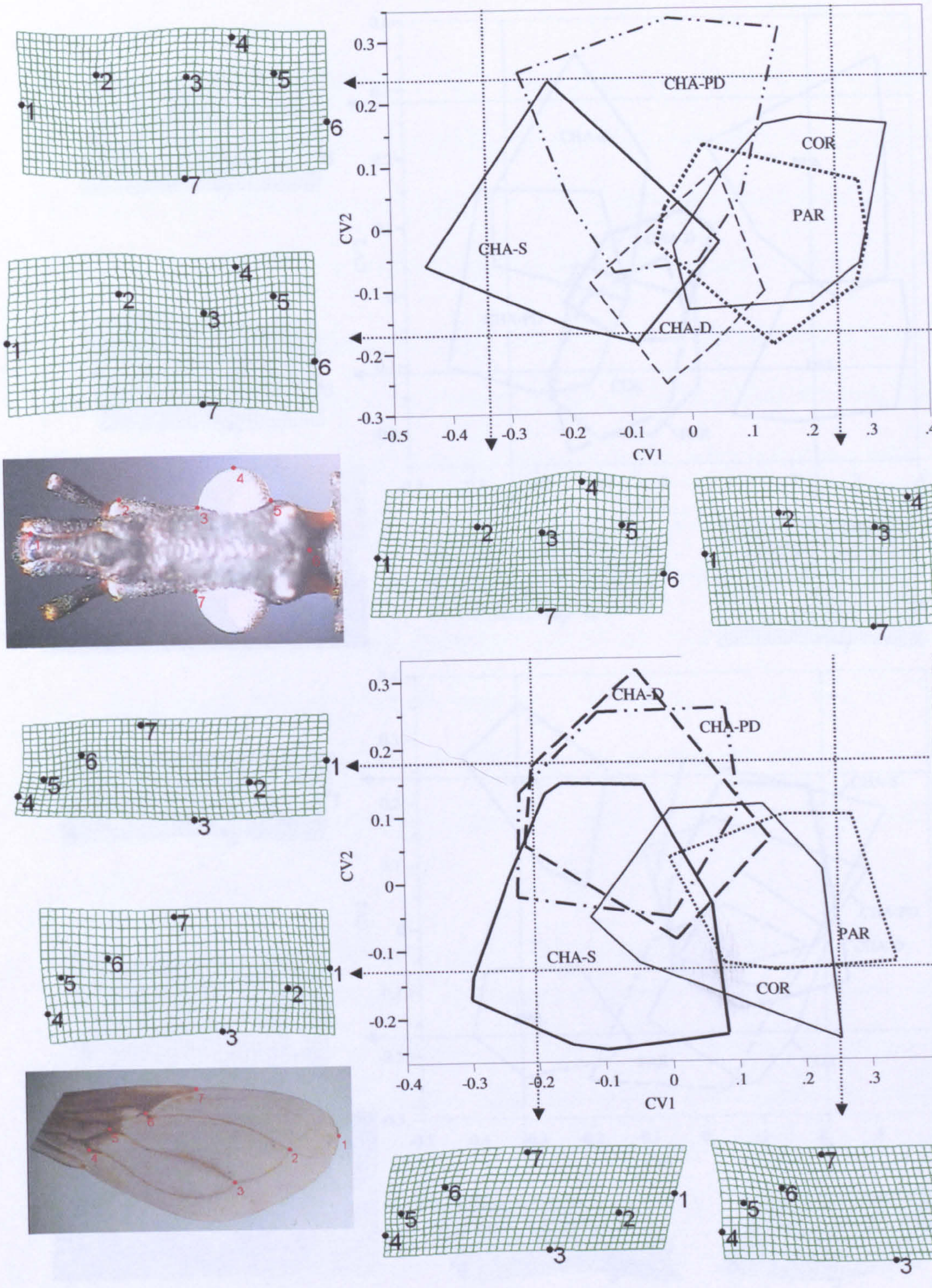

Figure 78. Morphometric analysis of *T. infestans* intraspecific groups: CVA analysis of shape components after GPA. Polygons enclose distribution of specimens in each group. The upper plot is derived from dorsal head landmarks and the lower from wings. For the heads CV1 accounts for 61.86% of the total variance and CV2 accounts for 23.7% (∑ = 85.5%). For the wings CV1 62.7%, CV2 22.7% (∑85.3 %). Thin plate splines are included showing, shape differences of the head and wing that correspond to the CV axes, as indicated by dashed lines and arrows. Group codes; CHA-D, CHA-PD and CHA-S from the Chaco, COR from Codillera state, and PAR from Paraguari state (see Table 33 for full details)

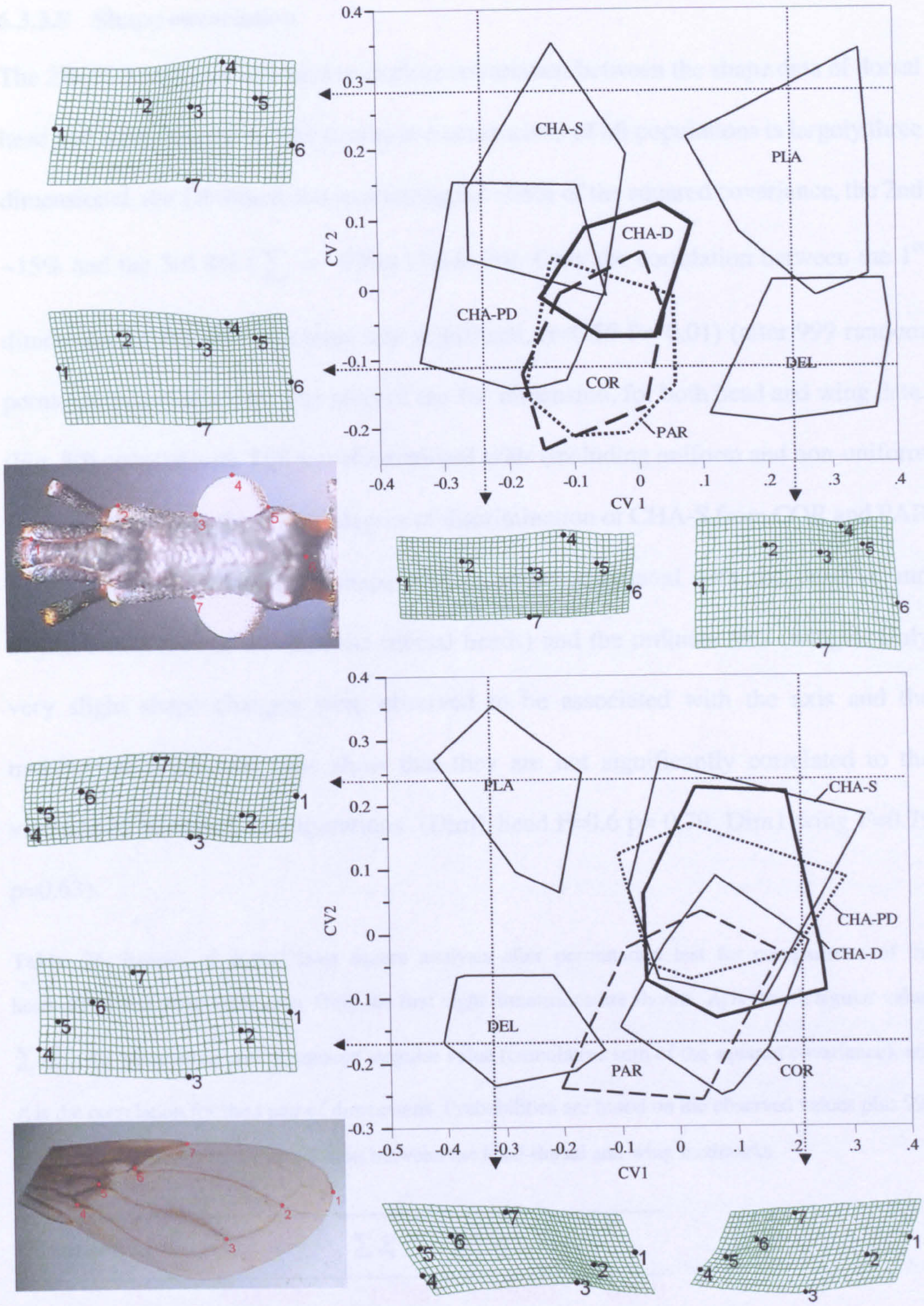

Figure 79. Morphometric analysis of *T. infestans* groups with interspecific out-groups (*Triatoma platensis* (PLA) and *T. delpontei* (DEL)) : CVA analysis of shape components after GPA. Polygons enclose distribution of specimens in each group. The upper plot is derived from dorsal head landmarks and the lower from wings. For the heads CV1 accounts for 64.6% of the total variance and CV2 accounts for 22.7% ($\sum$ = 87.3%). For the wings CV1 62.6%, CV2 31.6% ($\sum$94.2 %). Thin plate splines are included showing, shape differences of the head and wing that correspond to the CV axes, as indicated by dashed lines and arrows. Group codes; CHA-D, CHA-PD and CHA-S from the Chaco, COR from Codillera state, and PAR from Paraguari state (see Table 33 for full details)

6.3.3.5 Shape covariation

The 2B- PLS analysis was used to explore covariation between the shape data of dorsal head and wing structures. The results in a comparison of all populations is largely three dimensional, the 1st dimension accounting for ~68% of the squared covariance, the 2nd ~15% and the 3rd 8% ($\sum$ = ~93%) (Table 36). Only the correlation between the 1st dimension for the two structures was significant, (r=0.59 P= 0.01) (after 999 random permutations) (Table 36). The plots of the 1st dimension, for both head and wing data. (Fig. 80) coupled with TPS transformational grids (including uniform and non-uniform shape components) show some degree of discrimination of CHA-S from COR and PAR. TPS grids show the average shape configurations associated with the positive and negative extremes of the abscissa (dorsal heads) and the ordinate axis (wings). Only very slight shape changes were observed to be associated with the axis and the multivariate regression tests show that they are not significantly correlated to the variation in landmark configurations (Dim1-head F=0.6 p= 0.79; Dim1-wing F=0.79 p=0.63).

Table. 36. Results of partial least square analysis after permutation test for comparisons of the head-dorsal and wing landmarks. Only the first eight dimensions are shown. λ_i is the *i*th sigular value, $\sum \lambda_i^2$ is the cumulative sum of squared singular value (cumulative sum of the squared covariance), and r_i is the correlation for the *i* pair of dimensions. Probabilities are based on the observed values plus 999 random permutations of the association between the head-dorsal and wing landmarks.

Dimensions	λ_i	$\sum \lambda_i^2$	r_i	P
1	0.00009	0.6887	0.59302	0.010
2	0.00004	0.84173	0.30303	0.400
3	0.00003	0.92765	0.30568	0.320
4	0.00002	0.97431	0.31218	0.070
5	0.00001	0.98806	0.20107	0.720
6	0.00001	0.99572	0.20271	0.370
7	0.00001	0.9983	0.10007	0.960
8	0.00000	0.99985	0.13466	0.300

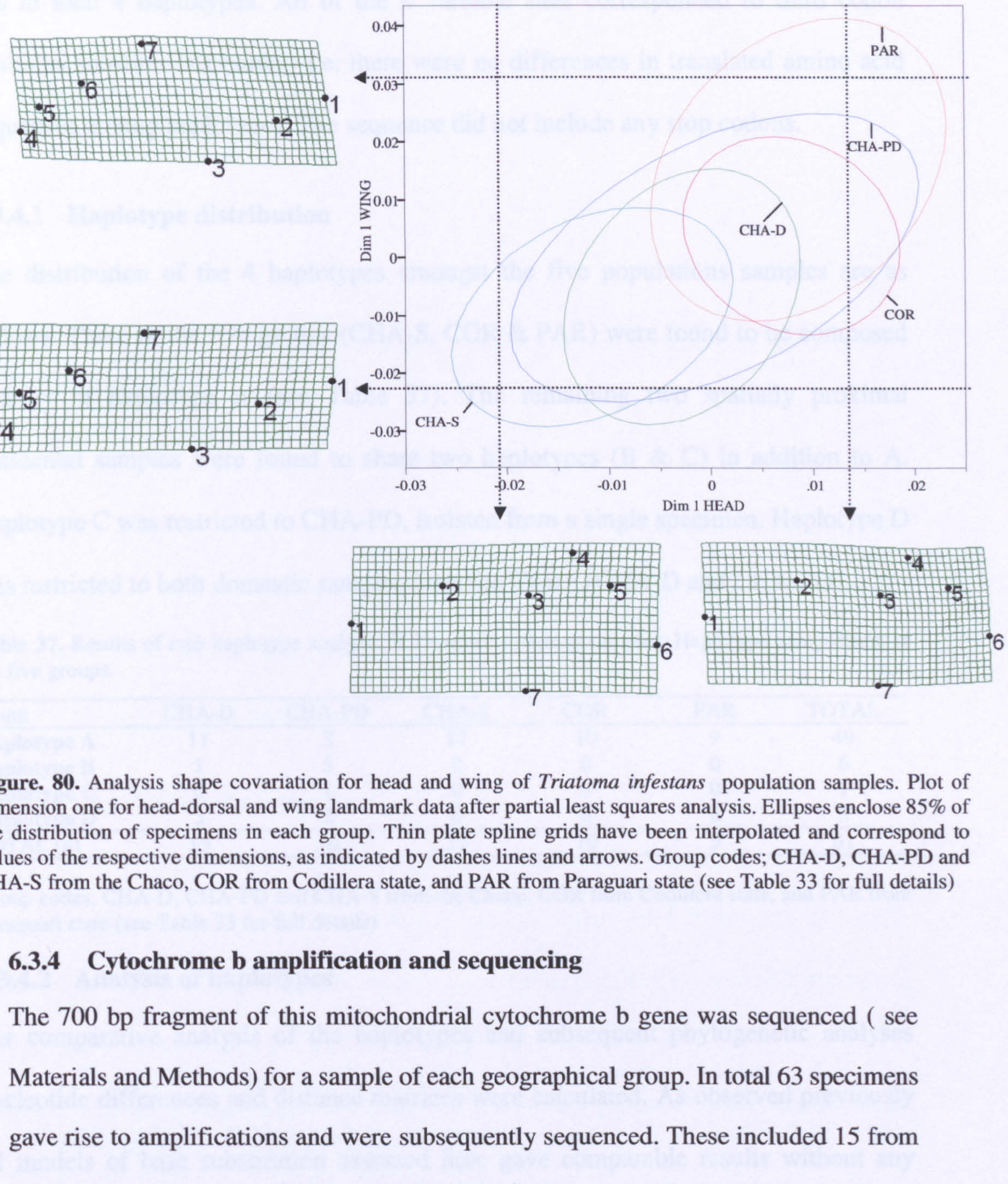

Figure. 80. Analysis shape covariation for head and wing of *Triatoma infestans* population samples. Plot of dimension one for head-dorsal and wing landmark data after partial least squares analysis. Ellipses enclose 85% of the distribution of specimens in each group. Thin plate spline grids have been interpolated and correspond to values of the respective dimensions, as indicated by dashes lines and arrows. Group codes; CHA-D, CHA-PD and CHA-S from the Chaco, COR from Codillera state, and PAR from Paraguari state (see Table 33 for full details)

6.3.4 Cytochrome b amplification and sequencing

The 700 bp fragment of this mitochondrial cytochrome b gene was sequenced (see Materials and Methods) for a sample of each geographical group. In total 63 specimens gave rise to amplifications and were subsequently sequenced. These included 15 from the CHA-D sample, 17 CHA-S, 10 CHA-PD, 10 COR and 9 PAR. The alignments of all sequences gave rise to a consensus of 407 bp and did not contain any gaps. Identity of the amplicons sequenced was confirmed by BLAST search and direct alignments to the complete cytochrome b gene of *T. dimidiata* (Dotson and Beard 2001; Genebank accession AF301594) revealed that the amplified fragment corresponded to the region of the gene between positions 340 and 1003 (total length of gene 1132 bp)

Alignments of all sequences revealed 8 variable sites (none parsimony-informative) and in total 4 haplotypes. All of the 8 variable sites corresponded to third codon positions substitutions (silent) i.e. there were no differences in translated amino acid sequences among haplotypes. The sequence did not include any stop codons.

6.3.4.1 Haplotype distribution

The distribution of the 4 haplotypes amongst the five populations samples are as follows. Three of the five groups (CHA-S, COR & PAR) were found to be composed entirely of haplotype A (see Table 37). The remaining two spatially proximal occidental samples were found to share two haplotypes (B & C) in addition to A. Haplotype C was restricted to CHA-PD, isolated from a single specimen. Haplotype D was restricted to both domestic samples form the Chaco (CHA-D and CHA-PD).

Table 37. Results of *cytb* haplotype analysis of *Triatoma infestans* samples: Haplotype composition of the five groups.

Count	CHA-D	CHA-PD	CHA-S	COR	PAR	TOTAL
Haplotype A	11	2	17	10	9	49
Haplotype B	1	5	0	0	0	6
Haplotype C	0	1	0	0	0	1
Haplotype D	3	2	0	0	0	5
TOTAL (n)	15	10	17	10	9	61

Group codes; CHA-D, CHA-PD and CHA-S from the Chaco, COR from Codillera state, and PAR from Paraguari state (see Table 33 for full details)

6.3.4.2 Analysis of haplotypes

For comparative analysis of the haplotypes and subsequent phylogenetic analyses nucleotide differences and distance matrices were calculated. As observed previously all models of base substitution assessed here gave comparable results without any significant differences in the results of the eventual phylogenetic analyses. For this reason, only K2 p distances and nucleotide differences are presented here. Among group differences are relatively small between haplotypes, ranging from 1 to 13 nucleotides (a sequence divergence of 0.15% - ~2%).

For each of the geographic samples/populations within group differences were assessed by absolute nucleotide differences (Table 38)

Table 38. Absolute number of nucleotide differences (for a 402 bp fragment of *cytb*) within populations of *Triatoma infestans*.

Geographical sample/ population	Within group; absolute no. of nucleotide differences
CHA-D	7
CHA-PD	8
CHA-S	0
COR	0
PAR	0

Group codes; CHA-D, CHA-PD and CHA-S from the Chaco, COR from Codillera state, and PAR from Paraguari state (see Table 33 for full details)

The data set of 4 haplotypes was found to have a relatively high transition to transversion ratio of 8.3. This observation, considered together with all p distances being < 0.09-0.1 (the saturation threshold for the cytochrome b gene, as recommended by Meyer (1994) negates the possibility that the models of base substitution used to calculate the genetic distances would be adversely affected by saturation of transitions.

6.3.4.3 Supplementary sequences

This dataset was supplemented by a specimen of *T. platensis,* collected from a bird nest in the Paraguayan Chaco. A sequence from *T. melanosoma* and further sequences of *T. infestans* from Bolivia, Brazil and Argentina were provided by Fernando Monterio and correspond to those used by Monterio *et al.*(1999b) (see Table 39).

Table 39. Supplementary *cytb* haplotypes of *Triatoma infestans* isolated by Monterio *et al.*(1999b) from countries bordering Paraguay.

Source of Material	Haplotypes
Bolivia	BOL-A and BOL-B
Brazil	Haplotype A and TM*
Argentina	Haplotype A

* TM represents a haplotype isolated from *T. melanosoma* found to share haplotype with a sample from Brazil

6.3.4.4 Phylogenetic analyses

6.3.4.4.1 Distance based

Neighbour-joining trees were generated (Fig. 81) using the various models of base substitution, and statistical support was evaluated by bootstrap resampling with 1000 replicates and a random seed number. In the alignment used to construct the trees a sequence from a closely related species (*T. brasiliensis*) was included as an outgroup. All models of base substitution investigated yielded essentially equivalent results, all trees with identical topologies and similar bootstrap supports.

6.3.4.4.2 Maximum parsimony

To support the phylogeny reported by the Neighbour-joining analysis the haplotypes were also subjected to a maximum parsimony analysis. The branch and bound algorithm was used to recover three equally parsimonious trees, from which a strict consensus tree was produced with bootstrap supports (Fig. 82).

The parsimony network constructed for all 4 haplotypes using TCS software (figure 83) shows the number of mutational steps separating any two of the haplotypes and the number and position of all inferred haplotypes that could conceivably be found with further sampling. (Fig 83). A further parsimony network was constructed to include the haplotypes provided by F. Monterio (Table 39) and originating from other geographical regions (Fig. 84).

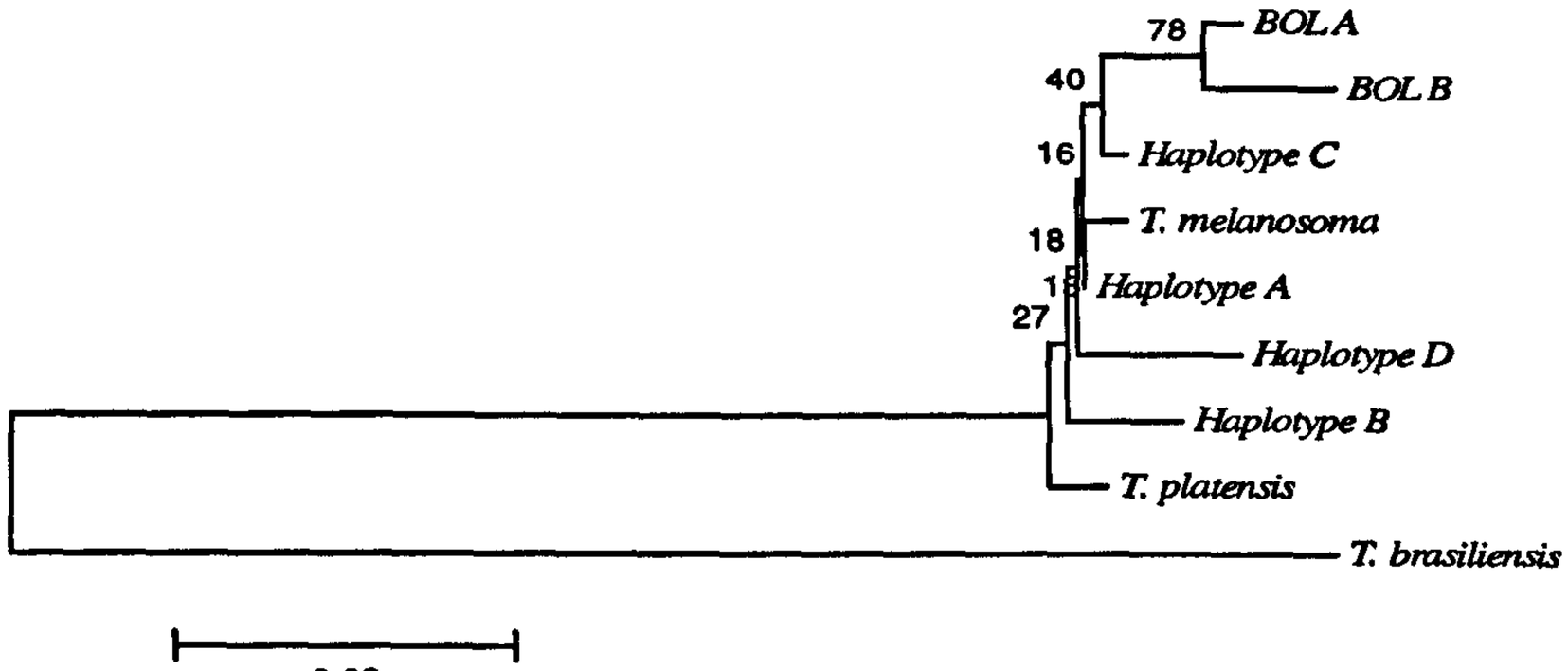

Figure 81. Analysis of *cytb* sequences: Neighbour-joining phylogenetic tree of the 10 *T. infestans* haplotypes including *T. platensis* and *T. brasiliensis* as outgroups. Constructed using k2p model, with 1000 bootstrap replicates sum of branch lengths = 0.196, scale: substitutions/site. Refer to Table 37 and 39 for details of haplotypes.

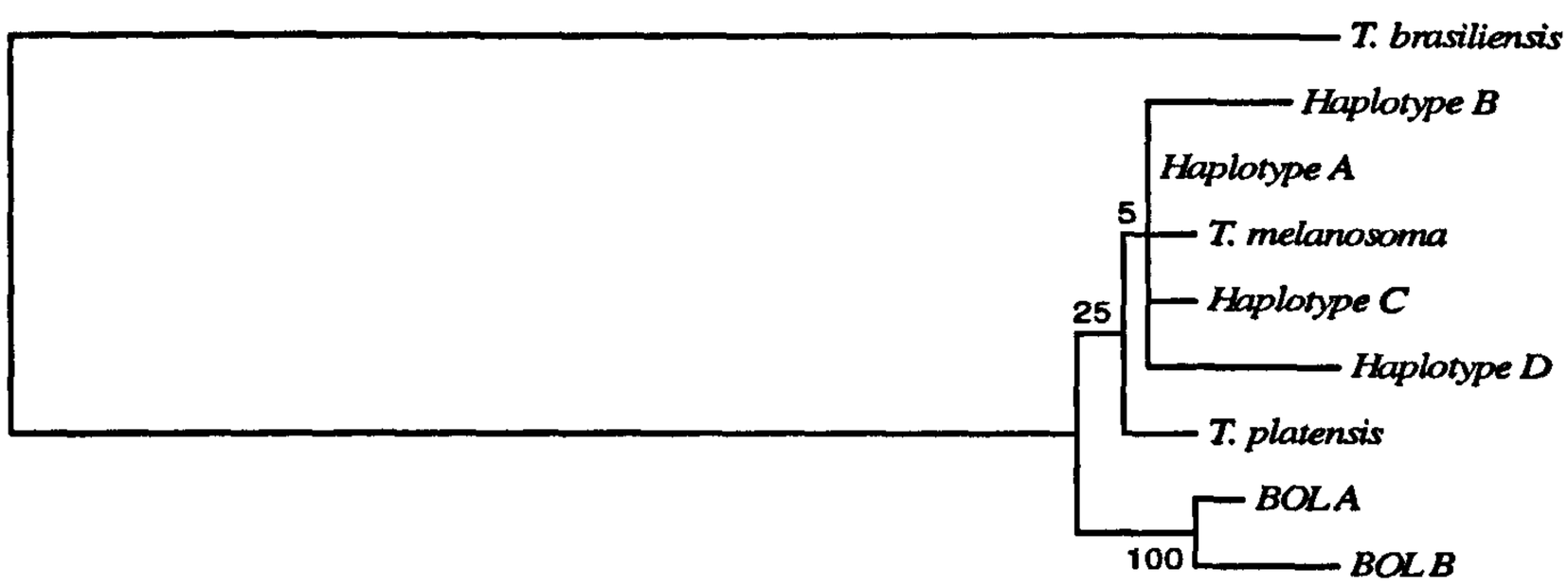

Figure 82. Analysis of *cytb* sequences: Maximum parsimony strict consensus phylogeny of the 10 *Triatoma infestans* haplotypes including *T. platensis* and *T. brasiliensis* as outgroups. Constructed using branch-and-bound algorithm with 1000 bootstrap replicates CI = 0.942 RI = 0.500 RCI= 0.471 (for all sites) and iCI = 0.636, iRI = 0.500, iRCI = 0.318 (for parsimony informative sites). Refer to Table 37 and 39 for details of haplotypes.

6.3.5 Morphometric/genetic comparisons

A subset of specimens used in the morphometric studies were matched to samples characterised by mitochondrial haplotype (Fig. 86). In light of the genetic results and phylogenetic analyses it became feasible to assess the morphometric data for phylogenetic signals. Using the Mahalanobis distances calculated during the canonical variate analysis, dendrograms were drawn by UPGMA cluster analysis to facilitate direct comparisons to the phylogenetic trees derived from the mitochondrial sequence

data. The only clear congruence of tree topologies is between head and wing shape datasets (Fig. 85). Mantel tests were used to assess correlation of distance matrices. Mahalanobis distances for head and wing, genetic distance and geographical distance between sampling locations were included. Only the correlation between morphological matrices was significant (Table. 40).

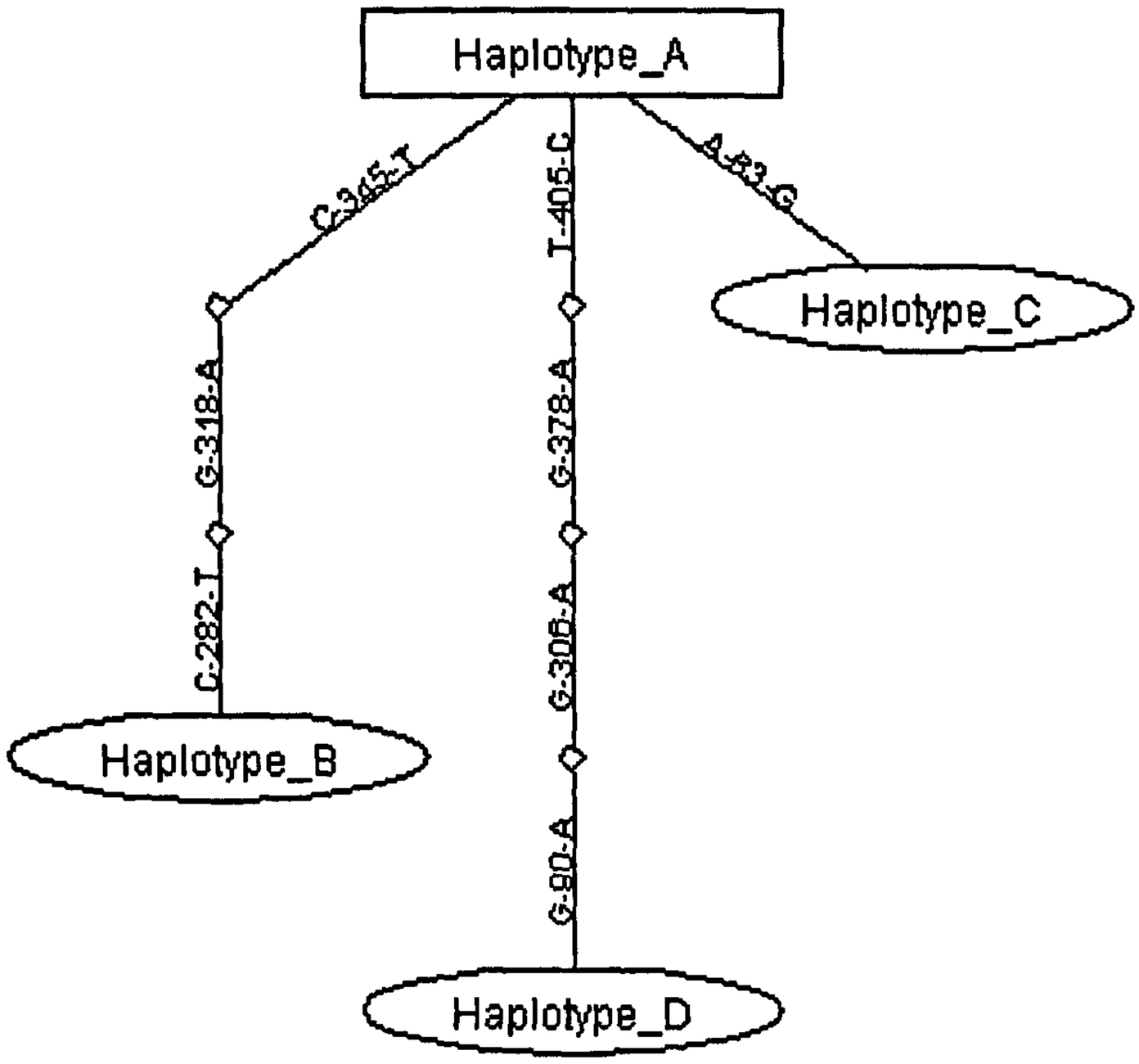

Figure 83. Analysis of *cytb* sequences: Network of Paraguayan *T. infestans* haplotypes. The maximum number of steps connecting parsimoniously two haplotypes is indicated; one step is indicated by a single line between two haplotypes and each additional base substitution by a small circle. The haplotype with the highest ancestral probability is displayed as a square, while other haplotypes are displayed as ovals. Refer to Table 37 for details of haplotypes.

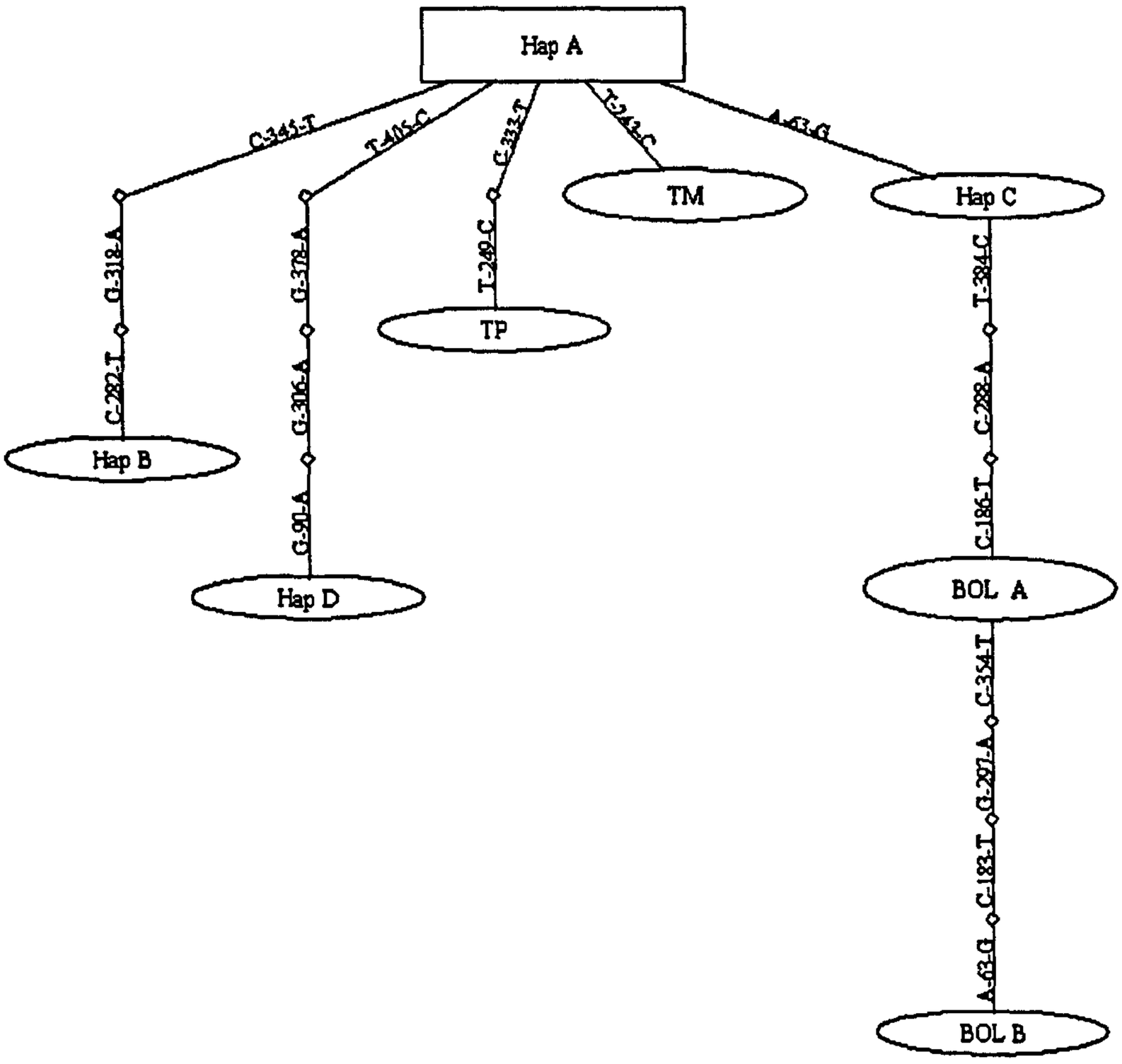

Figure 84 Analysis of *cytb* sequences: Network of *T. infestans* haplotypes, including Paraguyan, Brazilian and Bolivian isolates (see Table. 39) including The maximum number of steps connecting parsimoniously two haplotypes is indicated; one step is indicated by a single line between two haplotypes and each additional base substitution by a small circle. The haplotype with the highest ancestral probability is displayed as a square, while other haplotypes are displayed as ovals. See Table 37 and 39 for haplotypes. TP and TM represent *T. platensis* and *T. melanosoma* respectively.

Table 40. Analysis of correlation between data sets for Paraguayan *Triatoma infestans* samples: Results of pair-wise Mantel tests between morphometric (head and wing), geographical and genetic distance matices (K2p distances derived from analysis of 402 bp of *cytb*). P values are calculated after 10000 permutations

xy	Matrix correlation (rxy)	p
Head vs. Wing	0.68	0.02
Head vs. Geographical distance	0.50	0.18
Head vs. Genetic distance	0.042	0.36
Wing vs. Geographical distance	0.75	1.0
Wing vs. Genetic distance	-0.24	0.77
Geographical vs Genetic distances	-0.28	1.0

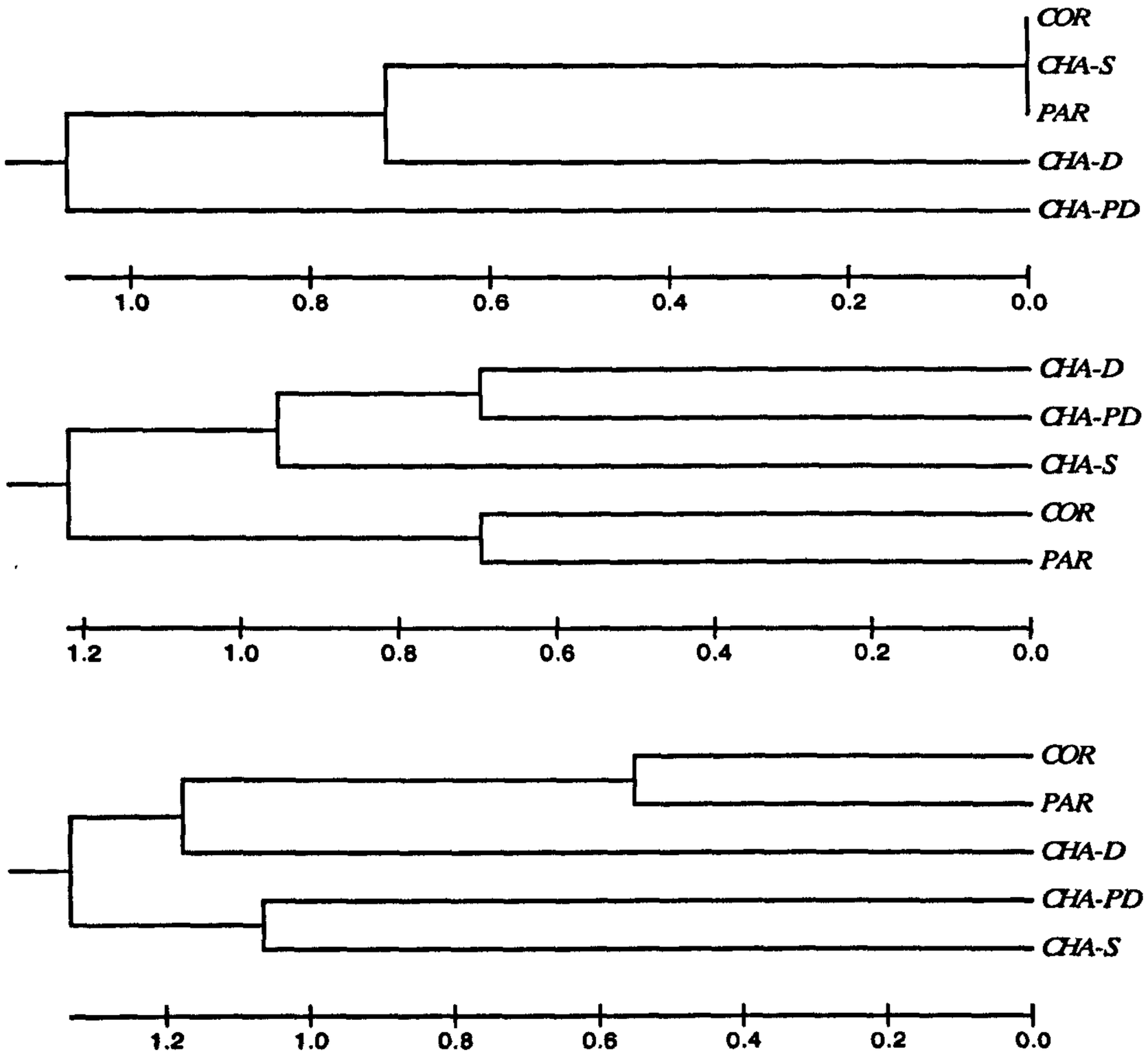

Figure 85. UPGMA cluster analysis of Mahalanobis distances (derived form morphometric analyses) and genetic distances (K2p distances derived from analysis of 402 bp fragment of *cytb*) for Paraguyan *Triatoma infestans* samples: Upper= genetic distance, Middle= wing shape, lower=. head shape. Group codes; CHA-D, CHA-PD and CHA-S from the Chaco, COR from Codillera state, and PAR from Paraguari state (see Table 33 for full details)

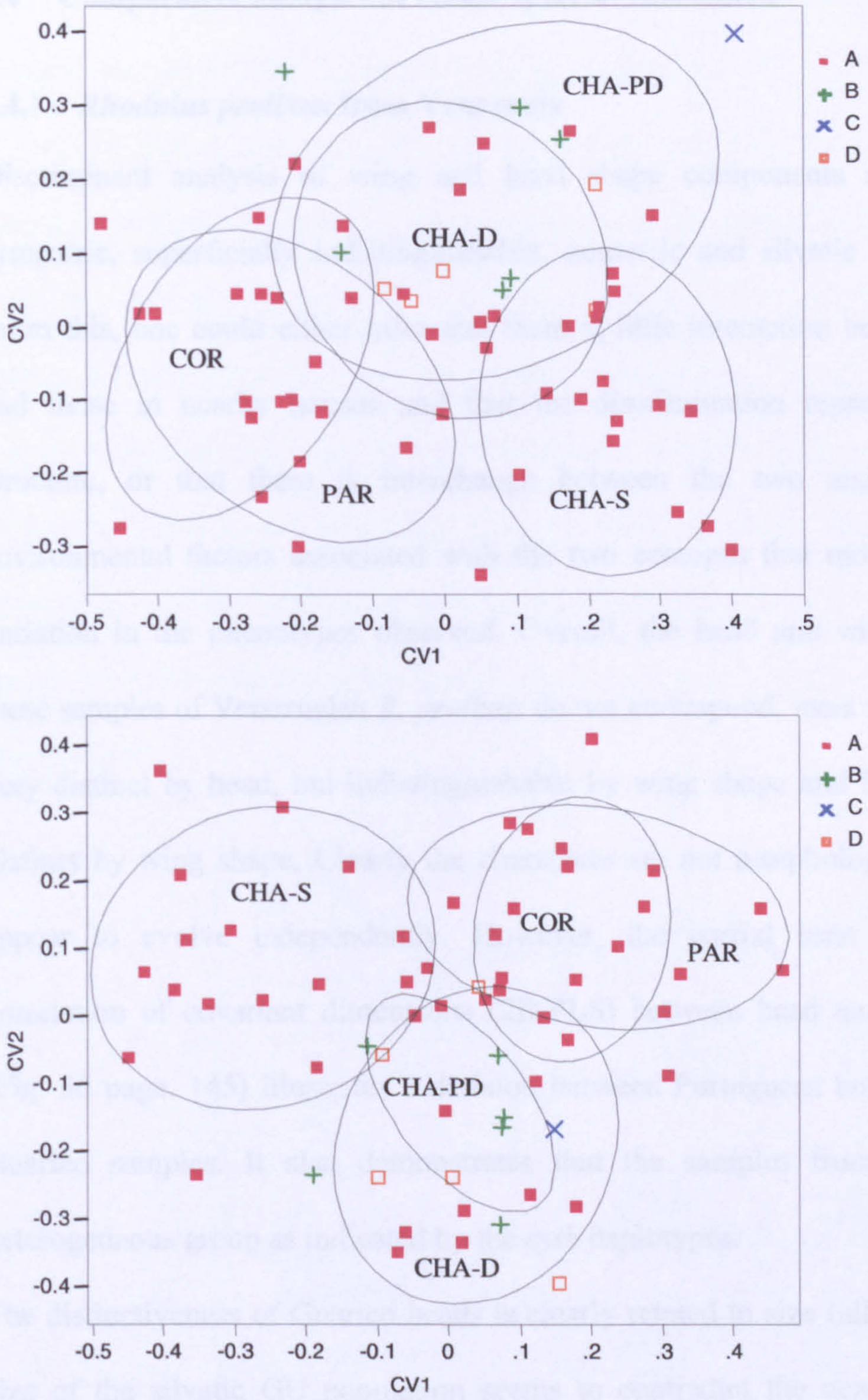

Figure. 86. Paraguayan *T. infestans cytb* mitochondrial haplotypes matched to morphometrics and superimposed on to CVA plot for head shape (upper) and wing shape (lower) groups enclosed by 85% density elipses. Group codes; CHA-D, CHA-PD and CHA-S from the Chaco, COR from Codillera state, and PAR from Paraguari state (see Table 33 for full details)

6.4 Comparative analyses of vector species: Discussion

6.4.1 *Rhodnius prolixus* from Venezuela

Discriminant analysis of wing and head shape components successfully separate sympatric, superficially indistinguishable, domestic and silvatic samples (PS & PD). From this, one could either infer that there is little interaction between bugs in palms and those in nearby houses and that the discrimination represents the population structure, or that there is interchange between the two and it is the differing environmental factors associated with the two ecotopes that modulate the directional variation in the phenotypes observed. Overall, the head and wing morphometrics of these samples of Venezuelan *R. prolixus* do not correspond, most strikingly Guarico are very distinct by head, but indistinguishable by wing shape and Lara bugs being most distinct by wing shape. Clearly the characters are not morphologically integrated and appear to evolve independently. However, the partial least squares analysis of correlation of covariant dimensions (2B-PLS) between head and wing morphologies (Fig. 56 page. 145) illustrates a division between Portuguesa bugs from the Lara and Guarico samples. It also demonstrates that the samples from Portuguesa form a heterogeneous group as indicated by the *cytb* haplotypes.

The distinctiveness of Guarico heads is clearly related to size (allometric). The smaller size of the silvatic GU population seems to contradict the general observation, that silvatic populations of triatomines are larger than derived domestic populations (Schofield *et al.*,1999, 2000 Dujardin *et al.* 1997a b 1998 a b). A possible explanation is Bergmann's rule, which states that smaller sized geographical races of a species are found in the warmer parts of the range and the larger-sized races in the cooler parts of the range. Originally Bergmann's rule was thought to apply only to homeothermic animals, however the rule has been observed to pertain to insects on several occasions

(Daly 1985). The lower altitude of the GU population relative to the other three Andean populations (see Fig. 50) may explain GUs smaller size.

R. prolixus and *R. robustus* are very similar species, morphologically discernable by only a few tenuous characters. One of the key characters used in differentiating between *R. prolixus* and *R. robustus* is the relative proportions of the head (Lent & Wygodzinsky 1979); the ratio of post-ocular to pre-ocular distances is ~ 1:3 for *R. prolixus* and ~1:4 for *R. robustus* (see Fig. 87). Visualisation of TPS grids (Fig. 54, page. 141) demonstrate that the GU population has an extreme "*prolixus*" like head while the other Venezuelan populations, both domestic and silvatic have relatively more "*robustus*" like heads. With the inclusion of a population of *R. robustus* (Fig. 55, page, 142) this trend is emphasised.

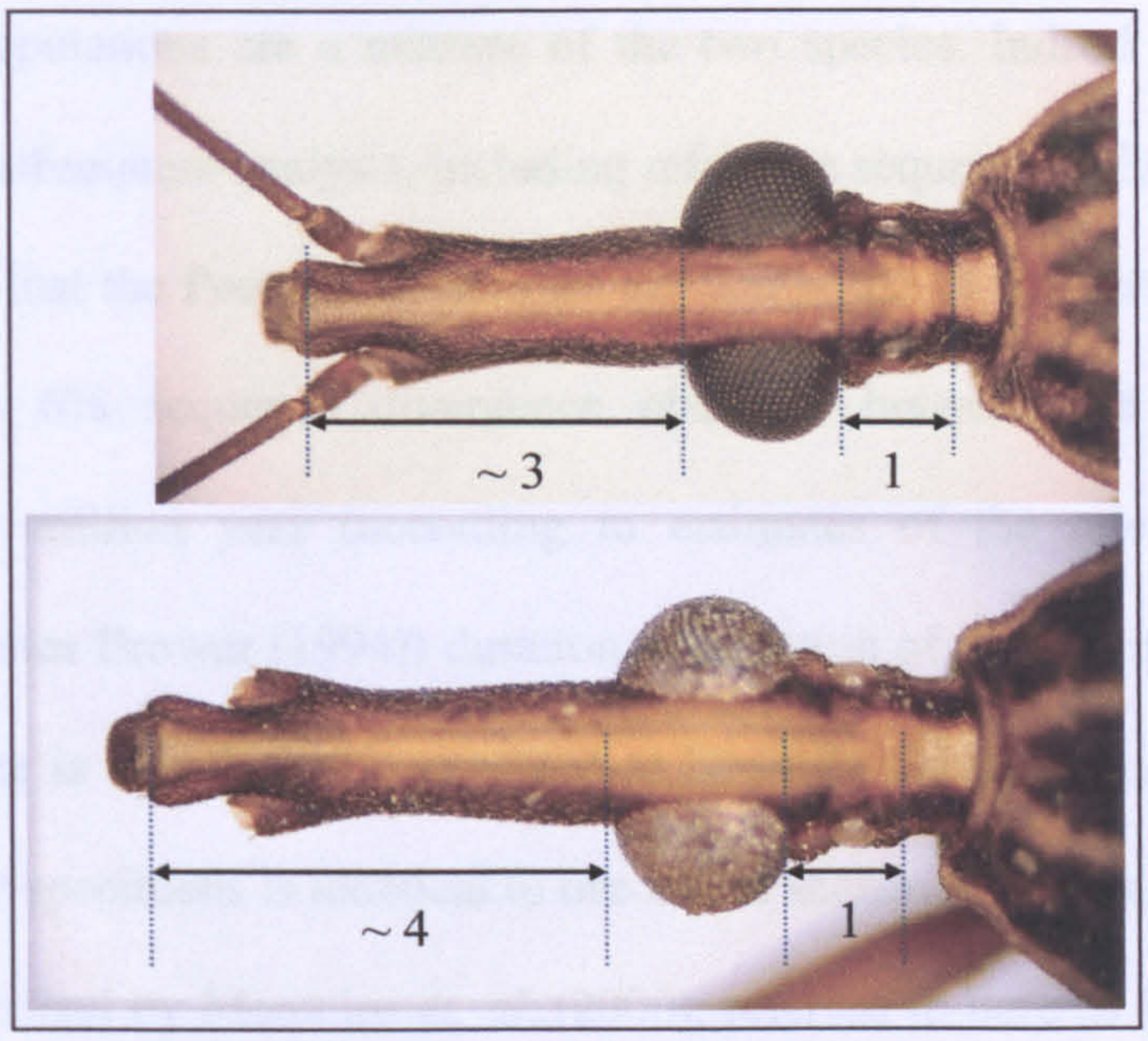

Figure 87 Comparison of *R. prolixus* (upper) and *R. robustus* (lower) demonstrating the general difference in pre-ocular to post-ocular ratios.

Recent work on the molecular phylogenetics of *R. robustus* and *R. prolixus* (Monteiro *et al.* 2000 and 2003) (also using *cytb* sequences) suggests that regardless of morphological phenotype the two species are assemblages of geographically defined

lineages. More specifically, *R. robustus* and *R. prolixus* from the Amazon form one clade and Central American, Colombian and Venezuelan *R. prolixus* and Venezuelan *R. robustus* form another. Therefore it seems that the traditional morphological characterisation of these two species masks the true patterns of convergence, biogeography and ecological specialisation that define the observed morphotypes. A morphometric comparison of Venezuelan *R. robustus* to domestic *R. prolixus* from a neighbouring state showed a clear difference between the wing shape of the two "species" (Villegas *et al.*, 2002). The morphological variation observed in the present study demonstrates morphological phenotypic gradation intermediate between *R. prolixus* and *R. robustus* head shape. This apparent clinal variation might indicate that there are intermediate forms between *R. prolixus* and *R. robustus* in Venezuela or that perhaps some populations are a mixture of the two species. Indeed the result of our sequencing and subsequent analysis, including reference sequences of *R. prolixus* and *R. robustus*, shows that the Portuguesa samples are composed of two extremely divergent haplotypes. The 6% sequence divergence observed between the two haplotypes represents a ~3 million year (according to estimates of the rate of mutation of mitochondrial genes Brower (1994)) duration of isolation of the two maternal lineages. Such a difference is usually to be expected at interspecific level. Indeed haplotype 3 isolated from our specimens is identical to one of the sequences of Brazilian Amazonian *R. robustus* described by Monteiro *et. al.*,(2000), referred to here as Brazil III (Fig.57, page 149). This striking result is difficult to reconcile by any other explanation other than introgression (Avise 1994). i.e. At some point the ancestors of the *R. prolixus* of Portuguesa hybridised with Amazonian type *R. robustus*, followed by the hybrid offspring backcrossing with the *R. prolixus*. This is particularly likely as the two species are known to be inter-fertile (Barrett 1996). The uniformity of the *prolixus* phenotype

and nuclear genome (as demonstrated by Fitzpatrick (2005) using microsatellite markers) among the Portuguesa samples are unequivocal support for introgression.

Therefore the introgressed haplotype 3 greatly distorts the trees drawn from genetic distances among groups and there are no correlations between the genetic distances and morphometric data matrices (Table 26 and Fig. 59). However, the plots of the haplotypes in discriminant plots for head and wing morphometrics (Fig. 60, page 152) suggest that if haplotype 3 were disregarded then the genetic data would best correspond to the differences in head shape. Indeed, disregarding haplotype 3, only Guarico would be distinguishable by mtcytb sequences.

With their introgressed robustus haplotype (haplotype 3) the Portuguesa samples are genetically heterogeneous. This is in contrast to domestic populations from Central America, which according to RAPD data (Dujardin *et al.*, 1998b) are genetically limited. This is reconcilable by the recent introduction of *R. prolixus* to Central America by the accidental escape of laboratory-bred insects in 1915 (Dujardin *et al.* 1998b and Zeledón 1996). Such an extreme bottle neck accounts for the limited genetic diversity, which could not be moderated since there are no natural silvatic populations in Central America. The continued isolation of Central American *R. prolixus* from those in South America was demonstrated by Dujardin *et. al.* (1998). Interestingly, haplotype 1, common to all samples of Venezuelan *R. prolixus* examined here has identity with Honduran samples (Fig. 57, page 149) isolated by Monteiro *et. al,* (2000, 2003), this suggests that mitochondrial haplotypes of <1 kb sequences may not give sufficiently high resolution as an estimate of population dynamics to be of epidemiological significance.

The genetic diversity within samples (Table 25, page 148) shows that the domestic bugs from Lara are the most homogeneous, with only one haplotype recovered from the entire sample.

If we recall that, despite equal effort to recover silvatic samples from the LA site, none could be found, the observed genetic homogeneity of the domestic LA sample might be due to genetic drift in the absence of silvatic populations to supplement the gene pool. The LA population is also least similar by wing landmark configuration (Fig. 54, page 141). As observed for other species examined here, distinctiveness of wing shape corresponds to apparent isolation from other domestic or silvatic populations. Therefore, variation in the formation of wing venation may be a common founder effect in isolated populations of limited genetic diversity.

Returning to the discordance between the head and wing morphometrics (Fig. 54, page 141), the analyses in which out-groups were included (Fig. 55, page. 142) demonstrate that the pattern of discrimination by wing morphometrics is more congruent to the phylogeny of the species, as shown by the *cytb* phylogenetic analysis (Fig. 57, page 149) and upheld by nuclear markers (Hypsa *et al.* 2002). This apparent phylogenetic signal is particularly interesting since *R. colombiensis* was initially misidentified as *R. prolixus* (Dujardin *et al.* 1999b). The head shape of *R. colombiensis* is clearly convergent to *R. prolixus* in this analysis and suggests that the trends observed in morphometric data of the head morphology maybe the result of homoplasies.

Phylogenetic relationships aside, the apparent inability of any population of *R. robustus* to adapt to life in houses is extremely interesting and the reasons for this are not clear. However, it is possible to theorise on the limiting factors involved: many silvatic species of triatomine bugs that require high levels of humidity, rarely establish domestic colonies and are notoriously difficult to culture in the laboratory, unless increased

humidity is maintained e.g. *Panstrongylus geniculatus*, *Psammolestes arturi* (D. Feliciangeli pers. Comm.); *R. robustus* and silvatic *R. ecuadoriensis* (F. Abad-Franch and M. A. Miles pers. comm.) Through most of its range *R. robustus* is restricted to humid tropical rainforest. Therefore it is possible that intolerence to low humidity is the factor that limits *R. robustus* to the highly humid microhabitat provided by palm trees and constrains it from adapting to exploit drier conditions, such as that found in houses. It is possible that Venezuelan *R. prolixus* and *R robustus* represent a derived lineage, this is consistent with phylogenetic data (Monteiro *et al.,* 2003), diverged from the ancestral Amazon clade and adapted to the drier conditions of the Venezuelan Llanos. This preadaptation to drier conditions, in turn predisposing them to domiciliation.

The most important inference that can be made from this pilot study is that domestic and silvatic populations are possibly interacting. This has serious implications for control of disease transmission; specifically for the study location in Portuguesa state, where sympatric domestic and silvatic populations occur. Further studies by Fitzpatrick (2005) using an extended sample of Venezuelan specimens have involved estimating population structure using an array of microsatellite loci. The results of that work indicate that there is panmixia among sympatric domestic and silvatic populations of *R. prolixus* in some localities. In light of these data the control strategy should be devised with contingency for reinvasion from silvatic bugs.

6.4.2 *R. ecuadoriensis* from Ecuador and Peru

The distinct variation in gross morphology of the *R. ecuadoriensis* geographic samples analysed here is supported by clear discrimination of all groups by head morphometrics (Table 27, page 159). Fairly good discrimination is also seen by wing morphometrics, the Peruvian sample being most distinct, with the remainder of the groups less clearly

discriminated; the Manabí sample demonstrating least cohesion and most error in reclassification (Table 27, page 159).

As demonstrated in the previous case study of Venezuelan *R. prolixus,* there is a lack of correspondence between the wing and head morphometrics, again the two morphologies clearly evolve independently. The partial least squares analysis does again reveal a significant axis of covariation for the two morphologies (table 29 and Fig. 67, page 164) but this seems to represent only the isometric trends among the groups separating large from small. In general, the head morphometric results relate well to ecological factors, The larger silvatic forms (Pichincha and Manabí), associated with cooler forest habitats, are distinguishable from the smaller domestic groups (El Oro, Loja and Peru) associated with warm, dry, non forested regions. Size variation associated with geographical and climatic factors, again appears to be in accordance with Bergmann's rule (see previous section on *R. prolixus*) i.e. large Pichincha bugs from Andean foothills; high altitude and cool; Manabí; intermediate in size from the warmer drier coastal region, and Loja, El Oro and Peruvian from yet warmer environments. The pattern of head shape also covaries with other patterns of morphological variation such as pigmentation, apparently in the role of camouflage (Abad-Franch 2003) (darker in silvatic populations and lighter in dry region domestic poulations). The congruence between ecological factors and head shape suggest that head shape may be under selective pressure, whereas wing shape variation does not correspond to ecological factors and may evolve mostly by random genetic drift.

This is supported by the analysis of *cytb* sequences, which correspond reasonably well with the pattern of wing shape variation (Fig.72, page 173). In particular, the Peruvian population, least similar by wing is also the most genetically divergent. Furthermore, the inclusion of outgroups *R. colombiensis* and *R. pallescens* in morphometric and genetic

analyses (see Figs 66, page 163 and Fig. 68, page 169) demonstrates a phylogenetic signal in wing shape extending to the interspecific level. The analyses also support the conspecific nature of the population samples considered here. Support for the usefulness of wing morphometrics in the assessment of population structure is also given by the correlation with geographical distances (table. 32, page 173). A diagram (Fig. 88, page 206) summarises the results of genetic and morphometric data in relation to the spatial arrangement of the populations sampled.

As in the *R. prolixus* study, wing shape also appears to be an indicator of genetic homogeneity. Three of the groups were composed of single haplotypes (Table. 30, page 167); El Oro, Pichincha, and Peru. Accordingly, these groups were most distinct, with 81%, 85% and 81% correct reclassification respectively. In comparison, Loja, was more heterogeneous (Table 30, page 167)

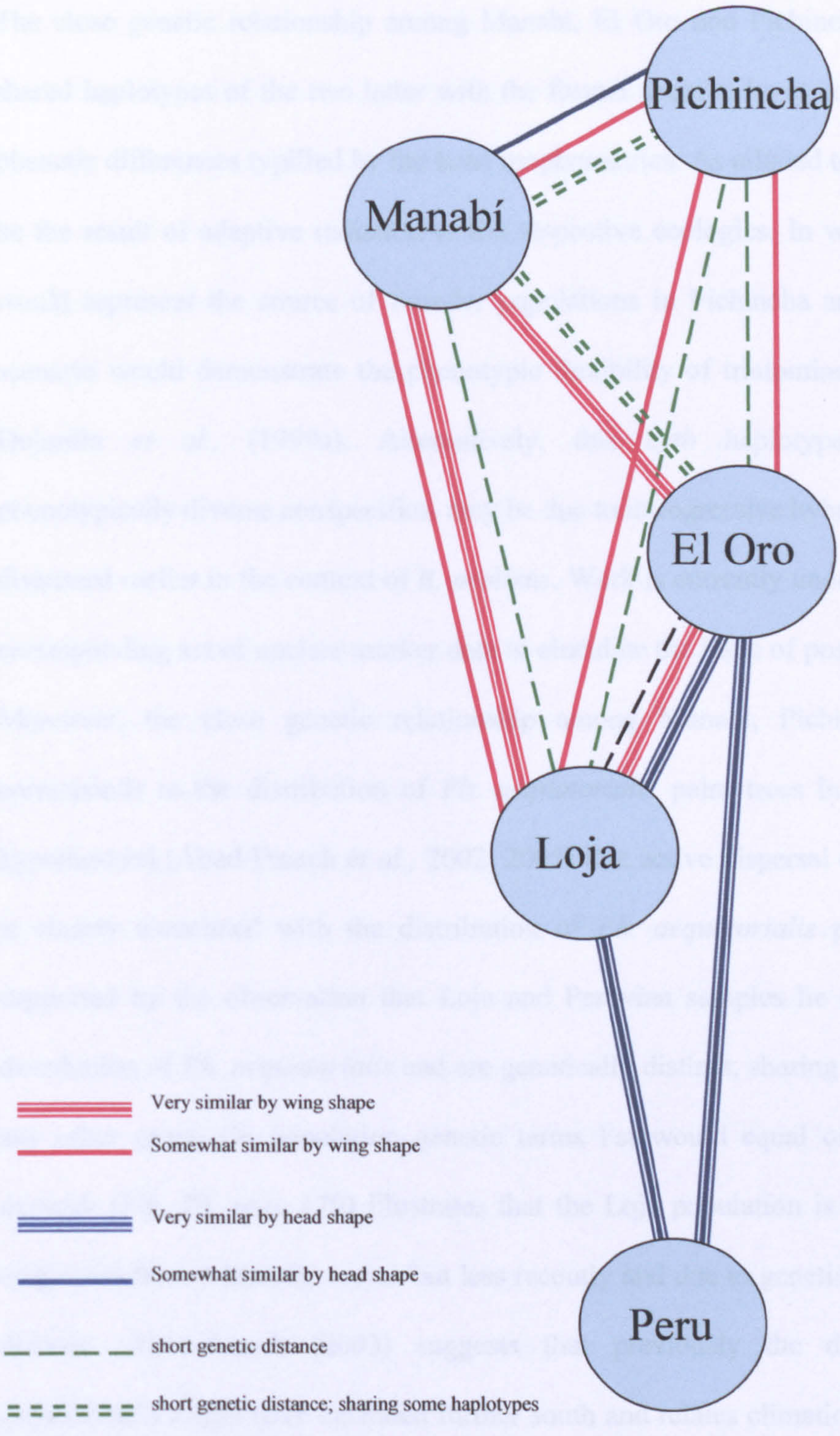

Figure 88. Affinities amongst populations of *Rhodnius ecuadoriensis*: A summary of morphometic and genetic results. The spatial arrangement of the groups represents the geographical distribution.

with 73% correct reclassification by wing, and Manabí, the most heterogenous genetically had only 53% correct reclassification.

The close genetic relationship among Manabí, El Oro and Pichincha samples due to shared haplotypes of the two latter with the former seem to be at odds with the strong phenetic differences typified by the head mophometrics. As alluded to above, this might be the result of adaptive radiation to the respective ecologies. In which case, Manabí would represent the source of founder populations in Pichincha and El Oro. Such a scenario would demonstrate the phenotypic flexibility of triatomines, as discussed by Dujardin *et al.*, (1999a). Alternatively, this *cytb* haplotype identity among phenotypically diverse conspecifics, may be due to introgressive hybridisation events, as discussed earlier in the context of *R. prolixus*. Work is currently underway to generate a corresponding set of nuclear marker data to elucidate the issue of possible introgression. Moreover, the close genetic relationship among Manabí, Pichincha and El Oro corresponds to the distribution of *Ph. aequatorialis* palm trees in Ecuador and it is hypothesised (Abad-Franch *et al.*, 2002, 2005) that active dispersal of *R. ecuadoriensis* is closely associated with the distribution of *Ph. aequatorialis* palm trees. This is supported by the observation that Loja and Peruvian samples lie beyond the current distribution of *Ph. aequatorialis* and are genetically distinct, sharing no haplotypes with any other group (In population genetic terms Fst would equal one). The haplotype network (Fig. 70, page 170) illustrates that the Loja population is also likely to have originated from a Manabí source but less recently and due to genetic drift is genetically discrete. Abad-Franch (2003) suggests that previously the distribution of *Ph. aequatorialis* might have extended further south and relates climatic vicariant events to episodic retreats in the distribution of *Ph. aequatorialis* palms resulting in the serial isolation of firstly the Peruvian (most genetically discrete with ~4% sequence divergence from other haplotypes, which applying the molecular clock (Brower 1994) implies a divergence date ~2 million years ago), and much more recently the Loja

population. The large genetic difference between Ecuadorian and Peruvian bugs is surprising, given the gross morphological (and head morphometric) similarity between Peruvian bugs and domestic Ecuadorian bugs from Loja and El Oro. The large genetic difference between Ecuadorian and Peruvian *R. ecuadoriensis* is supported by isoenzyme analyses (Chávez *et al.*, 1999 and Solano *et al.*, 1996). Therefore it seems certain that the Peruvian group converged morphologically with the domestic groups of Ecuador by parallel evolution. A report of *R. ecuadoriensis* captured from a hollow tree in northern Peru (Cuba Cuba *et al.* 2002) suggests that this might represent the ecotope which *R. ecuadoriensis* adapted in a warmer dry environment with the loss of palm trees, which in turn might have preadapted it for domiciliation.

This study, together with that of Fernando Abad-Franch (2003) highlights some important considerations for the control of vector populations in Ecuador and Peru. Firstly, genetically homogeneous domestic populations such as those in El Oro might be the result of a genetic bottle-neck, caused by several possible processes; either a residual population after habitat destruction or house spraying, the implication being either a recrudescence of a few survivors or reinvasion, of a single small founding population, either scenario presenting good prospects for control. Secondly, and in contrast, genetically heterogeneous domestic populations, like those sampled from Manabí and Loja, might represent populations in panmixia with silvatic bugs, in which case, vigilance should be heightened and contingency for reinvasion from silvatic sources considered.

6.4.3 *T. infestans* from Paraguay

Discriminant analysis of Paraguayan *T. infestans* samples examined here by morphometrics of wing and head did not show as extreme differences among groups as those observed for the previous two examples of *Rhodnius spp.* Also in contrast to the

previous two examples, there is congruence between wing and head morphometric analyses (see Fig. 85, page 196 & Table 40, page 195); the silvatic sample from the Chaco (CHA-S) was the most distinct single group. Additionally, the two oriental groups (COR and PAR) separate well together from the occidental Chaco population samples (see Fig. 78, page 186), this is further supported by the partial least squares analysis of morphological covariation. The overall agreement in the direction of variation of these two separate morphological modules suggests that they may represent trends due to genetic drift rather than adaptation to specific environmental factors. Moreover, in comparison to the two *Rhodnius* studies presented here, only one of the samples of *T. infestans* was silvatic, albeit coming from natural ecology not dissimilar in constituents to wattle and daub houses from which domestic samples are typically collected. Therefore, this comparative lack in habitat variation may account for the correlated variation in head and wing shape, without the apparent adaptive radiation of head shape observed in the examples of *Rhodnius spp.* Also, large differences in size are not observed for these conspecifics, contrary to the *Rhodnius spp.* examples, and so there are no large allometric trends in head shape. In accordance with the previous two case studies distinctiveness of wing shape is observed despite apparent genetic homogeneity. i.e. the oriental group (COR PAR, together 75% correctly reclassified) and CHA-S (60% correctly reclassified) have no detectable genetic variation (see Table 38, page 191). This is a further example of the facility of wing morphometrics in the detection of populations derived from genetic bottlenecks, and as such genetically isolated, implying low rates of recruitment/invasion and therefore identifying good targets for control.

Studies using sequences of rDNA internal transcribed spacer genes 1 and 2 (ITS-1, ITS-2) have not revealed an appreciable amount of genetic structure within *T. infestans* in

Paraguay (Marcilla *et al.*, 2000, Bargues *et al.*, 2006). In light of the genetic variation in mitochondrial DNA demonstrated here it seems that ITS genes do not mutate at a rate sufficient to make them informative population genetic markers, at least in this case

The phylogeny presented by Bargues *et al.*, (2006) suggests that *T. platensis* and *T. delpontei* are valid species; this is supported by morphometrics of head and wing (Fig. 79, page. 187). However, the *cytb* haplotype isolated here from a Paraguayan *T. platensis* lies well within the intraspecific genetic diversity of *T. infestans* (see Fig. 81, page 193). This could well be another example of introgressive hybridisation. More generally, there is agreement between the nuclear and mitochondrial DNA evidence, both of which subdivide *T. infestans* into two well suported clades; Andean and lowland (see Fig. 89, page 211). However, it remains unclear where the common ancestor originated, from the Chaco and adapting to the highlands or conversely originating in the Bolivian Andes and dispersing to the arid lowlands (Fig. 89, page 211).

Previous work also using *cytb* sequences (Monteiro *et al.* 1999b) included small samples from Argentina, Brazil and Bolivia. That study demonstrated distinctiveness and diversity of Bolivian samples (referred to here as BOL-A and BOL-B), with apparent homogeneity across Brazil and Argentina (identical to haplotype A isolated here), except for a further haplotype from Brazil, differing by a single nucleotide, and also isolated from *T. melanosoma* (a melanic morph, eventually synonymised by Gumiel *et al.*, 2003) (see Fig 81, page 191 and Fig. 82, page 193). Haplotypes B, C and D isolated here were not reported by Monteiro *et al.*, (1999b) and were isolated only from the domestic samples from the Chaco (CHA-D CHA-PD). Genetic diversity within these sympatric samples was high and they were not well discriminated by the morphometrics, in particular wing shape showed a large degree of overlap (see Fig. 85,

page 196 and Table 40, page 195). The differences in the haplotype diversity between the samples shows a

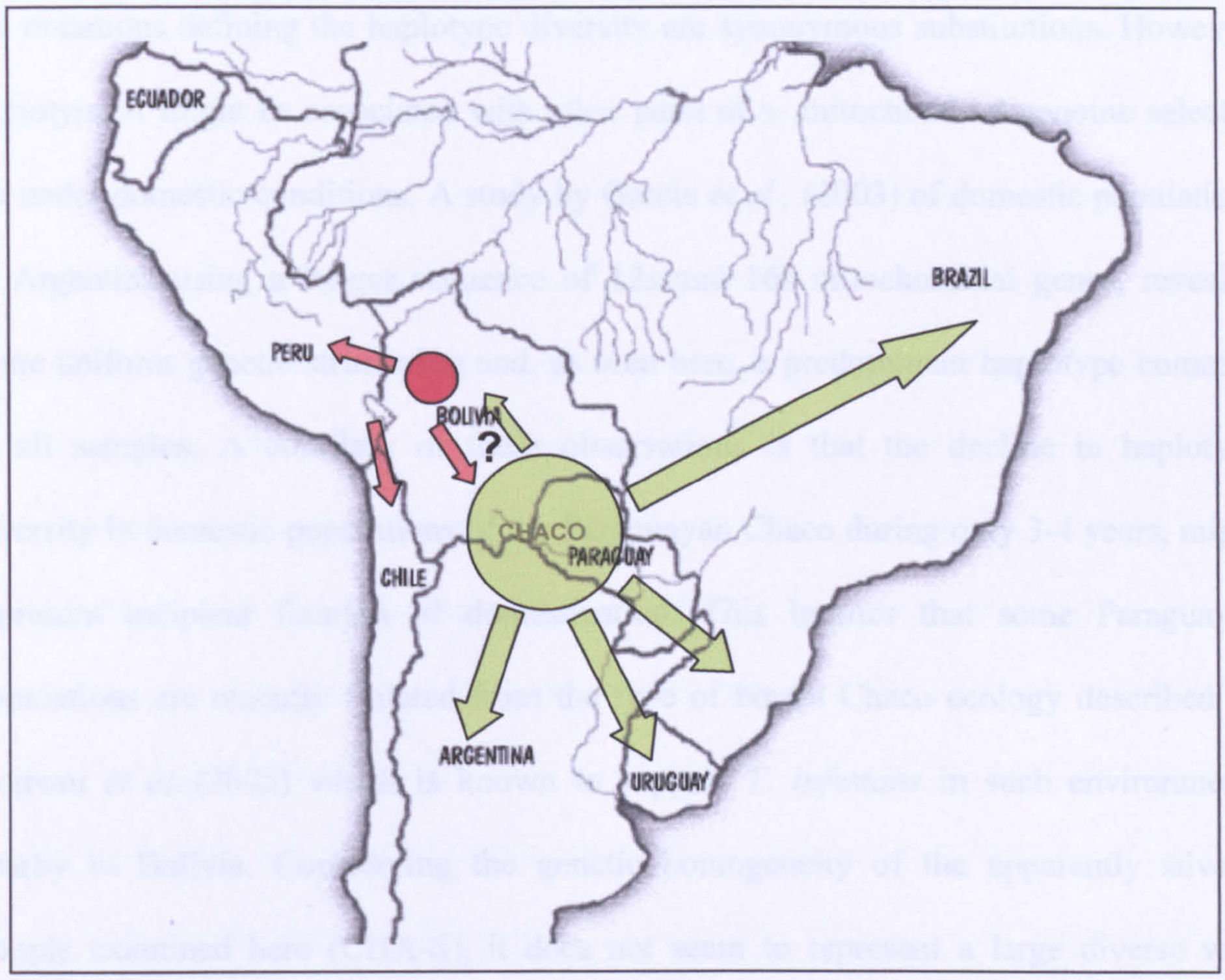

Figure 89. Map illustrating the phylogeography of *T. infestans* inferred from the results of Monteiro *et al.,* (1999) and Bargues *et al.,*(2006).The Andean clade is indicated in red, originating in Bolivia and the lowland clade is shown in green.

temporal decline, CHA-D collected 3-4 years after the collection of CHA-PD has lost Haplotype C and is mostly composed of haplotype A. This decrease in heterogeneity is apparently due to a genetic bottleneck, which might be attributable to sequential control efforts. However, the observation might be an artefact due to relatively small sample sizes and larger samples would have to be analysed to be able to assert this with confidence. However, the increase in the prevalence of Haplotype A is interesting, particularly when one considers that it appears to be the typical domestic genotype, homogeneously prevalent in Southern Paraguay (COR and PAR) and through geographically diverse regions of Brazil and Argentina (Monteiro *et al.,* 1999b). This

apparent selection for mtDNA seems unusual, but it is not unprecedented (Malhotra & Thorpe, 1994). The selection is apparently unrelated to the *cytb* gene specifically, as all the mutations defining the haplotype diversity are synonymous substitutions. However, haplotype A might be associated with other parts of a mitochondrial genome selected for under domestic conditions. A study by Garcia *et al.*, (2003) of domestic populations in Argentina using a longer sequence of 12s and 16s mitochondrial genes, revealed some uniform genetic structuring and, as seen here, a predominant haplotype common to all samples. A corollary of these observations is that the decline in haplotype diversity in domestic populations of the Paraguayan Chaco during only 3-4 years, might represent incipient fixation of domestication. This implies that some Paraguayan populations are recently isolated from the type of boreal Chaco ecology described by Noireau *et al.*,(2005) which is known to support *T. infestans* in such environments nearby in Bolivia. Considering the genetic homogeneity of the apparently silvatic sample examined here (CHA-S), it does not seem to represent a large diverse wild population. It might therefore represent a small colony, founded by a few individuals of domestic origin. This seems reasonable given the proximity of settlements and the similarity of the particular wild habitat to the dwellings themselves.

Clearly more work is needed to fully assess the extent to which domestic populations in the Chaco (including regions of Argentina Bolivia and Paraguay) are in isolation from silvatic populations. Prospects for achieving this using population genetics looks good, particularly given the recent development of microsatellite markers for *T. infestans* by Marcet *et al.*, (2006).

7 Evolution of head shape

Overall there seems to be a trend for congruence between wing morphometric data and mitochondrial gene data. In contrast, head shape seems to be generally far more variable and in most cases, appears to be relatively more plastic or under more rigorous selective pressure than wings. The clearest example of this is seen in the case of *R. ecuadoriensis*; the large Pichincha form departs greatly in head shape from other geographical samples despite having similar wing shape and shared mitochondrial haplotypes.

A general observation is that head shape in triatomines varies consistently according to size in a particular direction; i.e. large individuals/species have relatively elongate heads. Among the studies presented here this phenomenon is observed to occur intraspecifically, interspecifically and intergenerically. This was tested for across a representative sample of the subfamily by analysing the relationship between the ratio of head length to width (head shape) and total body length of 47 species (Fig.90). Head shape does not appear to simply correspond to specific ecological factors, such as ecotope. For example, both *R. prolixus* and *R. robustus* occupy similar palm habitats, but have strongly divergent head shapes.

I present here a theory for the evolutionary processes that are largely involved in determining the observed variation in head shape among Triatominae. As stated, the primary factor is size; across most of the subfamily relative size correlates with head shape i.e. large body size is associated with an elongated head shape (Fig 90) whereas small body size is associated with a relatively compact stout head. This allometric trend has been observed in all the studies presented here. A reason for this can be suggested along the following lines. Triatomines are far larger than most other blood feeding insects groups. Comparatively, other blood feeding groups have compact heads and mouthparts that, in part, (usually the labrum)

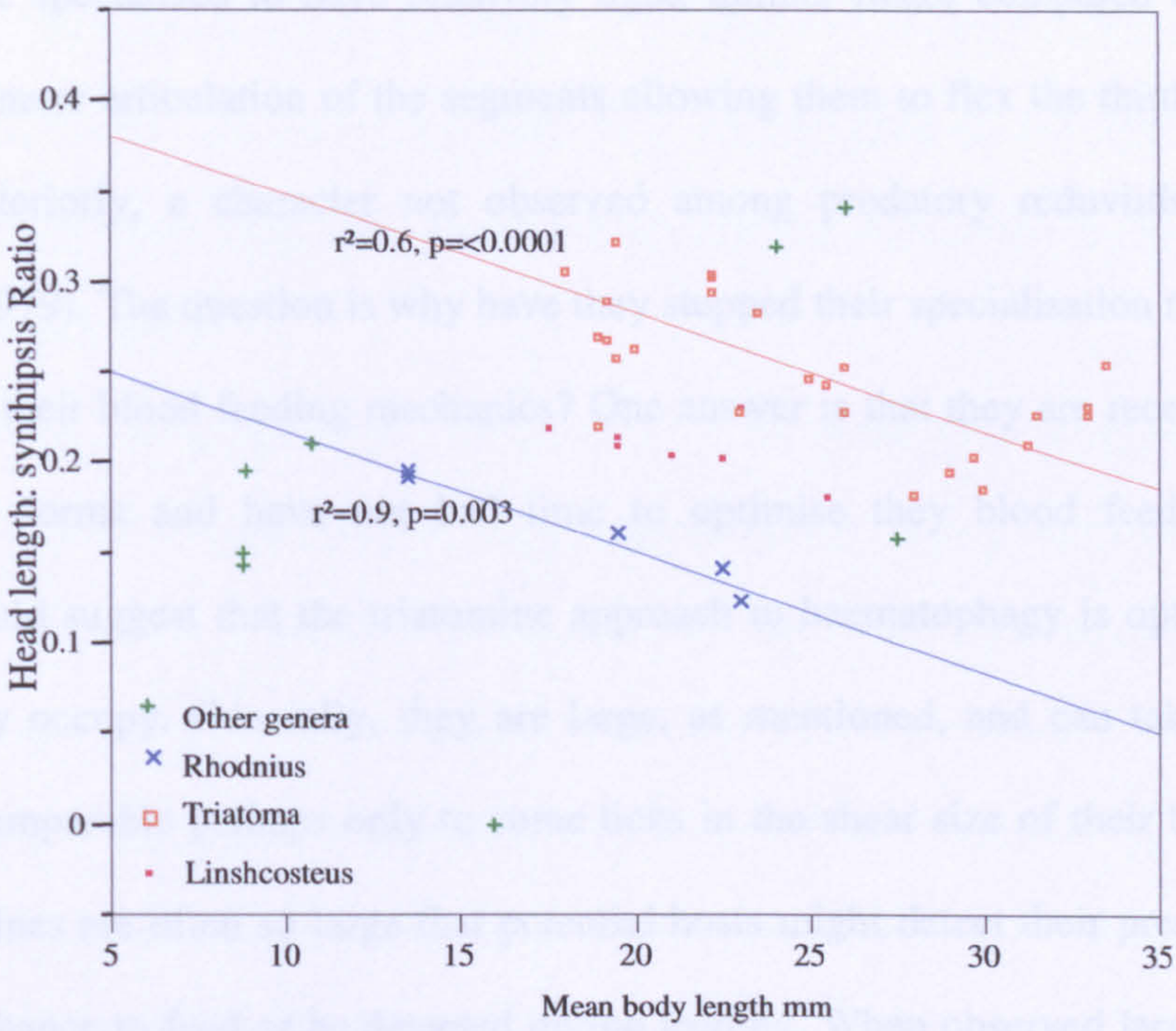

Figure 90. Plot showing relationship between head shape and body length. Head shape is represented as the ratio of head length to width (synthipsis= distance between eyes). The graph shows regression lines for *Triatoma* (red) and *Rhodnius* (blue). Data points represent species (47 in total)

are folded to "unsheathe" the penetrating maxillae and mandibles (the stylets). For a full comparative exposition on the comparative mouthparts of blood feeding insect groups see Lehane (2005). Suffice is to say that the manner in which triatomines feed is a little unusual. Triatomines, like another haematophagous group of Hemiptera, the bedbugs, have a three segmented labrum (rostrum). The bedbugs (family Cimicidae), are thought to be more derived, specialised bloodfeeders than triatomines (Schofield 2000). The Cimicidae feed like many phytophagous Hemiptera and many other vessel feeding haematophagous groups; i.e. by the previously mentioned unsheathing of the penetrative stylets. In contrast, triatomines have inherited a heavily sclerotised labrum from their predatory ancestors. Indeed, predatory reduviid groups have less facility to articulate their rostral segments and in some groups the rostrum functions as a raptorial apparatus first and mouthparts second. This pre-adaptive

history has given the triatomines a tool kit perhaps not optimal for blood feeding. However, triatomines have specialised to have relatively light, thinner rostra compared to predatory reduviids, with more articulation of the segments allowing them to flex the third segment or the rostrum anteriorly, a character not observed among predatory reduviids (Lent and Wygodzinsky 1979). The question is why have they stopped their specialisation there and not further adapted their blood feeding mechanics? One answer is that they are recently derived from predatory forms and have not had time to optimise they blood feeding facility. However, I would suggest that the triatomine approach to haematophagy is optimal for the niches that they occupy. Generally, they are large, as mentioned, and can take enormous blood meals, comparable perhaps only to some ticks in the shear size of their blood meals. Indeed, triatomines are often so large that potential hosts might detect their presence before they have the chance to feed or be detected during feeding. When observed large species of triatomines tend to blood feed while standing on the ground or a wall rather than ectoparasitically (standing/holding on to the host). Clearly such a strategy benefits from having an elongate head and long rostrum with which to reach through the pelage of the host. A corollary of this feeding strategy is that triatomines have followed a predominantly k strategy evolutionary path of carefully acquiring their blood meals by avoiding host alarm by keeping host contact to the minimum (i.e. with their mouthparts only), whilst at the same time maintaining large body sizes in general that allow for fewer bloodmeals.

This involves less risk while producing few, well developed offspring. Also, large body size can promote survival by allowing for longer periods without feeding. Conversely triatomines with small heads and small light bodies may, more safely enjoy a closer association with their hosts. Species like *Triatoma protracta, Paratriatoma hirsuta* and *Psammolestes spp.*,

occupy nests. Their heads are relaxed from the constraint of needing to reach through the pelage and they behave relatively ectoparasitically. Their short heads and short rostrums are less mechanically demanding, and in the continually/frequently occupied nests that they inhabit they feed regularly.

A further factor acting upon the evolution of head shape is stridulatory behaviour (Stridulation is the act of producing sound by rubbing together certain body parts. In the case of reduviids the sounds is produced by drawing the tip of the rostrum across a striated "stridulatory groove" or sulcus position on the ventral side of the thorax). Mechanistically this is reliant upon the rostrum being sufficiently long to reach the stridulatory sulcus on the ventral side of the thorax. Stridulation is an alarm mechanism shared with many predatory reduviids. To demonstrate the functional constraint of stridulation upon head shape and mouthpart evolution I have conducted an analysis of the relationship between head length and rostrum length (Fig. 91).

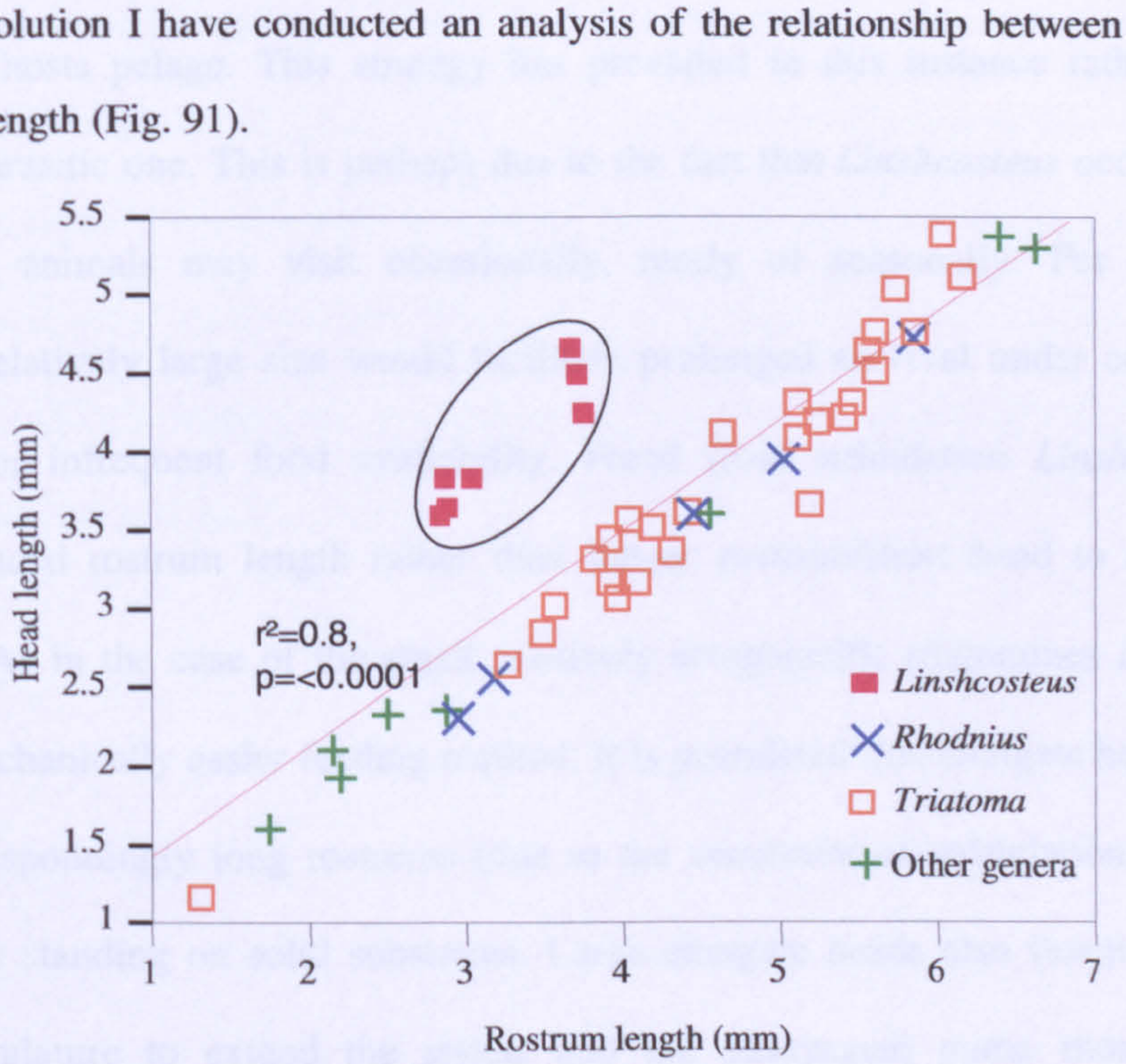

Figure 91. Analysis of the relationship between head length and rostrum length for Triatominae genera (47 species represented). Each data point represents a species average.

There is an almost constant 1:1 relationship between the two structures across the subfamily, with one exception; the genus *Linshcosteus*. *Linshcosteus* has a rostrum considerably shorter than its head and has a vestigial, non-striated stridulatory sulcus, and presumably does not stridulate. The cause for this departure from the normal condition is not clear. However, the cause is likely to be attributable to the specific ecology of *Linshcosteus spp.*, which is not shared with any other triatomine group i.e. rocky habitats in India. A possible evolutionary process is that the ecology in India presented a reduced threat from predators, relaxing the selective advantage of stridulation and subsequently resulting in selection for a short rostrum (not required to equal or surpass the head in length for stridulation) and elongate head. The maintenance of the elongate head is perhaps related to not standing on the host's body during feeding as described above. Moreover, by maintaining a long narrow head despite shortened mouthparts allows for the continuation of the strategy of feeding at a distance, and penetrating the hosts pelage. This strategy has prevailed in this instance rather than the relatively ectoparasitic one. This is perhaps due to the fact that *Linshcosteus* occupies rocky habitats, which animals may visit occasionally, rarely or seasonally. For this reason maintaining a relatively large size would facilitate prolonged survival under conditions of unreliable and/or infrequent food availability. Freed from stridulation *Linshcosteus* has favoured a reduced rostrum length rather than longer rostrum/short head to maintain its "reach", why? As in the case of the small relatively ectoparasitic triatomines *Linshcosteus* may attain a mechanically easier feeding method. It is postulated that elongate heads of large bugs with correspondingly long rostrums (due to the constraint of stridulation) tend to be cautious feeders standing on solid substrates. Large elongate heads also function to house sufficient musculature to extend the stylets and the pharyngeal pump muscles, which

according to Insausti (1994) occupy much of the head cavity. In particular, elongation promotes longer tendons and musculature for protrusion of mouthparts without folding the rigid rostrum, and the pharyngeal pump musculature can conceivably attain sufficient pressure with less frequent, longer waves of contraction along the head during feeding, thereby avoiding fatigue and prolonging feeding time. This is an issue as the terminal diameter of the feeding tube formed by the mouthparts is constrained not to exceed 8-10 μm in diameter. This is thought to be due to the trade off between keeping the terminal diameter small and inflicting less pain as opposed to a wider diameter that would reduce feeding time but possibly inflict more pain and disturb the host (Lehane 2005). It follows that the heads of small relatively ectoparasitic triatomines are, with some exceptions that will be dealt with later, relatively compact in shape. Less musculature is needed for a smaller blood meal, which may be acquired more quickly. A short reach to the skin, requires only a short (less mechanically demanding) feeding system i.e. short rostrum with short compact head. Moreover, the determinants of head shape evolution are the characteristics of particular niches, most prominently the availability of hosts. In general terms, triatomines are relatively sedentary, opportunistic bloodfeeders. They occupy a varied niche, ranging from close association with habitual nesting animals through to the sporadic opportunity of feeding from a mammal or bird which is seeking shelter .

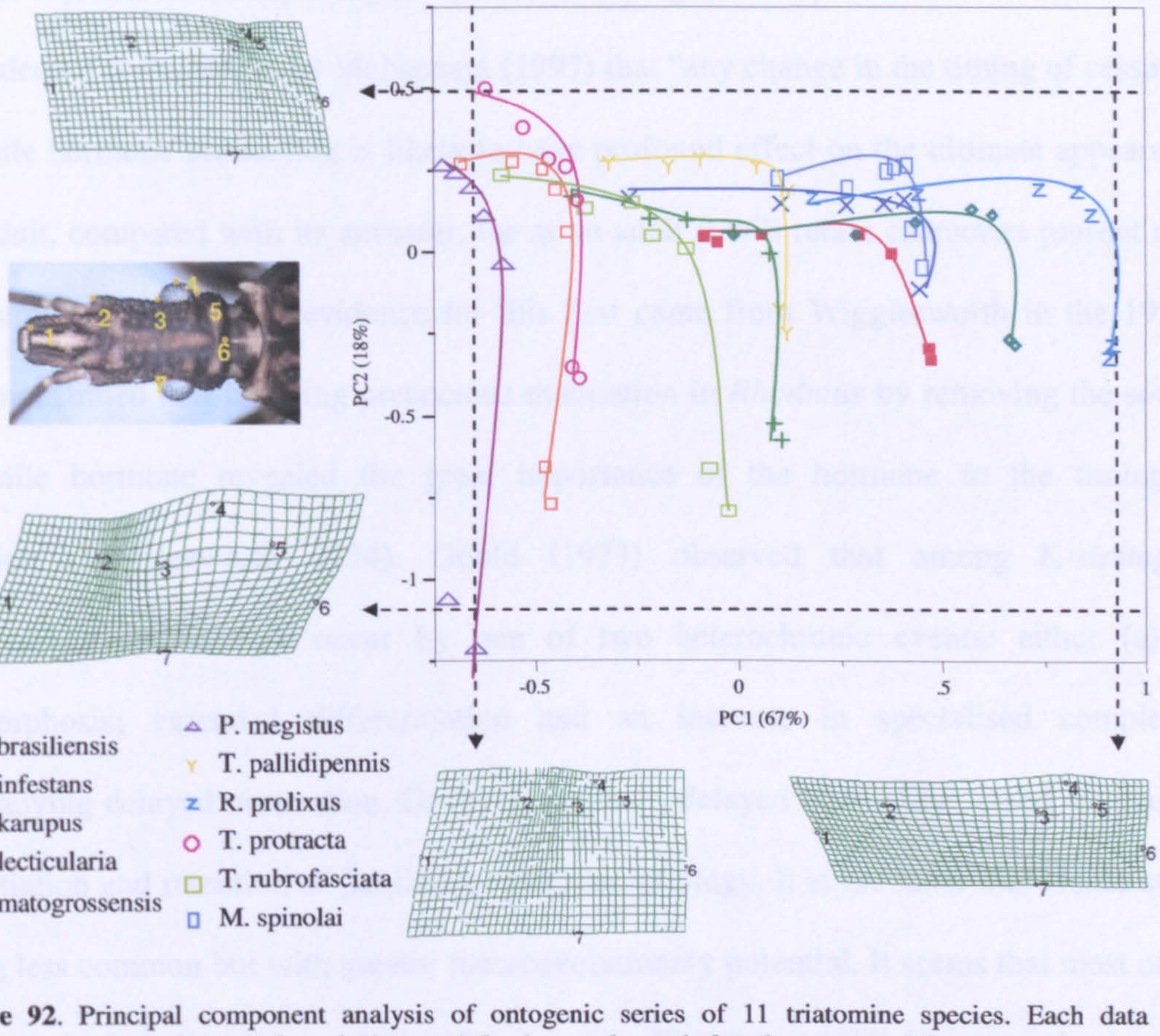

Figure 92. Principal component analysis of ontogenic series of 11 triatomine species. Each data point represents a group mean of each instar 1-5 plus male and female groups (10 specimens per stage). Transformation grids correspond to the shape changes associated with the extremes of the Principal component axes, as indicated by dashed lines and arrows. Lines are draw to fit the ontogenic trajectories.

This theory of head shape evolution can be extended to include the comparative ontogenic trajectories of different species. In an analysis of 11 species representative of 5 genera (Fig. 92) there is a clear pattern of positive allometry for head shape change within the life history of all species examined, i.e. from small and compact in early instars to large and elongate in the later instars and adults. This is represented by the shape change associated with PC1, accounting for 67% of variation (Fig. 92).

This allometric trend observed for all species examined recalls that observed among species. It seems to follow that in the early stages of development young instars of all species are optimally adapted to follow the "ectoparasitic" mode of feeding. In the context of

heterochrony the rate and extent of allometry can be of macroevolutionary significance (Gould 1977). It is this morphological flexibility through development that selection can act upon. Indeed it is suggested by McNamara (1997) that "any change in the timing of cessation of juvenile hormone production is likely to have profound effect on the ultimate appearance of the adult, compared with its ancestor, for as an adult it will retain characters present only in ancestral juveniles". The evidence for this first came from Wigglesworth in the 1930s, who demonstrated that inducing precocious maturation in *Rhodnius* by removing the source of juvenile hormone revealed the great importance of the hormone to the timing of maturation (Wigglesworth 1934). Gould (1977) observed that among K-strategists macroevolutionary changes occur by one of two heterochronic events: either (a) by hypermorphosis; extended differentiation and an increase in specialised complexity accompanying delayed maturation. Or (b) by neoteny; delayed maturation linked to retarded differentiation and retention of flexible juvenile morphology. It is the latter that Gould states as being less common but with greater macroevolutionary potential. It seems that most of the triatomines included in this analysis of ontogenic allometry exhibit hypermorphosis; with specialised head shapes as adults with long trajectories through the shape space. *Triatoma protracta* and *Mepraia spinolai* stand out a little as having rather shorter trajectories and may represent relatively neotenically derived species. *T. protracta* in particular varies little along PC1 from 1st instar to adult. This region of the shape space also coincides with many other juvenile Triatomini and may represent the ancestral head shape of the tribe.

8 Summary of Conclusions

Morphometrics and phylogeny of the Old World and New World Triatominae: patterns of parallel and divergent morphological evolution

- ***T. rubrofasciata* is homogenous:** Diversity among mitochondrial gene haplotypes from geographically disparate populations of *T. rubrofasciata* is well within the level of intraspecific variation observed for other triatomine species. This confirms the single species status for *T. rubrofasciata* and as a snapshot of population structure suggests that the global populations are relatively panmictic, supporting the hypothesis that they have dispersed passively and recently in association with shipping.
- **North American and Old World *Triatoma* demonstrate morphological convergence:** The morphometric similarities between *T. rubrofasciata* and the North and Central American species, particularly *T. rubida*, with less similarity to South American species of *Triatoma* have been revealed by the molecular analyses of mt-DNA and n-DNA to be affected by processes of parallel evolution and allopatric convergence.
- **Consistency in patterns of morphological covariation may be used to infer phylogenetic associations:** Partial least squares analysis revealed that patterns of covariation in head and wing shape were more variable between *T. rubida* and *T. rubrofasciata* compared to patterns seen between closely related species. Coupled with phylogenetic data, this reveals the potential of the partial least squares method for detecting discontinuous patterns of morphological evolution in morphometric studies.
- **Old World *Triatoma* and *Linshcosteus* have New World origins:** On the basis of the molecular evidence presented here and estimates of divergence dates it

seems likely that the Old World Triatominae originated as a result of ancestral American stock migrating across the Bering land bridge (BLB) in the warm Eocene ~30 MYA. This period corresponds to the appearance of the first modern mammals (including bats) and with the formation of the Himalayas. Therefore it seems reasonable to suggest that isolation of Old World lineages in India gave rise to *Linshcosteus* and subsequent limited dispersal of the Old World lineage from the Indian subcontinent gave rise to *T. rubrofasciata* and other Old World *Triatoma.*

- ***Linshcosteus* emerged as a result of radical morphological divergence:** In contrast, to the parallel evolution and convergence of head shape of North American and Old World *Triatoma, Linshcosteus* appears to have undergone a process of radical morphological divergence. Such processes of discontinuous morphological evolution, or type switching, are often only detectable by molecular methods. It seems that *Linshcosteus* adapted to exploit a novel ecological niche, which triggered its morphological diversification.
- **Patterns of wings shape variation corresponds to neutrally evolving molecular markers:** The demonstration of the phylogenetic signal in wing landmark data by correlation to genetic distances highlights the facility of morphometrics to detect conserved morphology that has evolved relatively neutrally.

Higher taxonomic relationships within the Triatominae and to other reduviid subfamilies: support for a polyphyletic origin of haematophagy within the Reduviidae.

- **Triatominae are polyphyletic:** The weight of evidence presented supports a polyphylectic origin for blood-feeding for the Triatominae. The apparent

independent development of blood feeding among the main lineages of the Triatominae represented by the genera *Triatoma* and *Rhodnius* highlights a fundamental biological difference among important vector species. This difference is likely to become evident when triatomine genome sequences become available and are applied to studies of vector/parasite interactions. Moreover, it highlights the importance of sequencing genomes from different vector genera.

- **Reduviids emerged in the Cretaceous in association with the emergence of flowing plants and many modern plant-associated insect groups:** 28S r-DNA dating indicated that most reduviid subfamilies assessed here diverged at around the same time, from 125-80 MYA. This corresponds to the date of earliest known reduviid fossil from the lower Cretaceous (Hong 1987) and the advent of the (flowering plants). The radiation of the angiopsperms was the cause/effect of contemporaneous radiation and emergence of many insect groups that coevolved mainly as pollinators or phytophages (Grimaldi & Engel 2005). Reduviidae responded at the next trophic level, apparently diversifying to exploit the predatory niches defined by the new plant-insect associations.
- **Haematophagous lineages of reduviids diverged in the late Cretaceous and haematophagy later emerged in associations with modern mammals:** Dating estimates suggest that the lineages that led to the Triatominae diverged in the late Cretaceous/ Palaeocene/ Eocene, diverging from one another 70-60 MYA, with *Microtriatoma* (Bolboderini) branching off earlier and Triatomini and Rhodniini diverging 50-60 MYA. For the Triatomini we have observed that they diverged from a predatory lineage (the Reduviinae) ~30 MYA and

radiated into haematophagous genera, coinciding with the emergence of modern mammals such as bats and other nest building mammals. It seems that this was the optimal time for the comparatively sedentary reduviids to adapt to haematophagy in some lineages. This is also the time period put forward as a possible date of divergence for lineages of *T. cruzi* (Kawasshita 2001).

Comparative analyses of vector species (*R. prolixus, R. ecuadoriensis* & *T. infestans*)

- **Wing shape is better than head shape for assessing population structure:** The results presented suggest that head shape variation is subject to morphological plasticity and/or selective pressure and functional constraint and does not correlate well with phylogenetic signals. However, wing shape appears to vary in a relatively neutral way in all examples and is congruent with the patterns inferred from sequence analysis. Consequently, I would recommend that wing shape and not head shape be used in morphometric assessments of population dynamics. I would also assert that if population structure is suggested by morphometrics, it should ideally be followed by intensive population genetic analysis. Thus morphometrics can be used as a tool for surveillance to identify areas that require more in-depth investigation.

- **Mitochondrial DNA sequences might not always be sufficiently polymorphic to resolve population structure at a level relevant to epidemiological surveillance.** Despite the indisputable power and relevance of the molecular approach, identity and general lack of heterogeneity among mitochondrial DNA haplotypes across geographical regions for important vectors such as *T. infestans* and *R. prolixus* suggests that sequences of <1 kb may not give a sufficiently high

resolution estimate of population dynamics to be of epidemiological significance. In all circumstances microsatellite analysis may provide an alternative approach.

- **Wing morphometry distinguishes samples of limited genetic diversity:** Genetically homogeneous populations consistently show distinctiveness by wing morphometry; e.g. the Lara sample of *R. prolixus*, Peru sample of *R. ecuadoriensis* and COR and PAR samples of *T. infestans*. These differences seem to be due to founder effects. These observations reveal the apparent usefulness of wing morphometrics for discrimination of genetically homogeneous populations. These apparent subtle founder effects could be used to detect populations derived from small isolated populations. In the context of control, this could constitute an important tool for the assessment of whether infestations are due to reinvasion or to recrudescence of survivors of spraying.

Evolution of Head shape

- **Head shape is strongly modulated by body size and feeding strategy:** Analysis of head shape variation among triatomines and by comparison of head shape through ontogeny reveals that head shape evolution is functionally contrained. A general observation is that head shape in triatomines varies consistently according to size in a particular direction; i.e. large individuals/species have relatively elongate heads. I have related this observation to feeding strategy and the potential fitness costs driving selection of head shape.

9 Future Work

- **Quantitative genetics**: The application of morphometrics continues to rest on some assumptions that could be elucidated by empirical studies to ascertain how much shape variation is attributable to environment. This issue could be addressed using quantitative genetic approaches to measure the additive genetic variance and give a measure of phenotypic heritability, i.e. of wing or head shape. Such an approach has been applied to study natural populations of *Drosophila* (Marsola Moraes & Melo Sene, 2004).
- **Population genetics:** Comparative studies of wing morphometrics in concert with, high resolution, population genetic analyses (using microsatellite markers) are needed to further test the application of morphometrics in the study of population structure. A comparison of instances where gene flow is proved or where it is disproved would be most informative.
- **Molecular phylogenetics:** Inclusion of more taxa, representing more reduviid and triatomine groups is required to elucidate the extent of polyphyly within the Triatominae and among the other subfamilies.

10 References

Abad-Franch, F. (2003). The ecology and genetics of Chagas disease vectors in Ecuador, with emphasis on `*Rhodnius ecuadoriensis'* (Triatominae). Thesis (PhD) University of London.

Abad-Franch, F. and F.A. Monteiro (2005). Molecular research and the control of Chagas disease vectors. *Anais Da Academia Brasileira De Ciencias,* **77,** 437-454.

Abad-Franch, F. and V.H.M. Aguilar (2000). Control de la enfermedad de Chagas en el Ecuador. Datos y reflexiones para una política de Estado. *Revista del Instituto Juan César García,* **25**, 12-32.

Abad-Franch, F., Aguilar, H.M., Paucar, A., Lorosa, E.S. and F. Noireau (2002). Observations on the domestic ecology of *Rhodnius ecuadoriensis* (Triatominae). *Memorias Do Instituto Oswaldo Cruz,* **97,** 199-202.

Abad-Franch, F., Noireau, F., Paucar, A., Aguilar, H.M., Carpio, C. and J. Racines (2000). The use of live-bait traps for the study of sylvatic *Rhodnius* populations (Hemiptera: Reduviidae) in palm trees. *Transactions of the Royal Society of Tropical Medicine and Hygiene,* **94**, 629-630.

Abad-Franch, F., Palomeque, F.S., Aguilar, H.M. and M.A. Miles (2005). Field ecology of sylvatic *Rhodnius populations* (Heteroptera, Triatominae): risk factors for palm tree infestation in western Ecuador. *Tropical Medicine and International Health,* **10** (12), 1258-1266.

Abad-Franch, F., Paucar, C.A., Carpio, C.C., Cuba Cuba, C.A., Aguilar, V.H.M. and M.A. Miles (2001). Biogeography of Triatominae (Hemiptera: Reduviidae) in Ecuador: implications for the design of control strategies. *Memórias do Instituto Oswaldo Cruz,* **96,** 611-620.

Aguilar, V.H.M., Abad-Franch, F., Guevara, A.G., Racines, V.J., Briones, L.A. and L.V. Reyes (2001). *Guía operacional para el control de la enfermedad de Chagas en el*

Ecuador. FASBASE–Ministerio de Salud Pública del Ecuador, Quito, Ecuador, 40 pp.

Aguilar, V.H.M., Abad-Franch, F., Racines, V.J. and C.A. Paucar (1999). Epidemiology of Chagas disease in Ecuador. A brief review. *Memórias do Instituto Oswaldo Cruz*, **94** (Suppl. 1), 387-393.

Ambrose, D. P. (1999). Assassin bugs, Science Publishers, Enfield, UK.

Ambrose, D.P. (2003). Biocontrol potential of assassin bugs (Hemiptera: Reduviidae) *Journal of Experimental Zoology, India*, **6**, 1-44.

Amino, R., Martins, R.M., Procopio, J., Hirata, I.Y., Juliano, M.A., and S. Schenkman (2002). Trialysin, a novel pore-forming protein from saliva of hematophagous insects activated by limited proteolysis. *The Journal of Biological Chemistry,* **277,** 6207-6213.

Anderson, J.M., Lai, J.E., Dotson, E.M., Cordon-Rosales, C., Ponce, C., Norris, D.E. and C.B. Beard (2002). Identification and characterization of microsatellite markers in the Chagas disease vector *Triatoma dimidiata. Infection, Genetics & Evolution,* **1** (3), 243-258

Andersson L. (1990). The driving force: Species concepts and ecology. *Taxon,* **39**, 375-382.

Avise JC (1994). *Molecular markers, natural history and evolution*. Chapman & Hall, New York, USA, 511 pp.

Barata J.M. (1998). Macroscopic and exochorial structures of Triatominae eggs, in (Carcavallo R.U., Galíndez Girón I., Jurberg J. and H. Lent eds.) *Atlas of Chagas disease vectors in the Americas*, Vol. II, Editora FIOCRUZ, Rio de Janeiro, Brazil, pp. 409-448.

Barata J.M.S. (1996). Aspectos morfológicos de ovos de Triatominae, in (Schofield, C.J., Dujardin, J.P and J. Jurberg eds.) *Proceedings of the International Workshop on Population Genetics and Control of Triatominae, Santo Domingo de los Colorados, Ecuador, Sept. 1995.* INDRE, Mexico City, Mexico, pp. 55-58.

Bargues, M.D., Klisiowicz, D.R., Panzera, F., Noireau, F., Marcilla, A., Perez, R., Rojas, M.G., O'Connor, J.E., Gonzalez-Candelas, F., Galvao, C., Jurberg, J., Carcavallo, R.U.,

Dujardin, J.P. and S. Mas-Coma (2006). Origin and phylogeography of the Chagas disease main vector *Triatoma infestans* based on nuclear rDNA sequences and genome size. *Infection, Genetics and Evolution,* **6** (1), 46-62.

Bargues, M.D., Marcilla, J.A., Ramsey, J., Dujardin, J.P., Schofield, C.J. and S. Mas-Coma (2000). RDNA-based molecular clock of the evolution of Triatominae (Hemiptera: Reduviidae), vectors of Chagas disease. Poster, *The Trypanosome Evolution Workshop, University of Exeter -London School of Hygiene and Tropical Medicine*, London, UK, February 2000.

Barrett, T.V. (1996). Species interfertility and crossing experiments in triatomine systematics, in (Schofield, C.J., Dujardin, J.P. and J. Jurberg eds.) *Proceedings of the International Workshop on Population Genetics and Control of Triatominae, Santo Domingo de los Colorados, Ecuador, Sept. 1995.* INDRE, Mexico City, Mexico, pp. 72-77.

Beard, C.B., Cordon-Rosales, C., and R.V. Durvasula (2002). Bacterial symbionts of the triatominae and their potential use in control of Chagas disease transmission. *Annual Review of Entomology,* **47,** 123-141.

Beard, C.B., Pye, G., Steurer, F.J., Rodriguez, R., Campman, R., Peterson, A.T., Ramsey, J., Wirtz, R.A. and L.E. Robinson (2003). Chagas disease in a domestic transmission cycle, southern Texas, USA. *Emerging Infectious Diseases,* **9** (1), 103-105.

Berenger, J.M. and D. Pluot-Sigwalt (1997). Special relationships of certain predatory Heteroptera Reduviidae with plants. First known case of a phytophagous Harpactorinae. *Comptes Rendus de l'Academie des Sciences. Serie III,* **320,** 1007-1012.

Bermudez, H., Balderrama, F. and F. Torrico (1993). Identification and characterization of wild foci of *Triatoma infestans* in Central Bolivia. *American Journal of Tropical Medicine and Hygiene* **49** (Suppl.), 371.

Billingsley P.F. and Downe A.E.R. (1988). Ultrastructural localization of cathepsin B in the

midgut of Rhodnius prolixus Stal (Hemiptera: Reduviidae) during blood digestion. *Intern J Insect Morphol Embryol* **17**: 295-302.

Bookstein F.L. (1991). *Morphometric tools for landmark data: geometry and biology.* Cambridge University Press, New York.

Bookstein, F.L. (1985). Modeling differences in cranial form, with examples from primates. In (Jungers, W.L. ed.). *Size and Scaling in Primate Biology*, Plenum Press: New York. pp 207-229.

Bookstein, F.L. (1990). Higher-order features of shape change for landmark data. In *Proceedings of the Michigan Morphometrics Workshop* (Rohlf, F.J. and F.L. Bookstein eds.). pp. 237-250, University of Michigan Museum of Zoology: Ann Arbor. USA.

Bookstein, F.L. (1996) Combining the tools of geometric morphometrics, in (Marcus, L.F.I., Corti, M., Loy, A., Naylor, G.J.P. and D.E. Slice eds) *Advances in morphometrics*, New York: Plenum Press, pp 131-151.

Borges, E.C., Pires, H.H.R., Barbosa, S.E., Nunes, C.M.S., Pereira, M., Romana, A.J. and L. Diotaiuti (1999). Genetic variability in Brazilian triatomines and the risk of domiciliation. *Memórias do Instituto Oswaldo Cruz*, **94** (Suppl. 1), 371-373.

Borges, E.C., Romanha, A.J. and L. Diotaiuti (2000). Uso do Random Amplified Polymorphic DNA (RAPD) no estudo populacional do *Triatoma brasiliensis* Neiva, 1911. *Cadernos de Saude Publica* **16** (Suppl. 2), 97-100.

Braga, M.V. and M.M Lima (1999). Feeding and defecation patterns of nymphs of *Triatoma rubrofasciata,* and its potential role as a vector for *Trypanosoma cruzi. Memórias do Instituto Oswaldo Cruz,* **94,** 127-129.

Breddin, G. (1903). Herr G. Breddin sprach uber "neue Palaotropische Reduviinen." (Description of a new Paleotropic Reduviid.) *Gesellschaft Naturforschender Freunde,* Berlin, **3,** 111-129.

Brower, A.V.Z. (1994). Rapid morphological radiation and convergence among races of the butterfly *Heliconius erato* inferred from patterns of mitochondrial DNA evolution. *Proceedings of the National Academy of Sciences of the USA*, **91,** 6491-6495.

Carcavallo R.U. and R.J. Tonn (1976). Pictorial key to the haematophagous Reduviidae (Hemiptera) of Venezuela. *Boletin de la Direccion de Malariologia y Saneamiento Ambiental,* **16,** 244-265.

Carcavallo, R.U., Galindez Girón, I., Catalá, S., Jurberg, J., Lent, H., Galvão, C. and J.M.S. Barata (1997). Some anatomic structures studied with Scanning Electron Microscopy (SEM), in (Carcavallo, R.U., Galindez Giron, I., Jurberg, J. and H. Lent eds.) *Atlas of Chagas disease vectors in the Americas,* Vol. I, Editom FIOCRUZ, Rio de Janeiro, Brazil. pp. 299-393.

Carcavallo, R.U., Galíndez Girón, I., Jurberg, J. and H. Lent (eds.) (1999). *Atlas of Chagas disease vectors in the Americas,* Vol.III, Editora FIOCRUZ, Rio de Janeiro, Brazil.

Carcavallo, R.U., Jurberg, J., Lent, H., Noireau, F. and C. Galvão (2000). Phylogeny of the Triatominae (Hemiptera: Reduviidae). Proposals for taxonomic arrangements. *Entomología y Vectores*, **7** (Suppl. 1), 1-99.

Carlier, L., Muñoz, M. and J.P. Dujardin (1996). A RAPD protocol for Triatominae, in (Schofield, C.J., Dujardin, J.P. and J. Jurberg eds.) *Proceedings of the International Workshop on Population Genetics and Control of Triatominae, Santo Domingo de los Colorados, Ecuador, Sept.* 1995. INDRE, Mexico City, Mexico, pp. 81-83.

Catalá, S. (1997). Antennal sensilla of Triatominae (Hemiptera, Reduviidae): a comparative study over five genera. *International Journal of Insect Morphology and Embriology,* **26,** 67-73.

Catalá, S. and C.J. Schofield (1994). The antennal sensilla of *Rhodnius. Journal of Morphology,* **21,** 193-203.

Catalá, S., Maida, D.M., Caro-Riano, H., Jaramillo, N. and J. Moreno (2004). Changes associated with laboratory rearing in antennal sensilla patterns of *Triatoma infestans, Rhodnius prolixus*, and *Rhodnius pallescens* (Hemiptera, Reduviidae, Triatominae). *Memorias Do Instituto Oswaldo Cruz,* **99,** 25-30.

Catalá, S., Sachetto, C., Moreno, M., Rosales, R., Salazar-Schettino, P. M. and D. Gorla (2005). Antennal phenotype of *Triatoma dimidiata* populations and its relationship with species of phyllosoma and protracta complexes. *Journal of Medical Entomology,* **42,** 719-725.

Chapman, M.D., Baggaley, R.C., Godfrey-Fausset, P.F., Malpas, T.J., White, G., Canese, J. and M.A. Miles (1984). *Trypanosoma cruzi* from the Paraguayan Chaco: isoenzyme profiles of strains isolated at Makthlawaiya. *Journal of Protozoology*, **31,** 482-486.

Chávez, T., Moreno, J. and J.P. Dujardin (1999). Isoenzyme electrophoresis of *Rhodnius* species: a phenetic approach to relationships within the genus. *Annals of Tropical Medicine and Parasitology*, **93,** 229-307.

Claridge, M.F. and M.C. Gillham (1992). Variation in populations of leafhoppers and planthoppers (Auchenorrhyncha): biotypes and biological species, in (Foottit, R.G. and J.T. Sorensen eds.), *Ordination in the study of morphology, evolution and systematics of insects: applications and quantitative genetic rationales*. Elsevier, New York. pp 241-259.

Clement, M., Posada, D. and K.A. Crandall (2000). TCS: a computer program to estimate gene genealogies. *Molecular Ecology*, **9,** 1657–1659.

Cobben, R.H. (1978). Evolutionary trends in Heteroptera Part II. Mouthpart-structures and feeding strategies. *Meded Landbouwhogeschool Wageningen,* **78,** 5-407.

Coluzzi, M. (1964). Morphological divergences in the *Anopheles gambiae* complex. *Rivista di Malariologia,* **43,** 197-232.

Costa, J., Barth, O., Marchon-Silva, V., de Almeida, C., Rosa-Freitas, M. and F. Panzera (1997). Morphological studies on the *Triatoma brasiliensis* Neiva 1911 (Hemiptera, Reduviidae, Triatominae). Genital structures and eggs of different chromatic forms. *Memórias do Instituto Oswaldo Cruz,* **92,** 493-498.

Cuba Cuba, A.C., Abad-Franch, F., Rodriguez, J.R., Vasquez, F.V., Velasquez, L.P. and M.A. Miles (2002). The triatomines of northern Peru, with emphasis on the ecology and infection by trypanosomes of *Rhodnius ecuadoriensis* (Triatominae). *Memorias Do Instituto Oswaldo Cruz,* **97,** 175-183.

Daly, H.V. (1985). Insect Morphometrics. *Annual Review Of Entomology*, **30**,415-438

Darroch, J.N. and J.E. Mosiman (1985). Canonical and principal components of shape. *Biometrika,* **72,** 241-252.

De Arias, A.R. (1996). Chagas disease in Paraguay. PAHO/HCP/HCT/72/96.

De Geer, C. (1773). *Mémoires pour servir a l'histoire des Insectes*, Pierrer Hesselberg, Stockholm **3**, 696.

De la Riva, J., Le Pont, F., Ali, V., Matias, A., Mollinedo, S. and J.P. Dujardin (2001). Wing geometry as a tool for studying the *Lutzomyia longipalpis* (Diptera: Psychodidae) complex. *Memórias do Instituto Oswaldo Cruz,* **96,** 1089-1094.

Dias, J.C., Silveira, A.C. and C.J. Schofield (2002). The impact of Chagas disease control in Latin America: a review. *Memórias do Instituto Oswaldo Cruz*, **97,** 603-12.

Dias, J.C.P. (1987). Control of Chagas-Disease in Brazil. *Parasitology Today*, **3,** 336-341.

Dias, J.C.P. (1991). Chagas disease control in Brazil: Which strategy after the attack phase? *Annales de la Societe de Medecine Tropicale,* **71**, (Suppl. 1), 75-86.

Distant, W.L. (1904) *The fauna of British India, including Ceylon and Burma. Rhynchota Vol. II (Heteroptera).* Taylor and Francis, Red Lion Court, Fleet Street, London 503pp.

Dotson, E.M. and C.B. Beard (2001). Sequence and organization of the mitochondrial genome

of the Chagas disease vector, *Triatoma dimidiata*. *Insect Molecular Biology,* **10,** 205-215.

Du Rietz, G.E. (1930). The fundamental units of biological taxonomy. *Svensk Botanisk Tidskrift*, **24,** 333-428.

Dujardin, J.P. (2006). PAD (Permutaciones, Analisis Discriminante) Software Version 82. http://www.mpl.ird.fr/morphometrics/pad.

Dujardin, J.P. and F. Le Pont (2000). Morphometrics of a neotropical sandfly subspecies *Lutzomyia carrerai thula*. *Comptes Rendus de l'Academie des Sciences. Series III Sciences de la Vie,* **323,** 273-279.

Dujardin, J.P., Bermudez, H. and C.J. Schofield (1997b). The use of morphometrics in entomological surveillance of sylvatic foci of *Triatoma infestans* in Bolivia. *Acta Tropica,* **66,** 145-53.

Dujardin, J.P., Bermudez, H., Casini, C., Schofield, C.J. and M. Tibayrenc (1997a). Metric differences between silvatic and domestic *Triatoma infestans* (Heteroptera: Reduviidae) in Bolivia. *Journal of Medical Entomology,* **34,** 544-51.

Dujardin, J.P., Chavez, T., Machane, M. and S. Solis (1999c). Size, shape and genetics. sexual dimorphism and environment, in (Schofield, C.J. and C. Ponce eds), *Proceedings of the Second International Workshop on Population Biology and Control of Triatominae, Tegucigalpa, Honduras,* INDRE, Mexico City.

Dujardin, J.P., Chavez, T., Moreno, J.M., Machane, M., Noireau, F. and C.J. Schofield (1999b). Comparison of isoenzyme electrophoresis and morphometric analysis for phylogenetic reconstruction of the Rhodniini (Hemiptera: Reduviidae: Triatominae). *Journal of Medical Entomology,* **36,** 653-659.

Dujardin, J.P., Forgues, G., Torrez, M., Martinez, E., Cordoba, C. and A. Gianella (1998a). Morphometrics of domestic *Panstrongylus rufotuberculatus* in Bolivia. *Annals of Tropical Medicine and Parasitology*, **92,** 219-228.

Dujardin, J.P., Munoz, M., Chavez, T., Ponce, C., Moreno, J., and C.J. Schofield (1998b). The origin of *Rhodnius prolixus* in Central America. *Medical and Veterinary Entomology,* **12,** 113-115.

Dujardin, J.P., Panzera, F. and C.J. Schofield (1999a). Triatominae as a model of morphological plasticity under ecological pressure. *Memórias do Instituto Oswaldo Cruz,* **94** (Suppl. 1), 223-228.

Dujardin, J.P., Schofield, C.J. and F. Panzera (2000). *Les Vecteurs de la Maladie de Chagas. Recherches Taxonomiques, Biologiques et Génétiques*. Academie Royale des Sciences d'Outre Mer, Brussels. 162 pp.

Dujardin, J.P., Tibayrenc, M., Venegas, E., Maldonado, L., Desjeux, P. and F.J. Ayala. (1987). Isoenzyme evidence of lack of speciation between wild and domestic *Triatoma infestans* (Heteroptera: Reduviidae) in Bolivia. *Journal of Medical Entomology,* **24,** 40-45.

Dujardin, J.P., Torrez, E.M., Le-Pont, F., Hervas, D. and D. Sossa (1997c). Isozymic and metric variation in the *Lutzomyia longipalpis* complex. *Medical and Veterinary Entomology,* **11,** 394-400.

Else, J.G., Cheong, W.H., Mahadevan, S. and L.G. Zarate (1977). A new species of cave inhabiting *Triatoma* (Hemiptera: Reduiidae) from Malaysia. *Journal of Medical Entomology*, **14,** 367-369.

El-Sebaey, I.I.A., El-Shazly, M.M. and H.A.A. El-Wahab (2002). Seasonal changes in the population density of *Coranus africana* El-Sebaey in Egypt as indicated by life table parameters. *Egyptian Journal of Agricultural Research,* **80,** 631-645.

Feliciangeli, M. D., Dujardin, J. P., Bastrenta, B., Mazzarri, M., Villegas, J., Flores, M., and

M. Munoz (2002). Is *Rhodnius robustus* (Hemiptera: Reduviidae) responsible for Chagas disease transmission in Western Venezuela? *Tropical Medicine and International Health,* 7, 280-287.

Fitzpatrick, S.O. (2005). The analysis of the relationship between silvatic and domestic populations of *Rhodnius prolixus/robustus* (Hemiptera:Reduviidae) in Venezuela by morphometric and molecular methods. Thesis (PhD) University of London.

Galvao, C., McAloon, F.M., Rocha, D.S., Schaefer, C.W., Patterson, J. and J. Jurberg (2005). Description of eggs and nymphs of *Linshcosteus karupus* (Hemiptera:Reduviidae: Triatominae). *Annals of the Entomological Society of America*, **98,** 861-872.

Galvao, C., Patterson, J.S., Rocha, D.D., Jurberg, J., Carcavallo, R., Rajen, K., Ambrose, D.P. and M.A. Miles (2002). A new species of Triatominae from Tamil Nadu, India. *Medical and Veterinary Entomology,* **16,** 75-82.

Gamboa, C.J. (1961). Comprobación de *Rhodnius prolixus* extradomesticos. *Boletin Informativo de !a Dirección de Malariologia y Saneamiento Ámbiental*, **1,** 139-142.

Gamboa, C.J. (1963). en Venezuela. *Boletin de la Ofcina Sanitaria Panamericana*, **54,** 18-25.

García, A.L., Carrasco, H.J., Schofield, C.J., Valente, S.A.S., Frame, I.A., Stothard, J.R. and M.A. Miles (1998). Random Amplification of Polymorphyc DNA as a tool for taxonomic studies of triatomine bugs (Hemiptera: Reduviidae). *Journal of Medical Entomology,* **35,** 38-45.

García, B.A. (1999). Molecular phylogenetic relationships among species of the genus *Triatoma*, in (Carcavallo, R.U., Galindez Giron, I., Jurberg, J. and H. Lent eds.) *Atlas of Chagas disease vectors in the Americas*, Vol. III, Editora FIOCRUZ, Rio de Janeiro, Brazil, pp. 971-980.

García, B.A. and J.R. Powell (1998). Phylogeny of species of *Triatoma* (Hemiptera: Reduviidae) based on mitochondrial DNA sequences. *Journal of Medical Entomology,*

35, 232-238.

García, B.A., Canale, D.M. and A. Blanco (1995). Genetic structure of four species of *Triatoma* (Hemiptera: Reduviidae) from Argentina. *Journal of Medical Entomology,* **32,** 134-137.

García, B.A., Manfredi, C., Fichera, L., Segura, E.L. (2003). Short report: variation in mitochondrial 12S and 16S ribosomal DNA sequences in natural populations of *Triatoma infestans* (Hemiptera: Reduviidae). *American Journal of Tropical Medicine and Hygiene,* **68,** 692-694.

García, B.A., Moriyama, E.N. and J.R. Powell (2001). Mitochondrial DNA sequences of triatomines (Hemiptera: Reduviidae): phylogenetic relationships. *Journal of Medical Entomology,* **38,** 675-683.

Garcia, B.A., Zheng, L., Perez de Rosa, A.R. and E.L. Segura (2004). Isolation and characterization of polymorphic microsatellite loci in the Chagas' disease vector *Triatoma infestans* (Hemiptera: Reduviidae). *Molecular Ecology Notes,* **4,** 568–571.

Gaunt, M.W. and M.A. Miles (2000). The ecotopes and evolution of triatomine bugs (triatominae) and their associated trypanosomes. *Memórias do Instituto Oswaldo Cruz,* **95,** 557-565.

Gaunt, M.W. and M.A. Miles (2002). An insect molecular clock dates the origin of the insects and accords with palaeontological and biogeographic landmarks. *Molecular Biology and Evolution*, **19,** 748-761.

Germar, E.F. and G.C. Berendt (1856). Die irn Bernstein befindlichen Organischen Reste der Vorwelt by G. C. Berendt, 1845-1856. Zweiter Band, I Abtheilung, Hemipteren und Orthopteren, pp. 12-16.

Ghauri, M.S.K. (1976). The Indian triatomine genus *Linshcosteus* (Reduviidae). *Systematic Entomology,* **1,** 183-187.

Gillett, J.D. (1934). Colour variation of *Triatoma rubrofasciata. Proceedings of the Royal Entomological Society Of London,* **9,** 4-5.

Goméz-Núñez, J.C. (1963). Notas sobre la ecología del *Rhodnius prolixus. Boletin Informativo de !a Dirección de Malariologia y Saneamiento Ámbiental,* **3,** 262-272.

Gorla, D.E., Dujardin, J.P. and C.J. Schofield (1997). Biosystematics of Old World Triatominae. *Acta Tropica,* **63,** 127-140.

Gorla, D.E., Jurberg J., Catalá, S.S. and C.J. Schofield. (1993). Systematics of *Triatoma sordida, T. guasayana* and *T. patagonica* (Hemiptera: Reduviidae), *Memórias do Instituto Oswaldo Cruz,* **88,** 379-385.

Gould, S.J. (1977). *Ontogeny and Phylogeny.* Belknap Press/Harvard University Press. 501 pp.

Gracco, M. and S. Catalá (2000). Inter-specific and developmental differences on the array of antennal chemoreceptors in four species of Triatominae (Hemiptera: Reduviidae). *Memórias do Instituto 0swaldo Cruz,* **95,** 67-74.

Grimaldi, D., and M.S. Engel (2005). *Evolution of the insects.* Cambridge University Press; Cambridge, UK.

Grundy, P. and D. Maelzer (2000). Assessment of *Pristhesancus plagipennis* (Walker) (Hemiptera: Reduviidae) as an augmented biological control in cotton and soybean crops. *Australian Journal of Entomology,* **39,** 305-309.

Grundy, P.R. and D.A. Maelzer (2002). Augmentation of the assassin bug *Pristhesancus plagipennis* (Walker) (Hemiptera: Reduviidae) as a biological control agent for *Helicoverpa* spp. in cotton. *Australian Journal of Entomology,* **41,** 192–196.

Guhl, F., and G.A. Vallejo (1999). Interruption of Chagas disease transmission in the Andean countries: Colombia. *Memórias do Instituto Oswaldo Cruz,* **94,** 413-415.

Gumiel, M., Catalá, S., Noireau, F., Rojas de Arias, A., García, A. and J.P. Dujardin (2003). Wing geometry in *Triatoma infestans* (Klug) and *T. melanosoma* Martinez, Olmedo &

Carcavallo (Hemiptera: Reduviidae). *Systematic Entomology,* **28,** 173–179.

Hall, T.A (1999). BioEdit: a user-friendly biological sequence alignment editor and analysis program for Windows 95/98/NT. *Nucleic Acids Symposium Series,*. **41,** 95-98.

Harry, M. (1993a). Isozymic data question the specific status of some blood-sucking bugs of the genus *Rhodnius*, vectors of Chagas disease. *Transactions of the Royal Society of Tropical Medicine and Hygiene,* **87,** 492.

Harry, M. (1993b). Use of the median process of the pygophore in the identification *of Rhodnius nasutus, R. neglectus, R. prolixus* and *R. robustus* (Hemiptera: Reduviidae). *Annals of Tropical Medicine and Parasitology,* **87,** 277-282.

Harry, M. (1994). Morphometric variability in the Chagas' disease vector *Rhodnius prolixus*. *Japanese Journal of Genetics,* **69,** 233-250.

Harry, M., Galindez, I. and M.L. Cariou (1992). Isozyme variability and differentiation between *Rhodnius prolixus, R.robustus* and *R. pictipes*, vectors of Chagas disease in Venezuela. *Medical and Veterinary Entomology,* **6,** 37-43.

Harry, M., Poyet, G., Romana, C.A. and M. Solignac (1998). Isolation and characterization of microsatellite markers in the bloodsucking bug *Rhodnius pallescens* (Heteroptera, Reduviidae). *Molecular Ecology,* **7,** 1784-1786.

Herwaldt, B.L., Grijalva, M.J., Newsome, A.L., McGhee, C.R., Powell, M.R., Nemec, D.G., Steurer, F.J and M.L. Eberhard (2000). Use of Polymerase Chain Reaction to diagnose the fifth reported US case of autochthonous transmission of *Trypanosoma cruzi*, in Tennessee, 1998. *The Journal of Infectious Diseases,* **181,** 395-399.

Hoare, C.A. (1972). *The Trypanosomes of Mammals*. Blackwell, Oxford.749 pp.

Hsaio, T.Y. (1965). A new species of *Triatoma* Laporte (Hemipterat Reduvudac). *Acta Zootaxonomica Sinica,* **2,** 197-200.

Hutcheson, H.J., Oliver, J.H., Houck, M.A. and R.E. Stauss (1995). Multivariate

morphometric discrimination of nymphal and adult forms of the black-legged tick (Acari:Ixodidae), a principal vector of the agent of lyme disease in Eastern North America. *Journal of Medical Entomology,* **32,** 827-842.

Hypsa, V., Tietz, D.F., Zrzavy, J., Rego, R.O.M., Galvao, C. and J. Jurberg (2002). Phylogeny and biogeography of Triatominae (Hemiptera : Reduviidae): molecular evidence of a New World origin of the Asiatic clade. *Molecular Phylogenetics and Evolution,* **23,** 447-457.

Insausti, T.C. (1994). Nervous system of *Triatoma infestans*. *Journal of Morphology*, **221,** 343-359.

Jahnke, S.M., Redaelli, L.R. and L.M.G. Diefenbach (2002). Population dynamics of *Cosmoclopius nigroannulatus* Stal (Hemiptera, Reduviidae) in tobacco culture. *Brasilian Journal of Biology,* **62,** 819-826.

Jaramillo, N., Castillo, D. and M.E. Wolff (2002). Geometric morphometric differences between *Panstrongylus geniculatus* from field and laboratory. *Memórias do Instituto Oswaldo Cruz*, **97,** 667–673.

Jaramillo, N.O. (2000). Partición en tamaño y forma de los caracteres métricos y su interés en los estudios poblacionales aplicados a los Triatominae. Thesis (PhD) University of Antioquia, Medellín, Colombia.

Jeannel, R. (1919). Henicocephalidae et Reduviidae. *Voyage de Ch. Alluaud et R. Jeannel en Afrique orientale (1911-1912). Resultats scientifiques- Hemiptera Paris,* **3,** 131-314.

Jurberg, J., Lent, H. and C. Galvão (1997). The male genitalia and its importance in taxonomy, in (Carcavallo, R.U., Girón, I.G., Jurberg, J. and H. Lent eds.) *Atlas of Chagas disease vectors in the Americas,* Vol. I, Editora FIOCRUZ, Rio de Janeiro, Brazil, pp. 85-106.

Kalshoven, L.G.E. (1970). Observations on the blood-sucking reduviid *Triatoma rubrofasciata* (De Geer) in Java. *Entomologische Berichten,* **30,** 41-47.

Kawashita, S.Y., Sanson, G.F.O., Fernandes, O., Zingales, B. and M.R.S. Briones (2001).

Maximum-Likelihood divergence date estimates based on rRNA gene sequences suggest two scenarios of *Trypanosoma cruzi* intraspecific evolution. *Molecular Biology and Evolution,* **18,** 2250-2259.

Klingenberg, C.P. (1996). Multivariate allometry, in (Marcus, L.F., Corti, M., Loy, A., Naylor, G.J.P. and D. Slice eds.) *Advances in morphometrics, Proceedings of the 1996 NATO-ASI on morphometrics*, Plenum press, New York, pp. 23-49.

Kumar, S., Tamura, K., and M. Nei (2004). MEGA3: Integrated software for Molecular Evolutionary Genetics Analysis and sequence alignment. *Briefings in Bioinformatics,* **5,** 150-163.

Lane, R.P. and P.D. Ready (1985). Multivariate discrimination between *Lutzomyia wellcomei*, a vector of mucocutaneous leishmaniasis, and *Lu. complexus* (Diptera: Phlebotominae). *Annals of Tropical Medicine and Parasit*ology, **79,** 469-472.

Larrousse, F. (1924). Triatomes d'Asie; description d'une nouvelle espece *Triatoma bouvieri* n.sp. *Annales de Parasitologie Humaine et Comparee,* Paris, **2** (1), 62-70.

Lehane, L. (2005). *The Biology of Blood-Sucking in Insects*. Second Edition. New York, NY: Cambridge University Press. pp 336.

Lent H., and A. Valdenama (1973). Hallazgo en Venezuela del triatomino *Rhodnius robustus* Lanousse, 1927 en la palma *Attalea maracaibensis* Martius (Hemiptera, Reduviidae). *Boletin de la Oficina Sanitaria Panamericana*, **13,** 175-179.

Lent, H. (1951). Triatominae das regioes Oriental, Australiana, Etiopica e Paleartica, com descricao de uma nova especie (Hemiptera, Reduviidae). *Revista Brasileira de Biologia*, **11,** 425- 429.

Lent, H. (1953). Nova especie de *Triatoma* da regiao oriental (Hemiptera, Reduiidae). *Revista Brasileira de Biologia,* **13,** 315-319.

Lent, H. and J. Jurberg (1983). Estudo comparativo da genitália externa masculina de

Linshcosteus costalis Ghauri e *L. kali* Lent & Wygodzinsky (Hemiptera, Reduviidae, Triatominae) *Memórias do Instituto Oswaldo Cruz,* **78,** 421-429.

Lent, H. and J. Jurberg (1985). Sobre a variaçao intra-específica em *Triatoma dimidiata* (Latreille) e *Triatoma infestans* (Klug) (Hemiptera: Reduviidae). *Memórias do Instituto Oswaldo Cruz,* **80,** 285-299.

Lent, H. and P. Wygodzinsky (1979). Revision of the Triatominae (Hemiptera, Reduviidae) and their significance as vectors of Chagas' disease. *Bulletin of the American Museum of Natural History,* **163,** 123-520.

López, G. and M.J. Moreno (1995). Genetic variability and differentiation between populations of *Rhodnius prolixus* and *Rhodnius pallescens,* vectors of Chagas Disease in Colombia. *Memórias do Instituto Oswaldo Cruz,* **90,** 353-357.

Louis, P. (1974). Biology of Reduviidae of cocoa farms in Ghana. *American Midl. Nature*, **9,** 68-89.

Lukashevich, E.D. and M.B. Mostovski (2001). Blood-sucking insects in the palaeontological record. in *Biodiversity in the Earth history*. XLVII session of All-Russia Palaeontological Society, Abstracts, , St. Petersburg, pp. 65-66.

Lyman, D.F., Monteiro, F.A., Escalante, A.A., Cordón-Rosales, C., Wesson, D.M., Dujardin, J.P. and C.B. Beard (1999). Mitochondrial DNA sequence variation among triatomine vectors of Chagas disease. *The American Journal of Tropical Medicine and Hygiene,* **60,** 377-386.

Macario-Rebelo, R.J.M., Alves, G.A., Lorosa, E.S., Pereira, Y.N.O., Silva, F.S. and V.L. Lopes de Barros (1999). Distribucao das especies do genero *Triatoma* Laporte, 1833 (Reduviidae, Triatominae) no estado de Maranhao Brazil. *Entomología y Vectores,* **6,** 91-109.

Maldonado Capriles, J. (1990). Systematic Catalogue of the Reduviidae of the World. Special

Pubishers, Caribbean Journal of Science, Mayaguez, PR.

Malhotra, A., and R. S. Thorpe (1994). Parallels between island lizards suggests selection on mitochondrial DNA and morphology. *Proceedings of the Royal Society of London (Series B),* **257,** 37-42.

Mantel, N. (1967) The detection of disease clustering and a generalized regression approach. *Cancer Research,* **27,** 209–220.

Marcet, P.L., Lehmann, T., Groner, G., Gurtler, R.E., Kitron, U. and E.M. Dotson (2006). Identification and characterization of microsatellite markers in the Chagas disease vector *Triatoma infestans* (Heteroptera: Reduviidae). *Infection, Genetics and Evolution,* **6,** 32-37.

Marcilla, A., Bargues, M.D., Abad-Franch, F., Panzera, F., Carcavallo, R.U., Noireau, F., Galvao, C., Jurberg, J., Miles, M.A., Dujardin, J.P. and S. Mas-Coma (2002). Nuclear rDNA ITS-2 sequences reveal polyphyly of *Panstrongylus* species (Hemiptera: Reduviidae: Triatominae), vectors of *Trypanosoma cruzi*. *Infection, Genetics and Evolution,* **1,** 225-235.

Marcilla, A., Canese, N., Acosta, E., López, A., Rojas de Arias, A., Bargues, M.D. and S. Mas-Coma (2000). Populations of *Triatoma infestans* (Hemiptera: Reduviidae) from Paraguay: a molecular analysis based on the second internal transcribed spacer of the rDNA. *Research and Reviews in Parasitology,* **60,** 99-105.

Marcilla, A., Dolores-Bargues, M., Ramsey, J.M., Magallon-Gatelum, E., Salazar-Schettino, P.M., Abad-Franch, F., Dujardin, J.P., Schofield, C.J. and S. Mas-Coma (2001). The ITS-2 of the nuclear rDNA as a molecular marker for populations, species, and phylogenetic relationships in Triatominae (Hemitera: Reduviidae), vectors of Chagas disease. *Molecular Phylogenetics and Evolution,* **18,** 136-142.

Marsden, P.D. and R.A. Penna (1982). 'Vigilance unit' for households subject to triatomine

control. *Transactions of the Royal Society of Tropical Medicine and Hygiene,* **76,** 790-792.

Marsola Moraes, E. and F. Melo Sene (2004). Heritability of wing morphology in a natural population of *Drosophila gouveai. Genetica,* **121,** 119-123.

Matias, A., de la Rive, J.X., Torrez, M. and J.P. Dujardin (2001). *Rhodnius robustus* in Bolivia identified by its wings. *Memórias do Instituto Oswaldo Cruz,* **96**, 947-50.

McNamara, K.J. (1997). *Shapes of Time: The Evolution of Growth and Development.* The Johns Hopkins University Press, USA, pp 360.

Meyer, A. (1994). Shortcomings of the cytochrome *b* gene as a molecular marker. *Trends in Ecology and Evolution*, **9,** 278-280.

Miller, N.C.E. (1941). New genera and species of Malaysian Reduviidae, Supplementary records. *Journal Fed. Malay States Mus*, **18,** 774-804.

Miller, N.C.E. (1958). On the Reduviidae of New Guinea and adjacent islands (Hemiptera-Heteroptera). Part 1. *Nova Guinea*, (n. s.), **9,** 13-143.

Moncayo, A. (2003). Chagas disease: current epidemiological trends after the interruption of vectorial and transfusional transmission in the Southern Cone countries. *Memórias do Instituto Oswaldo Cruz, 96,* 141-144.

Monteiro F., Pérez, R., Panzera, F., Dujardin, J.P., Galvão, C., Rocha, D., Noireau, F., Schofield, C.J. and C.B. Beard (1999b). Mitochondrial DNA variation of *Triatoma infestans* populations and its implication on the specific status of *T melanosoma. Memórias do Instituto Oswaldo Cruz,* **94** (Suppl. 1), 229-238.

Monteiro, F., Costa, J. and C.B. Beard (1999a). High levels of mitochondrial DNA sequence divergence among *Triatoma brasiliensis N*eiva, 1911 populations; (Hemiptera, Reduviidae, Triatominae). *Memórias do Instituto Oswaldo Cruz,* **94** (Suppl. 2), 244.

Monteiro, F.A., Barrett, T.V., Fitzpatrick, S., Cordon-Rosales, C., Feliciangeli, M.D. and C.B.

Beard (2003). Molecular phylogeography of the Amazonian Chagas disease vectors *Rhodnius prolixus* and *R. robustus*. *Molecular Ecology*, **12,** 997-1006.

Monteiro, F.A., Donnelly, M.J., Beard, C.B. and J. Costa (2004). Nested clade and phylogeographic analyses of the Chagas disease vector *Triatoma brasiliensis* in Northeast Brazil. *Molecular Phylogenetics and Evolution,* **32,** 46-56.

Monteiro, F.A., Escalante, A.A., and C.B. Beard (2001). Molecular tools and triatomine systematics: a public health perspective. *Trends in Parasitology,* **17,** 344-347.

Monteiro, F.A., Lazoski, C., Noireau, F. and A.M. Sole-Cava (2002). Allozyme relationships among ten species of *Rhodniini*, showing paraphyly of *Rhodnius* including *Psammolestes. Medical and Veterinary Entomology,* **16,** 83-90.

Monteiro, F.A., Wesson, D.M., Dotson, E.M., Schofield, C.J. and C.B. Beard (2000). Phylogeny and molecular taxonomy of the *Rhodniini* derived from mitochondrial and nuclear DNA sequences. *American Journal of Tropical Medicine and Hygiene,* **62,** 460-465.

Monteith, G.B. (1974). Confirmation of the presence of Triatominae (Hemiptera: Reduviidae) in Australia, with notes on Indo-Pacific species. *Journal Australian Entomology Society,* **13,** 89-94.

Moore, W.S. (1995). Inferring phylogenies from mtDNA variation: mitochondrial gene trees versus nuclear gene trees. *Evolution,* **49,** 718-726.

Noireau, F., Abad-Franch, F., Valente, S.A.S., Dias-Lima, A., Lopes, C.M., Cunha, V., Valente, V.C., Palomeque, F.S., Carvalho-Pinto, C.J.D., Sherlock, I., Aguilar, M., Steindel, M., Grisard, E.C. and J. Jurberg (2002). Trapping Triatominae in sylvatic habitats. *Memorias do Instituto Oswaldo Cruz,* **97,** 61-63.

Noireau, F., Bosseno, N.W., Vargas, F. and S.F. Breniére (1994). Apparent trend to domesticity observed in *Panstrongylus rufotuberculatus* Champion, 1899 (Hemiptera:

Reduviidae) in Bolivia. *Research and Reviews in Parasitology,* **54,** 263-264.

Noireau, F., Cortez, M.G., Monteiro, F.A., Jansen, A.M. and F. Torrico (2005). Can wild *Triatoma infestans* foci in Bolivia jeopardize Chagas disease control efforts? *Trends in Parasitology,* **21,** 7-10.

Noireau, F., Flores, R. and F. Vargas (1999). Trapping sylvatic Triatominae (Reduviidae) in hollow trees. *Transactions of the Royal Society of Tropical Medicine and Hygiene,* **99,** 13-14.

Noireau, F., Flores, R., Gutierrez, T. and J.P. Dujardin (1997). Detection of sylvatic dark morphs of *Triatoma infestans* in the Bolivian Chaco. *Memórias do Instituto Oswaldo Cruz,* **92,** 583-584.

Noireau, F., Flores, R., Gutierrez, T., Abad-Franch, F., Flores, E. and F. Vargas (2000). Natural ecotopes of *Triatoma infestans* dark morph and other sylvatic triatomines in the Bolivian Chaco. *Transactions of the Royal Society of Tropical Medicine and Hygiene,* **94,** 23-27.

Noireau, F., Gutiérrez, T., Flores, R., Breniére, S.F., Bosseno, M.F. and C. Wisnivesky-Colli (1999a). Ecogenetics of *Triatoma sordida* and *Triatoma guasayana* (Hemiptera: Reduviidae) in the Bolivian Chaco. *Memórias do Instituto Oswaldo Cruz,* **94,** 451-457.

Noireau, F., Gutierrez, T., Zegarra, M., Flores, R., Breniere, F., Cardozo, L. and J.P. Dujardin (1998). Cryptic speciation in *Triatoma sordida* (Hemiptera:Reduviidae) from the Bolivian Chaco. *Tropical Medicine and International Health,* **3,** 364-372.

Osawa, S. Su, Z.H. and Y. Imura (2004). *Molecular Phylogeny and Evolution of Carabid Ground Beetles.* Springer-Verlag, USA, pp 191.

Panzera, F., Álvarez, F., Sánchez-Rufas, J., Pérez, R., Suja, J.A., Scvortzoff, E., Estramil, E., Dujardin, J.P. and R. Salvatella (1992). C-heterochromatin polymorphism in holocentric chromosomes of *Triatoma infestans* (Hemiptera:Reduviidae). *Genome,* **35,** 1068-1074.

Panzera, F., Hornos, S., Pereira, J., Cestau, R., Canale, D., Diotaiuti, L., Dujardin, J.P. and R. Pérez (1997). Genetic variability and geographic differentiation among three species of triatomine bugs (Hemiptera: Reduviidae). *The American Journal of Tropical Medicine and Hygiene,* **57,** 732-739.

Panzera, F., Perez, R., Panzera, Y., Alvarez, F., Scvortzoff, E. and R. Salvatella (1995). Karyotype evolution in holocentric chromosomes of three related species of triatomines (Hemiptera-Reduviidae). *Chromosome Research,* **3,** 143-150.

Panzera, F., Scvortzoff, E., Pérez, R., Panzera, Y., Homos, S., Cestau, R., Nicolini, P., Delgado, V., Alvarez, F., Mazzella, M.C., Cossio, G., Martinez, M. and R. Salvatella (1998). Cytogenetics of triatomines, in (Carcavallo, R.U., Galindez Girón, I., Jurberg, J. and H. Lent eds.) *Atlas of Chagas disease vectors in the Americas,* Vol. II, Editora FIOCRUZ, Rio de Janeiro, Brazil, pp. 621-664.

Patterson J.W. and M. Schwarz (1977). Chemical structure, juvenile hormone activity and persistence within the insect of juvenile hormone mimics for *Rhodnius prolixus*. *Journal of Insect Physiology,* **23,** 121-129.

Patterson, J.S., Schofield, C.J., Dujardin, J.P. and M.A. Miles (2001). Population morphometric analysis of the tropicopolitan bug *Triatoma rubrofasciata* and relationships with Old World species of Triatoma: evidence of New World ancestry. *Medical and Veterinary Entomology,* **15,** 443-451.

Paula, A.S. de, Diotaiuti, L. and C.J. Schofield. (2005). Testing the sister-group relationship of the Rhodniini and Triatomini (Insecta : Hemiptera : Reduviidae : Triatominae). *Molecular Phylogenetics and Evolution,* **35,** 712-718.

Peakall, R. and P.E. Smouse (2006). GENALEX 6: genetic analysis in Excel. Population genetic software for teaching and research. *Molecular Ecology Notes,* **6,** 288-295.

Pereira J., Dujardin J.P., Salvatella R. and M. Tibayrenc (1996). Enzymatic variability and

phylogenetic relatedness among *Triatoma infestans, T. platensis, T delpontei,* and T *rubrovaria. Heredity,* **77,** 47-54.

Pinchin, R., Fanara, D.M., Castleton, C.W. and A.M. Oliveira-Filho (1981). Comparison of techniques for detection of domestic infestations with *Triatoma infestans* in Brazil. *Transactions of the Royal Society of Tropical Medicine and Hygiene,* **75,** 691-694.

Pires, H.H.R., Barbosa, S.E., Margonari, C., Jurberg J. and L. Diotaiuti (1998). Variations of the external male genitalia in three populations of *Triatoma infestans* Klug, 1834. *Memórias do Instituto Oswaldo Cruz,* **93**,479-483.

Poinar, G. (2005). *Triatoma dominicana* sp n. (Hemiptera : Reduviidae : Triatominae), and *Trypanosoma antiquus* sp n. (Stercoraria : Trypanosomatidae), the first fossil evidence of a triatomine-trypanosomatid vector association. *Vector-Borne and Zoonotic Diseases,* **5,** 72-81.

Poinar, G. Jr. and R. Poinar (1999). *The Amber Forest: A Reconstruction of a Vanished World.* Princeton University Press, USA.

Popov, P.V. and P.V. Putshkov (1998). *Redubinotus liedtkei* n. gen. n. sp. - The second Centrocnemina from the Baltic amber (Heteroptera: Reduviidae: Centrocnemidinae). - *Ann. up. siles. Mus. (Ent.),* **8-9,** 205-210.

Popov, P.V. Wroclaw, W.R. and P.E.S Whalley (1994). British upper triassic and lower jurassic Heteroptera and Coleorrhyncha (Insects : Hemiptera). *Genus,* **5,** 307-347.

Putshkov, P.V. and P.V. Popov (1993). A remarkable nymph of a centrocneminous bug from Baltic amber (Heteroptera:Reduviidae). *Mitt. Geol. Palaont. Inst. Univ. Hamburg,* **78,** 211-229.

Putshkov, P.V. and P.V. Popov (1995). Collarhampus mixtus n. gen. n. sp. – The first Collartidina (Heteroptera: Reduviidae, Emesinae) from the Baltic amber. *Mitt. Geol. Palaont. Inst. Univ, Hamburg,* **78,** 179-187.

Ready, P.D., Fraiha, H., Lane, I.P., Arias, J.R. and F.X. Pajot (1982). On distinguishing the female of *Psychodopygus wellcomei*, a vector of mulcocutaneous leishmaniasis, from other *squamiventris* series females. I. Characterization of *Ps. squamiventris squamiventris* and *Ps. s. maripaensis*. stat. nov. (Diptera: Psychodidae). *Annals of Tropical Medicine and Parasitology*, **76,** 201-214.

Remme, J.H.F., Feenstra, P., Lever, P.R., Médici, A., Morel, C., Noma, M., Ramaiah, K.D., Richards, F., Seketeli, A., Schmunis, G., van Brakel, W.H., and A. Vassall (2006). Tropical Diseases Targeted for Elimination: Chagas Disease, Lymphatic Filariasis, Onchocerciasis, and Leprosy, in *Disease Control Priorities in Developing Countries* (2nd edn), New York, Oxford University Press, pp 433-450.

Rohlf, F.J. (2002). Geometric morphometrics in systematics. in (Forey, P. and N. Macleod eds.) *Morphology, shape and phylogenetics*. Francis & Taylor, London, UK.

Rohlf, F.J and M. Corti (2000).The use of two-block partial least-squares to study covariation in shape. *Systematic Biology*, **49,** 740-753.

Rohlf, F.J. (1963). Congruence of larval and adult classifications in *Aedes* (Diptera: Culicidae). *Systematic Zoology*, **12,** 97-119.

Rohlf, F.J. (1997a). tpsDig., vol. 1.08, Department of Ecology and Evolution, State University of New York at Stony Brook: Stony Brook, NY.

Rohlf, F.J. (1997b). tpsPLS: partial least squares., vol. 1.01, Department of Ecology and Evolution, State University of New York at Stony Brook: Stony Brook, NY.

Rohlf, F.J. (1998a). tpsRelw: analysis of relative warps., vol. 1.15, Department of Ecology and Evolution, State University of New York at Stony Brook: Stony Brook, NY.

Rohlf, F.J. (1998b). tpsSuper: superimposition., vol. 1.03, Department of Ecology and Evolution, State University of New York at Stony Brook: Stony Brook, NY.

Rohlf, F.J. (1998c). tpsRegr: shape regression., vol. 1.13, Department of Ecology and

Evolution, State University of New York at Stony Brook: Stony Brook, NY.

Rohlf, F.J. (2001) NTSYS. Numerical taxonomy and multivariate analysis system. Version 2.10p, Exeter software, Setauket, New York.

Rohlf, F.J. and Bookstein F.L. (1990). Rohlf, F.J., Bookstein, F.L., (Eds.). Proceedings of the Michigan Morphometrics Workshop. Museum of Zoology Special Publication 2. University Michigan, Ann Arbor

Rohlf, F.J. and L.F. Marcus (1993). A revolution in morphometrics. *Trends in Ecology and Evolution*, **8**, 129-132.

Rojas de Arias, A., Lehane, M.J., Schofield, C.J. and A. Fournet (2003). Comparative evaluation of pyrethroid insecticide formulations against *Triatoma infestans* (Klug). Residual efficacy on four substrates. *Memorias do Instituto Oswaldo Cruz,* **98**, 975-980.

Rojas de Arias, A., Lehane, M.J., Schofield, C.J. and M. Maldonado (2004). Pyrethroid insecticide evaluation on different house structures in a chagas disease endemic area of the Paraguayan Chaco. *Memorias do Instituto Oswaldo Cruz*, **99**, 657-662.

Rozendaal, J. A. (1997). *Vector Control: Methods for use by individuals and communities.* World Health Organisation, Geneva.

Ryckman R.E. and C.M. Blankenship (1984). The Parasites, Predators and symbionts of the Triatominae (Hemiptera: Reduviidae: Triatominae*). Bulletin of the Society of Vector Ecologists*, **9,** 84-111.

Ryckman, R.E. and E.F. Archbold (1981). The Triatominae and Triatominae borne trypanosomes of Asia. Africa, Australia and the East Indies. *Bulletin of the Society of Vector Ecologists,* **6,** 43-166.

Sampson, P.D., Streissguth, A.P., Barr, H.M., and F.L. Bookstein (1989). Neurobehavioral effects of prenatal alcohol: part II. partial least squares analysis. *Neurotoxicology Teratology,* **11,** 477-491.

SAS Institute Inc. (2000) JMP® Statistics and graphics guide. Version 4.0.4. SAS Campus Drive, Cary

Schachter-Broide, J., Dujardin, J.P., Kitron, U. and R.E. Gurtler (2004). Spatial structuring of *Triatoma infestans* (Hemiptera, Reduviidae) populations from northwestern Argentina using wing geometric morphometry, *Journal of Medical Entomology,* **41** (4), 643-649.

Schaefer, A.W. and M.C. Coscaron (2004). The status of *Linshcosteus* in the Triatominae (Hemiptera: Reduviidae). *Journal of Medical Entomology*, **38** (6), 862-867.

Schaefer, C.W. (1998). Phylogeny, systematics, and practical entomology: the Heteroptera (Hemiptera). *Annals of the Society of Entomology, Brasil,* **27,** 499-511.

Schaefer, C.W. (2003). Triatominae (Hemiptera: Reduviidae); Systematic questions and some others. *Neotropical Entomology,* **32,** 1-10.

Schofield C.J. and J.C. Dias (1996). Introduction and historical overview, in (Schofield, C.J., Dujardin, J.P. and J. Jurberg eds.) *Proceedings of the International Workshop on population genetics and control of Triatominae, Santo Domingo de los Colorados, Ecuador, Sept. 1995*. INDRE, Mexico City, Mexico, pp. 11-16.

Schofield, C.J. and J.C. Dias (1999). The Southern Cone Initiative against Chagas disease. *Advances in Parasitology,* **42,** 1-27.

Schofield, C.J. and J.P. Dujardin (1999). Theories on the evolution of *Rhodnius*. *Actualidades Biologicas* (Medellin), **70,** 183-197.

Schofield, C.J. (1988). Biosystematics of the Triatominae, in (ed. M. W. Service) *Biosystematics of Haematophagous Insects.* Clarendon Press, Oxford.

Schofield, C.J. (1994). *Triatominae - Biology & Control.* Bognor Regis Eurocommunica Publications, West Sussex, UK.

Schofield, C.J. (1999). Overview: Evolution of the Triatominae, in (Schofield, C.J. and C. Ponce eds), *Proceedings of the Second International Workshop on Population Biology*

and Control of Triatominae, Tegucigalpa, Honduras, INDRE, Mexico City.

Schofield, C.J. (2000). *Trypanosoma cruzi* - The vector-parasite paradox. *Memórias do Instituto Oswaldo Cruz,* **95,** 535-544.

Schofield, C.J. (1985). Control of Chagas disease vectors. *British Medical Bulletin*, **41,** 187-194.

Schofield, C.J., Diotaiuti, L. and J.P. Dujardin (1999). The process of domestication in Triatominae. *Memórias do Instituto Oswaldo Cruz,* **94** (Suppl. 1), 375-378.

Schofield, C.J., Minter, D.M. and R.J. Tonn (1987).Vector Control Series, Triatomine Bugs, Training and information guide, WHO/VBC/87.941.

Schouteden, H. (1933) Resultats scientifiques du voyage aux Indies orientales neerlandaises de LL.AA.RR. Ie Prince et Ia Princesse de Belgique, Vol.4. *Memoires du Musee Royal d'Histoire Naturelle de Belgique*, Bruxelles, 43-70.

Shaw, K.L. (2002). Conflict between nuclear and mitochondrial DNA phylogenies of a recent species radiation: what *mt*DNA reveals and conceals about modes of speciation in Hawaiian crickets. *Proceedings of the National Academy of Science of the USA*, **25,** 16122–16127.

Simon, C., Frati, F., Beckenbach, A., Crespi, B., Liu, H. and P. Flook (1994). Evolution, weighting, and phylogenetic utility of mitochondrial gene sequences and a compilation *of* conserved Polymerase Chain Reaction primers. *Annals of the Entomological Society of America,* **87,** 651-701.

Sites, R.W. and M.R. Willig (1994). Efficacy of mensural characters in discriminating among species of Naucoridae (Insecta: Hemiptera): multivariate approaches and ontogenetic perspectives. *Systematics*, **87,** 803-814

Slice, D.E. (1998). Morpheus et al.: software for morphometric research. Revision 01-30-98. Department of Ecology and Evolution, State University of New York, Stony Brook, New

York.

Sneath, P.H.A. (1957). The application of computers to taxonomy. *Journal of Microbiology*, **17,** 201-206.

Sokal, R.R. (1973). The species problem reconsidered. *Systematic Zoology,* **22,** 360-374.

Solano, P., Dujardin, J.P., Schofield, G., Romaña, C. and M. Tibayrenc (1996). Isoenzymes as a tool for the identification of *Rhodnius* species. *Research and Reviews in Parasitology,* **56,** 41-47.

Sorensen, J.T. and R.G. Foottit (1992). The evolutionary quantitative genetic rationales for the use of ordination analyses in systematics: Phylogenetic implications. In RG Foottit & J T Sorensen (Editors). *Ordination in the study of morphology, evolution and systematics of insects: applications and quantitative genetic rationales*. Elsevier, New York. 29-55.

Spence, J.R. and N.M. Andersen (1994). Biology of water striders:interactions between systematics and ecology. *Annual Review of Entomology*, **39,** 101–128.

Stothard, J.R., Yamamoto, Y., Cherchi, A., García, A.L., Valente, S.A.S., Schofield, C.J. and M.A. Miles (1998). A preliminary survey of mitochondrial sequence variation within triatomine bugs (Hemiptera: Reduviidae) using Polymerase Chain Reaction-based single strand conformational polymorphism (SSCP) analysis and direct sequencing. *Bulletin of Entomological Research,* **88,** 553-560.

Swofford, D.L. (2002). PAUP*: Phylogenetic Analysis Using Parsimony (and Other Methods) 4.0 Beta., Sinauer Associates, Sunderland, MA.

Templeton, A.R., Crandall, K.A. and C.F. Sing (1992). A cladistic analysis of phenotypic associations with haplotypes inferred from restriction endonuclease mapping and DNA sequence data. 3. cladogram estimation. *Genetics,* **132,** 619–633.

Thompson D.W. (1917). *On growth and form*. Cambridge: Cambridge University Press.

Thompson, J.D., Higgins, D.G. and T.J. Gibson (1994). CLUSTALW: Improving the

sensitivity and progressive multiple sequence alignment through sequence weighting, positions-specific gap penalties and weight matrix choice. *Nucleic Acids Research,* **22,** 4673-4680.

Townson, H. and S.E.O. Meridith (1979). Identification of the Simuliidae in relation to onchocerciasis, in (ed Taylor, A.E.R. and Muller, R.) *Problems in the identification of parasites and their vectors*. Blackwell Scientific Publications, Oxford pp. 145-174.

Usinger, R.L. (1939). Descriptions of new Triatominae with a key to genera (Hemiptera, Reduviidae). *Univiversity of California Publications,* **7,** 33-56.

Usinger, R.L. (1943) A revised classification of the Reduvioidea with a new family of South American (Hemiptera). *Annals of the Entomological Society of America,* **36,** 602-617.

Usinger, R.L. (1944). The Triatominae of North and Central America and the West Indies and their public health significance. *Public Health Bulletin,* **288**. United States Government Printing Office, Washington

Usinger, R.L., Wygodzinsky, P. and R. Ryckman (1966). The biosystematics of Triatominae. *Annual Review of Entomology,* **11,** 309-330.

Velazquez, C.J. and G. Gonzalez (1959). Estado actual de la enfermedad de Chagas en el Paraguay. *Revista Medicina de Paraguay*, **3,** 308.

Villegas, J., Feliciangeli, M.D., and J.P. Dujardin (2002). Wing shape divergence between *Rhodnius prolixus* from Cojedes (Venezuela) and *Rhodnius robustus* from Mérida (Venezuela). *Infection, Genetics and Evolution*, **2,** 121–128.

Weitschat, W. and W. Wichard (2002). *Atlas of plants and animals in Baltic Amber.* Verlag Friedrich Pfeil, Munich, 256 pp.

Whitfield, J.B. (2002). Estimating the age of the polydnavirus/braconid wasp symbiosis. *Proceedings of the National Academy of Sciences of the USA*, **99,** 7508-7513.

WHO (1991). Control of Chagas Disease. Technical Report Series 811, Report of a WHO

Expert Committee. WHO, Geneva.

WHO (1999). Chagas disease, Venezuela. *Weekly epidemiological record*, **35,** 290-292.

WHO (2002). Control of Chagas disease. WHO Technical Report Series, 905.

WHO (2003). http://www.who.int/tdr/diseases/chagas/diseaseinfo.htm

Wigglesworth, V. B. (1934). The physiology of ecdysis in Rhodnius prolixus (Hemiptera). II. Factors controlling moulting and 'metamorphosis'. *Quart. J. Microsc. Sci.* **77**, 191-222.

Wootton, R.J. (1981). Palaeozoic Insects (1981). *Annual Review of Entomology, **26,*** 319-344.

World Bank. (1993). World development report 1993. Investing in Health. World development indicators. Oxford University Press, USA.

Yeo, M. (2003). The genetic diversity of `*Trypansoma cruzi'* multiclonality of natural populations, and characterisation of Paraguayan isolates and experimentally derived `*T cruzi'* I hybrids. Thesis (PhD) University of London.

Yeo, M., Acosta, N., Llewellyn, M., Sanchez, H., Adamson, S., Miles, G.A., Lopez, E., Gonzalez, N., Patterson, J.S., Gaunt, M.W., de Arias, A.R. and M.A. Miles (2005). Origins of Chagas disease: *Didelphis* species are natural hosts of *Trypanosoma cruzi* I and armadillos hosts of *Trypanosoma cruzi* II, including hybrids. *International Journal of Parasitology*, **35,** 225-233.

Zeledón, R (1996). Enfermedad de Chagas en Centro-américa. in (Schofield, C.J., Dujardin, J.P., and Jurberg, J. eds). *Proceedings of the International Workshop on Population Genetics and Control of Triatominae*, Santo Domingo de los Colorados, Ecuador, 24-28 Sept. 1995, INDRE, Mexico City, p. 40.

11 Glossary

affine transformation - A transformation for which parallel lines remain parallel. Affine transformations of the plane transform squares into parallelograms and circles into ellipses of the same shape.. Equivalent to "uniform transformation". (Antonyms; non-affine and non-uniform).

allometry - Any change of shape with size. It describes any deviation of the bivariate relation from the simple functional form y/x = c, where c is a constant and x and y are size measures in units of the same dimension.

autapomorphy - derived trait or apomorphy that is unique to only one group or OTU

autochtonous - something that has not been transported

bending energy - Bending energy is a metaphor borrowed for use in morphometrics from the mechanics of thin metal plates. Imagine a configuration of landmarks that has been printed on an infinite, infinitely thin, flat metal plate, and suppose that the differences in coordinates of these same landmarks in another picture are taken as vertical displacements of this plate perpendicular to itself, one Cartesian coordinate at a time. The bending energy of one of these out-of-plane "shape changes" is the (idealized) energy that would be required to bend the metal plate so that the landmarks were lifted or lowered appropriately.

biological species concept - The concept of species, according to which a species is a set of organisms that can interbreed among each other. Compare with cladistic species concept, ecological species concept, phenetic species concept, and recognition species concept.

bootstrap method - is used to assess the reliability of a dataset or statistical estimate, in phylogenetics, to assess clusters. Felsenstein's bootstrap for phylogenetic trees creates pseudoreplicates of the original dataset by random sampling with replacement. In each replicate a new data set is formed and analysed. The bootstrap value produced for each clade in the final tree is based on the frequency with which a given clade is found in the pseudoreplicates.

bottleneck - A drastic reduction in the population size followed by an expansion. This often results in altered gene pool as a result of genetic drift.

canonical variates analysis - A method of multivariate analysis in which the variation among groups is expressed relative to the pooled within-group covariance matrix. Canonical variates analysis finds linear transformations of the data which maximize the among group variation relative to the pooled within-group variation. The canonical variates then may be displayed as an ordination to show the group centroids and scatter within groups. This may be thought of as a "data reduction" method in the sense that one wants to describe among group differences in few dimensions.

centroid size - Centroid Size is the square root of the sum of squared distances of a set of landmarks from their centroid, or, equivalently, the square root of the sum of the variances of the landmarks about that centroid in x- and y-directions. Centroid Size is used in geometric morphometrics because it is approximately uncorrelated with every shape variable when landmarks are distributed around mean positions by independent noise of the same small variance at every landmark and in every direction. Centroid Size is the size measure used to scale a configuration of landmarks so they can be plotted as a point in Kendall's shape space. The denominator of the formula for the Procrustes

distance between two sets of landmark configurations is the product of their Centroid Sizes.

character - heritable trait possessed by an organism; characters are usually described in terms of their states, for example: blue and red as character states for the character flower color

clade - a group of organisms that share a common ancestor; lineage; a monophyletic group

cladistic species concept - The concept of species, according to which a species is a lineage of populations between two phylogenetic branch points (or speciation events). Compare with biological species concept, ecological species concept and phenetic species concept.

cladistics - A method of grouping organisms that is based on synapomorphies or shared derived traits or characters.

cladogram - a dichotomous phylogenetic tree that branches repeatedly, suggesting a classification of organisms based on the sequence in which evolutionary branches arise; a nested diagram of synapormorphies indicating relations between groups; each point of branching represents divergence from a common ancestor

cluster analysis - A method of analysis that represents multivariate variation in data as a series of sets. In biology, the sets are often constructed in a hierarchical manner and shown in the form of a tree-like diagram called a dendrogram.

co-evolution - Joint evolution of two unrelated species that have a close ecological relationship resulting in reciprocal adaptations as happens between host and parasite, and plant and insect.

consensus configuration - A single set of landmarks intended to represent the central tendency of an observed sample for the production of superimpositions, of a weight matrix, or some other morphometric purpose. Often a consensus configuration is computed to optimize some measure of fit to the full sample: in particular, the Procrustes mean shape is computed to minimize the sum of squared Procrustes distances from the the consensus landmarks to those of the sample.

convergent evolution, convergence - the independent development of similar (analogous) structures in different groups; convergent evolution is thought to be the result of similar environmental selection pressures on different groups

coordinates - A set of parameters that locate a point in some geometrical space. Cartesian coordinates, for instance, locate a point on a plane or in physical space by projection onto perpendicular lines through one single point, the origin. The elements of any vector may be thought of as coordinates in a geometric sense.

derived trait - same as apomorphy; a derived character / trait is inferred to be a modified version of a more primitive condition of that character and therefore inferred to have arisen later in the evolution of the clade

discriminant analysis - A broad class of methods concerned with the development of rules for assigning unclassified objects/specimens to previously defined groups. See discriminant function.

disparity - distinct in morphological characters; morphological variation; compare to diversity

divergent evolution - A kind of evolutionary change that results in increasing morphological difference between initially more similar lineages.

ecological species concept - A concept of species, according to which a species is a set of organisms adapted to a particular, discrete set of resources (or "niche") in the

environment. Compare with biological species concept, cladistic species concept and phenetic species concept.

eigenvalues - are the diagonal elements of the diagonal matrix in the equation: . In the common data analysis case, S is a symmetrical variance-covariance matrix, E is a matrix of eigenvectors, , and . The order of the columns of E and is arbitrary, but by convention they are usually sorted from largest to smallest eigenvalue. See eigenvectors and singular value decomposition.

endemic - belonging or native to a particular region or area and found only in that area. endosperm

entomophage - An organism that feeds on insects (noun); the corresponding adjective is entomophagous.

extant - currently existing; living now

facultative parasitism - A condition in which a free-living organism may exist by parasitism (parasitoidism) but does not rely upon this way of life.

form - In morphometrics, we represent the form of an object by a point in a space of form variables, which are measurements of a geometric object that are unchanged by translations and rotations. If you allow for reflections, forms stand for all the figures that have all the same interlandmark distances. A form is usually represented by one of its figures at some specified location and in some specified orientation. When represented in this way, location and orientation are said to have been "removed."

founder effect - A type of genetic drift in which allele frequencies are altered in a small population, which is a nonrandom sample of a larger (main) population.

FST (Fixation index) - FST = 1/(4Nm+1) can be used to estimate gene flow; *N* is the effective population size, *m* is the effective proportion of immigrants. FST=1 indicates an absence of gene flow.

gamma distribution - this parameter allows for variation in the rate of nucleotide substitution changes from site to site e.g. depending on the gene target certain areas of gene maybe more likely to undergo mutation than other sites.

generalized superimposition - The superimposition of a set of configurations onto their consensus configuration. The fitting may involve least-squares, resistant-fit, or other algorithms and may be strictly orthogonal or allow affine transformations.

genetic drift - Evolutionary change over generations due to random events in small populations (not to be mixed with sampling error due to a small sample size). It operates unless overcome by strong selective forces.

geometric morphometrics - Geometric morphometrics is a collection of approaches for the multivariate statistical analysis of Cartesian coordinate data, usually (but not always) limited to landmark point locations. The "geometry" referred to by the word "geometric" is the geometry of Kendall's shape space: the estimation of mean shapes and the description of sample variation of shape using the geometry of Procrustes distance. The multivariate part of geometric morphometrics is usually carried out in a linear tangent space to the non-Euclidean shape space in the vicinity of the mean shape. More generally, it is the class of morphometric methods that preserve complete information about the relative spatial arrangements of the data throughout an analysis. As such, these methods allow for the visualization of group and individual differences, sample variation, and other results in the space of the original specimens.

haematophagy – Blood feeding (usually refers to vertebrate blood).

heterochrony - an evolutionary change in phenotype based on an alteration in timing of developmental events

heuristic method - Finding the optimal tree in phylogenetics often requires extensive analysis, to overcome this heuristics is often used. This is a method of searching data for the most parsimonious tree, thereby increasing the speed of analysis, but possibly giving less than accurate results.

holophyletic - A holophyletic taxon is one in which all descendants of a singular common ancestor are united into one lineage. It is synonymous with clade.

homology - likeness and correspondence in structure between parts of different organisms, due to common ancestry of the organisms.

homoplasy - see convergence;

hypermorphosis - The phyletic extension of ontogeny beyond its ancestral termination (usually to larger body sizes and increased complexity of differentiating organs) producing recapitulation as a result because ancestral adult stages are now intermediate stages of a lengthened descendant ontogeny.

indels - insertion\deletion; the alignment of multiple sequences often needs the introduction of gaps as some sequences may have insertions or deletions, these alignment gaps are called indels.

introgression - Infiltration of the genes of one species into the gene pool of another through repeated backcrossing of an interspecific hybrid with one of its parents.

isometry - An isometry is a transformation of a geometric space that leaves distances between points unchanged. If the space is the Euclidean space of a picture or an organism, and the distances are distances between landmarks, the isometries are the Euclidean translations, rotations, and reflections. If the distances are Procrustes distances between shapes, the isometries (for the simplest case, landmarks in two dimensions) are the rotations of Kendall's shape space. For triangles, these can be visualized as ordinary rotations of Kendall's "spherical blackboard."

Jukes-Cantor - when calculating the distance between sequences this model assumes equal frequencies each of the 4 bases, A, T, C, and G, and an equal rate of nucleotide substitution.

Kendall's shape space - The fundamental geometric construction, due to David Kendall, underlying geometric morphometrics. Kendall's shape space provides a complete geometric setting for analyses of Procrustes distances among arbitrary sets of landmarks. Each point in this shape space represents the shape of a configuration of points in some Euclidean space, irrespective of size, position, and orientation. In shape space, scatters of points correspond to scatters of entire landmark configurations, not merely scatters of single landmarks. Most multivariate methods of geometric morphometrics are linearizations of statistical analyses of distances and directions in this underlying space.

Kimura 2-parameter - when calculating the distance between sequences this model assumes equal frequencies each of the 4 bases, A, T, C, and G, and differential transitional and transversional substitutions rates (a transitional\transversional bias).

landmark - A specific point on a biological form or image of a form located according to some rule. Landmarks with the same name, homologues in the purely semantic sense, are presumed to correspond in some sensible way over the forms of a data set.

least-squares estimates - Parameter estimates that minimize the sum of squared differences between observed and predicted sample values.

linear combination - A sum of values each multiplied by some coefficient. A linear combination can be expressed as the inner product of two vectors, one representing the data and the other a vector of coefficients.

macroevolution - The study of evolutionary events and processes that require long times for their occurrence or operation conventionally defined at taxonomic levels involving the origin and deployment of species and higher taxa, not changes of gene frequencies within local populations

mahalanobis distance - Defined by the equation for two row vectors xi and xj for two individuals, and p variables as: $\left(\left(\mathbf{x}_i - \mathbf{x}_j\right)\mathbf{S}^{-1}\left(\mathbf{x}_i - \mathbf{x}_j\right)^t\right)^{\frac{1}{2}}$, where S is the pxp variance-covariance matrix. It takes into consideration the variance and correlation of the variables in measuring distances between points, i. e., differences in directions in which there is less variation within groups are given greater weight than are differences in directions in which there is more variation.

maximum likelihood - is a discrete method of tree building, which uses an evolutionary model set by the user to score and rank trees, in terms of their likelihood. It analyses data in its raw form, not derived distances and as such is often thought to be more powerful. The correct evolutionary tree is that with the highest likelihood score under that model.
maximum parsimony - Parsimony aims to recreate the ancestral sequences of the data on the basis of a minimum number of evolutionary changes, giving the optimal tree or network.

monophyletic - A group composed of a collection of organisms, including the most recent common ancestor of all those organisms and all the descendants of that most recent common ancestor. A monophyletic taxon is also called a clade.

morphometrics - method to define and describe morphological characters and character states based on quantifiable measurements; morphometrics can also help define taxa by evaluating ranges of variation within and between groups

Mya - Million years ago.

Neighbour-joining - is a tree building method based on a clustering algorithm and the minimum evolutionary principle. Pairwise genetic distances are calculated between the sequences according to an evolutionary model e.g. the Kimura-2 parameter. A phylogenetic tree is then constructed by linking the least distant pairs of sequences, the tree with the least total branch length is preferred at each step. The tree produced is unrooted.

neoteny - Paedomorphosis (retention of formerly juvenile characters by adult descendants) produced by retardation of somatic development.

node - The branching points on a cladogram, which are supported by synapomorphies

non-synonymous substitution - A nucleotide substitution (mutation) that results in a different amino acid. More likely for first and second position codons.

ontogeny - the course of development of an individual organism

orthogonal - At right angles. In linear algebra, being "at right angles" is defined relative to a symmetric matrix P, such as the bending-energy matrix; two vectors x and y are orthogonal with respect to P if xtPy=0. Principal warps are orthogonal with respect to bending energy, and relative warps are orthogonal with respect to both bending energy and the sample covariance matrix.

orthogonal superimposition - A superimposition using only transformations that are all Euclidean similarities, i. e., involve only translation, rotation, scaling, and, possibly, reflection.

OUT - or Operational Taxonomic Unit; definitions or names of the taxa included in a phylogenetic analysis

parallell evolution - see convergent evolution

paraphyly, paraphyletic group - terms applied to a group of organisms that include an ancestor and some, but not all of its descendants; compare to monophyly, monophyletic groups and polyphyly, and polyphyletic groups

parsimony-informative - A site is parsimony-informative if it contains at least two types of nucleotides (or amino acids), and at least two of them occur with a minimum frequency of two.

partial least squares - Partial Least Squares (PLS) is a multivariate statistical method for assessing relationships among two or more sets of variables measured on the same entities. Partial Least Squares analyses the covariances between the sets of variables rather than optimizing linear combinations of variables in the various sets. Their computations usually do not involve the inversion of matrices.

partial warp scores - Partial warp scores are the quantities that characterize the location of each specimen in the space of the partial warps. They are a rotation of the Procrustes residuals around the Procrustes mean configuration. For the nonuniform partial warps, the coefficients for the rotation are the principal warps, applied first to the x-coordinates of the Procrustes residuals, then to the y-coordinates and, for three-dimensional data, the z-coordinates.

phenetic species concept - A concept of species according to which a species is a set of organisms that are phenotypically similar to one another. Compare with biological species concept, cladistic species concept and ecological species concept.

phylogenetics - Study of reconstructing evolutionary genealogical ties between taxa and line of descent of species or higher taxon.

phytophagy - The habit of feeding upon plants or vegetable matter (noun); herbivory; also phytophage (noun) and phytophagous (adjective).

plesiomorphy, plesiomorphic trait - A character that is present in the common ancestor of a clade; a primitive trait is inferred to be the original character state of that character within the clade under consideration; compare to derived trait

polyphyly, polyphyletic group - a group of organisms with different most recent ancestors

polytomy - In cladistics, a polytomy refers to a node with more than two descendant branches. A "hard" polytomy refers to a situation in which data is insufficient to resolve it down to two branches, which may be interpreted as a multiple speciation event. A "soft" polytomy, on the other hand, refers to a conflict between two resolved cladograms.

predatory - Living by preying on others, here it usually refers to entomophagy.

principal components analysis - The eigenanalysis of the sample covariance matrix. Principal components (PC's) can be defined as the set of vectors that are orthogonal both with respect to the identity matrix and the sample covariance matrix. They can also be defined sequentially: the first is the linear combination with the largest variance of all those with coefficients summing in square to 1; the second has the largest variance (when normalized that way) of all that are uncorrelated with the first one; etc. One way to

compute principal components is to use a singular value decomposition. Relative warps are principal components of partial warp scores.

procrustes superimposition - The construction of a two-form superimposition by least squares using orthogonal or affine transformations. The adjective "Procrustes" refers to the Greek giant who would stretch or shorten victims to fit a bed.

purines - the nucleotides Adenine (A) and Guanine (G) are purines.

pyrimidines - the nucleotides Cytosine (C) and Thymine (T) are pyrimidines.

relative warps - Relative warps are principal components of a distribution of shapes in a space tangent to Kendall's shape space. They are the axes of the "ellipsoid" occupied by the sample of shapes in a geometry in which spheres are defined by Procrustes distance. Each relative warp, as a direction of shape change about the mean form, can be interpreted as specifying multiples of one single transformation, a transformation that can often be usefully drawn out as a thin-plate spline. In a relative warps analysis, the parameter can be used to weight shape variation by the geometric scale of shape differences. Relative warps can be computed from Procrustes residuals or from partial warps.

relative rates mutation model - when calculating the distance between sequences this model allows for unequal base frequencies (A, T, G, C), and allows for different rates of base substitution e.g. in AT rich insect mitochondria A and T are more frequent and more likely to undergo base substitution. This model also allows for back mutations.

synonymous change - a nucleotide substitution that does not change the encoded amino acid (antonym nonsynonymous).

shape variable - Any measure of the geometry of a biological form, or the image of a form, that does not change under similarity transformations: translations, rotations, and changes of geometric scale (enlargements or reductions). Useful shape variables include angles, ratios of distances, and any of the sets of shape coordinates that arise in geometric morphometrics.

sister group - Two clades that resulted from the splitting of a single lineage; sister groups share a common ancestor

strict consensus – A method for choosing among several most parsimonious trees generated by a phylogenetic analysis; strict consensus means that only clades that show up in all the most parsimonious trees are recognized

synapomorphy - Shared derived trait (apomorphy); a derived character that is shared between organisms; compare to autapormorphy

Tajima-Nei - when calculating the distance between sequences this model allows variation in the frequency of the four nucleotides bases, A, T, C, and G, but the rate of nucleotide substitution is equal for all.

Tamura-Nei - when calculating the distance between sequences this model allows for variation in the frequency of the four nucleotides bases, A, T, C, and G, and differential transitional and transversional substitutions rates (a transitional\transversional bias).

thin-plate spline - In continuum mechanics, a thin-plate spline models the form taken by a metal plate that is constrained at some combination of points and lines and otherwise free to adopt the form that minimizes bending energy. (The extent of bending is taken as so small that elastic energy - stretches and shrinks in the plane of the original plate - can be neglected.) One particular version of this problem - an infinite, uniform plate constrained only by displacements at a set of discrete points - can be solved algebraically by a simple

matrix inversion. In that form, the technique is a convenient general approach to the problem of surface interpolation for computer graphics and computer-aided design. In morphometrics, the same interpolation (applied once for each Cartesian coordinate) provides a unique solution to the construction of D'Arcy Thompson-type deformation grids for data in the form of two landmark configurations.

traditional morphometrics - Application of multivariate statistical methods to arbitrary collections of size or shape variables such as distances and angles. "Traditional morphometrics" differs from the geometric morphometrics discussed here in that even though the distances or measurements are defined to record biologically meaningful aspects of the organism, but the geometrical relationships between these measurements are not taken into account. Traditional morphometrics makes no reference to Procrustes distance or any other aspect of Kendall's shape space. See geometric morphometrics

transition - a transition is the substitution of purine by a purine, or a pyrimidine by a pyrimidine at a nucleotide site.

transition/transversion ratio - the ratio of the number of transitions to the number of transversions in a data set. In sequence data transitions occur more frequently than transversions, and can reach saturation quickly. As the rate of transitional changes differs from the rate of transversions this could bias distance analysis.

transversion - a transversion is a change from a purine to a pyrimidine at a nucleotide site, or vice versa.

UPGMA - Unweighted Pair Group Method with Arithmetic Mean is a clustering method for creating phylogenetic trees that assumes a constant evolution rate and produces a rooted tree. Initial clusters are formed based on minimum distance between pairs, the average distance between paired clusters is then calculated and those separated by the minimum distance grouped into a higher-level cluster, the average distance is recalculated until the last two clusters are joined.

vicariance - Separation of a continuously distributed ancestral population or species into separate populations, due to the development of a topographic or ecological barrier (vicariant events)

weight matrix , W matrix -The matrix of partial warp scores, together with the uniform component, for a sample of shapes. The weight matrix is computed as a rotation of the Procrustes-residual shape coordinates; like them, they are a set of shape coordinates for which the sum of squared differences is the squared Procrustes distance between any two specimens.

This Glossary has been complied and adapted from the following sources:

Page, R. D. M. and E. C. Holmes (2000). *Molecular Evolution - A Phylogenetic Approach.* Oxford, U.K., Blackwell Science, pp 346.

Gould, S.J. (1977). *Ontogeny and Phylogeny.* Belknap Press/Harvard University Press. 501 pp.

http://www.dorak.info/genetics/glosgen.html

http://www.ucmp.berkeley.edu/IB181/VPL/Glossary.html

http://life.bio.sunysb.edu/morph/glossary/gloss1.html

http://biocontrol.ifas.ufl.edu/glossary.htm

12. Appendix

Table. 41 The fossil record of major insect groups over the main geological periods

ERA	PERIOD	MAX. AGE [1] (millions of years)	INSECT FOSSILS (earliest found)	OTHER FOSSILS (earliest found)
CAENOZOIC (Quaternary)	Holocene	(present) — 0.01		
	Pleistocene	2		modern man
CAENOZOIC (Tertiary)	Pliocene	5		
	Miocene	25	butterflies, ants	
	Oligocene	40	many insects similar or identical to our present fauna trapped in baltic amber	
	Eocene	60		
	Palaeocene	65		
MESOZOIC (Secondary)	Cretaceous	145		birds, flowering plants (last dinosaurs & ammonites)
	Jurassic	210	earwigs, sawflies	mammals
	Triassic	245	caddis flies, beetles, true flies	dinosaurs, coniferous plants
PALEOZOIC (Primary)	Permian	285	dragonflies, mayflies, stoneflies, lacewings, crickets, true bugs	reptiles, ammonites (last trilobites)
	Carboniferous	360	cockroaches, many archaic insects that all disappear in the late Permian leaving no modern descendants	amphibians
	Devonian	410	springtails	spiders, ferns and other similar land plants
	Silurian	440		scorpions
	Ordovician	505		fishes
	Cambrian	540		trilobites, worms, molluscs, corals
PRE-CAMBRIAN	Proterozoic	2500		unicellular organisms (algae, fungi, bacteria)
	Azoic (Archaean)	3900		

[1] The figures cited are approximate and are subject to continual revision

Old World *Triatoma*

T. rubrofasciata *T. migrans* *T. cavernicola* *T. amicitae* *T. leopoldi* *T. pugasi*

Linshcosteus spp.

L. carnifex *L. confumus* *L. costalis* *L. chota* *L. kali* *L. karupus*

North & Central American *Triatoma*

T. rubida *T. sanguisuga* *T. gerstaeckeri* *T. pallidipennis* *T. dimidiata* *T. protracta* *T. flavida*

South American *Triatoma*

T. infestans *T. rubrovaria* *T. platensis* *T. matogrossensis*

Figure 93. Comparison of representative Old & New World *Triatoma* and *Linshcosteus spp.*

Reduviinae (PRO+) Reduviinae (PRZ+) Reduviinae (PRZ) Reduviinae (PRO) Reduviinae (RPB)

Vesciinae (PVP) Reduviinae (PRL) Reduviinae (VRL) Stenopodinae (SV) Emesinae (PEE) Ectrichodiinae (PER)

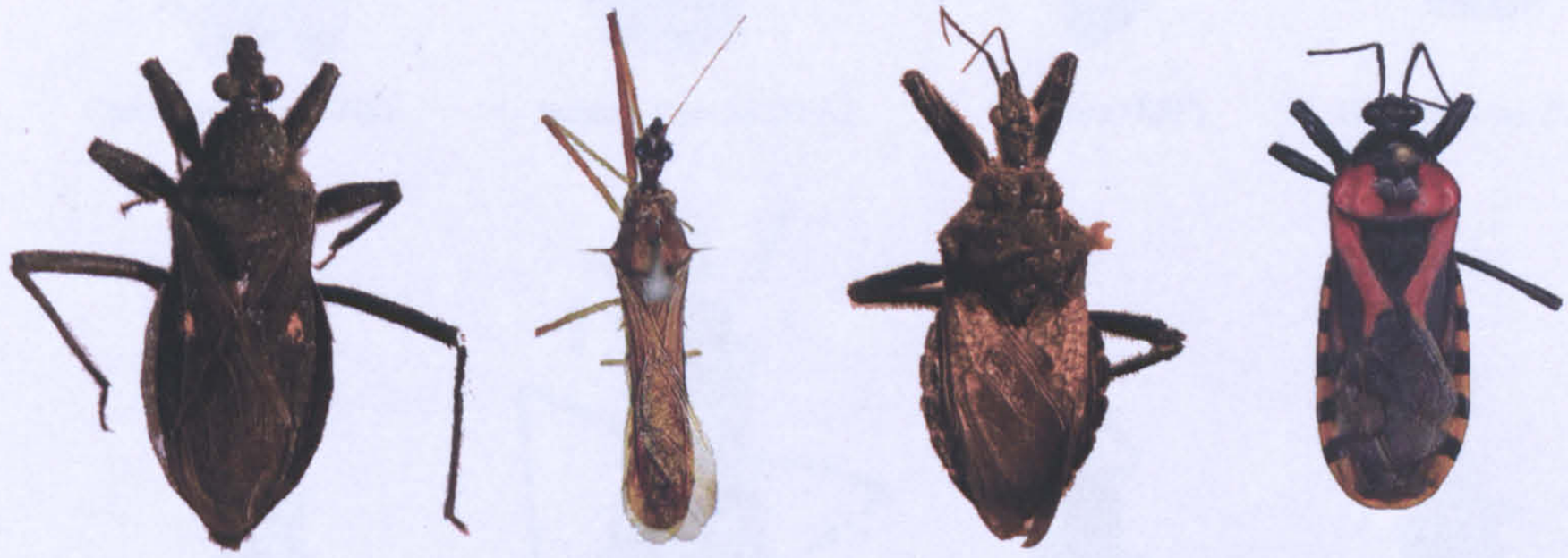

Hammacerinae (PH) Harpactorinae (VH) Harpactorinae (VHA) Ectrichodiinae (VEB)

Figure 94. A selection of field caught Reduviidae examined (see **Table. 19** for details)

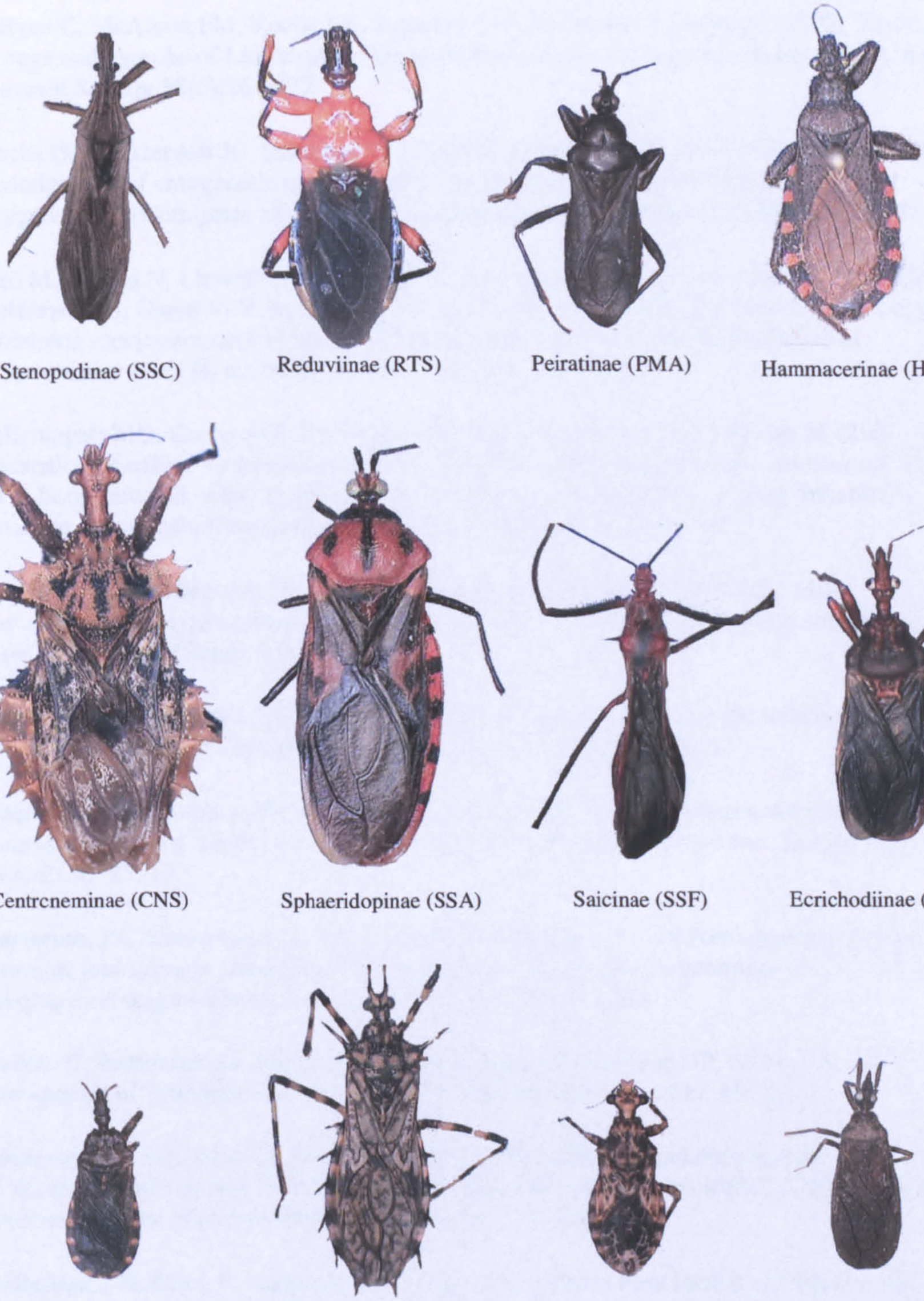

Stenopodinae (SSC) | Reduviinae (RTS) | Peiratinae (PMA) | Hammacerinae (HHG)

Centrcneminae (CNS) | Sphaeridopinae (SSA) | Saicinae (SSF) | Ecrichodiinae (ECT)

Physoderinae (PPB) | Salyavatinae (SSV) | Cetherinae (CCM) | Tribelocephalinae (TTT)

Figure 95 A selection of Reduviidae examined from the Natural History Museum London (see **Table 19** for details)

Publications related to this work

- Galvao C, McAloon FM, Rocha DS, Schaefer CW, **Patterson J**, Jurberg J. 2005. Description of eggs and nymphs of Linshcosteus karupus (Hemiptera : Reduviidae : Triatominae). *Ann Entomol Soc Am* **98**(6):861-872.

- Rocha DD, **Patterson JS**, Sandoval CM, Jurberg J, Angulo VM, Esteban L, Galvao C. 2005. Description and ontogenetic morphometrics of nymphs of Belminus herreri Lent & Wygodzinsky (Hemiptera : Reduviidae, Triatominae). *Neotrop Entomol* **34**(3):491-497.

- Yeo M, Acosta N, Llewellyn M, Sánchez H, Adamson S,. Miles GAJ, López E, González N, **Patterson JS**, Gaunt MW, Rojas de Arias A & Miles MA. (2005) Origins of Chagas disease: *Didelphis* species are natural hosts of *Trypanosoma cruzi* I and armadillos hosts of *Trypanosoma cruzi* II, including hybrids. *Int. J. Parasit.* (In press).

- Feliciangeli MD, Carrasco H,**Patterson JS**, Suarez B, Martínez C, Medina M (2004). Mixed domestic infestation by *Rhodnius prolixus* Stäl, 1859 and *Panstrongylus geniculatus* Latreille, 1811,both infected with *Trypanosoma cruzi*,and seroprevalence among inhabitants in El Guamito, Lara State, Venezuela *Am. J. Trop. Med. Hyg.* 71: 501-505.

- Abad-Franch F, Monteiro FA, **Patterson JS**, Aguilar HM, Beard CB, Miles MA (2003) Population phenotypic plasticity linked to ecological adaptations in Triatominae. *Rev. Inst. Trop. S. Paulo* 45 (Suppl. 13): 201.

- **Patterson JS**, Fitzpatrick SO (2003) Morphometrics of triatomine bugs: indicators of evolutionary processes and population diversity. *Inf. Gen. Evol.* 85: 13

- Abad-Franch F,Monteiro FA, **Patterson JS**, Miles MA (2003) Phylogenetic relationships among members of the Pacific *Rhodnius* lineage (Hemiptera: Reduviidae: Triatominae) *Inf., Gen. Evol.* 85: 10.

- **Patterson JS**, Abad-Franch F, Cuba Cuba CA Miles MA (2002)Morphometric distinction of domestic and sylvatic populations of *Rhodnius ecuadoriensis* (Triatominae) from different geographical origins *Trans. Roy. Soc. Trop. Med. Hyg* 96: 365.

- Galvão C, **Patterson JS**, Rocha D, Jurberg J, Rajen K, Ambrose DP, Miles MA. (2002) A new species of Triatominae from Tamil Nadu Indian. *Med. Vet. Ent.* 16: 75-82.

- **Patterson JS**, Schofield CJ, Dujardin JP, Miles MA (2001) Population morphometric analysis of the tropicopolitan bug *Triatoma rubrofasciata* and relationships with Old World species: evidence of New World ancestry. *Med. Vet. Ent.* 15: 443-451.

- **Patterson J S**, Rajen K, Ambrose D P, Miles M A. (2001) First record of trypanosomes from the endemic Indian genus of Triatominae, *Linshcosteus sp.* nov. *Trans. Roy. Soc. Trop. Med. Hyg.* 95: 248-249

Related work on Tsetse flies.

- **Patterson JS** & Schofield CJ (2005) Preliminary study of wing morphometry in relation to tsetse population genetics. *South African Journal of Science* 101, 132-134

- Schofield CJ & **Patterson JS** (2005) Preparing for tsetse eradication. *South African Journal of Science* 101, p.116